The *in vitro* effects of heavy metals and nanoparticles on the immune system

By

Kim Leigh Lategan

Submitted in fulfillment of the requirements for the degree

Doctor of Philosophy

In the

Department of Medical Bioscience

Faculty of Science

University of the Western Cape

Supervisor

Prof. E.J. Pool

December 2017

Declaration

I declare that:

The in vitro effects of heavy metals and nanoparticles on the immune system is my own work, that it has not been submitted for any degree or examination at any other university, and that all the sources I have used or quoted have been indicated and acknowledged by complete references.

Kim. L. Lategan

Signature:

Date: December 2017

ii

Abstract

Heavy metals and nanoparticles may be released into the environment due to their use and applications. Sources of high, toxic metal concentrations may result from leachates from hazardous waste sites, discharge from industrial plants, and effluents from wastewater treatment plants being released into the environment. Nanoparticles may be found in a number of consumer products, and are used in medical applications such as drug delivery, bioimaging and biosensing. The release of heavy metals and nanoparticles to the environment may directly or indirectly impact abiotic and biotic systems.

Three heavy metals and three nanoparticles were selected for this study. The heavy metals selected include cadmium (Cd), silver (Ag) and copper (Cu). The nanoparticles (NPs) chosen were silver nanoparicles (AgNPs), graphene oxide nanoparticles (GONPs) and carbon dots (CDs). These compounds were selected to evaluate the potential effects these compound may have on the immune system.

The murine macrophage cell line RAW 264.7 and human whole blood cell cultures (WBCs) were selected as immune system representatives to assess the effects of heavy metals and nanoparticles on the immune system. The effects of heavy metals and NPs on RAW cells were monitored either in the absence or presence of the mitogen, lipopolysaccharide (LPS). The effects of heavy metals and NPs on WBCs were evaluated under basal conditions or in the presence of LPS or phytohaemmagglutinin (PHA). A number of parameters were monitored. These

iii

parameters included cytotoxicity, inflammatory biomarkers, cytokines of the acquired immune system and a proteome profile analysis.

The first objective of this study was to assess the effects Cd, Ag and Cu on immune system biomarkers. No effects on were seen on cultures not stimulated by LPS. Cd was more cytotoxic than Ag, with Cu having no effect on cell viability of the RAW cells. The same trend was seen when evaluating the inflammatory biomarkers, nitric oxide (NO) and interleukin 6 (IL-6). Evaluating the effects of the metals on WBCs and the cytokines representing the innate (IL-6), humoral (IL-10) and cell mediated immunity (IFNγ) found that all the cytokines were reduced by the metals. The results show IL-6 was inhibited by Cu at lower concentrations than Cd, while Ag upregulated its synthesis. IL-10 was inhibited by Cd at lower concentrations than Cu, and Ag inhibited the production of this cytokine the least. IFNγ was reduced by higher concentrations of Ag, followed by Cu, and then Cd.

The second objective of this study was to evaluate the effects AgNPs had on the immune system biomarkers. AgNP concentrations had no negative effect on RAW cell viability at concentrations used. However, AgNP cytotoxicity of WBCs was evident. Under basal conditions, AgNPs induced inflammation in RAW cells and WBCs respectively. Under a simulated inflammatory response, AgNPs inhibited the inflammatory response for both RAW and WBCs. The acquired immune cytokines IL-10 and IFNγ were both induced by AgNPs in the absence of PHA. IL-10 was partially inhibited by AgNPs when evaluated in the presence of PHA. Proteome profiles of RAW cell supernatants show that AgNPs do in fact modulate specific

iv

protein synthesis. Upregulated proteins due to AgNP exposure indicate induction of specific proteins indicative of inflammatory responses and wound healing. WBC supernatant proteome analysis indicates modulation of anti-inflammatory properties by AgNPs.

The third objective was to monitor the effects of GONPs on the immune system biomarkers. GONPs were cytotoxic to both RAW and WBCs. In the absence of mitogens, GONPs elicited an inflammatory response from RAW and WBCs respectively. This activation was further corroborated by proteome profile analysis of both experimental cultures. GONPs inhibited LPS induced IL-6 synthesis and PHA induced IFNγ synthesis by WBCs in a dose dependent manner. In the absence of mitogens, GONPs stimulated IL-10 synthesis by WBCs. GONPs modulate immune system biomarkers and these may pose a health risk to individuals exposed to this type of nanoparticle.

The last objective of this study was to evaluate the effects of CDs on the immune system. CDs were cytotoxic to RAW and WBCs respectively. Biomarkers associated with inflammation was induced by CDs under basal conditions for both RAW and WBCs respectively. The humoral immune system regulating cytokine IL-10 was increased by CDs under both basal and PHA activated WBCs. Proteome analysis supported the inflammatory data as proteins identified are associated with inflammation and provide potential biomarkers to be assessed upon CD exposure.

The heavy metals and NPs assessed in this study can potentially be detrimental to human health as they are cytotoxic and induce immunomodulatory cytokines. This could potentially result in immunosuppression or immunostimulation in individuals exposed to these compounds.

UNIVERSITY *of the*
WESTERN CAPE

Acknowledgements

I wish to express my sincere gratitude to my supervisor, Prof. Edmund John Pool for his unwavering support, encouragement, supervision, guidance and inspiration throughout this research. Without his guidance, the completion of this research project would not have been possible.

I would like to thank Prof. Maria Fidalgo and Mohamed Bayati from the University of Missouri for providing and characterizing the graphene oxide nanoparticles and carbon dots.

I express appreciation to my fellow peers in and outside of our lab, with whom none of this would have been possible.

My heartfelt gratefulness to my parents and family for their unconditional love and support during this PhD study. To my parents, for always affording me the best opportunities, and for always pushing me to complete things to the best of my ability.

I wish to thank my friends for being there when venting was necessary and giving me a new perspective on things if needed.

I am grateful to the NRF for their financial support during this research project.

List of acronyms and abbreviations

°C	degrees Celsius
2-D	two-dimensional
Ag	silver
AgNO$_3$	silver nitrate
AgNPs	silver nanoparticles
ANOVA	analysis of variance
APCs	antigen presenting cells
ATCC	American Type Culture Collection
BSA	bovine serum albumin
BSNPs	sodium borohydride nanoparticles
Ca	calcium
CAT	catalase
CCL2/MCP-1/JE	monocyte chemoattractant protein-1
CCL3/MIP-1α	macrophage inflammatory protein 1 alpha
CCL4/MIP-1β	macrophage inflammatory protein 1 beta
CCL5/RANTES	T cell expressed and secreted
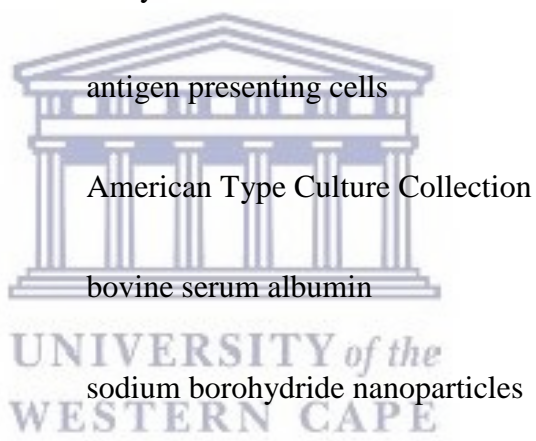
Cd	cadmium
Cd/l	cadmium per litre
CD54/sICAM-1	intracellular adhesion molecule-1
$CdCl_2$	cadmium chloride
CDs	carbon dots
cells/ml	cells per milliliter
CNTs	carbon nanotubes
CO_2	carbon dioxide
CTLs	cytotoxic T-cells
Cu	copper
$CuSO_4$	copper sulphate
CXCL10/CGR-2/IP-10	interferon gamma induced protein 10
CXCL2/MIP-2	macrophage inflammatory protein 2
DAS ELISA	double antibody sandwich enzyme-linked immunosorbent assay
DCs	dendritic cells
DEA	Department of Environmental Affairs

ix
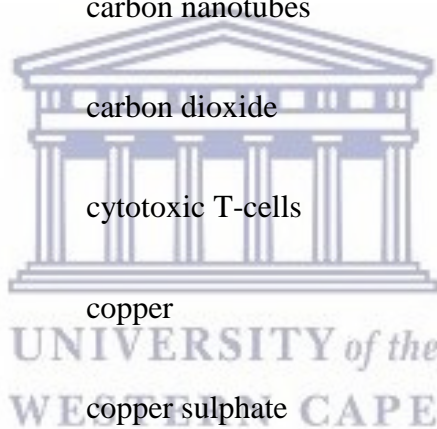
DMEM	Dulbecco's modified Eagle's medium
DNA	deoxyribonucleic acid
DPBS	Dulbecco's phosphate buffered saline
DWAF	Department of Water Affairs and Forestry
DWNTs	double-walled carbon nanotubes
ER	endoplasmic reticulum
EU	European Union
FAO	Food and Agricultural Organization
FasL	Fas ligand
FBS	fetal bovine serum
FBS/well	fetal bovine serum per well
FTIR	Fourier-transform infared spectroscopy
G	graphene
g/l	gram per liter
GALT	gut associated lymphoid tissue
G-CSF	granulocyte colony-stimulating factor
GM-CSF	granulocyte-macrophage colony-stimulating factor
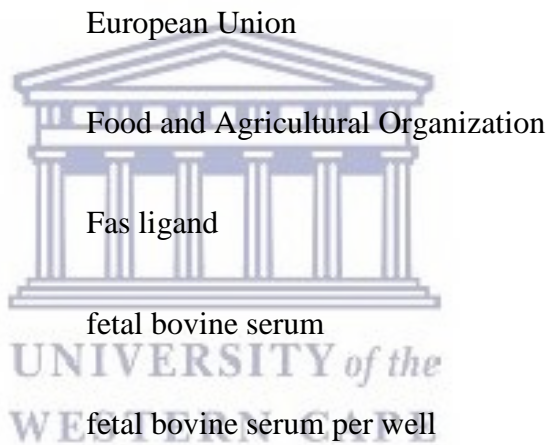
GO	graphene oxide
GONPs	graphene oxide nanoparticles
gp130	glycoprotein 130
GPx	glutathione peroxidase
GSH	glutathione
GST	glutathione-S-transferase
HSA	human serum albumin
hrs	hours
IC_{50}	half maximal inhibitory concentration
IFNα	interferon alpha
IFNγ	interferon gamma
IgD	immunoglobulin D
IgE	immunoglobulin E
IgG	immunoglobulin G
IgM	immunoglobulin M
IL-1	interleukin 1
IL-10	interleukin 10

IL-12	interleukin 12
IL-1R	interleukin 1 receptor
IL-1ra	interleukin 1 receptor antagonist
IL-1β	interleukin 1 beta
IL-27	interleukin 27
IL-4	interleukin 4
IL-6	interleukin 6
IL-8	interleukin 8
ILs	interleukins
ISO	International Organization for Standardization
JAK	Janus kinase
K	potassium
K_2SO_4	potassium sulphate
KNO_3	potassium nitrate
LDH	lactate dehydrogenase
LPO	lipid peroxidation
LPS	lipopolysaccharide

MAC	membrane attack complex
MALT	mucosal associated lymphoid tissue
MAPK	mitogen-activated protein kinase
MASP	mannan-binding lectin-associated serine proteases
MBL	mannan-binding lectin
M-CSF	macrophage colony-stimulating factor
Mg	magnesium
mg/l	milligram per litre
mg/ml	milligram per millilitre
MgCl$_2$	magnesium chloride
MHC	major histocompatability complex
MIF	macrophage migration inhibitory factor
mins	minutes
mm	millimeter
mM	millimolar
MTs	metallothioneins
mV	millivolts

MWCNTs	multi-wall carbon nanotubes
n	sample size
$NaCl_2$	sodium chloride
NF-κβ	nuclear factor kappa beta
NK	natural killer cells
nm	nanometer
NO	nitric oxide
NPs	nanoparticles
OECD	Organization for Economic Co-operation and Development
PAMPs	pathogen-associated molecular patterns
PEG	ploy(ethylene glycol-amine)
pH	potential of hydrogen
PHA	phytohaemmagglutinin
PMA	phorbol 12-myristate 13-acetate
PMBCs	peripheral blood mononuclear cells
ppb	parts per billion
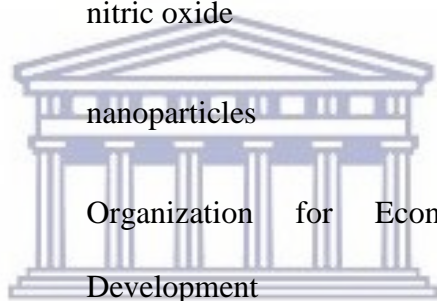
ppm   parts per million

PRRs   pattern recognition receptors

rcf   relative centrifugal force

ROS   reactive oxygen species

RPMI 1640   Roswell Parks Memorial Institute 1640

SANS   South African National Standard

SD   standard deviation

SDF-1   stromal cell-derived factor 1

secs   seconds

Serpin E1   Serpin family E member 1

SOD   superoxide dismutase

STAT   signal transducers and activators of transcription

HRP   horseradish peroxidase

SWCNTs   single-walled carbon nanotubes

Tc   cytotoxic T-cells

TCRs   T-cell antigen receptor

TEM   transmission electron microscopy

TLRs	Toll-like receptors
TMB	3,3',5,5'-tetramethylbenzidine
TNF-α	tumour necrosis factor alpha
UN	United Nations
US EPA	United States Environmental Protection Agency
UV-vis	ultraviolet-visible spectrophotometry
v/v	volume per volume
w/v	weight per volume
WBCs	whole blood cultures
WHO	World Health Organization
WST-1	2-(4-Iodophenyl)-3-(4-nitorphenyl)-5-(2,4-dislfophenyl)-2H-tetrazolium
Zn	zinc
Zn/l	zinc per liter
μg/g	microgram per gram
μg/l	microgram per liter
μg/ml	microgram per milliliter

μl   microliter

μM   micromolar

μm   micrometer

Oral and poster presentations at Conferences

- Lategan, K. and Pool, E., 2013. *Saccharomyces cerevisiae* as a Rapid Bio-indicator for Sewage Related Water Toxicity- an ecosystem perspective 16th Biennial International Symposium for Toxicity Assessment (ISTA), Cape Town, 21-26 February 2013.

- Lategan, K. and Pool, E. 2013. Development of rapid assays to monitor adverse effects of pollutants on humans. Social Innovation and Public Health, Cape Town, South Africa, 25 October 2013.

- Lategan, K. and Pool, E. 2015. The effects of cadmium on RAW 264.7 macrophage cells. China-Africa Water Forum, Cape Town, South Africa, August 2015.

- Lategan, K. and Pool, E, 2015. Molecular biomarkers for monitoring heavy metal and heavy metal nanoparticle toxicity. SETAC Africa, Langebaan, South Africa, 5-8 October 2015.

- Lategan, K., Leach, L., Alghadi, H., Fowler, J., Fidalgo, M. and Pool, E., 2017. The use of proteome profiling to detect potential biomarkers for monitoring the immunotoxicity of engineered nanoparticles. SETAC Europe, Brussels, Belgium, 7-11 May 2017.

- Lategan, K., Walters, C. and Pool, E. The effects of silver nanoparticles on RAW 264.7 macrophages and human whole blood cell cultures. International Conference on Immunology and Immunotechnology, Barcelona, Spain, 1-3 November 2017.

Table of Contents

xxiii

List of Figures

xxxv

xl

mean ± SD with n = 3. Bars marked with the letter a indicate significantly different (P < 0.001) compared to 0 μg/ml AgNPs…………………………………………………..114

Figure 4.3. Interleukin 6 (IL-6) production by RAW 264.7 macrophage cells exposed to AgNPs in LPS stimulated cell cultures. Data represents mean ± SD with n = 3. Unstimulated cultures did not synthesize IL-6 (data not presented). Bars marked with the letter a indicate significantly different (P < 0.001) compared to 0 μg/ml AgNPs. …………………………………………………………………………………...115

Figure 4.4. Cell viability of RAW 264.7 macrophage cells exposed to AgNPs. Data represents mean ± SD with n = 9. Bars marked with the letter a indicate significantly different (P < 0.001) compared to negative control, 0 μg/ml AgNPs………………116

Figure 4.5. Nitric oxide (NO) production by RAW 264.7 macrophage cells exposed to AgNPs. Data represents mean ± SD with n = 9. Bars marked with letters indicate significant difference (P < 0.01) to control. Significance demarcated by: a- significantly different (P < 0.001) compared to 0 μg/ml AgNPs, -LPS; b- significantly different (P < 0.001) compared to 0 μg/ml AgNPs, +LPS…………………………117

Figure 4.6. Interleukin 6 (IL-6) production by stimulated RAW 264.7 macrophage cells exposed to AgNPs. Data represents mean ± SD with n = 9. Unstimulated cultures did not synthesize IL-6 (data not presented). Bars marked with the letter a indicate significantly different (P < 0.001) compared to 0 μg/ml AgNPs………….118

Figure 4.7. The effect of AgNPs on RAW 264.7 cells. Cells were incubated with (a) medium only, (b) medium containing LPS or (c) 250 μg/ml AgNPs in the absence of

xli

xliii

xliv

xlvi

l

UNIVERSITY *of the*
WESTERN CAPE

List of Tables

0.001) compared to negative control, b- GONP at 15.6 µg/ml significantly different (P < 0.001) compared to the positive control……………………………………166

Table 5.2. Quantification of cytokines and chemokines secreted by WBCs not stimulated with LPS after treatment with medium only (negative control), medium containing LPS (positive control) or medium containing 5 µg/ml GONPs. Membranes were subjected to chromogenic exposure. Data is represented as mean ± SD. Significance indicated by a- GONP at 5 µg/ml significantly different (P < 0.001) compared to negative control, b- GONP at 5 µg/ml significantly different (P < 0.001) compared to the positive control…………………………………………………178

Table 6.1. Quantification of cytokines and chemokines secreted by RAW 264.7 cultures not stimulated with LPS after treatment with medium only (negative control), medium containing LPS (positive control) or medium containing 500 µg/ml CDs. Membranes were subjected to chromogenic exposure. Data is represented as mean ± SD. Significance indicated by a- CD at 500 µg/ml significantly different (P < 0.001) compared to negative control, b- CD at 500 µg/ml significantly different (P < 0.001) compared to the positive control…………………………………………………201

Table 6.2. Quantification of cytokines and chemokines secreted by WBCs not stimulated with LPS after treatment with medium only (negative control), medium containing LPS (positive control) or medium containing 500 µg/ml CDs. Membranes were subjected to chromogenic exposure. Data is represented as mean ± SD. Significance indicated by a- CDs at 500 µg/ml significantly different (P < 0.001)

Permissions List for the Use of Copyrighted Materials

Figure 4.19. Reprinted from Circulation, B. L. Hoh, K. Hosaka, D. P. Downes, K. W. Nowicki, C. E. Fernandez, C. D. Batich and E. W. Scott. Monocyte chemotactic protein-1 promotes inflammatory vascular repair of murine carotid aneurysms via a macrophage inflammatory protein-1α and macrophage inflammatory protein-2–dependent pathway. Page 2250, Copyright (2011), with permission from Wolters Kluwer Health, Inc.

<div align="center">**Chapter 1:**</div>

<div align="center">**Introduction, Thesis Structure and Objectives**</div>

1.1. Heavy metals in the environment

Heavy metals are prevalent in the environment due to both natural and anthropogenic activities. Humans can be exposed to this via different pathways (Khan et al., 2008). The rapid increase in the use of heavy metals and chemicals in process industries has resulted in the production of large quantities of effluent containing elevated levels of toxic heavy metals. The disposal of the metal containing effluents pose problems due to the non-degradable and persistent nature of heavy metals (Ahluwalia and Goyal, 2007). Heavy metals are known to be bioaccumulative and are biomagnified in biotic and abiotic systems (Florea and Busselberg, 2006). Sources of exposure may include mining, industries, wastewater, and agriculture (Khan et al., 2008, De Lurdes Dinis and Fiúza, 2011). Humans need certain heavy metals in trace amounts for optimum physiological functioning. Guidelines have been implemented to minimize human exposure to heavy metals via the various routes, as most heavy metals are toxic or carcinogenic to humans, even at low concentrations. Heavy metals are known to affect several physiological systems such as the central nervous function, lungs, kidneys, liver and blood composition (De Lurdes Dinis and Fiúza, 2011). However, the permissible levels of heavy metals may vary from country to country, with some countries having more stringent guidelines.

1

The levels of heavy metals permitted in drinking water are relatively similar for South Africa and international standards like the United States Environmental Protection Agency (US EPA), World Health Organisation (WHO) and European Union (EU) (Table 1.1). This is important as South Africa is a water scarce country, where only 65 % of the country experiences an average annual rainfall of ≥ 500 mm (Rodda et al., 2011). Therefore, the limited water supply needs to be of great quality and must be kept as pristine as possible.

Table 1.1. Maximal levels of heavy metal permitted in drinking water (μg/l) according to international and national standards.

Heavy Metal	WHO	US EPA	EU	South African DWAF
Aluminum	-	-	-	150
Arsenic	10	10	50	10
Cadmium	3	5	5	5
Chromium	50	100	-	50
Copper	2000	1300	50	1000
Iron	-	300	-	100
Lead	10	15	50	10
Magnesium	-	-	-	30000
Manganese	-	50	50	50
Nickel	70	-	-	-
Potassium	-	-	-	50000
Silver	-	100	-	-
Sodium	-	-		100000
Zinc	-	500	3000	3000
Reference	WHO (2006)	Araujo et al. (2013), Fernández-Luqueño et al. (2013)	O'Connor (2004)	DWAF (1996)

The levels of heavy metals in soil for agriculture (Table 1.2) also need to be monitored, as this is required for exporting agricultural crops to some countries. Export of these agricultural products is a major source of revenue for South Africa. Crops containing high amounts of heavy metals, may pose a health risk to consumers. The maximum allowed levels vary significantly across governing bodies, with the food and agricultural organization (FAO) of the United Nations (UN) seemingly having more stringent restrictions on the amount of certain heavy metals permitted in the soil. However, the South African Department of Environmental Affairs (DEA) has higher maximum allowed levels for certain heavy metals, such as, chromium (46 000 μg/g) and nickel (91 μg/g) permitted in soil compared to other international guidelines. Copper (16 μg/g) and lead (20 μg/g) levels in South Africa were noted to be lower than international standards.

The concentration of heavy metals in soils is also dependent on the season, as these concentrations are found to be higher in dry seasons compared to wet seasons (Oluyemi et al., 2008, Malan et al., 2015). These variations could be attributed to the types of soil found in the respective regions and the season in which the heavy metal concentrations were analysed. Malan et al. (2015) stated that the pH of the soil also plays a vital role in the bioavailability of heavy metals to plants as an alkaline soil results in the decrease of the bioavailability of the heavy metals in the soil as they are more tightly bound to the soil. This could result in the accumulation of the heavy metals in the soil and if the pH of the soil should become acidic, the heavy metals become more bioavailable for uptake by the plants and in turn human consumption.

3

Table 1.2. Maximum allowed levels of heavy metals in soil (μg/g) according to international and South African standards

Heavy Metal	FAO of the UN	US EPA	South African DEA
Arsenic	29	75	58
Cadmium	0.8	85	7.5
Chromium	100	3000	46000[*]
Copper	36	4300	16[*]
Iron	-	-	-
Lead	85	420	20[*]
Magnesium	-	-	-
Manganese	-	-	740
Nickel	35	75	91[*]
Potassium	-	-	-
Silver	-	-	-
Sodium	-	-	-
Zinc	140	7500	240
Reference	Van Lynden et al. (2004), Chiroma et al. (2014)	USEPA (2000)	DEA (2012)

[*]DEA maximum allowed heavy metal levels higher than both the FAO and US EPA maximal allowed limits for soil (μg/g).

Rivers across South Africa have been analysed (Table 1.3) in order to ascertain the levels of heavy metals in them as rivers are used as a source of drinking water in certain parts of the country. Heavy metal levels vary greatly from river to river with majority of the rivers having extremely high levels of the metals and several are exceeding the maximal allowable amount as stipulated by the South African Department of Water and Forestry (DWAF), along with other international standards. The extremely high levels of heavy metals, bar the Thohoyandou River, Limpopo could be due to effluents from mining and industrial operations and also the season in

4

which the water was analyzed. The heavy metal levels detected in these rivers may pose a risk to human health due to compromised water quality.

Table 1.3. A non-exhaustive summary of levels of heavy metals (Mean ± SD) found in river water across South Africa (μg/l)

Heavy Metals	South African DWAF	Diep River, Western Cape	Thohoyandou River, Limpopo	Swartkops River, Eastern Cape	Philippi Horticulture Area, Western Cape
Aluminum	150	4000 ± 900[*]	-	-	-
Cadmium	5	-	3.3 ± 0.2	-	9 ± 2[*]
Chromium	50	-	-	20300 ± 12350[*]	60 ± 9[*]
Copper	1000	500 ± 100	2.6 ± 1.2	6800 ± 4830[*]	10 ± 2
Iron	100	72000 ± 12700[*]	-	-	-
Lead	10	-	12.3 ± 2.3[*]	33000 ± 27640[*]	50 ± 8[*]
Manganese	50	0 ± 0	-	115000 ± 94250[*]	20 ± 4
Nickel	-	100 ± 100	-	-	20 ± 2
Zinc	3000	1800 ± 100	2.1 ± 3.8	36000 ± 26630[*]	50 ± 2
Reference	DWAF (1996)	Jackson et al. (2009)	Okonkwo and Mothiba (2005)	Binning and Baird (2001)	Malan et al. (2015)

[*]Levels of heavy metals higher than the South African DWAF maximal allowed limits in water (μg/l).

UNIVERSITY of the

WESTERN CAPE

1.2. *In vivo* methods to monitor potential toxicity of heavy metals in the aquatic environment

Commonly used methods of biological monitoring looks at changes in various parameters within an ecosystem. These parameters include: community structure, genetic integrity and morphological, physiological and biochemical characteristics at individual or population levels (Figure 1.1) (Ravera, 2001). Heavy metals are known to affect all of the above, which can be attributed to their bioaccumulative, and biomagnified nature. This can result in morphological and physiological changes. These changes will eventually affect populations and subsequently whole ecosystems.
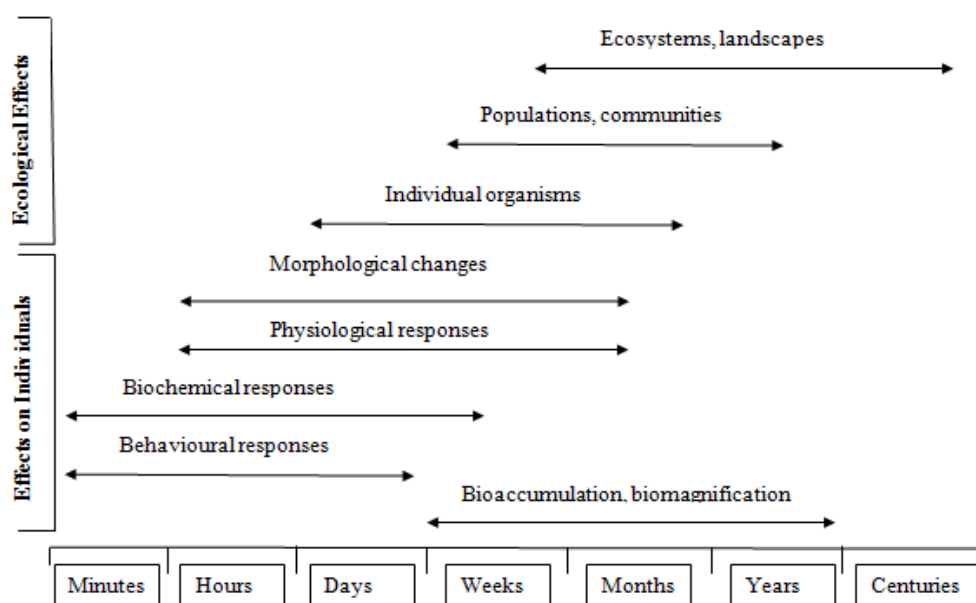
Figure 1.1. The duration of biological effects by heavy metals (Adapted from Chapman et al. (1996)).

Heavy metal toxicity in the aquatic environment has been studied extensively (Jezierska and Witeska, 2001, Pinto et al., 2003, Clemens, 2006, Horvat et al., 2007, Mishra and Tripathi, 2008), with multiple models used in order to assess the effects of heavy metals in the environment. *In vivo* models for monitoring include the effects of metals on aquatic plants, invertebrates and vertebrates.

Some South African *in vivo* studies include the vertebrate, *Oreochromis mossambicus* exposed to sub-lethal manganese concentrations which resulted in the decrease in haematological and osmoregulation (Barnhoorn and Van Vuuren, 2001). An invertebrate study by Reinecke et al. (1999) found that *Eisenia fetida* (Oligochaeta), exposed to sub-lethal doses of cadmium over a period of time (more than 10 generations), developed resistance to the heavy metal compared to those that were unexposed and noted that they had a gross increase in body fluids. *Physa acuta,* another invertebrate, were also exposed to sub-lethal levels of engineered nanoparticles and it was noted that this resulted in a reduction in embryo growth rate and hatchability, along with developmental deformities (Musee et al., 2010).

There are also *in vitro* models where well established fish and other cell lines and primary cell cultures are used to monitor the effects of the heavy metals. All these models allow researchers to assess the overall effect of the heavy metals as it moves up higher trophic levels and food chains.

1.2.1. Aquatic algae

A variety of algal species are found in fresh and marine aquatic habitats. These species are vital for oxygen production, nutrient cycling, controlling water quality, sediment stabilization and providing habitat and shelter for other aquatic species (Lewis, 1995). Heavy metal exposure may cause a disturbance of normal metabolism and biological function, inhibition of photosynthesis, reduction of cytochrome P450, and an increase in cell mutations and death (Zhou et al., 2008).

Studies have investigated the effects of heavy metals on aquatic plants (Campanella et al., 2001, Koukal et al., 2003, Miretzky et al., 2004, Gubbins et al., 2011, Piotrowska-Niczyporuk et al., 2012) (Table 1.4). These studies indicated that heavy metals reduce algae growth, photosynthetic activity and metabolite accumulation, regardless of the aquatic algae species. This indicates that aquatic plants species have similar reactions when exposed to heavy metals. Certain algal species may be more sensitive to metal exposure compared to others. This was evident in a study conducted by Miretzky et al. (2004), where *Lemna minor* did not survive their experimental conditions, compared to the other algal species, *Pista stratiotes* and *Spirodela intermedia.*

Table 1.4. A non-exhaustive summary of the toxic effects of heavy metals and nanoparticles on aquatic plants

Test species	Metal	Metal Concentration	Major Findings	Reference
Spirulina subsalsa	Mercury Copper	1, 2.5, 5 mg/l	Dose dependent inhibition of photosynthetic activity	Campanella et al. (2001)
Pista stratiotes, Spirodela intermedia, Lemna minor	Iron Copper Zinc Manganese Chromium Lead	1 mg/l	*L. minor* did not survive conditions. Rate of metal uptake was dependent on metal concentration for 3 species studied.	Miretzky et al. (2004)
Chlorella vulgaris	Cadmium Lead Copper	100 μM	Metals inhibited algal growth, metabolite accumulation, enzymatic and non-enzymatic antioxidant systems.	Piotrowska-Niczyporuk et al. (2012)
Pseudokirchneriella subcapita	Cadmium Zinc	97, 195, 292, 389, 486 μg Cd/l 152, 305, 610, 764, 910 μg Zn/l	Photosynthetic activity decreased in a dose dependent manner	Koukal et al. (2003)
Lemnar minor	Silver nanoparticles (20 and 100 nm)	5, 10, 20, 40 μg/l	Inhibition of growth at 5 μg/l	Gubbins et al. (2011)

1.2.2. Aquatic invertebrates

Trace metals accumulate in tissues of all aquatic invertebrates, whether the metals are essential for metabolism or not. However, different invertebrates accumulate trace metals at different concentrations in their tissues, organs and bodies (Rainbow, 2002). Crustaceans are represented by daphniidae for biomonitoring of aquatic metal exposure, with responses that include growth, fertilization, behaviour, morphologic characters and biological alterations (Zhou et al., 2008). Daphnids are used internationally by the US EPA, Organisation for Economic Co-operation and Development (OECD) and International Organisation for Standardisation (ISO) to monitor water quality and lethality of a pollutant. Other invertebrates used to monitor heavy metals in aquatic ecosystems such as sediments include: aquatic insects, molluscs and worms.

A range of aquatic invertebrates exposed to heavy metals and nanoparticles have been investigated (Figure 1.5). The water-flea, *Daphnia magna,* the most common aquatic invertebrate, exhibited toxicity when exposed to heavy metals and nanoparticles (Münzinger, 1990, Lan and Lin, 2005, Zhu et al., 2010, Asghari et al., 2012). Due to the small size of the nanoparticles, 21 and 15.83 nm, used by Zhu et al. (2010) and Asghari et al. (2012) respectively, allowed for easier translocation and ingestion, thus resulting in the toxic effects of the nanoparticles on the Daphnia as smaller nanoparticles are known to be more toxic. The mussel, *Mytilus galloprovincialis,* showed accumulation of heavy metals which affected morphology (Domouhtsidou and Dimitriadis, 2000), with the loss of body weight observed in the aquatic insect, *Hydropsyche betteni* (Balch et al., 2000).

Exposing invertebrates to heavy metals allowed for various biomarkers to be monitored. Radwan et al. (2010) assessed the effects of heavy metal exposure on catalase (CAT) activity, lipid peroxidation (LPO), glutathione peroxidase (GPx), glutathione-S-transferase (GST), and glutathione (GSH) as biomarkers indicative of cellular stress. These biomarkers are indicative of reactive oxygen species (ROS) mechanisms which drives the cellular stress response.

South African studies have been conducted on a number of aquatic invertebrates, which include monitoring metal exposure on different crab species, earthworms and snails. These studies have found that *Potamonautes warreni* exposed to sub-lethal concentrations of copper showed that oxygen consumption and glyconeogenesis significantly increased after a 21 day exposure period (Vosloo et al., 2002). *Potamonautes perlatus,* the freshwater crab, contained the highest accumulated concentration of lead and cadmium in the gonads and carapace, with the digestive glands having the lowest concentration of the metals after a two year exposure period (Reinecke et al., 2003). The African earthworm, *Eudrilus eugeniae* (Oligochaeta) was more susceptible to the effects of copper than zinc. However, both metals affected growth and maturation, with the metals being absorbed via the body wall of the earthworm after a 73 day exposure period (Reinecke et al., 1997). All the mentioned studies indicated that heavy metals had negative effects regardless of the test species monitored.

Table 1.5. A non-exhaustive summary of the toxic effects of heavy metals and nanoparticles on aquatic invertebrates

Test Species	Metal	Metal Concentration	Major Findings	Reference
Daphnia magna	Thallium	24-203 µg/l	Extremely toxic to daphnids.	Lan and Lin (2005)
Daphnia magna	Nickel	40-160 ppb	Toxicity to daphnids.	Münzinger (1990)
Daphnia magna	Titanium oxide nanoparticles (21nm)	0-100 mg/l	High toxicity at 72hrs. Growth impairment, mortality, and reproductive defects at 21 days.	Zhu et al. (2010)
Daphnia magna	Silver nitrate Silver nanoparticles (15.83 nm)	0.001-0.32 mg/l	AgNPs accumulate under carapace. All silver species caused abnormal swimming.	Asghari et al. (2012)
Mytilus galloprovincialis	Mercury Silver Lead Copper	0.1 mg/l	Black silver deposits on gills. Morphology of digestive cells affected.	Domouhtsidou and Dimitriadis (2000)
Theba pisana	Copper Lead Zinc	0.5-5 mg/ml 50-200 mg/ml 5-20 mg/ml	Increase in LPO and CAT activity, GPx, and GST. Decrease in GSH.	Radwan et al. (2010)
Hydropsyche betteni	Zinc	7.6-30.2 mg/ml	Significant loss in live-body weight.	Balch et al. (2000)
Mytilus edulis	Carbon dots	1, 5, 10 µg/ml	Nitric oxide release, decrease in mitochondrial weight	Canesi et al. (2008)

1.2.3. Aquatic Vertebrates (Fish)

Fish has attracted a lot of attention with regards to the biomonitoring of water pollution as it has unique biological characteristics, such as; its body size, long life cycle, simple to raise and they are at the top of the aquatic food chain and may directly impact human health due to consumption (Zhou et al., 2008). Metals tend to distribute differentially in the liver and muscle, which could be attributed to the metal-binding proteins like metallothioneins in certain organs of the fish (Ploetz et al., 2007).

Exposing fish to various heavy metals allows various parameters to be monitored (Table 1.6). Accumulation of the heavy metals occur in the kidneys, liver, flesh tissue and gills of the fish (Paris-Palacios et al., 2000, Vinodhini and Narayanan, 2008). Examining the effects of the heavy metals at a cellular level indicated cellular and deoxyribonucleic acid (DNA) damage (Cavas et al., 2005, Chae et al., 2009).

Similar to the aquatic invertebrates, biomarkers may also be monitored to indicate cellular stress as was performed by Paris-Palacios et al. (2000) and Talas et al. (2008). These studies monitored superoxide dismutase (SOD), GSH, LPO, GPx, and CAT and these levels gave indications on the mechanism whereby the metals would impact the fish. Fish models allow researchers to monitor macro- and microscopic effects of heavy metals. Fish molecular biomarkers are also available that can provide a holistic picture of the effects of the metals on the organism.

Table 1.6. A non-exhaustive summary of the toxic effects of heavy metals and nanoparticles on aquatic vertebrates (fish)

Test Species	Metal	Metal Concentration	Major Findings	Reference
Cyprinus carpio	Chromium Nickel Cadmium Lead	5 ppm	Accumulation of metals in the kidneys, liver, flesh tissue and gills.	Vinodhini and Narayanan (2008)
Oncorhynchus mykiss	Cadmium Chromium	2 ppm	Significant decrease in CAT activity, GPx, and SOD. Increase in LPO.	Talas et al. (2008)
Cyprinus carpio *Carassius gibelio* *Corydoras paleatus*	Cadmium Copper	0.005-0.1 mg/l 0.01-0.25 mg/l	Micronucleated and binucleated cells increased. Increased micronuclei and binuclei in gill and liver cells. Cytotoxic and genotoxic effects.	Cavas et al. (2005)
Brachydanio rerio	Copper	40 and 140 μg/l	Accumulation, lysing of parenchyma near hepatic veins and toxicity. Increase in GSH, as well as CAT and GST activity.	Paris-Palacios et al. (2000)
Oryzias latipes	Silver nanoparticles (49.6 nm)	1 and 25 μg/l	Cellular, DNA damage, carcinogenic and oxidative stress.	Chae et al. (2009)
Danio rerio	Graphene oxide	1, 5, 10, 50 mg/l	Oxidative stress and immunotoxicity	Chen et al. (2016a)

15

1.3. *In vitro* **methods to monitor potential toxicity of heavy metals in the aquatic environment**

Due to the economic and ethical constraints associated with *in vivo* tests, *in vitro* bioassays, like cell cultures derived from aquatic animal species, are preferred to monitor heavy metal toxicity in aquatic environments. Performing *in vitro* experiments in established fish cell lines is favoured as experiments are relatively rapid, cost-effective, and reproducible (Tan et al., 2008). Cell lines allow for a number of parameters to be monitored like viability, metabolism and proliferation.

Multiple fish derived cell lines and primary cultures have been used to assess heavy metal toxicity in the aquatic environment (Table 1.7). The *in vitro* cultures mainly monitored cell viability and the phagocytic capabilities of the cells exposed to the various heavy metals and nanoparticles. All the heavy metals and nanoparticles were cytotoxic to all the cell lines monitored (Sauvé et al., 2002, Tan et al., 2008, Goswami et al., 2014, Connolly et al., 2015). However, conflicting results regarding phagocytic activity of the cell lines exposed to cadmium was reported. Olabarri et al. (2001) reported an increase in phagocytic activity while Sauve et al. (2002) had an inhibition of phagocytic activity. This discrepancy could be due to the concentration range used and the source of the haemocytes (test species). Heavy metals and nanoparticles are cytotoxic, and inhibit other cellular functions.

Table 1.7. A non-exhaustive summary of the toxic effects of heavy metals and nanoparticles in the aquatic environment using *in vitro* methods

Test Species	Cell Type	Metal	Metal Concentration	Major Findings	Reference
Marine species: *Cyrtodaria siliqua, Mactromeris polynyma, Mesosdesma arctatum, Mya sp.*	Haemocytes	Silver, Cadmium, Mercury, Zinc	0.001-1000 μM	Dose dependent inhibition of haemocyte phagocytosis	Sauvé et al. (2002)
Freshwater species: *Dreissena polymorpha* and *Elliptio complanata*	Haemocytes	Silver, Cadmium, Mercury, Zinc	0.001-1000 μM	Dose dependent inhibition of haemocyte phagocytosis	Sauvé et al. (2002)
Labeo rohita	Fin Tissue	Zinc Cadmium	1.563-25 mg/l	Cytotoxicity of cells	Goswami et al. (2014)
Ctenopharyngodon idellus	Fin, Kidney	Cadmium Chromium Zinc Copper	1-100 μM 1-100 μM 10-600 μM 10-600 μM	Cytotoxic	Tan et al. (2008)
Ictalurus punctatus	Ovary	Cadmium Chromium Zinc Copper	1-100 μM 1-100 μM 10-600 μM 10-600 μM	Exhibited cytotoxicity	Tan et al. (2008)
Ameiurus nebulosus	Caudal trunk	Cadmium	1-100 μM	Cytotoxicity	Tan et al. (2008)

Table 1.7. A non-exhaustive summary of the toxic effects of heavy metals and nanoparticles in the aquatic environment using *in vitro*
methods

Test Species	Cell Type	Metal	Metal Concentration	Major Findings	Reference
Ameiurus nebulosus	Caudal trunk	Chromium Zinc Copper	1- 100 μM 10-600 μM 10-600 μM	Cytotoxicity	Tan et al. (2008)
Pimephales promelas	Muscle	Cadmium Chromium Zinc Copper	1-100 μM 1-100 μM 10-600 μM 10-600 μM	Cytotoxic	Tan et al. (2008)
Mytilus galloprovincialis	Haemocytes	Cadmium	10-2000 μM	Dose dependent increase phagocytic ability and acid phosphatase activity	Olabarrieta et al. (2001)
Oncorhynchus mykiss	Liver, Hepatoma, Fibroblast-like gonadal, Primary Hepatocytes	Silver Nanoparticles (7.5 and 65 nm) Silver	0-93.5 μg/ml 0-345 μg/ml	Toxicity of silver and nanoparticles	Connolly et al. (2015)

1.4. South African Legislature on *in vivo* Experiments

South Africa has strong legislation regarding *in vivo* experiments and experiments are expected to bide by the "Three R" principle for humane animal research. These principles include: the replacement of animals wherever possible, reduction of the number of animals in experiments that allow for smaller sample size that will allow for valid information, and refinement of animal sourcing to eliminate physical and psychological distress of the animal within experiments. These principles are implemented in order to comply with The South African National Standard for the Care and Use of Animals for Scientific Purpose (SANS 10386:2008) (Mohr, 2013). Therefore, South Africa is attempting to steer away from *in vivo* experiments as far as possible as investigators first need to understand what happens on a cellular level.
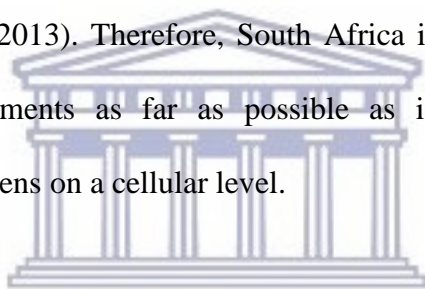
1.5. Methods in *in vitro* toxicology using mammalian cell lines

An in-depth review conducted by Eisenbrand et al. (2002) outlines the various parameters monitored in *in vitro* toxicity assays. These include cytotoxicity, which are the most prominent parameter monitored, cellular and functional responses, metabolism, inflammatory responses and biomarkers of exposure to a toxicant. Most studies mainly monitor the potential of a compound to induce cell death and DNA damage, along with ROS production (Reardon and Lucas, 1987, Rossi et al., 1996, Steiner et al., 1998, Kawata et al., 2009, Aziz et al., 2014) (Table 1.8). In order to combat the production of ROS from heavy metals, the major mechanism employed is the metabolism of GSH to protect cells from toxicants (Eisenbrand et al., 2002, Aziz et al., 2014). Reactive oxygen species

19

describes a variety of molecules and free radicals derived from molecular oxygen for either physiological concentrations needed for normal cellular function or excess amounts which leads to oxidative stress (Nordberg and Arner, 2001, Liebsch and Spielmann, 2002, Turrens, 2003). Oxidative stress, if not counter reacted will result in excessive membrane permeability, LPO, DNA damage and protein inactivation.

Table 1.8. A non-exhaustive summary of the toxic effects of heavy metals and nanoparticles using mammalian cell lines

Cell Type	Cell Type Representing	Metal	Metal Concentration	Major Findings	Reference
Human Caco-2	Intestinal tract	Zinc Copper Cadmium	0-2000 μM 0-1200 μM 0-125 μM	Toxicity to cells.	Rossi et al. (1996)
Mouse B- and T-lymphocytes	Humoral and cell mediated immunity	Zinc, Mercury	10-100 μM	Cellular toxicity.	Reardon and Lucas (1987)
Human HepG2	Liver hepatocytes	Silver Nanoparticles	0-1 mg/l	Toxicity at high doses and cell proliferation at <0.5 mg/ml.	Kawata et al. (2009)
Human HepG2	Liver hepatocytes	Cadmium, Silver, Copper, Manganese, Lead, Tin, Nickel, Zinc, Mercury, Aluminium	0.1-100 μM	Decrease in cell viability and hsp70 synthesis.	Steiner et al. (1998)
Human Caco-2 HL-7702	Intestinal tract Liver hepatocytes	Cadmium	0.25-10 mg/ml	Cytotoxicity and dose dependent decrease in SOD and GPx.	Aziz et al. (2014)
Human U87	Brain cells	Graphene oxide	0 – 100 μg/ml	Cytotoxicity	Jaworski et al. (2015)

A limited amount of research has been conducted on the *in vitro* effects of heavy metal exposure on mammalian cells. Most studies focused on functions, such as ROS production. However, there is a lack of data in the literature on heavy metal effects on the cellular processes such as inflammation, metabolic processes, and the proteome in general. This is a major shortfall in the *in vitro* toxicology stream. This will allow researchers to understand the mechanisms of how heavy metals impact an individual.

1.6. Silver nanoparticles (AgNPs)

The investigation into the effects of silver (Ag) and silver nanoparticles (AgNPs) have increased considerably as there have been dramatic increases in commercial products which contain AgNPs. In 2014 alone 420 tons of AgNPs were produced and this amount is expected to rise in the future. Products containing AgNPs range from health and fitness, cleaning products, and food (Pulit-Prociak and Banach, 2016) (Figure 1.2). However, relatively little is known about the potential adverse effects of AgNPs. Silver has known antimicrobial properties; hence AgNPs has been introduced into commercial products due to its superior antimicrobial properties in comparison to silver micro- and macro-particles. Nanoparticles, in general have superior reactivity characteristics, mainly due to their higher surface to volume ratio (Chen and Schluesener, 2008, Stone et al., 2010, Fabrega et al., 2011, Liu et al., 2011, Martínez-Gutierrez et al., 2012). This factor has also been speculated to result in higher toxicity of these smaller particles when compared to the bulk reagents.
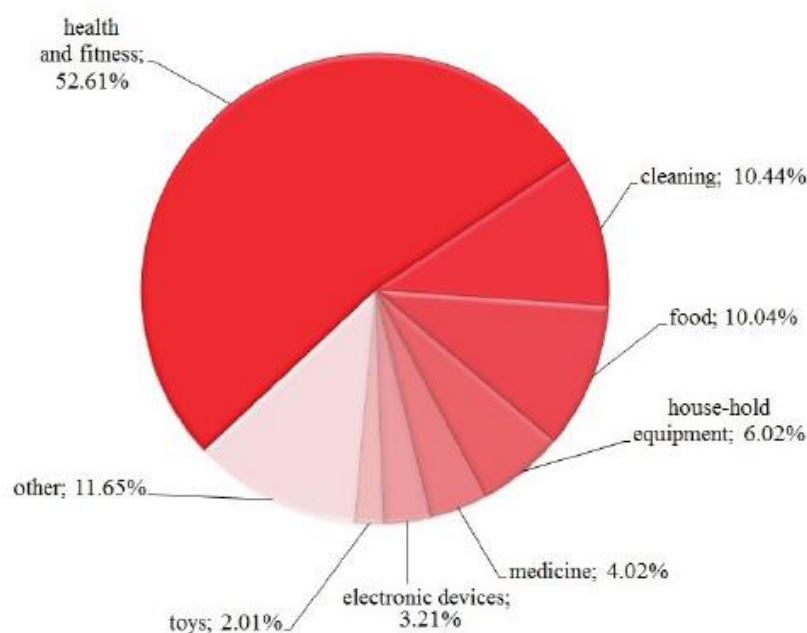
Figure 1.2. Groups of products containing silver nanoparticles (Pulit-Prociak and Banach, 2016).

1.6.1. Toxicity of AgNPs

Storage of AgNPs, if not stable, results in the aggregation of the AgNPs. Aggregation results in the change of their unique characteristics and nanoscale properties as the surface area is reduced (Kaur and Tikoo, 2013). Aggregation is caused when there is a reduction in stability (Liu et al., 2011). It changes particle properties and particle transport which alters bioavailability and cellular toxicity (Figure 1.3). The oxidation of the AgNPs causes the release of Ag ions (Zhang et al., 2011). Ahamed et. al (2010) proposed that AgNPs induce cytotoxicity via the generation of ROS, which results in lipid and DNA damage and ultimately apoptosis. An increase in ROS consequently causes the inhibition of mitochondrial function and membrane lipid peroxidation which ultimately results in apoptosis.

23
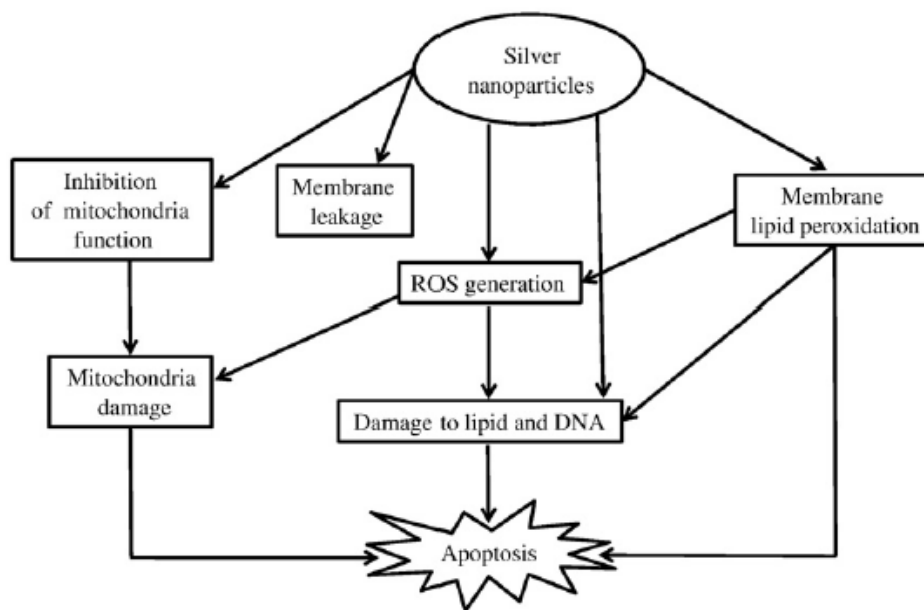
Figure 1.3. Possible mechanism for silver nanoparticle induced toxicity (Ahamed et al., 2010).

Studies show that prolonged exposure to AgNPs and Ag cause bio-accumulation and this results in damage to the lungs, liver and kidney. Prolonged exposure can also result in adverse effects like a permanent bluish-grey discolouration of the skin and eyes (argyria/ argyrosis) (Panyala et al., 2008).

Since AgNPs are so regularly found in consumer products, it may leach out during washing and may be a potential risk to human health and environmental biota (Liu et al., 2011, Singh and Ramarao, 2012). The leaching of silver ions can disrupt the helpful bacteria in wastewater treatment plants and endangers aquatic species (Kaur and Tikoo, 2013). Dissolved Ag ions in the environment have adverse effects on prokaryotes, many marine- and freshwater invertebrates and fish (Fabrega et al., 2011). Silver nanoparticles are classified as an ecotoxicological hazard as it undergoes biodegradation, persists and bioaccumulates in the food

24

chain, and many studies have been done to document the toxic effects AgNPs have on fish (Bystrzejewska-Piotrowska et al., 2009, Fabrega et al., 2011).

Studies also suggest that Ag and AgNPs can negatively affect the immune system (Fabrega et al., 2011). There are relatively few studies looking at the immunotoxicity of nanoparticles on mammalian cell lines, let alone AgNPs. A ScienceDirect search of published peer reviewed articles per year when either entering the search term 'mammalian cells, nanoparticles, immunotoxicity' or 'mammalian cells, silver nanoparticles, immunotoxicity' indicated that not many articles have been published regarding those search terms but show a steady increase across 2008-2017 (Figure 1.4).
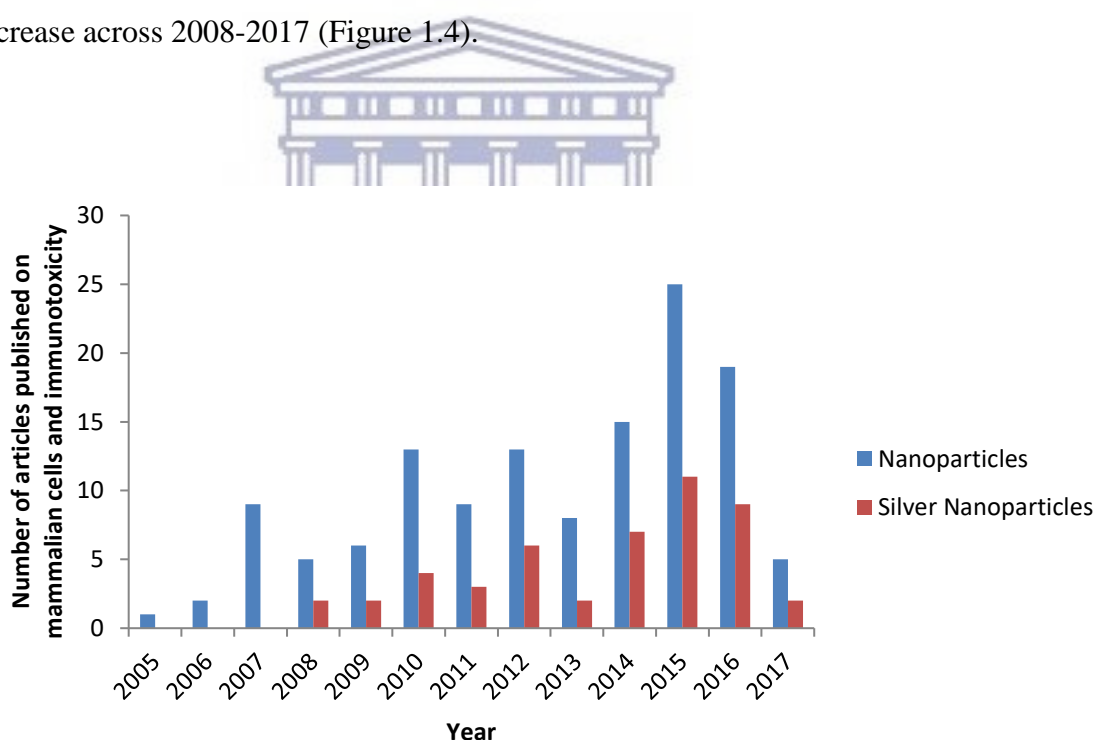
Figure 1.4. Graphical representation of a ScienceDirect search of the amount of peer reviewed articles published per year by either using the search term 'mammalian cells, nanoparticles, immunotoxicity' or 'mammalian cells, silver nanoparticles, immunotoxicity' as of 25 January 2017.

25

Silver nanoparticles induce cytotoxicty and elicited inflammatory responses from various mammalian immune cell lines (Table 1.9). The smaller the diameter of the nanoparticle, the greater toxicity and inflammatory response evoked from the cells, regardless of the concentration ranges that were investigated in the various studies (Shin et al., 2007, Park et al., 2011, Martínez-Gutierrez et al., 2012, Yang et al., 2012). Although the above studies exhibited certain immune responses, the exact mechanism is not yet apparent as it could be due to biological variability and dependent on the composition of the nanoparticle, cell type, cell cycle, and animal model (Elsabahy and Wooley, 2013).

Table 1.9. A non-exhaustive summary of immunotoxic effects of silver nanoparticles on mammalian cell lines.

Cell Line	Silver Nanoparticle Concentration	Size	Major Findings	Reference
Human THP-1 monocytes	0.5-100 µg/ml	24 nm	Cytotoxic to cell and elicited an inflammatory response.	Martínez-Gutierrez et al. (2012)
Peripheral blood mononuclear cells (PMBCs) from humans	0, 1, 5, 10, 15, 20 and 30 µg/ml	1.5 nm	Cytotoxic at high concentrations and affected the modulation of cytokine production in a concentration dependent manner.	Shin et al. (2007)
Primary human monocytes (PMBCs)	0-6.25 µg/ml	5 nm 28 nm	Cytokine IL-1β (innate immunity) and cytotoxicity was monitored after AgNP exposure. The IL-1β synthesis increased as AgNP cell size decreased.	Yang et al. (2012)
Murine cells: Peritoneal macrophage cell line RAW 264.7 and Mouse fibroblasts L929	0-0.3 µg/ml	20 nm 80 nm 113 nm	L929 and RAW 264.7 metabolic activity decreased concentration dependently. The AgNPs caused the release of inflammation markers from the cells.	Park et al. (2011)

1.7. Carbon based nanoparticles

1.7.1. Graphene oxide nanoparticles (GONPs)

Graphene (G) is a two-dimensional (2-D) carbon material, with a hexagonal structure (honeycomb lattice) consisting of sp^2 hybridized atoms, which has been isolated from its three dimensional parent material, graphite (Chen et al., 2016a, Chen et al., 2016b, Liu et al., 2016). Graphene oxide (GO) is a single carbon layer graphene derivative, containing oxygen-bearing functional groups such as carboxyl and hydroxyl groups (Chen et al., 2016b, Lu et al., 2017, Sotirelis and Chrysikopoulos, 2017). These groups are acquired when graphene undergoes oxidization (Chen et al., 2016b) (Figure 1.5). These oxidized graphene nanoparticles possess unique characteristics such as electronic and thermal conductivity, superior mechanical strength and optical properties (Cherian et al., 2014). Due to these exceptional physiochemical properties of graphene oxide nanoparticles (GONPs), it has a broad range of applications in a number of fields. These fields include electrochemistry, biomedicine, biosensing, drug delivery, high energy capacity batteries and super capacitors to name a few (Chen et al., 2016b, Sotirelis and Chrysikopoulos, 2017).
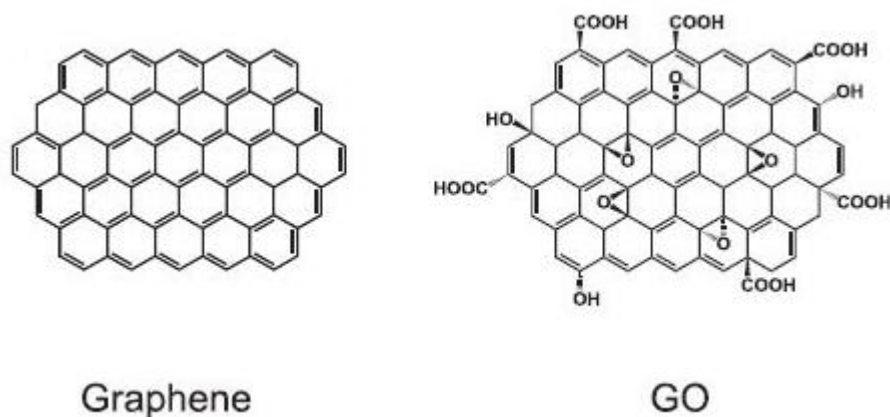
Figure 1.5. Structure of graphene and graphene oxide (Zhang et al., 2016)

1.7.2. Toxicity of GONPs

Studies have mostly focused on the uptake and bioimaging of cells using GONPs (Sun et al., 2008, Wang et al., 2010, Chen et al., 2011). This is evident as only a limited amount of studies have focused on the effects of GONPs on the immune system (Figure 1.6). Studies focusing on *in vitro* exposure to GONPs, have found that GONPs decreases cell viability, induces DNA damage, increased ROS production (Lu et al., 2017, Peruzynska et al., 2017). Only two studies have focused on mammalian cells and immunotoxicty, which showed that GONPS induce inflammatory factors (Zhi et al., 2013, Yan et al., 2017) (Table 1.10).

29
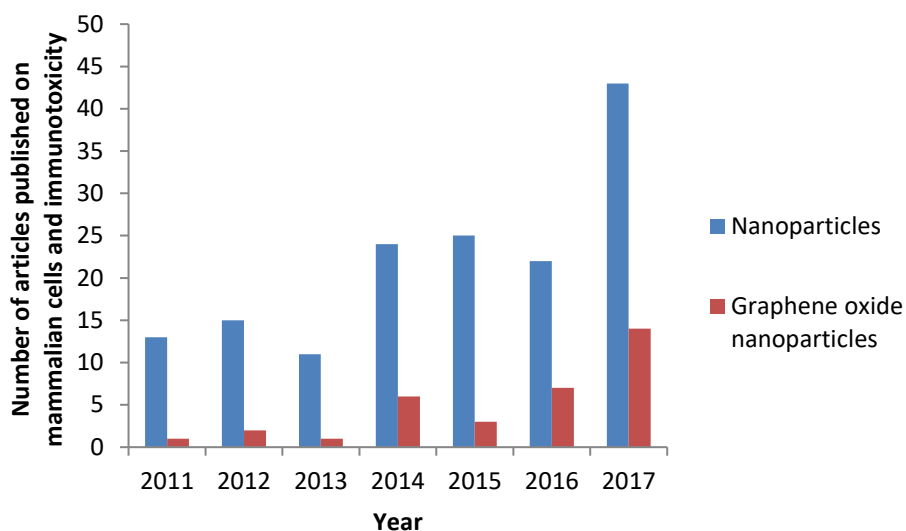
Figure 1.6. Graphical representation of a ScienceDirect search of the amount of peer reviewed articles published per year by either using the search term 'mammalian cells, nanoparticles, immunotoxicity' or 'mammalian cells, graphene oxide nanoparticles, immunotoxicity' as of 27 October 2017.

Table 1.10. A non-exhaustative summary of immunotoxic effects of graphene oxide nanoparticles on mammalian cell lines.

Cell Line	GONP Concentration	Major Findings	Reference
Human: Dendritic cells T-lymphocytes Macrophages	0, 25, 50, 100 µg/ml	Immunotoxicity	Zhi et al. (2013)
THP-1	0 – 50 µg/ml	Immunotoxicity	Yan et al. (2017)

1.7.3. Carbon Dots (CDs)

CDs, also known as carbon quantum dots or carbon nanoparticles are a relatively new fluorescent quasi spherical, zero dimensional nanomaterial with a diameter less than 10 nm (Bayati et al., 2017, Sun and Lei, 2017, Tuerhong et al., 2017). Recently, there has been an increase in CD popularity as they possess unique optical properties, biocompatibility, low toxicity, facile synthesis and aqueous stability (Peng et al., 2017, Sun and Lei, 2017, Tao et al., 2017). These unique properties have allowed CDs to be used in bioapplications, such as bioimaging, drug delivery and theranostic developments (Peng et al., 2017).

1.7.4. Toxicity of CDs

Very few studies have evaluated the potential effects of CDs on cells and the immune system (Figure 1.7). *In vivo* and *in vitro* studies have mainly focused on sensing and bioimaging of cells via the photoluminescent properties of CDs (Pierrat et al., 2015, Kudr et al., 2017, Pandey et al., 2017, Wang et al., 2017). Only a few studies have reported on the toxicity of CDs, and agree with the reports of their low toxicity. However, the toxicity is dependent on the functionalization of the CDs (Havrdova et al., 2016, Yuan et al., 2017). To date, no studies have reported on the effects of CDs on the immune system utilizing the experimental conditions in this study. However, a number of studies have been conducted on the effects of other carbon based nanoparticles, such as carbon black nanoparticles, single-walled carbon nanotubes (SWNTs) and double-walled carbon nanotubes (DWNTs) on the immune system of aquatic wildlife (Canesi et al., 2008, Mouchet et al., 2008, Liu et al., 2009). These

31

studies show that the various carbon based nanoparticles exhibited cytoxic, genotoxic and immunotoxic effects on the larvae of *Xenopus laevis, Drosophilia* and blue mussel hemocytes.
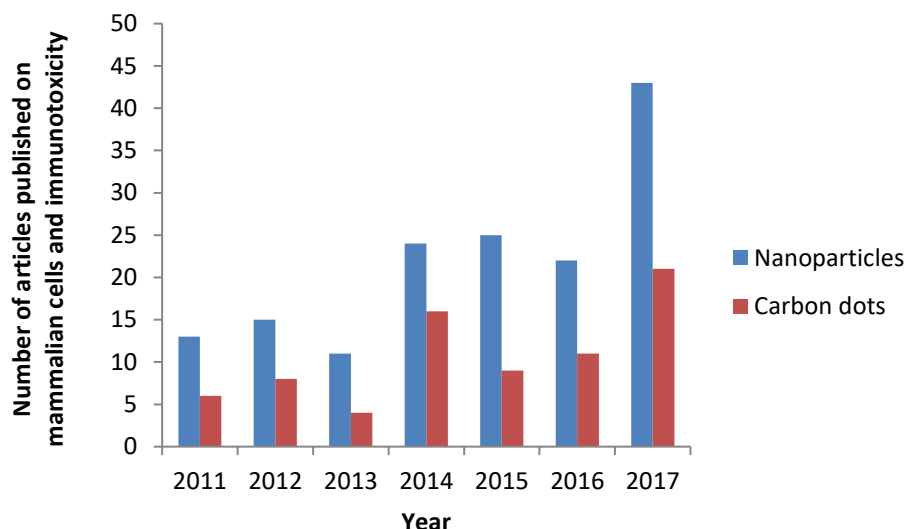
Figure 1.7. Graphical representation of a ScienceDirect search of the amount of peer reviewed articles published per year by either using the search term 'mammalian cells, nanoparticles, immunotoxicity' or 'mammalian cells, carbon dots, immunotoxicity' as of 27 October 2017.

1.8. Project Objectives

Demands for heavy metals and nanoparticles increased dramatically over the last few decades due to increased applications of these products in consumer goods, pharmaceuticals and industries, and also due to the rapid increase in population demanding these products. The production of metal and carbon based nanoparticles are expected to rise dramatically and become more readily available in products. It is thus very important to investigate the effects of these emerging nanoparticles on

physiological systems such as the immune system to prevent potential long term adverse effects on health and the environment in the future. This is vital as the metal ions can leach out of the various products and result in numerous damaging effects, as previously discussed. The nanoparticles can also impact physiological processes due to their structure and ability to enter cells and can also cross physiological barrier systems.

1.9. Aims

- The aim of this project is to utilize mammalian cell cultures to monitor the effects of the heavy metals silver, copper and cadmium on the immune system, utilizing *in vitro* techniques. Once the *in vitro* cell cultures have been optimized by using the heavy metals, the effects of various nanoparticles (silver, graphene oxide and carbon dots) on the immune system will also be evaluated.

- Identify molecular biomarkers that can be employed in rapid bioassays to monitor adverse effects of heavy metals and nanoparticles.

1.10. Hypothesis

H_0: Heavy metals and nanoparticles have no effects on pathways regulating the immune system.

H_1: Heavy metals and nanoparticles have an effect on pathways regulating the immune system.

1.11. Thesis Structure

The main aim of this thesis is to establish and identify potential biomarkers that can be used to monitor heavy metal and nanoparticle exposure. To achieve this aim, the effects of the heavy metals, cadmium, copper and silver on the murine macrophage cell line RAW 264.7 cells and human whole blood cell cultures will be assessed (Chapter 3). Based on the results and methodology employed in chapter 3, the effects of various nanoparticles on the immune system will be evaluated. The chapters focusing on the effects of the various nanoparticles on the immune system (Chapters 4, 5 and 6) have been submitted to peer reviewed journals. This dissertation consists of seven chapters including an introduction (Chapter 1), an overview of the immune system (Chapter 2) and a final chapter consisting of conclusions and recommendations for further work (Chapter 7).

Details of each chapter are given below:

Chapter 1: Introduction, thesis structure and objectives

This chapter gives an introduction to heavy metals and nanoparticles and a review of available research. This chapter also highlights why an *in vitro* approach has been taken as opposed to an *in vivo* one. This chapter also describes the outlines of the thesis and the aims and objectives of the thesis.

Chapter 2: Overview of the immune system

This second chapter gives an overall view of the immune system and how it responds to an invasion due to a microbe.

34

Chapter 3: The Effects of Heavy Metals on the Immune System

This chapter evaluates the effects of the heavy metals, cadmium, copper and silver on the immune system. It uses an *in vitro* method to determine whether these metals cause immunomodulation under basal and simulated immune response conditions.

Chapter 4: The effects of silver nanoparticles on RAW 264.7 macrophages and human whole blood cell cultures

This chapter aims to evaluate a number of parameters after exposing RAW cells and whole blood cells to AgNPs. These parameters include, cell viability, inflammatory biomarkers, cytokines of the acquired system and a proteome profile analysis of cytokines and chemokines. This chapter also aimed to identify potential biomarkers for AgNP exposure. This chapter has been submitted for publication.

Chapter 5: Effects of graphene oxide nanoparticles on the immune system biomarkers produced by RAW 264.7and human whole blood cell cultures

This chapter aims to evaluate a number of parameters after exposing RAW cells and whole blood cells to GONPs. These parameters include, cell viability, inflammatory biomarkers, cytokines of the acquired system and a proteome profile analysis of cytokines and chemokines. This chapter also aimed to identify potential biomarkers for GONP exposure. This chapter has been submitted for publication.

Chapter 6: The effects of carbon dots on immune system biomarkers, using the murine macrophage cell line RAW 264.7 and human whole blood cell cultures

This chapter aims to evaluate a number of parameters after exposing RAW cells and whole blood cells to CDs. These parameters include, cell viability, inflammatory biomarkers, cytokines of the acquired system and a proteome profile analysis of

35

cytokines and chemokines. This chapter also aimed to identify potential biomarkers for CD exposure. This chapter has been submitted for publication.

Chapter 7: Conclusions and recommendations

This final chapter highlights the main findings of this research and also gives recommendations for future work.

Chapter 2: Immune System

2.1. Overview of the Immune System

The main function of the immune system is to protect hosts from infectious pathogens by recognizing self from non-self (Cebo et al., 2001, Chaplin, 2006). Many environmental substances, such as metals, organic pesticides, and gaseous pollutants, disrupt the immune response and increase susceptibility to infectious disease (Parkin and Cohen, 2001). The immune system is comprised of various cells, cell products, tissues and organs, which together form an efficient, interactive and intricate network that protects the host from infectious agents (Parkin and Cohen, 2001, Ladics, 2007, Moser and Leo, 2010). Before encountering the immune systems, the pathogen encounters different barriers, comprising of external (skin etc.) and chemical barriers (stomach acids etc.) (Moser and Leo, 2010). The immune system consists of two types of immunity, namely; the innate immunity, that is present from birth and acquired immunity, that only develops after birth and upon contact with a specific pathogen (Chaplin, 2006).

2.2. Organs of the Immune System

The organs of the immune system, lymphoid organs, are distributed throughout the body and can be divided into primary lymphoid organs, where lymphocytes are generated and secondary lymphoid organs, where the adaptive immune responses are initiated. The primary lymphoid organs comprise of the bone marrow and thymus. The spleen, lymph nodes, and mucosal- and gut-associated lymphoid tissues (MALT

and GALT) (i.e. tonsils, adenoids, appendix and Peyer's patches) are the secondary lymphoid organs. The cells of the immune system are dependent on these organs for their production, maturation, storage and transportation (Moser and Leo, 2010, Zhao et al., 2012).

2.2.1. Bone marrow

Bone marrow is considered to be the primary site of haematopoiesis and functions as an active site for trafficking immune cells, which include T cells, B cells, dendritic cells (DCs), natural killer (NK) cells, neutrophils, myeloid-derived suppressor cells and mesenchymal stem cells. This is the site where B cells are also produced and matured (Zhao et al., 2012).

2.2.2. Thymus

The thymus produces T lymphocytes from thymocytes (T cell precursor), which migrate via the circulatory system from the bone marrow. The thymus is the site where these T cells undergo development, differentiation and expansion. Thymocytes undergo a rigorous selection process, of which ~96% undergo apoptosis and only ~3-5% becomes fully competent T cells that are able to recognize foreign antigens but do not recognize self-antigens, and eventually enter into the circulation as naïve T cells. A variety of other cells are also found in the thymus, such as; antigen-presenting cells (APCs), macrophages and a minute amount of B cells (Ribatti et al., 2006).

2.2.3. Spleen

The spleen is the largest secondary immune organ as it contains about a quarter of the body's lymphocytes (Cesta, 2006). The spleen uniquely combines the innate and adaptive immune systems in an organized way. This secondary lymphoid organ removes old erythrocytes and cellular debris by filtering the blood and removes any blood-borne microorganisms. It also serves as a storage site for erythrocytes and platelets. Due to its highly organized lymphoid compartments, it has distinctive antibacterial and antifungal reactivity (Mebius and Kraal, 2005, Cesta, 2006). Various cells are also found within this immune organ, such as, T cells, B cells, DCs, macrophages and NK cells (Mebius and Kraal, 2005).

2.2.4. Lymph nodes

Lymph nodes are composed of a complex network of fibroblasts, that when filled with lymphocytes, B and T cells have their own compartments that kill bacterial and viral agents respectively (Roozendaal et al., 2008). This immune organ is crucial for the commencement of immune responses by creating an environment where lymphocytes and APCs can interact optimally (Willard-Mack, 2006, Roozendaal et al., 2008). Apart from B and T cells, DCs and macrophages are also present at this secondary immune organ site (Roozendaal et al., 2008).

2.2.5. Overview of the cells of the Immune System

Table 2.1. Summary of the immune cells and their functions (Murphy and Weaver, 2016)

Cells of the Immune System		
Leukocyte (White Blood Cells)	**Function**	**Type of Leukocyte**
Neutrophils	Phagocytosis and activation of bactericidal mechanisms	Polymorphonuclear Leukocytes (Granulocytes)
Basophils	Promotion of allergic responses and enhancement of anti-parasitic immunity	
Eosinophils	Killing of antibody-coated parasites	
Mast cells	Release of granules containing histamine and active agents	
Monocytes	Phagocytosis	Mononuclear Leukocytes
Macrophages	Phagocytosis and activation of bactericidal mechanisms Antigen Presentation	
Lymphocytes	Specific Immune Responses	
Dendritic Cells	Antigen uptake in peripheral sites. Antigen Presentation	

Table 2.2. The effector cells (lymphocytes) of the immune system (Murphy and Weaver, 2016)

Lymphocytes	Function
B-lymphocytes	Production and secretion of antibodies specific to the pathogen that activated its production
Cytotoxic T-cells (T-lymphocyte)	Kills cells that are infected with viruses or other intracellular pathogens
T-helper Cells (T-lymphocyte)	Provides additional signals that influence the behaviour and activity of other cells such as antigen-stimulated B-cells
Regulatory T-cells (T-lymphocyte)	Suppress the activity of other lymphocytes and helps to control immune responses
Natural Killer Cells	Releases lytic granules that kill some virus-infected cells

2.3. Innate Immunity

Innate immunity is the type of immunity which an individual is born with and is the first line of defense against a pathogen (Moser and Leo, 2010). However, this type of immunity is broadly specific, lacks memory and is focused on a limited set of antigenic determinants which are shared by numerous pathogens (Flores et al., 2004). Due to these characteristics of the innate immune system, a very rapid response, which is put into effect without delay is exhibited when a pathogen is encountered (Storni et al., 2005). The external and chemical barriers, along with phagocytosis forms part of the innate immune system (Mogensen, 2009, Moser and Leo, 2010).

2.3.1. Pathogen recognition via Toll-like receptors (TLR)

Discovery of the Toll protein originated in the *Drosophila,* where it was shown to be vital for dorsal-ventral pattern determination during embryogenesis and the early formation of the innate immune system (Lu et al., 2008). Toll is a type 1 transmembrane protein with abundant leucine repeats in the extracellular domain and an area of high homology to the human interleukin 1 (IL-1) receptor (IL-1R) in the cytoplasmic domain (Fitzgerald et al., 2004). The leucine rich repeats are responsible for the recognition of specific pathogen components (Kawai and Akira, 2007). Mammalian homologues of the Toll receptor were subsequently identified and were named Toll-like receptors (TLRs) (Takeda and Akira, 2004). TLRs recognize specific patterns of microbial components that are conserved among pathogens, but are not found in mammals (Takeda and Akira, 2005) and this plays a crucial role in innate immune responses as TLRs signal via a common pathway that leads to the expression

of various inflammatory genes (Kumar et al., 2009). Host cells express various pattern recognition receptors (PRRs) that detect various pathogen-associated molecular patterns (PAMPs) such as lipids, proteins and nucleic acids (Kawai and Akira, 2007, Moser and Leo, 2010). Secreted PRRs bind to microbial cells and flag them for destruction either by the complement system or by phagocytosis (Janeway and Medzhitov, 2002, Medzhitov, 2007). When PRRs recognize PAMPs, it activates intracellular signaling pathways in the immune system cells which induce inflammatory cytokines and chemokines, and forms a link with the adaptive immune response (Kawai and Akira, 2007, Mogensen, 2009).

2.3.2. Phagocytosis

Phagocytosis is an important effector mechanism of the innate immunity (Moser and Leo, 2010). Immune cells such as neutrophils, macrophages, monocytes and DCs are capable of phagocytosing a pathogen upon which the pathogen can be broken down via a series of defined steps (Aderem, 2003, Rosales and Uribe-Querol, 2017). When a pathogen encounters a phagocyte, the receptors on the phagocytic cell surface recognize and bind to the pathogen. Signals are then produced, which generate actin polymerization under the membrane at the binding site. The actin rich membrane appendages, called pseudopodia reach out around the pathogen, fusing the membranes to form a phagosome inside the phagocyte (Richards and Endres, 2014). The pathogen is then pulled towards the centre of the cell, allowing the phagosome to mature via a series of fusion and fission events to become a phagolysosome (Aderem 2003). Thus, the pathogen is engulfed and trapped within an intracellular vesicle,

43

called a phagolysosome (Richards and Endres, 2014). This phagolysosome is an acidic, hydrolytic compartment which destroys the pathogen by exposing it to digestive enzymes and free radicals in preparation for antigen presentation (Aderem 2003; Moser & Leo 2010).

APCs such as DCs, macrophages and B lymphocytes use phagocytosis to express antigens to major histocompatibility complex (MHC) (Greenberg & Grinstein 2002; Aderem 2003). Antigen presentation by molecules encoded by the MHC to T-lymphocytes is a key event in the detection and elimination of foreign protein antigens. Once exogenous proteins are internalized, the proteins are degraded before being loaded onto MHC II molecules. These MHC II molecules are then presented to CD4^{+} T-lymphocytes (Zufferey et al., 2017).

On the other hand, antigen presentation via MHC I, usually relies on the degradation of exogenous proteins by the cytosolic proteasome. Thereafter, peptides are translocated into the endoplasmic recticulum (ER) and loaded onto emerging MHC I molecules. These molecules are then transported to the cell surface, which leads to CD8^{+} T cell activation via T cell receptors (Zufferey et al., 2017). Therefore, phagocytosis serves as a link between the innate and acquired immune responses.

2.3.3. Complement System

The complement system comprises of more than 30 proteins in the plasma and on cell surfaces, amounting to more than 3 g/L and constituting more than 15 % of the globular fraction of plasma (Dunkelberger and Song, 2010). These vast amounts of proteins are organized in a hierarchy of proteolytic cascades that commence with the

recognition of antigenic surfaces and leads to the production of proinflammatory mediators (anaphylatoxins), opsonization of antigenic surfaces through different opsonins after which the pathogen is targeted for lysis of the antigenic surface by the assembly of membrane penetrating pores, identified as membrane attack complexes (MAC) (Figure 2.1) (Dunkelberger and Song, 2010, Trouw and Daha, 2011, Noris and Remuzzi, 2013). The complement system also aids and directs the adaptive/acquired immune responses, as well as coordinating non-inflammatory removal of cellular debris (Zipfel, 2009).

The activation of the complement system can result from the activation of at least three different pathways, namely; the classical pathway, lectin pathway and the alternative pathway. The initiation of each pathway is unique but all three pathways result in the cleavage of C3 (Hawlisch and Kohl, 2006).

2.3.3.1. The Classical Pathway

The classical pathway is activated when C1q binds to an antigen-antibody complex (Hawlisch and Kohl, 2006). After binding to the F_c region of either an immunoglobulin G/M (IgG/ IgM) antibody, an interaction with C1q occurs and results in a conformational change and this ultimately results in the activation of C1r and C1s (Noris and Remuzzi, 2013). Activated C1s cleaves C4 and C2 into larger fragments (C4b and C2a) and smaller fragments (C4a and C2b). The larger fragments associate to form C4bC2a, known as C3 convertase. This convertase has the ability to cleave C3. The C3 convertase forms on the surface of pathogens (Dunkelberger and Song, 2010). C3 convertase cleaves C3 into the anaphylatoxin C3a and the opsonin

45

C3b, which is the central component of the complement cascade (Noris and Remuzzi, 2013). The C3b opsonin binds to the pathogen by a thioester group and this effectively 'tags' the pathogen as foreign (Trouw and. Daha, 2011). This process ultimately leads to further complement activation on and around the opsonized surface and ends in the production of anaphylatoxins and the assembly of MAC (Dunkelberger and Song, 2010). The assembly of MAC occurs as C3b also activates C5 converatses, which proteolytically degrade C5 into C5a and C5b. C5b (opsonin) along with C6-9 forms a molecular complex (MAC) which penetrates microbial cell membranes and causes them to lyse (Cota and Midwinter, 2009).

2.3.3.2. The Lectin Pathway

The lectin pathway is activated by recognition molecules through a mechanism similar to that of the classical pathway, the mannan-binding lectin (MBL) or ficolins (lectins that consist of a fibrogen-like and a collagen-like domain) (Dodds and Matsushita, 2007). These molecules recognize carbohydrate PAMPs that activates C2 and C4 through MBL-associated serine proteases (MASP-1, MASP-2 and MASP-3) (Dunkelberger and Song, 2010). This results in the cleaving of C2 and C4 and generates C4bC2a (C3 convertase complex) in a reaction similar to the classical pathway (Noris and Remuzzi, 2013).

2.3.3.3. The Alternative Pathway

The alternative pathway is initiated by the slow and continuous turnover of the complement, C3, to C3a and C3b (Trouw and Daha, 2011). This then initiates the spontaneous cleavage of C3 to C3(H_2O) which functions similarly to C3b as it has the

ability to bind to factor B (Descotes, 2004, Noris and Remuzzi, 2013). Factor B is then cleaved by factor D to Bb and results in the formation of C3 convertase C3(H_2O)Bb, which is similar to the classical C3 convertase C2bC2a as it can cleave C3 to C3a and C3b (Noris and Remuzzi, 2013). C3b then binds to factor B on the pathogen membrane, after which factor B is cleaved to Ba ad Bb by factor D, forming the alternative convertase C3bBb (Descotes, 2004). The newly formed C3bBb binds to the plasma protein properdin for stabilization (Noris and Remuzzi, 2013). The C3 convertase (C3bBb) then binds to the opsonin (C3b) to form C5 convertase (C3bBbC3b), which ultimately results in the formation of MAC and destruction of the microbe (Cota and Midwinter, 2009, Trouw and Daha, 2011).
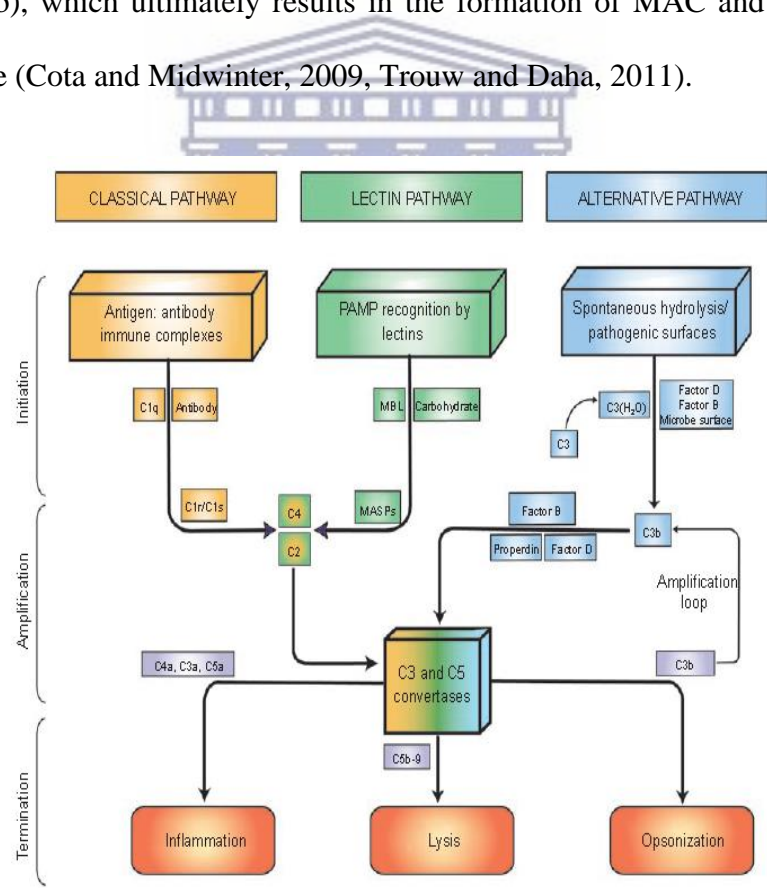
Figure 2.1. The three pathways whereby the complement system is activated (Dunkelberger and Song, 2010).

47

2.3.4. Inflammation

Inflammation is employed as a protective mechanism against tissue injury or destruction. In the inflammatory process, numerous inflammatory cells enter into injured tissue and produce inflammatory mediators that magnify inflammatory responses which is characterized by swelling, redness, pain and fever (Ryu et al. 2013). The infiltrated cells or damaged tissues produce numerous inflammatory molecules such as nitric oxide (NO), prostanoids, tumour necrosis factor-α (TNF-α) and interleukins (ILs). These molecules act as pleotropic effector molecules that intensify acute inflammation and leads to the activation of the adaptive immune response (Murphy and Weaver, 2016). The transduction of the inflammatory process involves a number of signaling pathways such as nuclear factor kappa B (NF-κB), which is an important signaling molecule that increases the production of effector molecules that are directly related to inflammation (Janeway and Medzhitov, 2002, Ryu et al., 2013).
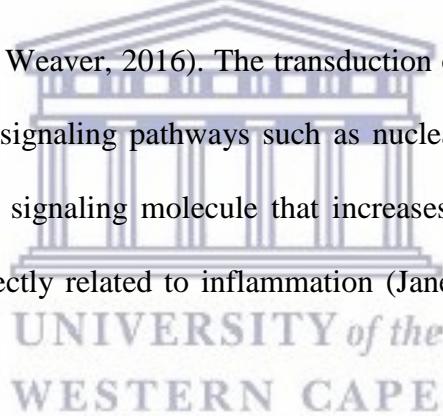
2.4. Acquired or Adaptive Immunity

The acquired immune response is the result of continual exposure to the pathogen and becomes more intense after every exposure (Flores et al. 2004). The acquired immune response is mediated and maintained by B and T lymphocytes (Storni et al., 2005). B-cells, the precursor of antibody secreting cells, can directly recognize native antigens through their B-cell receptor. However, T lymphocytes need the antigen to be processed and presented to them by an APC. The T-cell antigen receptor (TCRs) can only recognize fragments of antigens bound to molecules of the MHC on the surface

48

of an APC (Banchereau and Steinman, 1998). Upon the eradication of the pathogen, memory of the pathogen is acquired and maintained to defend against future encounters with the pathogen (Moser & Leo 2010). The acquired immunity comprises of two types of defense mechanisms; cell mediated immunity and humoral immunity (Murphy and Weaver, 2016).

2.4.1. Humoral Immunity

MHC is cell surface glycoprotein that binds peptide fragments of proteins that have been ingested by the cell and is proteolytically processed, either by endocytosis or phagocytosis to give rise to MHC-II antigen complex. These MHC-II antigen complexes are constitutively expressed on B cells, DCs, monocytes and macrophages (APCs) and these cells present antigens to CD4$^+$ T cells (Chaplin, 2010).

The MHC-II antigen complex stimulates the precursor Th$_0$ lymphocytes to differentiate into Th$_2$ cells (Parkin and Cohen, 2001). This process occurs as interleukin 4 and 10 (IL-4 and IL-10) induce differentiation of Th$_0$ cells to Th$_2$ cells. B-lymphocytes are then stimulated to produce antibodies by the cytokines IL-4 and IL-10 (Tan and Coussens, 2007). These Th$_2$ cells secrete higher levels of IL-4 and IL-10. IL-4 and IL-10 are responsible for the maturation of B cells. The mature B cells secrete the antibodies a few days after exposure into the general circulation and antibodies are able to recognize the specific pathogen that induced its production (Maddaly et al., 2010, Brewer, 2013). Some B cells are stored as memory cells after the exposure event. These affinity-matured B-cells are long lived CD27$^+$ cells that express surface immunoglobulins but do not secrete antibody. However, when these

49

cells re-encounter the antigen, they divide swiftly and expand their numbers or differentiate into antibody secreting cells (LaRosa and Orange, 2008). Whereas, long-lived plasma cells are CD138^{+}, terminally differentiated B-cells which are incapable of further division, return to the bone marrow to secrete high-affinity class-switched antibodies (LaRosa and Orange, 2008). Therefore, after infection, activated naïve B cells can switch from expressing immunoglobulin M (IgM) and IgD on their surface to expressing IgG, IgE or IgA. This isotype/class switch changes the effector function of the antibody, and improves its ability to eliminate the pathogen that induced the response (Stavnezer and Schrader, 2014). Class switching is directed by cytokines secreted by T cells and other cells (Stavnezer et al., 2008). This allows immune memory and protects an individual from extracellular pathogens, such as bacteria and parasites (McGlauchlen and Vogel, 2003).

2.4.2. Cell Mediated Immunity

Intracellular pathogens such as mycobacteria, viruses and cancer replicate inside the hosts cell and some of their proteins are cleaved into peptides in the cytoplasm of the infected cell and are then bound to MHC-I complex. The MHC-I-antigen complex is presented on the surface of the infected cell membrane. This complex is then recognized by CD8^{+} cytotoxic T cells. Once the cytotoxic T cells (CTLs) are activated, they can directly kill a target cell (Banchereau and Steinman, 1998, Chaplin, 2010). CTLs can kill target cells via two major pathways. First, the CTLs can express the death- inducing molecule Fas ligand (FasL) on their cell surface. Once FasL interacts with its receptor Fas on the target cell, the activation of a suicide

50

pathway in the target cell is induced, similar to apoptosis (Kaufmann, 1999). CTLs also have unique cytoplasmic granules containing various effector molecules with cytolytic activity, such as perforin and granzymes. Once CTLs are in close contact with the target cell, they release their granular content. The granular content causes the formation of pores in the target cell membrane, which causes swelling, rupture and eventual cell death. These processes work synergistically to cause effective, targeted cell death (Kaufmann, 1999). This process is regulated by cytokines interleukin 12 and interferon gamma (IL-12 and IFNγ) that also activated T helper cells release. This promotes the Th_0 lymphocytes to differentiate into Th_1 cells and this is required for the activation of cytotoxic T cells (Flores et al., 2004).

2.5. Cytokines

The immune system needs to be regulated and the activity of the immune system is controlled by cytokines (Cebo et al., 2001). Cytokines are small glycoprotein molecules produced by a number of cells that are responsible for regulating a variety of processes, including, immunity, inflammation, apoptosis and hematopoiesis (House, 2001). The cytokines that control the innate, humoral and cell mediated immune responses are briefly discussed below.

2.5.1. IL-6

IL-6 is a pleiotropic cytokine, which means that it has the potential to elicit different biological responses on different cell types (Niemand et al., 2003). Some of these pleiotropic effects include the ability of IL-6 to stimulate T cell proliferation and their differentiation into cytotoxic T cells, stimulate antibody production by B-cells, and

51

also induce production of acute phase proteins (Hibi et al., 1996, Niemand et al., 2003). IL-6 is an important inflammatory mediator as it is mainly synthesized by immune cells and play a crucial role in the acute phase of inflammation (Ryu et al., 2013). IL-6 also has the ability to exhibit both pro-inflammatory and anti-inflammatory effects (Niemand et al., 2003). Its classic pro-inflammatory characteristics are vital in normal cell inflammatory processes, host immune responses and the modulation of cellular growth (Ataie-Kachoie et al., 2013).

The IL-6 cytokine exerts their action by binding to the signal transducing receptor chain, glycoprotein 130 (gp130). This signal transduction involves the activation Janus kinase (JAK) tyrosine kinase family members, which leads to the activation of transcription factors of the signal transducers and activators of transcription (STAT) family (Heinrich et al., 2003, Kishimoto, 2006). IL-6 cytokines can also be activated by another major signaling pathway, which is the mitogen-activated protein kinase (MAPK) pathway (Heinrich et al., 2003, Kishimoto, 2010).

2.5.2. IL-10

IL-10 is a pleiotropic cytokine that belongs to the class II cytokine receptor family, where it has numerous effects on various cell types (Riley et al., 1999). IL-10 has the unique ability to inhibit the expression and production of many LPS-inducible genes, mainly pro-inflammatory cytokines, by macrophages (Donnelly et al., 1999, Riley et al., 1999). Therefore, IL-10 serves as an anti-inflammatory cytokine as during infection it inhibits the activity of Th_1 cells, NK cells and macrophages, all of which are needed for optimal pathogen removal but also contribute to tissue damage

(Couper et al., 2008). Active IL-10 receptors are comprised of two subunits that also contain receptors for IFNα and IFNγ. The IL-10 receptor α chain functions as a signal transducer and has the principal role in mediating high affinity ligand binding. Whereas, the β subunit is a polypeptide and is mainly needed for signaling (Riley et al., 1999).

2.5.3. IFNγ

IFNγ (originally called macrophage-activating factor) is a cytokine that is produced mainly by activated CD4^{+} or CD8^{+} T cells and NK cells and is recognized as the principal mediator of innate and adaptive immunity (Mühl and Pfeilschifter, 2003, Schroder et al., 2004). Activation of IFNγ is via the JAK/STAT pathway and this leads to the production of IFN stimulated genes that block viral replication (Harvey et al., 2015). Stimulation of macrophages with IFNγ induces direct antimicrobial and antitumour mechanisms as well as the up-regulation of antigen processing and presentation pathways. IFNγ also plays a role in attracting leukocytes and directs growth, maturation and differentiation of several cell types (Schroder et al., 2004).

2.6. Immunotoxicity

The immune system can be the target of many chemicals, which may potentially have severe adverse effects on the host's health. An immunotoxic compound can be defined as a compound that can change one or more functions of the immune system that will result in an adverse effect for the host (Descotes, 2004, Corsini et al., 2013). The adverse effects may be immunosuppression (decreased immunocompetence) which may result in repeated, more severe, or prolonged infection, as well as the

development of cancer. The other adverse effect may be over/hyper immunostimulation, which may cause immune-mediated disease like hypersensitivity reactions and autoimmune diseases (Corsini et al., 2013).

2.6.1. Immunosuppression

Immunosuppression has a direct impact on the function of immune cells/organs as there will be a decrease in the weight of the lymphoid organ and/or decrease in the amount of immune cells. Due to these effects, it may result in reduced immune function, which will decrease one's ability to defend against infections (De Jong and Van Loveren, 2007, DeWitt et al., 2012).

2.6.2. Immunostimulation

Since immunosuppression causes a decrease in immune function, immunostimulation causes an increase in the activity of immune cells/organs that may produce an elevated immune response. These effects may be exacerbated immune responses against pathogens and a decrease in the ability of the immune system to appropriately act against external challenges (De Jong and Van Loveren, 2007, DeWitt et al., 2012, Corsini et al., 2013)

2.6.3. Hypersensitivity

A hypersensitivity reaction refers to a state of altered reactivity in which the body mounts an amplified immune response to a xenobiotic (Marc and Olson, 2009). The effects of a hypersensitivity reaction may be an allergic response to a xenobiotic (De Jong and Van Loveren, 2007, Corsini et al., 2013).

There are four types of hypersensitivities. Type I, or immediate hypersensitivity, happens within approximately 30 mins. It is IgE antibody-mediated, and the allergic signs or symptoms are initiated by cross-linking of mast cell-bound IgE by antigens and this result in mast cell degranulation and the release of inflammatory mediators (Baldo and Pham, 2013). Type II hypersensitivities, which are also known as cytotoxic hypersensitivities, are uncommon reactions that are typically caused by IgG and IgM antibodies. This response can occur when the target antigen is part of the surface of a specific host cell. Examples may include drug reactions and transplantations. This happens when the antibodies bind to host cells to form complexes that activate the complement pathway (Marc and Olson, 2009, Baldo and Pham, 2013). Like type II hypersensitivities, type III hypersensitivities are also mediated by IgG and IgM antibodies. However, type III hypersensitivities are associated with responses to soluble antigens that are not attached to host cells/tissues but with antibodies in the blood that can lead to the formation of immunoprecipitates, resulting in an inflammatory response (Marc and Olson, 2009). Type IV hypersensitivities or delayed type hypersensitivities are mediated by antigen specific T cells and the reaction can occur more than 12 hrs after exposure to an antigen (Marc and Olson, 2009, Baldo and Pham, 2013).

2.6.4. Autoimmunity

Autoimmunity is induced in response to auto-antigens that are initiated by either a superior immune reactivity, immune stimulation, or reactions to distorted self antigens after a xenobiotic encounter with tissue compartments. It can also cause the

55

induction of antinuclear antibodies (De Jong and Van Loveren, 2007, DeWitt et al., 2012).

Therefore an immunotoxic response can be categorized according to their immune response. It is the activation of the immune system (i.e. immunostimulation and autoimmunity); sensitization of the immune response (i.e. hypersensitivity reactions); and the impairment of an immune response (i.e. immunosuppression) (Langezaal et al., 2001).

The Effects of Heavy Metals on the Immune System

Abstract

Heavy metals occur naturally in the environment. However, due to mining activities and anthropogenic use, high levels of heavy metals are currently found in soil and also in our water resources. Most heavy metals are toxic to biota. The current study investigated the effects of metals on the immune system using *in vitro* assays. The metals investigated are cadmium (Cd), silver (Ag) and copper (Cu). Cell culture assays were employed using RAW 264.7 murine macrophages and human whole blood cells (WBCs). Effects of metals on inflammation were investigated under basal (unstimulated) or lipopolysaccharide (LPS) stimulated conditions. RAW 264.7 cells indicate that Cd is more cytotoxic than Ag, while Cu had no cytotoxic effects at the concentrations investigated. None of the metals investigated had an effect on inflammatory markers under basal conditions. LPS stimulated RAW cells show that Cd inhibited the inflammatory markers nitric oxide (NO) and IL-6 at lower concentrations than Ag, while Cu had no effects on the synthesis of these biomarkers. Upon investigating LPS stimulated WBCs it was found that Cu inhibited the inflammatory marker IL-6 at a lower concentration than Cd, while Ag activated IL-6 synthesis. Effects of metals on T-helper (T_h) cytokines were also investigated under basal and phytohaemagglutinin (PHA) stimulated conditions. T_h cytokines regulate the acquired immune pathways namely humoral immunity by interleukin 10 (IL-10)

and cell mediated immunity by interferon gamma (IFNγ). Results show that Cd inhibited IL-10 production at a lower concentration than Cu, and Ag was least inhibitory for this cytokine. Contrary to this, Ag inhibited IFNγ production at a lower concentration than Cu, and Cd was least inhibitory for this cytokine. From this it can be concluded that heavy metals act differently on the various immune components and that they could potentially have adverse health effects on people exposed to high levels of environmental metal pollutants.

Keywords: Heavy metals, immune system, cytokines, autoimmunity, immunosuppression

3.1. Introduction

Metal and metal compounds are constituents of the natural environment. Their distribution depends on the existence of natural sources and human activity (Florea and Busselberg, 2006). Metals are persistent environmental contaminants as they cannot be degraded or destroyed (Duruibe et al., 2007). Therefore, metal and metal compounds released into the environment can accumulate in abiotic and biotic systems (Florea and Busselberg, 2006). Sources of metal pollution include leachate from hazardous waste sites, discharge from industrial plants, and effluents from wastewater treatment plants and chemical waste from land disposal sites that may contain high concentrations of toxic metals (Said and Lewis, 1991).

Most heavy metals are toxic or carcinogenic to humans, such as cadmium (Cd), a known group I carcinogen (Pathak and Khandelwal, 2006) and silver (Ag). Exposure

58

to Ag can result in the permanent discolouration of the skin called arygria (Hadrup and Lam, 2014). Toxicity may occur upon exposure to low concentrations of the heavy metal (Pathak and Khandelwal, 2006, De Lurdes Dinis and Fiúza, 2011). Some metals like copper (Cu), magnesium (Mg), potassium (K), and calcium (Ca) are essential trace elements which can be found in small or large amounts in a number of cells and tissues (Bia and DeFronzo, 1981, Hartwig, 2001, Gaetke, 2003, Maier et al., 2004). Some of the essential trace elements are involved in metabolic pathways and may also serve as a cofactor of numerous enzymes involved in redox reactions and electron transport in biological systems (Hartwig, 2001, Maier et al., 2004, Jomova and Valko, 2011). However, exposure to large quantities of essential trace elements may also result in toxicity. Heavy metals are known to affect several physiological systems such as the central nervous function, lungs, kidneys, endocrine system, liver and blood composition (Handy, 2003, Bertin and Averbeck, 2006, De Lurdes Dinis and Fiúza, 2011). However, the effects of various heavy metals on the immune system, in an *in vitro* environment, are not that well established (Colombo et al., 2004, Shin et al., 2007, Yang et al., 2012).

This study aimed to monitor the effects of Cd, Ag and Cu on the immune system by using *in vitro* exposures to murine RAW 264.7 cells and human whole blood cell cultures. Cytotoxicity, inflammatory biomarkers, molecular biomarkers and cytokines of the acquired immune system were assessed in the study.

59
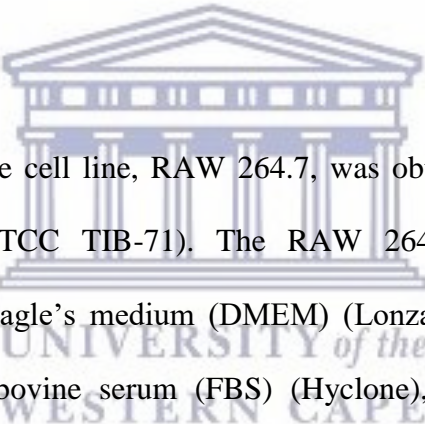
3.2. Materials and Methods

3.2.1. Preparation of metal salts

Stock concentrations (100 mM) of the metal salts cadmium chloride ($CdCl_2$), magnesium chloride ($MgCl_2$), silver nitrate ($AgNO_3$), potassium nitrate (KNO_3), copper sulphate ($CuSO_4$) and potassium sulphate (K_2SO_4) (all obtained from Merck) were prepared using distilled water and were thereafter 0.45 µm (Starlab Scientific) sterile filtered.

3.2.2. RAW 264.7 Cells

3.2.2.1. Cell culture

The murine macrophage cell line, RAW 264.7, was obtained from American Type Culture Collection (ATCC TIB-71). The RAW 264.7 cells were cultured in Dulbecco's modified Eagle's medium (DMEM) (Lonza) supplemented with 10 % heat inactivated fetal bovine serum (FBS) (Hyclone), glutamax (Sigma-aldrich), antibiotic/antimycotic (Sigma-aldrich) and gentamicin (Sigma-aldrich). The cells were incubated in a humidified atmosphere of 5 % CO_2 at 37 ºC and the cells were sub-cultured every 2-3 days.

The RAW 264.7 cells (5 x 10^5 cells/ml) were cultured in treated 96 well plates and incubated in a humidified atmosphere of 5 % CO_2 at 37 ºC for approximately 48 hrs until the cells reached 80-90 % confluence. The cells were then pre-exposed for 4 hrs to various concentrations of the metal salts. Thereafter the cells were either left unstimulated or stimulated by lipopolysaccharide (LPS) (0.2 µg/ml) overnight (~18

60

hrs) in complete medium under standard tissue culture conditions. Culture supernatants were collected (100 µl assigned to each assay) for nitric oxide and interleukin 6 (IL-6) determination.

3.2.2.2. Cytotoxicity Assay

After the removal of the supernatants, cytoxicity was measured by adding 50 µl of a 1/10 dilution of 2-(4-Iodophenyl)-3-(4-nitrophenyl)-5-(2,4-disulfophenyl)-2H-tetrazolium (WST-1) (Roche) reagent in complete medium to each well. Formazan formation was determined by reading the plate at 450 nm (Multiskan Ex, Thermo Electron Corporation) immediately after WST-1 addition and again after an incubation period of 15 min at 37 °C. The increase in absorbance at 450 nm is proportional to formazan formation.

3.2.2.3. Nitric Oxide (NO) Determination

After the overnight incubation of the RAW 264.7 cells, the amount of nitrite that was produced by the cells was measured in the supernatant as an indication of NO production. The NO assay is based on the Griess reaction (Granger et al., 1996). The amount of NO production was measured against a doubling dilution range of an initial 100 µM nitrite standard (Sigma-Aldrich). 100 µl of the supernatant collected or nitrite standard were mixed with 100 µl of Griess reagent (1:1 of 1 % sulfanilamide and 0.1 % naphtylethlemidimine-dihydrochloride in 2.5 % phosphoric acid) (all reagents obtained from Sigma-Aldrich). Thereafter, the plate was incubated at room temperature for 15 min. The absorbance was read at 540 nm by a microplate reader

61

(Multiskan Ex, Thermo Electron Corporation) and the amount of NO produced by the RAW cells quantified.

3.2.2.4. Mouse IL-6 Double Antibody Sandwich (DAS) Enzyme Linked Immunosorbent Assay (ELISA)

The mouse IL-6 ELISA (e-Bioscience, Ready-Set-Go) kits were used to measure IL-6 cytokine levels in the cell culture supernatants (1/40 v/v). Assays were performed in 96 well Nunc maxisorb plates. The kit contained all the reagents for the assay and was performed as per the manufacturer's instructions.

3.2.3. Whole Blood Cell (WBC) Culture

3.2.3.1. Blood collection

Blood was collected by a doctor/nurse from a healthy male who was not using any medication. The blood was collected using venipuncture directly into 3.2 % sodium citrate vacuum tubes (Greiner bio-one). The blood was processed immediately. The whole blood cell cultures were performed under sterile conditions. Ethical clearance was obtained from the University of the Western Cape (Ethics No.10/9/43). Informed consent was also obtained from the participant.

3.2.3.2. Cell Culture

Human whole blood was diluted with Roswell Parks Memorial Institute (RPMI) 1640 media (Sigma-Aldrich) to give rise to a 10% (v/v) mixture. Blood was either left unstimulated or stimulated with LPS (Sigma-Aldrich) (0.1 μg/ml) or phytohaemmagglutinin (PHA) (Sigma-Aldrich) (1.6 μg/ml). Unstimulated or

62

stimulated whole blood cell cultures were incubated overnight at 37 °C with various concentrations of the metal salts in sterile eppendorf tubes (Greiner bio-one). After the incubation period, culture supernatants were screened for interleukin 6 (IL-6), interleukin 10 (IL-10) and interferon gamma (IFNγ) using commercially available ELISA kits (e-Bioscience).

3.2.3.3. Cytokine Analysis using DAS ELISAs

Commercially available kit (e-Bioscience, Ready-Set-Go) were used to analyze the level of cytokine secretion from the whole blood cell cultures. The kits were used as per the manufacturer's instructions and contained all the reagents to complete the assay. The unstimulated and LPS stimulated samples were analysed using a 1/40 v/v dilution for the IL-6 assay. The unstimulated and PHA stimulated samples were assayed neat for interleukin 10 (IL-10) and interferon gamma (IFNγ) analysis. The same protocol was used as previously described for the mouse cytokine ELISA.

3.2.4. Statistical Analysis

All experiments were performed in triplicate and the data was calculated as a percentage of the control using Microsoft Excel. Data is presented as mean ± standard deviation (SD). One way analysis of variance (ANOVA) using SigmaPlot 12.0 was used to assess statistical differences with $P < 0.01$ being deemed significant.

3.3. Results

3.3.1. The effects of $MgCl_2$ and $CdCl_2$ on RAW 264.7 cells

3.3.1.1. Cytotoxicity

The WST-1 assay was used to assess the toxicity of the metal salt $CdCl_2$ on RAW 264.7 macrophage cells. At concentrations ≥ 20 μM, cell viability was significantly reduced ($P < 0.001$) compared to the control 0 μM $CdCl_2$ (Figure 3.1). Where at 20 μM $CdCl_2$, cell viability was reduced by ~35 % and at 25 μM $CdCl_2$ viability was reduced by ~70 % (Figure 3.1). Based on the reduction in cell viability an IC_{50} of 21.9 μM $CdCl_2$ was determined (Figure 3.2). No cytotoxicity was exhibited across all concentrations for the control metal salt, $MgCl_2$ and at concentrations ≤ 15 μM $CdCl_2$ (Figure 3.1).

UNIVERSITY of the
WESTERN CAPE
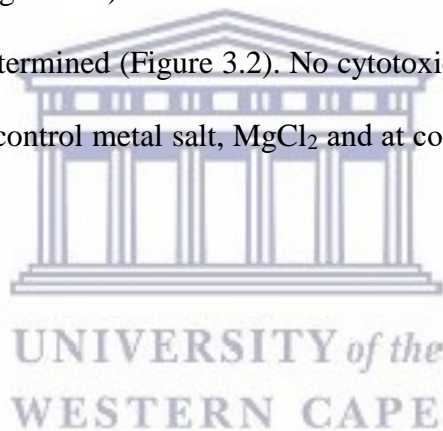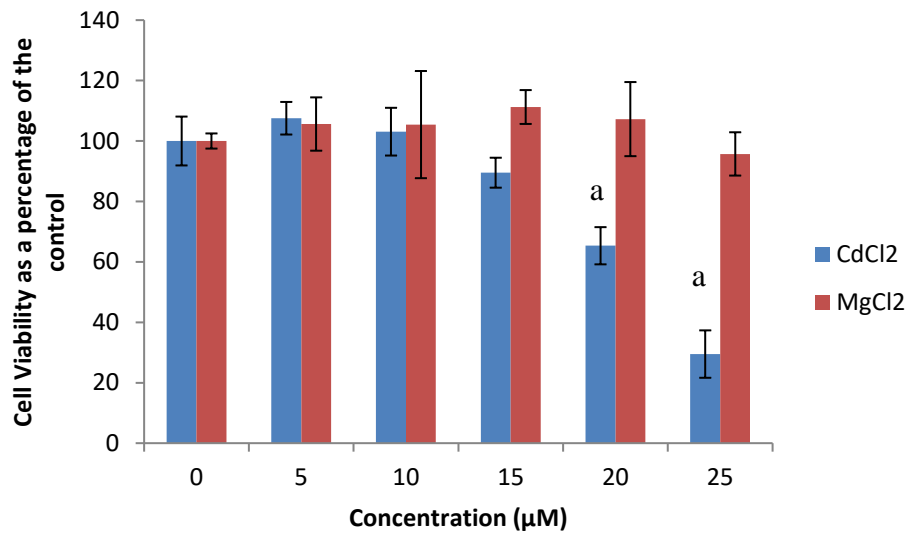
Figure 3.1. Cell viability of RAW 264.7 macrophage cells exposed to $CdCl_2$ and $MgCl_2$. Data represents mean percentage $\pm$ SD with n = 9. Bars marked with letters indicate significant difference (P < 0.01) to control. Significance demarcated by: a-significantly different (P < 0.001) compared to 0 µM $CdCl_2$.
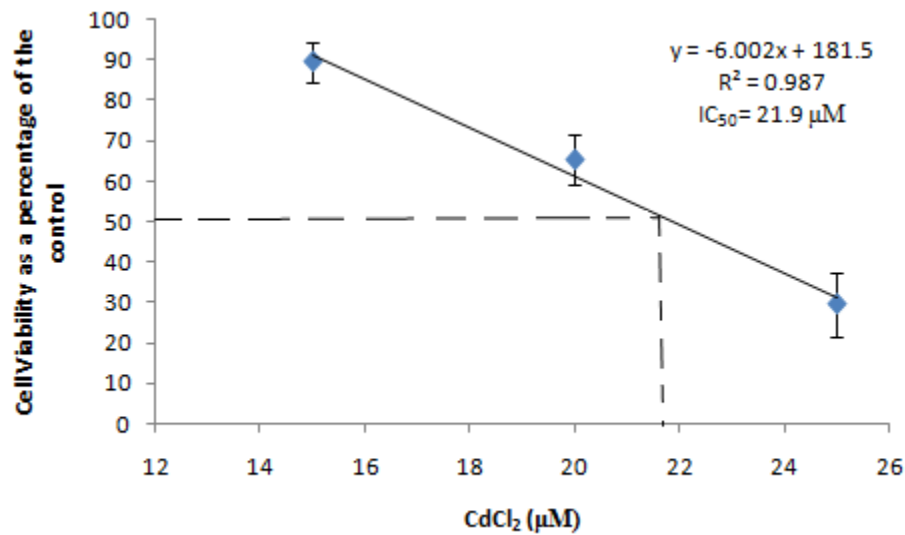
Figure 3.2. IC_{50} determination of $CdCl_2$ on cell viability as a percentage of the 0 µM $CdCl_2$

3.3.1.2. The effects of $MgCl_2$ and $CdCl_2$ on the inflammatory biomarker NO using RAW 264.7 cells

The amount of NO produced by the cells exposed to $CdCl_2$, revealed a considerable reduction ($P < 0.001$) in the pro-inflammatory biomarker at concentrations ≥ 10 µM compared to the control, 0 µM $CdCl_2$ (Figure 3.3). This steady decrease in NO production showed that at 10, 15, 20 and 25 µM there was an approximate 40, 90, 95 and 100 % reduction in NO production respectively (Figure 3.3). This decrease in NO production allowed for an IC_{50} of 10.46 µM to be determined (Figure 3.4). Unstimulated cells did not synthesize NO when exposed to $MgCl_2$ and $CdCl_2$ (results not shown). However, the control metal, $MgCl_2$ notably increased ($P \leq 0.004$) the

66

amount of NO produced at concentrations ≥ 5 μM by approximately 10-20 % compared to the control, 0 μM $MgCl_2$ (Figure 3.3).
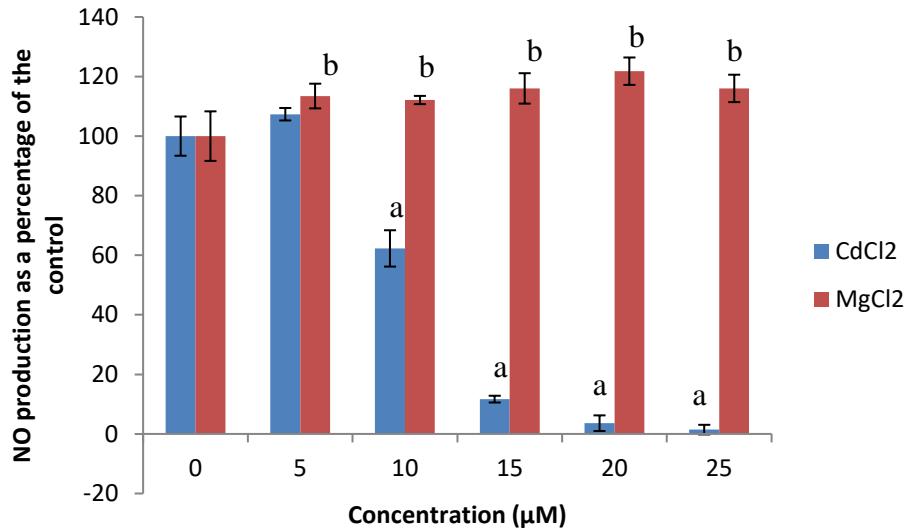
Figure 3.3. NO levels of RAW 264.7 cell cultures exposed to $CdCl_2$ and $MgCl_2$ in the presence of LPS. Unstimulated cultures did not produce NO and are not presented. Data represents mean percentage $\pm$ SD with n = 9. Bars marked with letters indicate significant differences (P < 0.01). Significance demarcated by: a- significantly different (P < 0.001) compared to 0 μM $CdCl_2$, b- significantly different (P $\leq$ 0.004) compared to 0 μM $MgCl_2$.
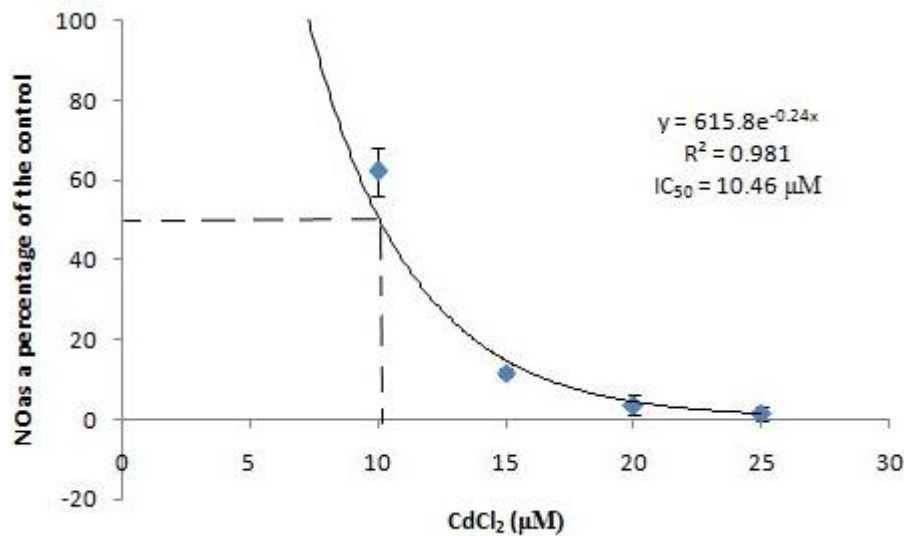
Figure 3.4. IC_{50} determination of $CdCl_2$ on NO production as a percentage of the 0 µM $CdCl_2$

3.3.1.3. The effects of $MgCl_2$ and $CdCl_2$ on the inflammatory biomarker IL-6 using RAW 264.7 cells

Cadmium chloride exhibited a biphasic immunomodulatory effect on the pro-inflammatory cytokine, IL-6 as it significantly upregulated ($P < 0.001$) IL-6 more than 2 fold at concentrations ≤ 10 µM, while significantly inhibiting ($P \leq 0.003$) the cytokine's synthesis at concentrations ≥ 15 µM compared to the control, 0 µM $CdCl_2$ (Figure 3.5). The synthesis of IL-6 was reduced by approximately 25 % for 15 µM $CdCl_2$ and 90 % for 20 and 25 µM $CdCl_2$ (Figure 3.5), thus allowing an IC_{50} of 16 µM to be determined (Figure 3.6). A similar trend was seen in the reduction of NO when RAW cells were exposed to ≥ 10 µM $CdCl_2$ (Figure 3.3). Whereas, $MgCl_2$ considerably upregulated ($P < 0.001$) the synthesis of IL-6 from the RAW cells exposed to all concentrations (Figure 3.5), by approximately 60 %, which was also

68

seen with the production of NO (Figure 3.3). Results are not shown for unstimulated cultures as they did not synthesize IL-6 when exposed to the metals.
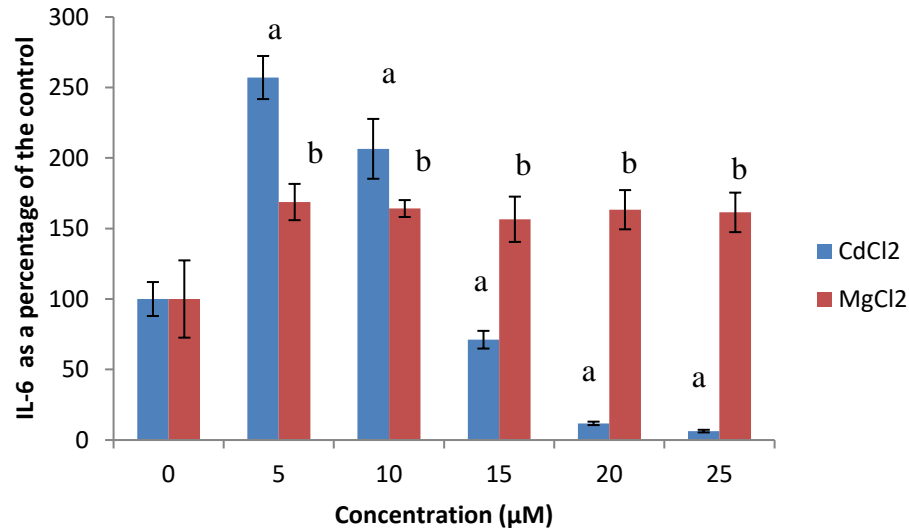
Figure 3.5. IL-6 levels of RAW 264.7 cell cultures exposed to $CdCl_2$ and $MgCl_2$ in the presence of LPS. Unstimulated cultures did not produce IL-6 and are not presented. Data represents mean ± SD with n = 9. Bars marked with letters indicate significant differences (P < 0.01). Significance demarcated by: a- significantly different (P ≤ 0.003) compared to 0 μM $CdCl_2$, b- significantly different (P < 0.001) compared to 0 μM $MgCl_2$.

The figure shows a plot with y-axis "IL-6as a percentage of the control" ranging from 0 to 250, and x-axis "CdCl₂ (µM)" ranging from 0 to 30. The equation shown is $y = 2332.e^{-0.24x}$, $R^2 = 0.970$, $IC_{50} = 16\ \mu M$.
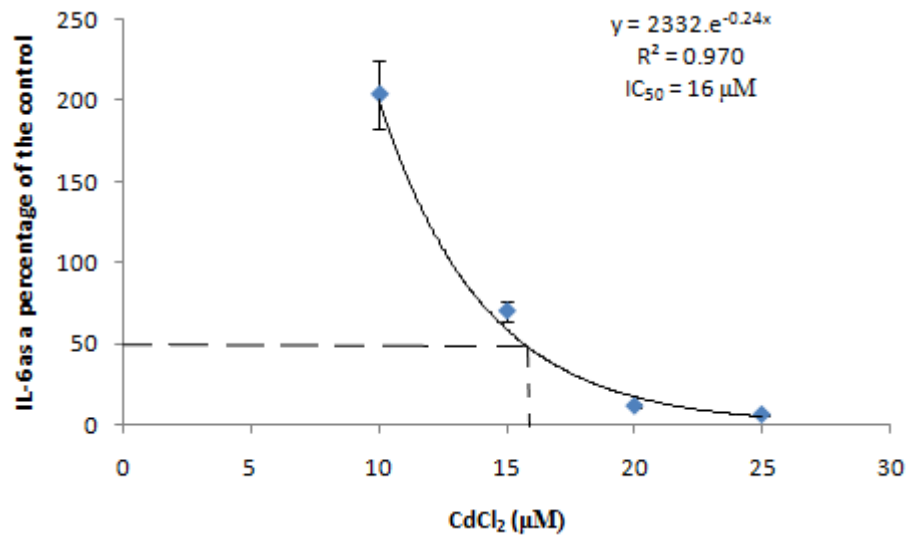
Figure 3.6. IC_{50} determination of $CdCl_2$ on IL-6 synthesis as a percentage of the 0 µM $CdCl_2$

3.3.2. The effects of $MgCl_2$ and $CdCl_2$ on cytokine synthesis by WBC

3.3.2.1. The effects of $MgCl_2$ and $CdCl_2$ on the inflammatory biomarker IL-6 using WBC

Whole blood cell cultures not stimulated by LPS did not synthesize any IL-6 (results not shown). Exposure to high concentrations of $CdCl_2$ (250 and 500 µM) significantly inhibited ($P < 0.001$) IL-6 synthesis by 70 and 90 % respectively when compared to 0 µM $CdCl_2$ (Figure 3.7). The IC_{50} of $CdCl_2$ for IL-6 synthesis by WBC was 220 µM (Figure 3.8). The control metal $MgCl_2$ had no effect on the production of IL-6 at all concentrations, bar one (7.8125 µM) which elicited a slightly higher IL-6 synthesis from the WBC (Figure 3.7).

70
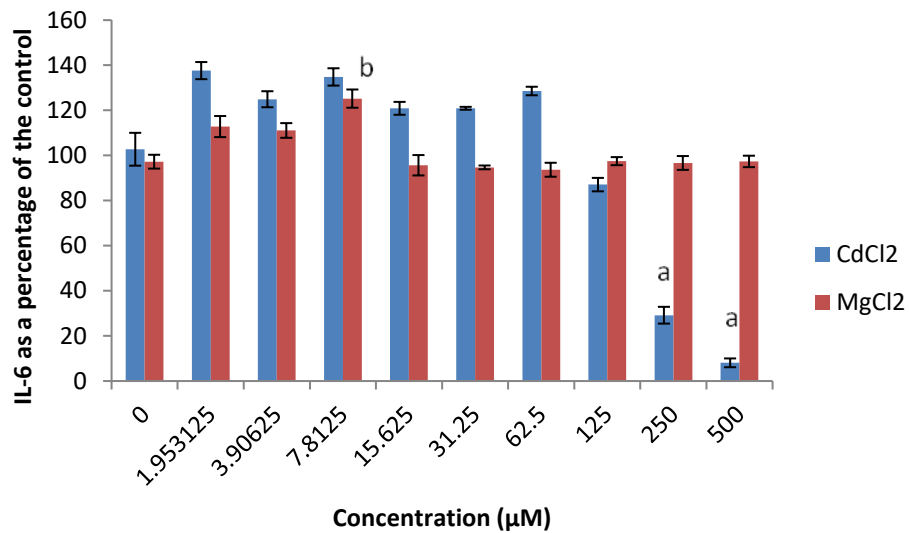
Figure 3.7. The effect of CdCl$_2$ and MgCl$_2$ on IL-6 synthesis by LPS stimulated whole blood cell (WBC) cultures. Data are presented as mean ± SD (n = 9). Unstimulated WBC cultures did not synthesize IL-6 (data not presented). Bars marked with letters indicate significant difference (P < 0.01) to control. Significance demarcated by: a- significantly different (P < 0.001) compared to 0 µM CdCl$_2$, b-significantly different (P < 0.001) compared to 0 µM MgCl$_2$
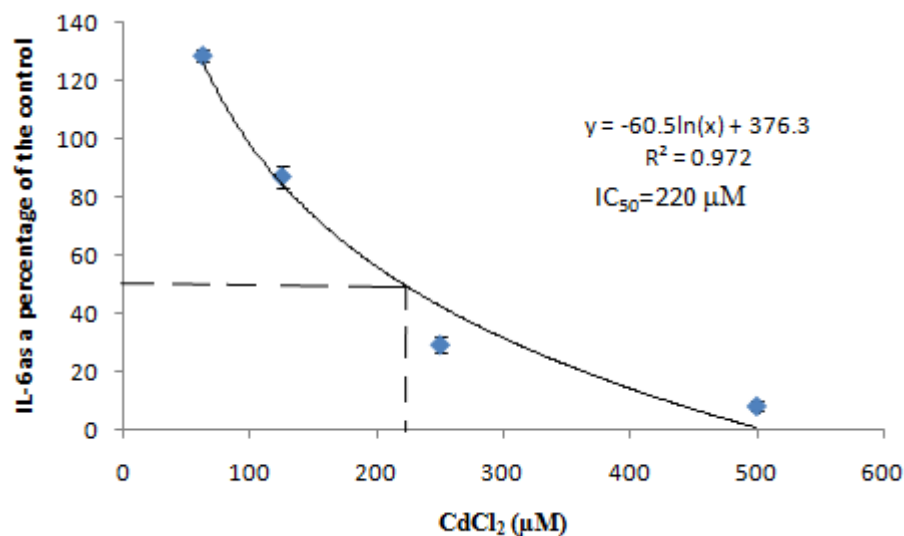
Figure 3.8. IC$_{50}$ determination of CdCl$_2$ on IL-6 production by LPS stimulated WBC as a percentage of the 0 µM CdCl$_2$

3.3.2.2. The effects of MgCl$_2$ and CdCl$_2$ on the humoral immunity biomarker IL-10 using WBC

Exposure to CdCl$_2$ significantly decreased (P < 0.001) the synthesis of IL-10 by PHA stimulated WBC in a dose-dependent manner. The IL-10 production was lower at all CdCl$_2$ concentrations compared to the 0 µM CdCl$_2$ (Figure 3.9). At the lowest, intermediate and highest concentration (1.95, 31.25 and 500 µM) CdCl$_2$ reduced the synthesis of IL-10 from the WBC by approximately 10, 40 and 100 % (Figure 3.9). The IC$_{50}$ of CdCl$_2$ for the inhibition of IL-10 synthesis was 54 µM (Figure 3.10). The control metal MgCl$_2$ had no effect on IL-10 synthesis (Figure 3.9). Cultures that were not stimulated with PHA did not produce any IL-10 (results not shown).
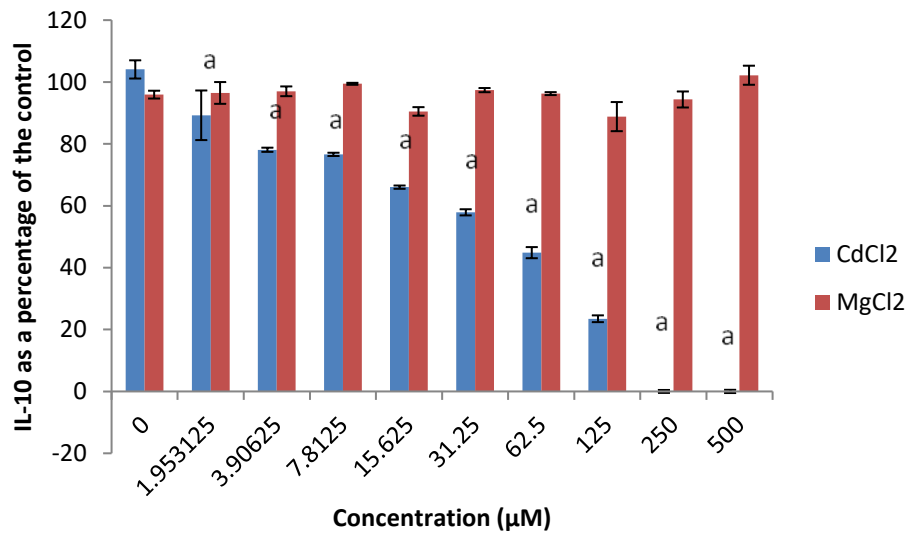
Figure 3.9. The effect of $CdCl_2$ and $MgCl_2$ on IL-10 synthesis by PHA stimulated whole blood cell (WBC) cultures. Data are presented as mean ± SD (n = 9). Unstimulated WBC cultures did not synthesize IL-10 (data not presented). Bars marked with letters indicate significant difference (P < 0.01) to control. Significance demarcated by: a- significantly different (P < 0.001) compared to 0 µM $CdCl_2$.
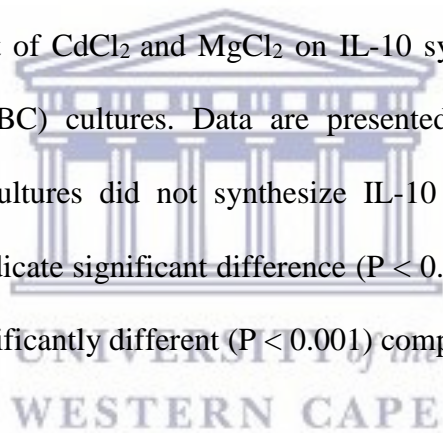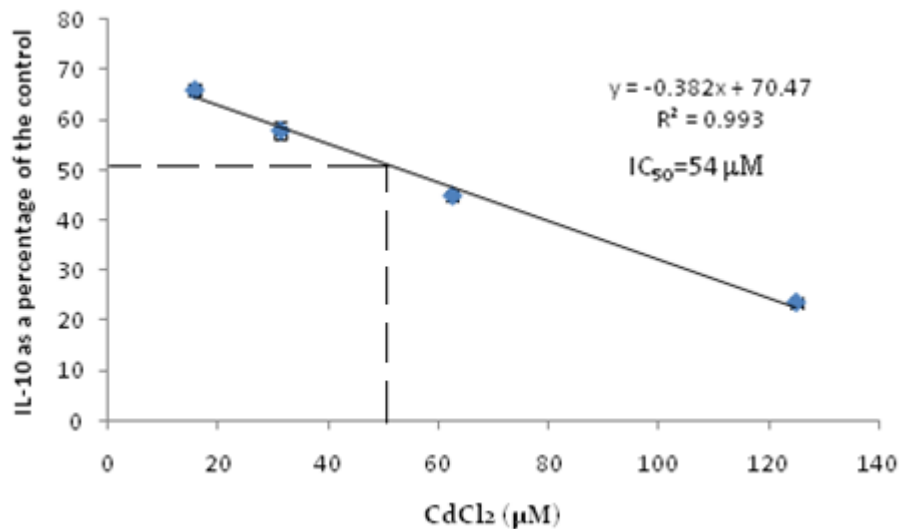
Figure 3.10. IC_{50} determination of $CdCl_2$ IL-10 production by PHA stimulated WBC as a percentage of the 0µM $CdCl_2$

3.3.2.3. The effects of $MgCl_2$ and $CdCl_2$ on the cell mediated immunity biomarker IFNγ using WBC

$CdCl_2$ at concentrations ≤ 62.5µM had no effect on IFNγ synthesis by PHA stimulated WBC compared to the 0 µM $CdCl_2$ controls. However, $CdCl_2$ concentrations of ≥ 125 µM significantly reduced ($P < 0.001$) IFNγ synthesis by ≥ 35 % in PHA stimulated WBC compared to control cultures (Figure 3.11). The IC_{50} of $CdCl_2$ for the inhibition of IFNγ synthesis was 155 µM (Figure 3.12). The addition of $MgCl_2$ to culture medium had no effect on IFNγ synthesis by PHA stimulated cultures compared to the 0 µM $MgCl_2$ control (Figure 3.11). Unstimulated cultures did not synthesize IFNγ (results are not shown).

74
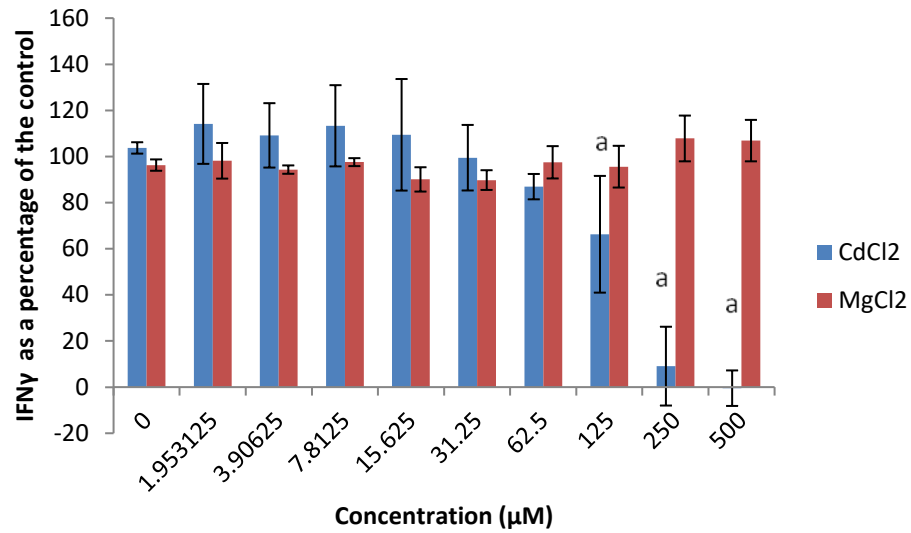
Figure 3.11. The effect of CdCl$_2$ and MgCl$_2$ on IFNγ synthesis by PHA stimulated whole blood cell (WBC) cultures. Data are presented as mean ± SD (n = 9). Unstimulated WBC cultures did not synthesise IFNγ (data not presented). Bars marked with letters indicate significant difference (P < 0.01) to control. Significance demarcated by: a- significantly different (P < 0.001) compared to 0 µM CdCl$_2$.
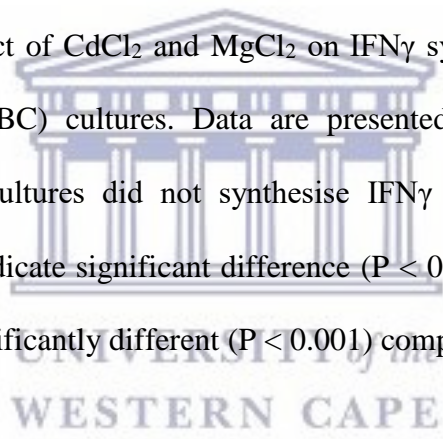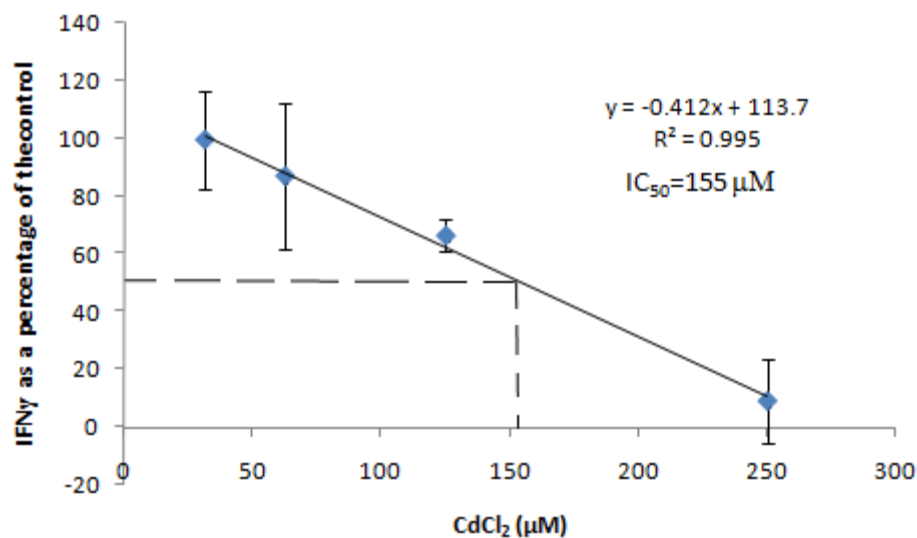
Figure 3.12. IC_{50} determination of $CdCl_2$ IFNγ production by PHA stimulated WBC as a percentage of the 0 µM $CdCl_2$

3.3.3. The effects of KNO_3 and $AgNO_3$ on RAW 264.7 cells

3.3.3.1. Cytotoxicity

Cytotoxicity of the RAW cells exposed to concentrations > 25 µM $AgNO_3$ resulted in a 100 % cell death (P < 0.001) when compared to the control 0 µM $AgNO_3$ (Figure 3.13). Concentrations ≤ 25 µM $AgNO_3$ exhibited no significant effects on cell viability and this trend was also seen across all the concentrations for KNO_3 (Figure 3.13).
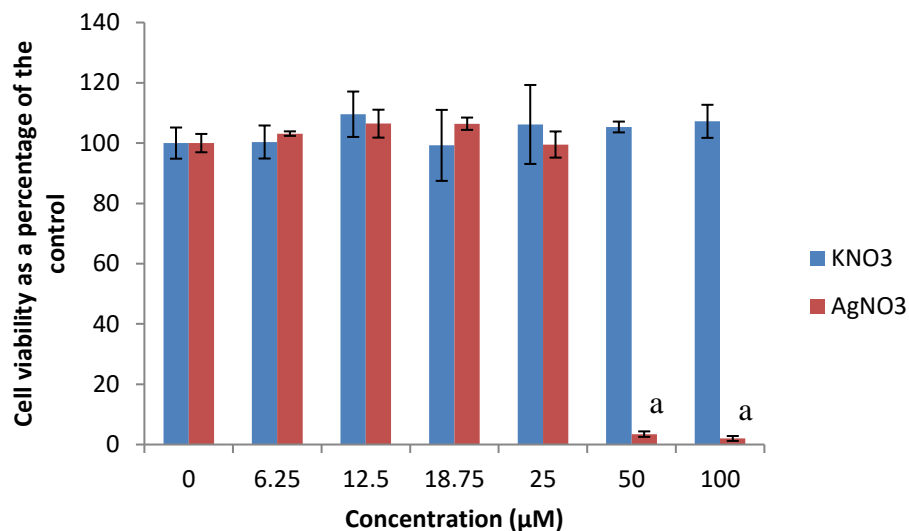
Figure 3.13. Cell viability of RAW 264.7 macrophage cells exposed to $AgNO_3$ and KNO_3. Data represents mean percentage $\pm$ SD with n = 9. Bars marked with letters indicate significant difference (P < 0.01) to control. Significance demarcated by: a- significantly different (P < 0.001) compared to 0 μM $AgNO_3$.

3.3.3.2. The effects of KNO_3 and $AgNO_3$ on the inflammatory biomarker NO using RAW 264.7 cells

Exposure of RAW cells to concentrations $\geq$ 18.75 μM $AgNO_3$ resulted in a significant reduction (P < 0.001) in NO of more than a 70 % (Figure 3.14) and resulted in an IC_{50} of 15.78 μM (Figure 3.15). Concentrations $\leq$ 12.5 μM $AgNO_3$ had no effect on the production of NO compared to the control. The control metal, KNO_3 did not affect NO production from the RAW cells (Figure 3.14). Data for unstimulated cultures are not shown as they did not produce NO.
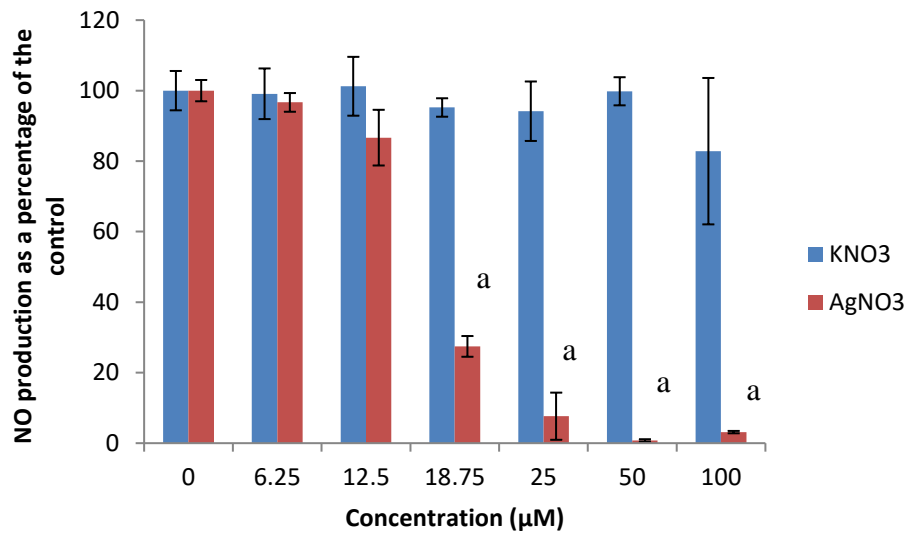
Figure 3.14. NO levels of RAW 264.7 cell cultures exposed to $AgNO_3$ and KNO_3 in the presence of LPS. Unstimulated cultures did not produce NO (data not presented). Data represents mean percentage $\pm$ SD with n = 9. Bars marked with letters indicate significant differences (P < 0.01). Significance demarcated by: a- significantly different (P < 0.001) compared to 0 μM $AgNO_3$.

The graph shows:
$y = 1003.e^{-0.19x}$
$R^2 = 0.999$
$IC_{50} = 15.78\ \mu M$
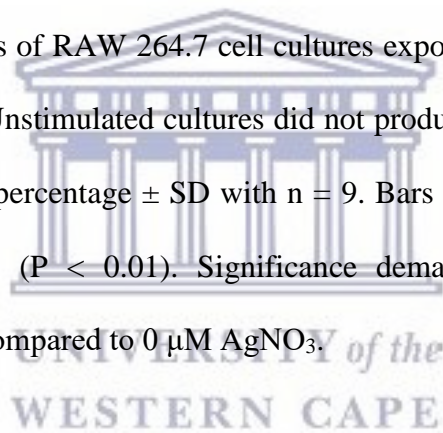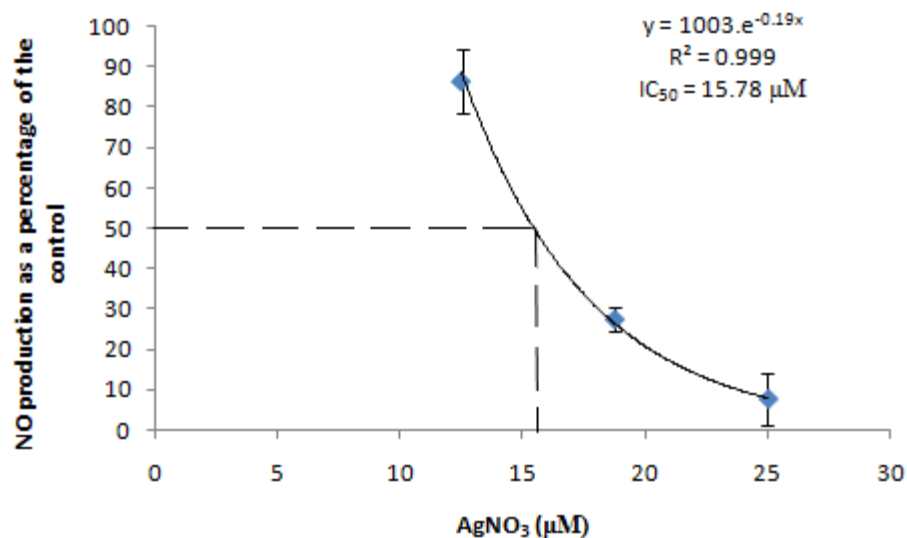
Figure 3.15. IC_{50} determination of $AgNO_3$ on NO production as a percentage of the 0 µM $CdCl_2$

3.3.3.3. The effects of KNO_3 and $AgNO_3$ on the inflammatory biomarker IL-6 using RAW 264.7 cells

The production of IL-6 (Figure 3.16) followed the same trend to that of the NO (Figure 3.14) for RAW cells exposed to $AgNO_3$. $AgNO_3$ reduced the production of IL-6 considerably (P < 0.001) by more than 50 % at concentrations ≥ 18.75 µM (Figure 3.16) and resulted in an IC_{50} of 18.86 µM (Figure 3.17). The production of IL-6 was not affected when exposed to KNO_3 (Figure 3.16). Cultures not stimulated by LPS did not synthesize any IL-6 when exposed to the metal salts and therefore the data is not presented.

79
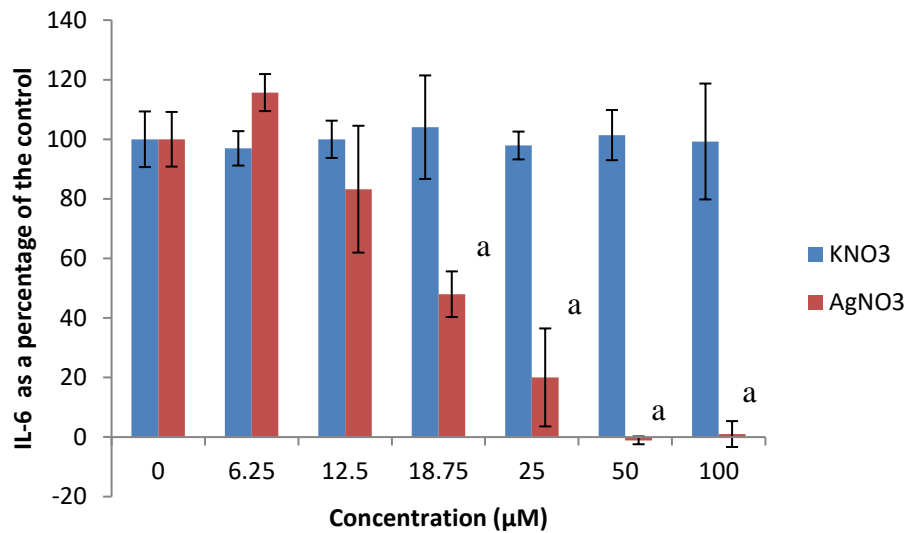
Figure 3.16. IL-6 levels of RAW 264.7 cell cultures exposed to $AgNO_3$ and KNO_3 in the presence of LPS. Unstimulated cultures did not produce IL-6 (data not presented). Data represents mean ± SD with n = 9. Bars marked with letters indicate significant differences (P < 0.01). Significance demarcated by: a- significantly different (P < 0.001) compared to 0 μM $AgNO_3$.
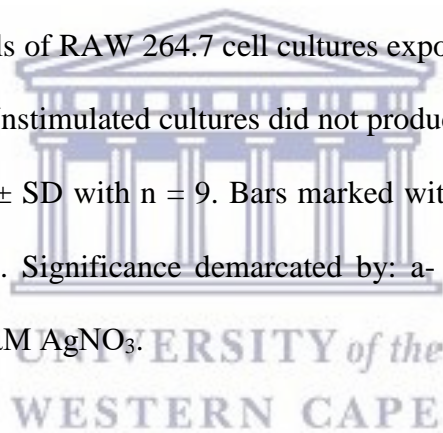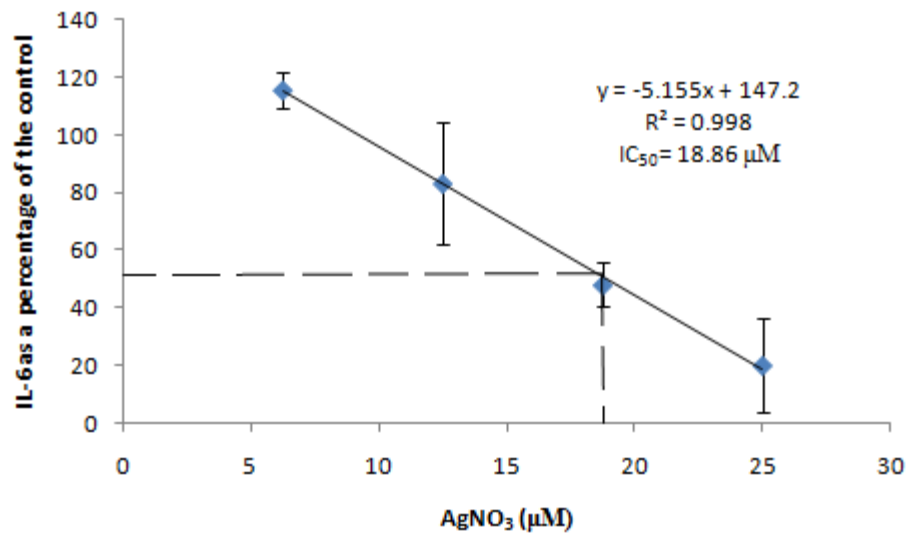
Figure 3.17. IC_{50} determination of $AgNO_3$ on IL-6 production on LPS stimulated RAW cells as a percentage of the 0 µM $AgNO_3$.

3.3.4. The effects of KNO_3 and $AgNO_3$ on cytokines production of WBC

3.3.4.1. The effects of KNO_3 and $AgNO_3$ on the inflammatory biomarker IL-6 using WBC

IL-6 was used as a biomarker to monitor the effects of $AgNO_3$ and KNO_3 on the inflammatory response. The addition of the metals to unstimulated WBCs had no effects on the inflammatory response (results not shown). The results for IL-6 secretion in stimulated WBCs are depicted in Figure 3.18. When $AgNO_3$ was added to stimulated WBCs, it was found to significantly increase ($P < 0.001$) IL-6 secretion at concentrations ≥ 1.5625 µM by more than 10 % compared to the control. Unlike the various concentrations of $AgNO_3$, the control metal KNO_3 had no effect on the secretion of IL-6 across all concentrations.

81
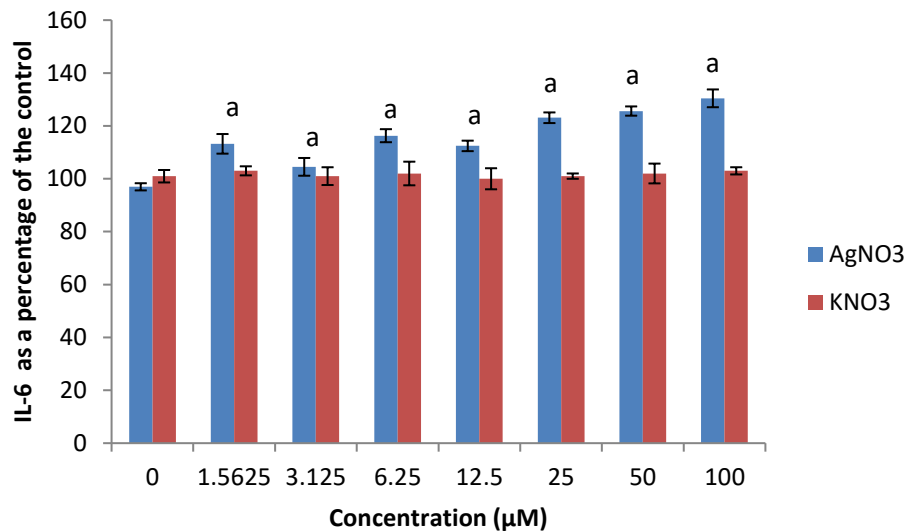
Figure 3.18. IL-6 production by human whole blood cell cultures exposed to $AgNO_3$ and KNO_3 in the presence of LPS. Data represents mean ± SD with n = 9. Unstimulated WBC cultures did not synthesize IL-6 (data not presented). Bars marked with letters indicate significant differences ($P < 0.01$) to control. Significance demarcated by: a- significantly different ($P < 0.001$) compared to 0 μM $AgNO_3$.

3.3.4.2. The effects of KNO_3 and $AgNO_3$ on the humoral immunity biomarker IL-10 using WBC

IL-10 was used as the biomarker to monitor humoral immunity in response to being exposed to $AgNO_3$ and KNO_3. The samples had no effect on IL-10 secretion by unstimulated cells (data not shown). However, IL-10 secretion by stimulated WBC was modulated by $AgNO_3$ (Figure 3.19). In the presence of the stimulus PHA, $AgNO_3$ significantly reduced ($P < 0.001$) the secretion of IL-10 at 100 μM by 55 % and resulted in an IC_{50} of 99.4 μM (Figure 3.20). However, the synthesis of IL-10

82

was notably upregulated (P < 0.001) by 20 % at 6.25 µM when compared to the control. The control metal KNO_3 across all concentrations had no notable effect on IL-10 secretion.
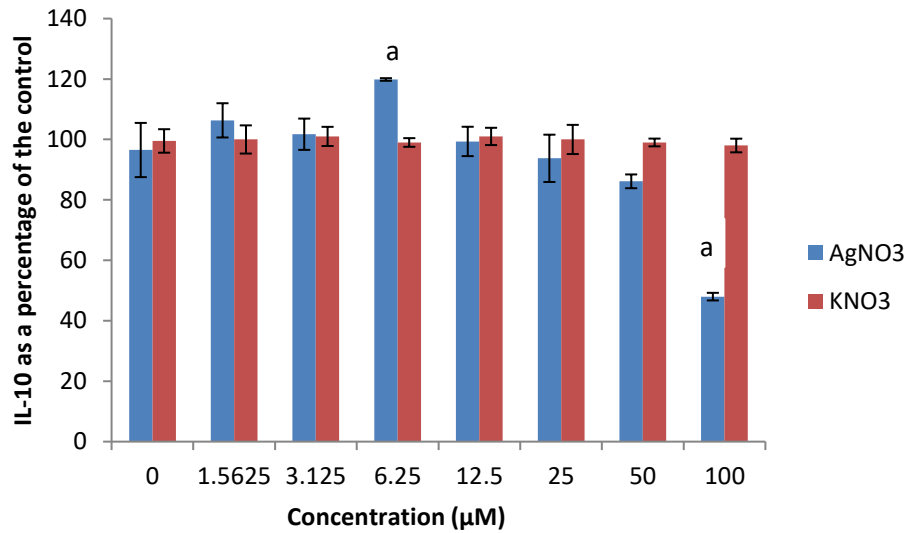
Figure 3.19. IL-10 production by human whole blood cell cultures exposed to $AgNO_3$ and KNO_3 in the presence of PHA. Data represents mean ± SD with n = 9. Unstimulated WBC cultures did not synthesize IL-10 (data not presented). Bars marked with letters indicate significant differences (P < 0.01) to control. Significance demarcated by: a- significantly different (P < 0.001) compared to 0 µM $AgNO_3$.
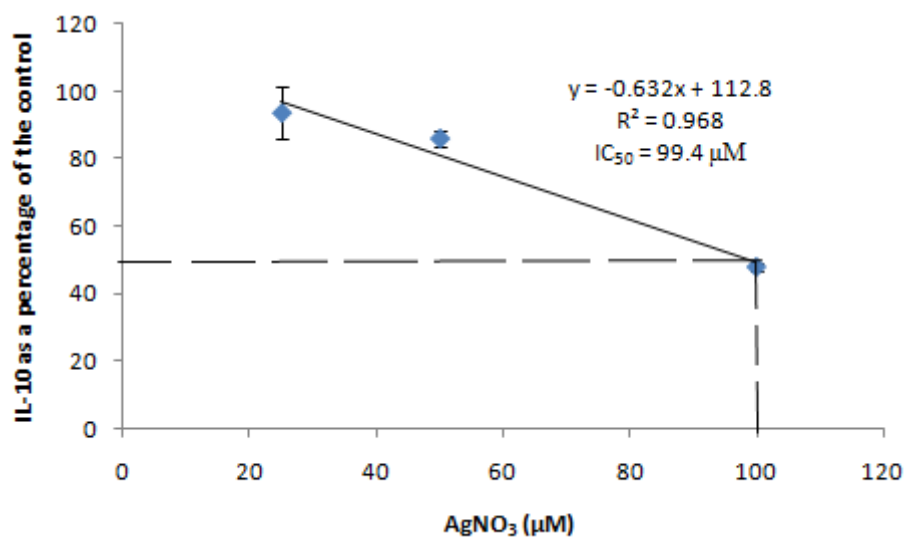
Figure 3.20. IC_{50} determination of $AgNO_3$ IL-10 production by PHA stimulated WBC as a percentage of the 0µM $AgNO_3$

3.3.4.3. The effects of KNO_3 and $AgNO_3$ on the cell mediated immunity biomarker IFNγ using WBC

IFNγ was used as the biomarker to monitor cell mediated immunity. $AgNO_3$ and KNO_3 had no effect on IFNγ secretion by unstimulated WBC and therefore, the results are not shown. Graphs showing the results for the stimulated cultures are shown in Figure 3.21. IFNγ secretion was inhibited ($P < 0.001$) at concentrations ≥ 3.125 µM $AgNO_3$ when compared to the control. The reduction of IFNγ ranged from approximately 5 - 25 % (Figure 3.21), due to this reduction an IC_{50} of 122.6 µM was determined (Figure 3.22). KNO_3 had no effects on IFNγ at the concentrations investigated.
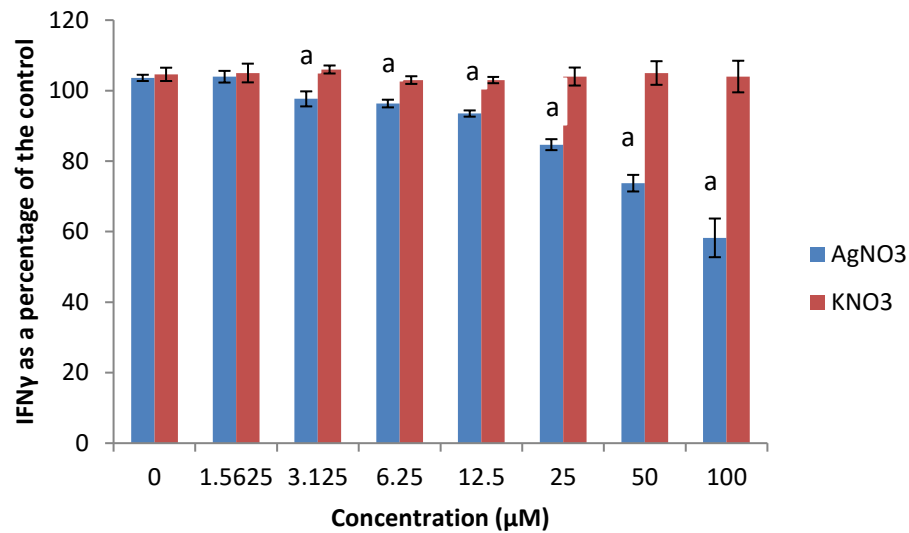
Figure 3.21. IFNγ production by human whole blood cell cultures exposed to AgNO$_3$ and KNO$_3$ in the presence of PHA. Data represents mean ± SD with n = 9. Unstimulated WBC cultures did not synthesize IFNγ (data not presented). Bars marked with letters indicate significant differences (P < 0.01) to control. Significance demarcated by: a- significantly different (P <0.001) compared to 0 μM AgNO$_3$.
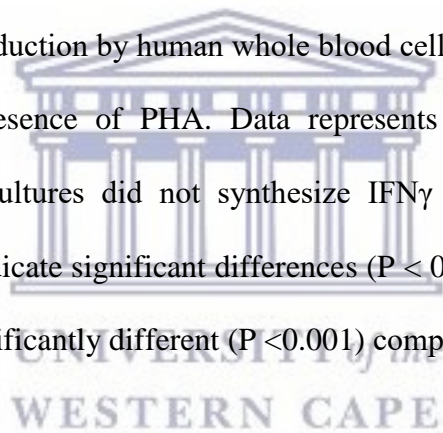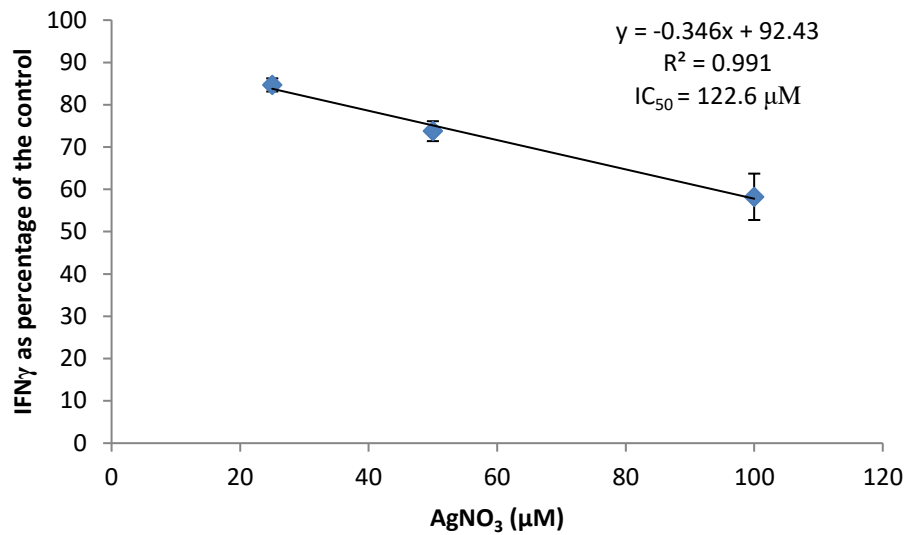
Figure 3.22. IC_{50} determination of $AgNO_3$ IFNγ production by PHA stimulated WBC as a percentage of the 0μM $AgNO_3$

3.3.5. The effects of K_2SO_4 and $CuSO_4$ on RAW 264.7 cells

3.3.5.1. Cytotoxicity

The K_2SO_4 and $CuSO_4$ did not affect cell viability of RAW 264.7 cells at all concentrations monitored in this study (Figure 3.23).
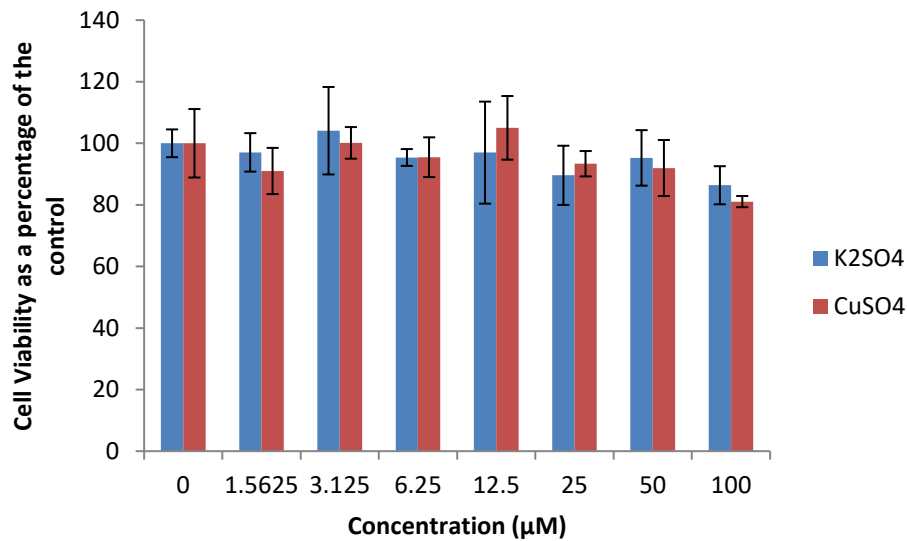
Figure 3.23. Cell viability of RAW 264.7 macrophage cells exposed to K_2SO_4 and $CuSO_4$. Data represents mean percentage $\pm$ SD with n = 9.

3.3.5.2. The effects of K_2SO_4 and $CuSO_4$ on the inflammatory biomarker NO using RAW 264.7 cells

Similarly to the cell viability (Figure 3.23), data obtained shows that K_2SO_4 and $CuSO_4$ did not modulate the production of NO by RAW cells under stimulated conditions (Figure 3.24). RAW cells not stimulated with LPS did not produce NO in the presence of the metals (results not shown).
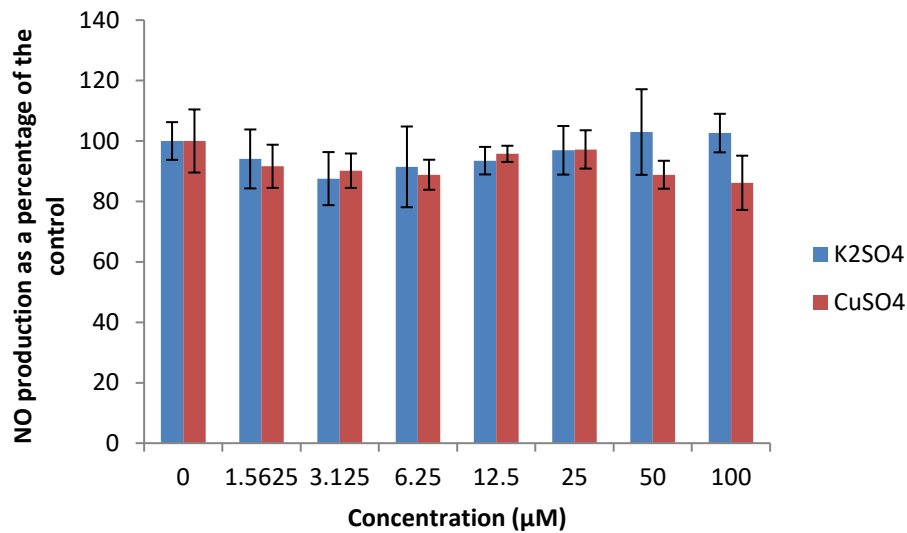
Figure 3.24. NO levels of RAW 264.7 cell cultures exposed to K_2SO_4 and $CuSO_4$ in the presence of LPS. Unstimulated cultures did not produce NO (data not presented). Data represents mean percentage ± SD with n = 9.

3.3.5.3. The effects of K_2SO_4 and $CuSO_4$ on the inflammatory biomarker IL-6 using RAW 264.7 cells

The IL-6 data obtained from exposing RAW cells to K_2SO_4 and $CuSO_4$ under stimulated conditions followed the same trend as the cell viability and NO data, (Figures 3.23 and 3.24) where the metals had no impact on the synthesis of the pro-inflammatory cytokine (Figure 3.25). These metal salts did not affect the synthesis of IL-6 in cultures not stimulated by LPS (results not shown).
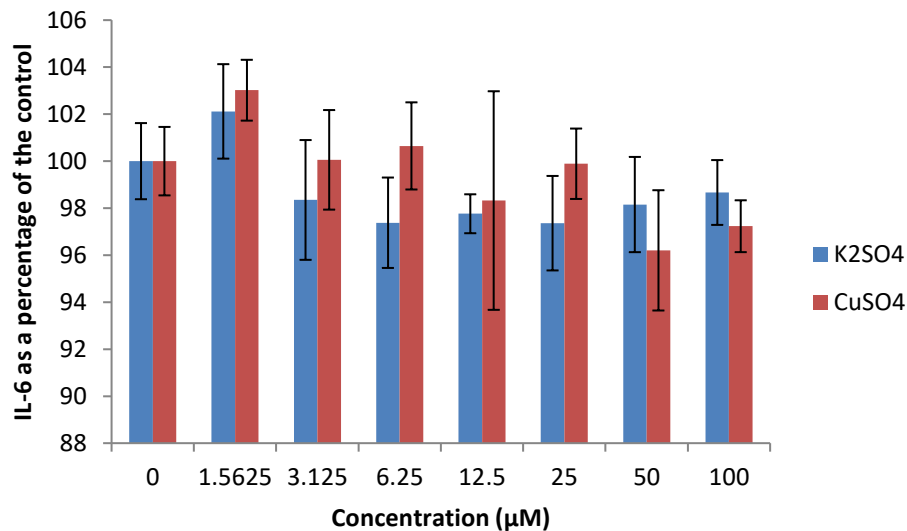
Figure 3.25. IL-6 levels of RAW 264.7 cell cultures exposed to K_2SO_4 and $CuSO_4$ in the presence of LPS. Unstimulated cultures did not produce IL-6 (data not presented). Data represents mean ± SD with n = 9.

3.3.6. The effects of K_2SO_4 and $CuSO_4$ on cytokines production of WBC

3.3.6.1. The effects of K_2SO_4 and $CuSO_4$ on the inflammatory biomarker IL-6 using WBC

Whole blood cell cultures exposed to K_2SO_4 and $CuSO_4$ in unstimulated conditions did not elicit an inflammatory response. Exposure to concentrations ≥ 12.5 μM $CuSO_4$ significantly inhibited (P < 0.001) the synthesis of IL-6 when compared to the positive control by more than 10 % across the above mentioned concentration range (Figure 3.26). The extrapolated IC_{50} of $CuSO_4$ for IL-6 synthesis was 279 μM (Figure 3.27). The control metal, K_2SO_4 at concentrations of 1.625 and 6.25 μM was notably (P < 0.001) different in synthesizing ≥ 10 % IL-6 compared to the positive control,

89

whereas there was no difference in the synthesis of IL-6 at the other concentrations (Figure 3.26).
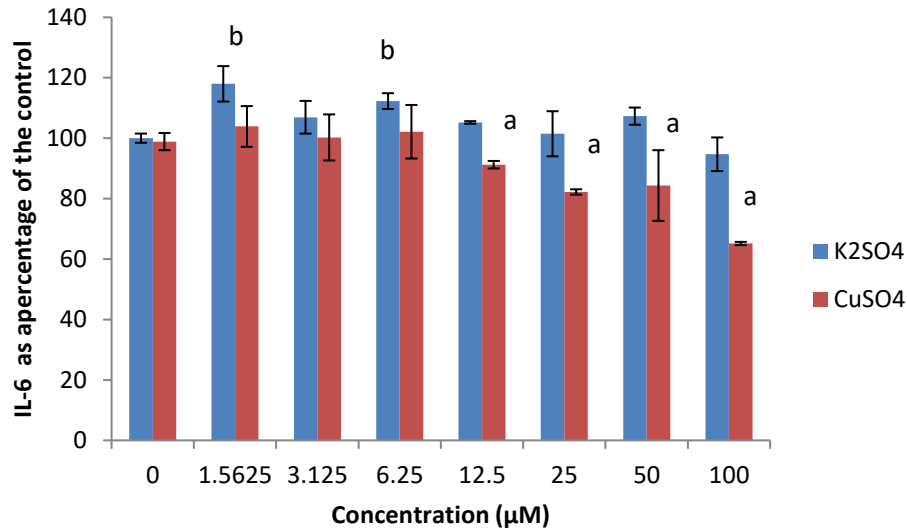
Figure 3.26. IL-6 production by human whole blood cell cultures exposed to K_2SO_4 and $CuSO_4$ in the presence of LPS. Data represents mean $\pm$ SD with n = 9. Unstimulated cultures did not produce IL-6 (data not presented). Bars marked with letters indicate significant differences (P < 0.01) to control. Significance demarcated by: a- significantly different (P < 0.001) compared to 0 μM $CuSO_4$, b- significantly different (P < 0.001) compared to 0 μM K_2SO_4.

The chart shows a plot with y-axis labeled "IL-6 as a percentage of the control" ranging from 0 to 120, and x-axis labeled "CuSO₄ (µM)" ranging from 0 to 120. The trendline equation and statistics shown:

$$y = -0.174x + 98.51$$
$$R^2 = 0.997$$
$$IC_{50} = 279\ \mu M$$
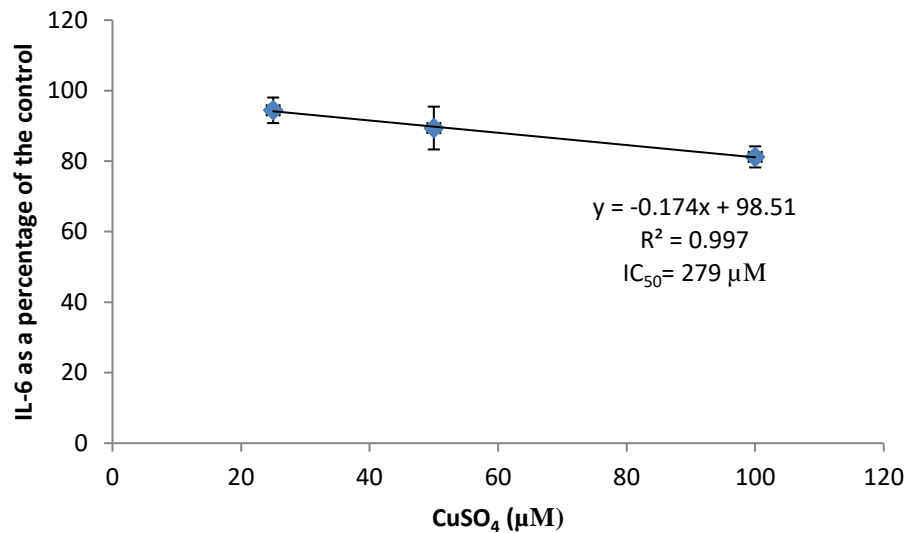
Figure 3.27. IC_{50} determination of $CuSO_4$ IL-6 production by LPS stimulated WBC as a percentage of the 0µM $CuSO_4$.

3.3.6.2. The effects of K_2SO_4 and $CuSO_4$ on the humoral immunity biomarker IL-10 using WBC

Exposure to $CuSO_4$ significantly decreased ($P < 0.007$) the synthesis of IL-10 in PHA stimulated WBC when exposed to concentrations ≥ 12.5 µM when compared to the positive control (Figure 3.28). The reduction in IL-10 synthesis ranged from 10 – 30 % when exposed to the concentration range 12.5 – 100 µM $CuSO_4$. The IC_{50} of $CuSO_4$ for IL-10 synthesis was 211 µM (Figure 3.29). The control metal K_2SO_4 notably increased ($P < 0.008$) the synthesis of IL-10 at 6.25 µM, and slightly decreased IL-10 synthesis at 100 µM when compared to the positive control (Figure 3.28). These metals did not affect the synthesis of IL-10 in cultures not stimulated by PHA.

91
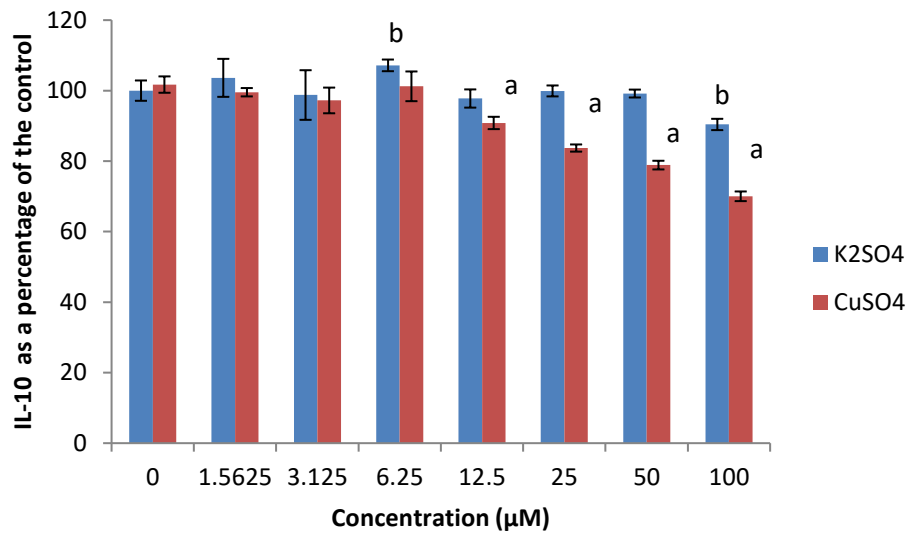
Figure 3.28. IL-10 production by human whole blood cell cultures exposed to K_2SO_4 and $CuSO_4$ in the presence of PHA. Data represents mean ± SD with n = 9. Unstimulated cultures did not produce IL-10 (data not presented). Bars marked with letters indicate significant differences (P < 0.01) to control. Significance demarcated by: a- significantly different (P < 0.007) compared to 0 μM $CuSO_4$, b- significantly different (P < 0.008) compared to 0 μM K_2SO_4.
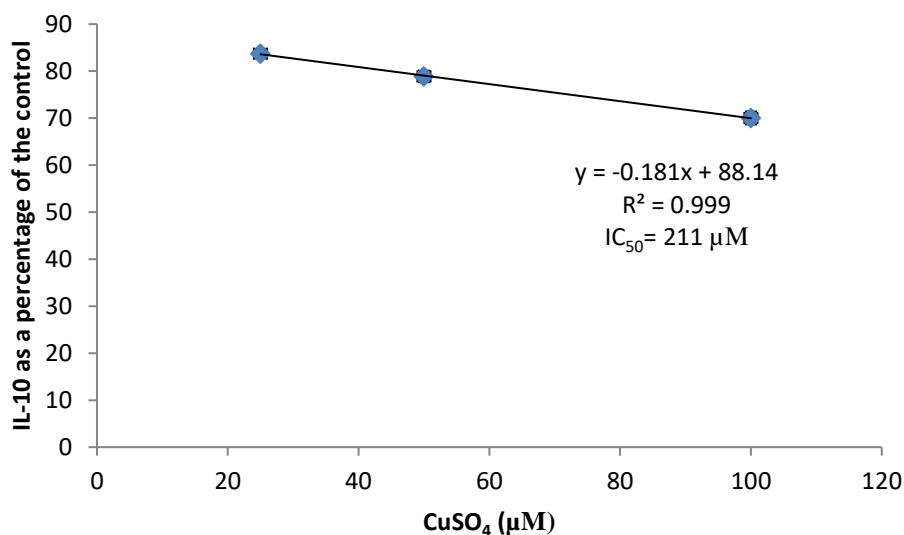
Figure 3.29. IC$_{50}$ determination of CuSO$_4$ IL-10 production by PHA stimulated WBC as a percentage of the 0µM CuSO$_4$.

3.3.6.3. The effects of K$_2$SO$_4$ and CuSO$_4$ on the cell mediated biomarker IFNγ using WBC

Unstimulated cultures exposed to the above mentioned metals did not affect IFNγ synthesis. The PHA stimulated WBC exposed to concentrations ≤ 6.25 µM CuSO$_4$ had no effect on the synthesis of IFNγ compared to the positive control. However, CuSO$_4$ concentrations ≥ 12.5 µM considerably reduced ($P < 0.001$) the synthesis of IFNγ by more than 20 % in PHA stimulated WBC compared to the control cultures (Figure 3.30). The IC$_{50}$ of CuSO$_4$ for IFNγ synthesis was 95 µM (Figure 3.31). The control metal K$_2$SO$_4$ significantly increased ($P < 0.001$) the synthesis of IFNγ by more than 30 % in PHA stimulated WBC at concentrations above 50 µM when compared to the positive control (Figure 3.30).
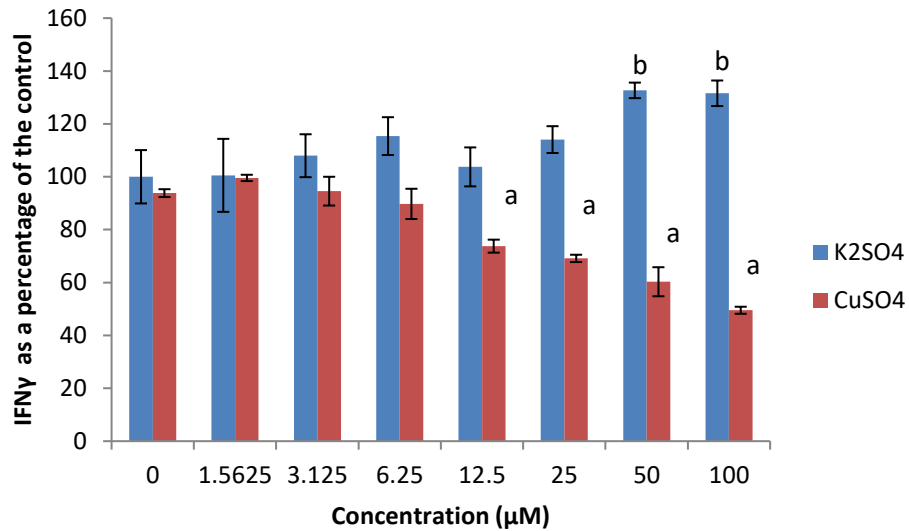
93

Figure 3.30. IFNγ production by human whole blood cell cultures exposed to K_2SO_4 and $CuSO_4$ in the presence of PHA. Data represents mean ± SD with n = 9. Unstimulated cultures did not produce IFNγ (data not presented). Bars marked with letters indicate significant differences (P < 0.01) to control. Significance demarcated by: a- significantly different (P < 0.001) compared to 0 μM $CuSO_4$, b- significantly different (P < 0.001) compared to 0 μM K_2SO_4.

94
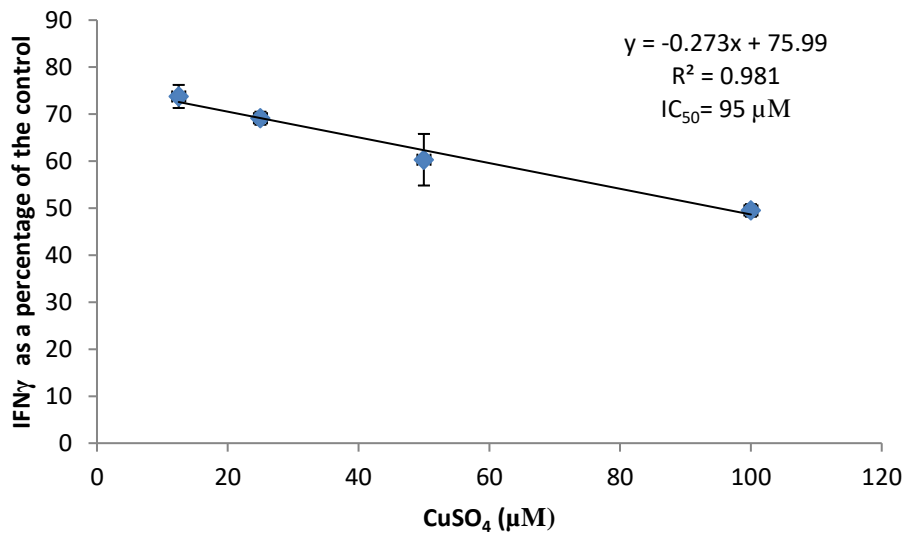
Figure 3.31. IC$_{50}$ determination of CuSO$_4$ IFNγ production by PHA stimulated WBC as a percentage of the 0µM CuSO$_4$.

3.4. Discussion and conclusion

Human whole blood cell culture contains a heterogeneous population of cells and contains all the vital components for the stimulation of both the innate and acquired immune system (Gill et al., 2016). The experimental conditions used for this study mimick an *in vivo* environment. RAW 264.7 is a macrophage line producing several inflammatory cytokines and chemokines upon stimulation with an inflammatory stimulus (He et al., 2011). The WBC and RAW cells have previously been used to study the effects of heavy metals on immune responses under *in vitro* experimental conditions (Marth et al., 2001, Riemschneider et al., 2015). Exposure of the heavy metals to RAW cells and WBCs would also allow for the various sensitivities of the heavy metals to the cell sub-sets to be evaluated.

95

Evaluating the acute effects of Cd, Ag and Cu on RAW cells revealed Cd (IC_{50} = 21.9 μM) to be more cytotoxic than Ag, as Ag only became cytotoxic at concentrations > 25 μM, while Cu had no cytotoxic effects. Exposure to cadmium and silver *in vitro* reduced cell viability in a number of other cell types. These cell types include Jurkat T cells (Colombo et al., 2004, Eom and Choi, 2010), liver cells (Baldi et al., 1988, Ye et al., 2007), human T, B and lymphoidblastoid cells (Tsangaris and Tzortzatou-Stathopoulou, 1998); human dermal fibroblasts (Hidalgo and Domınguez, 1998); human leukocytes (Jansson and Harms-Ringdahl, 1993) and murine macrophage cells (J774.1) (Arai et al., 2015). The mechanism of action resulting in Cd and Ag toxicity is poorly understood. The reduction in cell viability could be due to the ion interaction with a number of biomolecules such as nucleic acids, cell wall components, metallothioneins (MTs), glutathione (GSH), the production of highly reactive chemical entities such as free radicals which include reactive oxygen species (ROS), oxidation of sulphydryl groups of proteins, depletion of proteins, deoxyribonucleic acid (DNA) damage, and lipid peroxidation which can all lead to cellular dysfunction (Herzog et al., 2013, Arai et al., 2015, Jan et al., 2015).

Since Cd has a stronger affinity for MT than zinc (Zn), Cd can easily replace Zn in MT which inhibits MT from acting as a free radical scavenger within the cell (Jaishankar et al., 2014). Silver ions have a strong tendency to interact with thiol groups of important enzymes and phosphorous containing bases. Silver also induces free radicals and leads to membrane and DNA damage (Herzog et al., 2013).

96

Contrary to what was found in this study, copper has been reported to reduce cell viability in human epithelial and liver cells when Cu homeostasis is disrupted (Rossi et al., 1996, Steiner et al., 1998).

Similar effects were seen for the inhibition of inflammatory biomarkers NO and IL-6. Cadmium was the most potent in inhibiting NO and IL-6. Silver affected NO and IL-6 production at higher concentrations, while Cu had no effect on these biomarkers at the concentrations investigated. Haase et al. (2010) has reported that Cd can cause immunomodulation at sub-toxic concentrations. This was also evident in the current study when examining IL-6 levels, as this inflammatory biomarker is upregulated at non-toxic concentrations of Cd (5 and 10 μM). Jin et al. (2016) also reported an upregulation of inflammatory biomarkers when RAW cells were exposed to Cd for 6 hrs and the down-regulation of inflammatory biomarkers when exposed to Cd for 24 hrs. In this study, similar results were seen when RAW cells were exposed to Cd for 18 hrs.

Exposure of the metals to WBCs yielded contradictory inflammatory responses compared to the RAW cells. Cadmium inhibited an inflammatory response at concentrations $\geq$ 250 μM (IC_{50}= 220 μM), while Ag upregulated inflammatory responses across all concentrations. Copper suppressed the synthesis of IL-6 at concentrations $\geq$ 12.5 μM (IC_{50} = 279 μM). Therefore, indicating that an inflammatory response from the WBCs is more sensitive to Cu and Cd exposure than Ag. The RAW cells were more sensitive to Cd and Ag exposure compared to Cu. Inflammation is a vital protective response to cell or tissue damage. The function of

inflammation is to destroy and remove the agent causing the damage and the affected cell/tissues, in so doing, promoting repair of the affected area. However, if this process occurs uncontrollably, it could result in excessive cell or tissue damage that results in chronic inflammation and the damage of normal cells or tissues (Rahman and MacNee, 2000). Silver caused an upregulation of IL-6, and if it is sustained over a period of time, chronic effects could occur. IL-6 was reduced by Cu and Cd, which could result in the inability to mount an effective inflammatory response.

The humoral immunity cytokine, IL-10 proved to be very sensitive to Cd, which reduced the synthesis of IL-10 in a dose dependent manner (IC$_{50}$= 54 μM). Copper reduced IL-10 at concentrations ≥ 12.5 μM, (IC$_{50}$= 211 μM), while Ag only reduced IL-10 synthesis at 100 μM. Humoral immunity protects an individual from extracellular pathogens, such as bacteria and parasites (McGlauchlen & Vogel, 2003). Humoral immunity employs B-lymphocytes/cells which produce antibodies to recognize a specific pathogen (Brewer, 2013). This process occurs as IL-4 and IL-10 induce differentiation of Th$_0$ cells to Th$_2$ cells and these Th$_2$ cells secrete higher levels of IL-4 and IL-10. IL-4 and IL-10 are responsible for the maturation of B cells which secrete the antibodies (Maddaly et al, 2010). All the metals reduced the synthesis of IL-10, and could result in an impaired humoral immune response, as B cells have been compromised.

The cell mediated cytokine; IFNγ was inhibited by all the metals. Cadmium reduced its synthesis at concentrations ≥ 125 μM (IC$_{50}$= 155 μM), Ag in a dose dependent manner (≥ 3.125 μM) and Cu at concentrations ≥ 12.5 μM (IC$_{50}$= 95 μM). This

98

indicates that WBCs are more sensitive to Ag, followed by Cu and then Cd. Cell mediated immunity acts against intracellular pathogens such as mycobacteria, viruses and cancers (McGlauchlen & Vogel, 2003, Moser & Leo, 2010). This process is triggered by cytokines interleukin 12 and interferon gamma (IL-12 and IFNγ) secreted by T_h1 cells. IFNγ and IL-12 further activate T_c to kill cancers and infected cells (Flores et al, 2004). The cell mediated immune response of an individual would be impaired if exposed to the metals at the concentrations mentioned.

A review conducted by Mishra (2009) suggested that heavy metals interact with the immune system in an antigen non-specific manner. By doing this the metal employs direct toxicity to compounds of the immune system and this can either lead to an entire immune system malfunction or the metal disrupts its regulatory processes, which may result in exacerbated responses. All this may cause immunosuppression or immunodysregulation, which was seen in this study, as the WBCs cytokines have various sensitivities to the metals monitored. IL-6 was most sensitive to Cu, followed by Cd and then Ag. While IL-10 was most sensitive to Cd, followed by Cu, and then Ag. Where IFNγ proved to be most sensitive to Ag, followed by Cu and then Cd. Based on this, each metal would affect the innate, humoral and cell mediated immune responses slightly differently but would still impair them and the immune system as a whole. RAW cells were most sensitive to Cd, then Ag and Cu having no effects on viability, NO and IL-6. The molecular biomarkers corroborated the inflammatory data from the RAW cells. However, the exact mechanism whereby these metals exert their effects are not yet fully understood and needs to be investigated further as metals are known to have long half-lives in biological systems.

99

The effects of silver nanoparticles on RAW 264.7 macrophages and human whole blood cell cultures

Abstract

Silver nanoparticles (AgNPs) are commonly found in consumer products due to their antimicrobial properties. However, very little is known about the effects of AgNPs on the immune system. This current study evaluated the effects of AgNPs on the murine macrophage cell line RAW 264.7 and human whole blood cell cultures (WBCs). The effects of AgNPs on immune system biomarkers produced by RAW 264.7 were assessed in the presence or absence of a mitogen, lipopolysaccharide (LPS). The effects of AgNPs on immune system biomarkers produced by WBCs were monitored under basal conditions and also in the presence of either LPS or phytohaemmagglutinin (PHA). A number of parameters were evaluated for both cultures, which included cytotoxity, biomarkers of inflammation, cytokines of the acquired immune system and a proteome profile analysis. AgNP concentrations had no negative effect on RAW cell viability at concentrations used. However, cytotoxicity of WBCs was evident at 250 μg/ml. Under basal conditions, AgNPs concentrations ≥ 62.5 μg/ml and > 25 μg/ml induced inflammation in RAW cells and WBCs respectively. Under a simulated inflammatory response, 250 μg/ml AgNP inhibited the inflammatory response for both RAW and WBCs. The acquired immune

cytokines IL-10 and IFNγ were both induced by 250 μg/ml AgNP in the absence of PHA. IL-10 was partially inhibited by 250 μg/ml AgNP when evaluated in the presence of PHA. Proteome profiles of RAW cell supernatants show that AgNPs do in fact modulate specific protein synthesis. Upregulated proteins due to AgNP exposure indicate specific induction of proteins indicative of inflammatory responses and wound healing. WBCs proteome analysis indicates anti-inflammatory properties. Monitoring those proteins in future experiments will give a better indication of the effects of AgNPs.

Keywords: Silver nanoparticles, cell viability, inflammatory biomarkers, proteome analysis, cytokines and chemokines

4.1. Introduction

Commercial silver nanoparticle (AgNP) production has increased rapidly, with 420 tons produced in 2014 alone. Due to the potent antimicrobial properties of AgNPs, it is predicted production of AgNPs will increase due to consumer demands. Silver nanoparticles are commonly found in a wide range of consumer products ranging from cleaning products, food, and health and fitness products (Pulit-Prociak and Banach, 2016). Relatively little is known about toxicological risks posed by these nanoparticles on human and environmental health. Research data on the toxicological effects of AgNPs is increasing rapidly.

In vitro AgNP exposure studies have been conducted on several mammalian immune system cell line types such as human THP-1 monocytes, human peripheral blood

101

mononuclear cells (PMBCs), and the murine macrophage cell line RAW 264.7. These studies found that the smaller the diameter of the nanoparticle, the greater the toxicity and inflammatory response elicited from the cells. This was regardless of the concentration range investigated (Shin et al., 2007, Park et al., 2011, Martínez-Gutierrez et al., 2012, Yang et al., 2012). There are also conflicting reports on the effects on AgNPs where no negative effects were seen (Carlson et al., 2008, Greulich et al., 2011, Kaur and Tikoo, 2013). However, the mechanisms whereby AgNPs cause these effects are not fully understood.

It is important to understand the mechanism whereby nanoparticles interfere with biological processes to develop strategies to prevent adverse effects. Proteomics would be key in comprehending this dilemma, as proteomics plays a vital role in aiding the discovery of pathways behind certain cellular processes (Lacerda and Reardon, 2009). To date only a limited number of proteome profiles of cells treated with AgNPs have been conducted. These include various bacteria such as *Eschericia coli, Bacillus subtilis,* and *Staphylococcus aureus* to evaluate the antimicrobial properties of AgNPs (Ruparelia et al., 2008, Ivask et al., 2010). However, none has investigated the effects of AgNPs on macrophages, which is one of the first immune cells the AgNPs encounter in the immune system (Gustafson et al., 2015).

The aim of this study was to evaluate the effects of AgNPs on murine macrophages and human whole blood cell cultures (WBC) by monitoring cell viability, inflammatory biomarkers, and cytokines of the acquired immune system.

Furthermore, proteome profiling of cells were also conducted to identify potential biomarkers that can be used in future biomonitoring studies.

4.2. Materials and Methods

4.2.1. Characterization of silver nanoparticles

Silver nanoparticles were purchased from Sigma-Aldrich (Cat. No.576832) and were subsequently characterized by Walters et al. (2013). The nanoparticles were noted to be spherical. Transmission electron microscopy (TEM) of the dry particles revealed that 65 % of the silver nanoparticles were 10 nm in diameter, while a lower percentage (≤ 5 %) was between 50-100 nm. When in an aqueous solution (water), ~35 % of the particles were between 20-40 nm and ~15 % were between 70-1000 nm in diameter.
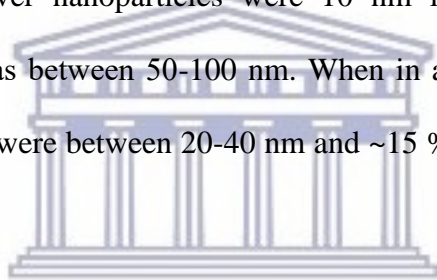
4.2.2. Preparation of silver nanoparticles

A freshly prepared stock solution (5 mg/ml) of silver nanoparticles in distilled water was used for each experiment. The nanoparticles were subjected to sonication, using a tip sonicator for 5 mins (QSonica, LLC. Misonix sonicators, XL-200 Series) prior to cellular exposures.

4.2.3. RAW 264.7 Cells

4.2.3.1. Cell Culture

The murine macrophage cell line, RAW 264.7, was obtained from American Type Culture Collection (ATCC TIB-71). Cells were maintained in Roswell Park

103

Memorial Institute 1640 (RPMI 1640) media (Sigma-Aldrich) supplemented with 5 % heat inactivated fetal bovine serum (FBS) (Biowest), glutamax (Thermofisher), gentamicin (Sigma-Aldrich) and antibiotic/antimycotic mixture (Sigma-Aldrich). Cells were grown in non-treated tissue culture flasks (SPL Life Sciences) and were subjected to standard tissue culture conditions, with sub-culturing occurring approximately every 2-3 days.

4.2.3.2. Nanoparticle exposure

Initially cells were cultured (5 x 10^5 cells/ml) in 96 well tissue culture treated plates (Falcon) in complete Dulbecco's modified Eagle's medium (DMEM) (Lonza). The complete medium was supplemented with 10 % heat inactivated FBS, glutamax, gentamicin and antibiotic/antimycotic mixture. Cells were incubated overnight at 37 °C and 5 % CO_2. Cells were then exposed to a low, intermediate and high concentration of AgNPs in various FBS concentrations. These FBS concentrations include 10, 5, 2 and 1 %. Cells were incubated in the absence or presence of lipopolysaccharide (LPS) (0.2 µg/ml). The unstimulated or stimulated samples were incubated overnight. After the overnight incubation, cytotoxicity was monitored and supernatants were immediately used for nitric oxide (NO) and interleukin 6 (IL-6) analysis.

Cells were cultured (1 x 10^6 cells/ml) in 48 well tissue culture treated plates (Falcon) in complete DMEM medium. The complete medium was supplemented with 10 % heat inactivated FBS, glutamax, gentamicin and antibiotic/antimycotic mixture. Cells were incubated overnight at 37 °C and 5 % CO_2. Cells were then pre-exposed to

104

various concentrations of AgNPs for 2 hrs. Thereafter, cells were either left unstimulated or stimulated with 0.2 μg/ml LPS. Unstimulated or stimulated samples were incubated overnight (~18 hrs) under standard tissue culture conditions. After the overnight incubation, supernatants were removed, and centrifuged at 12 100 rcf for 3 mins. Supernatants were used immediately for analysis of NO, IL-6, macrophage inflammatory protein 1α (MIP-1α), MIP-1β, MIP-2, and proteome profiling.

4.2.3.3. Cytotoxicity Assay

After the overnight incubation, supernatants were removed and cells washed with Dulbecco's Phosphate Buffered Saline (DPBS) (Lonza). Thereafter, 150 μl of a 1/10 dilution of 2-(4-Iodophenyl)-3-(4-nitrophenyl)-5-(2,4-disulfophenyl)-2H-tetrazolium (WST-1) (Roche) reagent in complete medium was added to each well. Metabolically active cells convert WST-1 reagent to a formazan that can be measured spectrophotometrically. Formazan formation was determined by reading the plate at 450 nm (Multiskan Ex, Thermo Electron Corporation) immediately after WST-1 addition and again after an incubation period of 1 hr at 37 °C. The increase in absorbance at 450 nm is proportional to formazan formation. The level of fomazan formed is directly proportional to cell viability.

4.2.3.4. Nitric Oxide (NO) Assay

This assay is based on the Griess reaction. The amount of nitrite produced by cells was determined using the supernatants. This was used as an indicator of the amount of NO produced upon exposure to the AgNPs. The total NO produced was measured

against a doubling dilution range of nitrite standard (Sigma-Aldrich), with an initial concentration of 100 μM. Nitrite standards or culture supernatant collected (100 μl) were mixed with 100 µl of Griess reagent (1:1 of 1 % sulfanilamide and 0.1 % naphtylethlemidimine-dihydrochloride in 2.5 % phosphoric acid) (all reagents obtained from Sigma-Aldrich). Thereafter, the plate was incubated at room temperature for 15 min. The absorbance was read at 540 nm using a microplate reader (Multiskan Ex, Thermo Electron Corporation). The amount of NO produced by the RAW cells quantified using a linear fitting standard curve constructed by Excel.

4.2.3.5. Mouse Interleukin 6 (IL-6) Double Antibody Sandwich Enzyme Linked Immunosorbent Assay (DAS ELISA)

A mouse IL-6 ELISA (e-Bioscience, Ready-Set-Go) kit was used to measure cytokine levels in cell culture supernatants. The kit contained all the reagents for the assay and was performed as per the manufacturer's instructions. The assay was performed in Nunc maxisorb plates (Nunc, Germany). Supernatants from cells not stimulated with LPS were assayed at a 1/5 v/v dilution in assay diluent, while supernatants of cultures stimulated with LPS were assayed at a 1/40 v/v dilution in assay diluent.

4.2.3.6. Mouse Proteome Profiling Analysis

A commercially available antibody array kit (Proteome Profiler, Mouse cytokine Array Panel A, R & D Systems) was used. The kit screens for 40 proteins in duplicate

106

on a nitrocellulose membrane using a dot blot assay. The kit contained all the reagents for the assay and was performed as per the manufacturer's instructions. This cytokine and chemokine antibody array was used to determine the effects of AgNPs on cytokine and chemokine secretion when exposed to RAW 264.7 macrophage cells. The assay required 500 µl of cell culture supernatants. Supernatants from cultures incubated (a) without LPS and AgNPs, (b) in the presence of 250 μg/ml AgNPs without LPS, (c) in the presence of LPS without AgNPs and LPS, and (d) in the presence of LPS and 250 μg/ml AgNPs were screened. Membranes were subjected to chemiluminescence (UVP, Biospectrum Imaging System, Chemi HR 410) in 30 sec intervals to reveal sample-antibody complexes labeled with streptavidin-HRP. Photographs were taken at the end of each exposure period.

4.2.3.7. Quantification of pixel density for cytokine and chemokine membranes

Membrane images were quantified using the image processing and analysis Java software, ImageJ. Levels of cytokines and chemokines were expressed as a percentage of the reference spot. Microsoft Excel was used to calculate the percentages which are expressed as mean ± standard deviation (SD).

The upregulated cytokines and chemokines detected by the proteome profiler were selected for ELISA quantification. The cytokines and chemokines selected belonged to the MIP family, namely; MIP-1α, MIP-1β and MIP-2.

107

4.2.3.8. Mouse MIP (MIP-1α, MIP-1β and MIP-2) DAS ELISAs

Mouse MIP-1α, MIP-1β and MIP-2 ELISAs (R & D Systems) were performed on the unstimulated and LPS stimulated culture supernatants of the RAW 264.7 macrophage cells subjected to 0, 31.25 and 250 μg/ml AgNP exposure respectively. The kits contained all the reagents required for the ELISA and assays were performed as per the manufacturer's instructions. The samples were all diluted in reagent diluent, 1% bovine serum albumin (BSA) (w/v). The MIP-1α unstimulated culture supernatants were assayed at 1/27 v/v and stimulated supernatants at 1/1000 v/v dilution in assay diluent. For the MIP-1β ELISA, the unstimulated culture supernatants were assayed at 1/2 v/v while the LPS stimulated supernatants were assayed at 1/500 v/v dilution in assay diluent. While the MIP-2 ELISA unstimulated supernatants were assayed undiluted and the mitogen stimulated supernatants were used at a 1/100 v/v dilution in assay diluent.
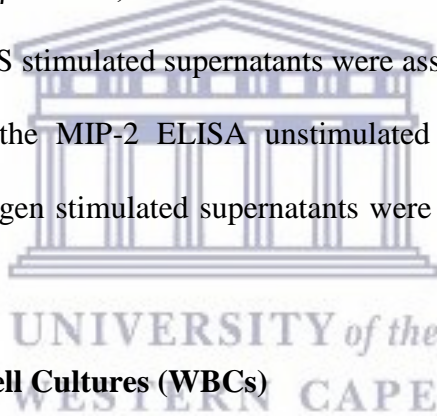
4.2.4. Whole Blood Cell Cultures (WBCs)

4.2.4.1. Blood collection

Blood was collected by a health practitioner, in a clinical practice, from healthy males who were not using any medication. Ethical clearance to collect blood was obtained from the University of the Western Cape (Ethics No.10/9/43). Informed consent was also obtained from the participant. The blood was collected using venipuncture directly into 3.2 % sodium citrate vacuum tubes (Greiner bio-one). The blood was processed immediately. The preparation of whole blood for cell culture was performed under sterile conditions.

108

4.2.4.2. Effects of AgNPs on inflammation

Human whole blood was diluted with RPMI 1640 media to give a 10 % v/v mixture. Blood was either left unstimulated or stimulated with lipopolysaccharide (LPS) (Sigma-Aldrich) (0.1 µg/ml). Unstimulated or LPS stimulated WBCs were incubated overnight with various concentrations of AgNPs (2.5, 25 and 250 μg/ml) or 0.1% Tween20 v/v (Merck) in 48 well cell culture trays (Falcon) at 37 °C. After the incubation period, culture supernatants were collected and screened for IL-6 and MIP-1β (R & D Systems) using commercially available ELISA kits.

4.2.4.3. Effects of Ag and AgNPs on Th cytokines

Human whole blood was diluted with RPMI 1640 media (Sigma-Aldrich) to give a 10 % v/v mixture. Blood was either left unstimulated or stimulated with phytohaemmagglutinin (PHA) (Sigma-Aldrich) (16 μg/ml). Unstimulated or PHA stimulated WBCs were incubated overnight with various concentrations of AgNPs (2.5, 25 and 250 μg/ml) or 0.1% Tween20 v/v in tissue culture treated 48 well plates at 37 °C. After the incubation period, culture supernatants were collected and screened for interleukin 10 (IL-10) and interferon gamma (IFNγ) using commercially available ELISA kits (e-Bioscience).

4.2.4.4. Lactate Dehydrogenase (LDH) Cytotoxicity Assay

The assay was performed as per the manufacturer's instructions (BioVision, LDH-Cytotoxicity Colorimetric Assay Kit II). Unstimulated culture supernatants were used for the assay. Briefly, 100 µl of LDH reaction mix was added to 10 µl sample

109

supernatants and incubated for 30 mins at room temperature. Thereafter, plates were read at 450 nm. The amount of LDH in supernatant is directly proportional to cytotoxicity.

4.2.4.5. Human IL-6, MIP-1β, IL-10, and IFNγ Double Antibody Sandwich Enzyme Linked Immuno-Sorbent Assay (DAS ELISA)

Human DAS ELISA kits (IL-6, IL-10 and IFNγ) (e-Bioscience, Ready-Set-Go) and MIP-1β (R & D Systems) were used to measure cytokine levels in WBC supernatants. Supernatants used for IL-6 and MIP-1β analysis were diluted 1/10 v/v in assay diluents while the supernatants for IL-10 and IFNγ were assayed undiluted. Assays were performed in 96 well Nunc maxisorb plates (Nunc, Germany). The kits contained all the reagents for the assay and were performed as per the manufacturer's instructions.

4.2.4.6. Human Proteome Profile Analysis

A commercially available proteome profile kit (Proteome Profiler, Human Cytokine Array Kit, R & D Systems) was used. The kit screened for 36 proteins in duplicate on a nitrocellulose membrane using a dot blot assay. The kit contained all the reagents for the assay and was performed as per the manufacturer's instructions. Supernatants from cultures incubated (a) without LPS and AgNP, (b) in the presence of 25 μg/ml AgNP without LPS, (c) in the presence of LPS without AgNP, and (d) in the presence of LPS and 25 μg/ml AgNPs were screened. The same procedure was followed as previously stated. Membranes were subjected to a ultra sensitive chromogenic

3,3',5,5'-Tetramethylbenzidine (TMB) membrane substrate (Thermo Scientific) to reveal sample-antibody complexes labeled with streptavidin-HRP. Photographs were taken of the blots after the exposure to the substrate. Quantification of pixel density was calculated as previously mentioned.

4.2.5. Statistical Analysis

Assays were performed in triplicate. Data was calculated using Microsoft Excel and is presented as mean ± SD. One way analysis of variance (ANOVA) using SigmaPlot 12.0 was used to assess statistical differences with $P < 0.01$ being deemed significant.

4.3. Results

4.3.1. The effects of AgNPs on RAW 264.7 Cells

4.3.1.1. The effects of AgNPs on RAW 264.7 cells cultured in various FBS concentrations

4.3.1.1.1. The effects of AgNPs on RAW 264.7 cell viability

Silver nanoparticles at 50 μg/ml in medium containing 2 % FBS upregulated ($P < 0.001$) cell viability of unstimulated RAW cells, while AgNP at 250 μg/ml in medium containing 2 and 5 % FBS inhibited ($P < 0.001$) cell viability (Figure 4.1 a).

Silver nanoparticles at 250 μg/ml in medium containing 1, 2 and 5 % FBS significantly decreased cell viability. The other AgNP concentrations had no effect on viability of stimulated RAW cells cultured in medium containing 1-10 % FBS (Figure 4.1 b).

111
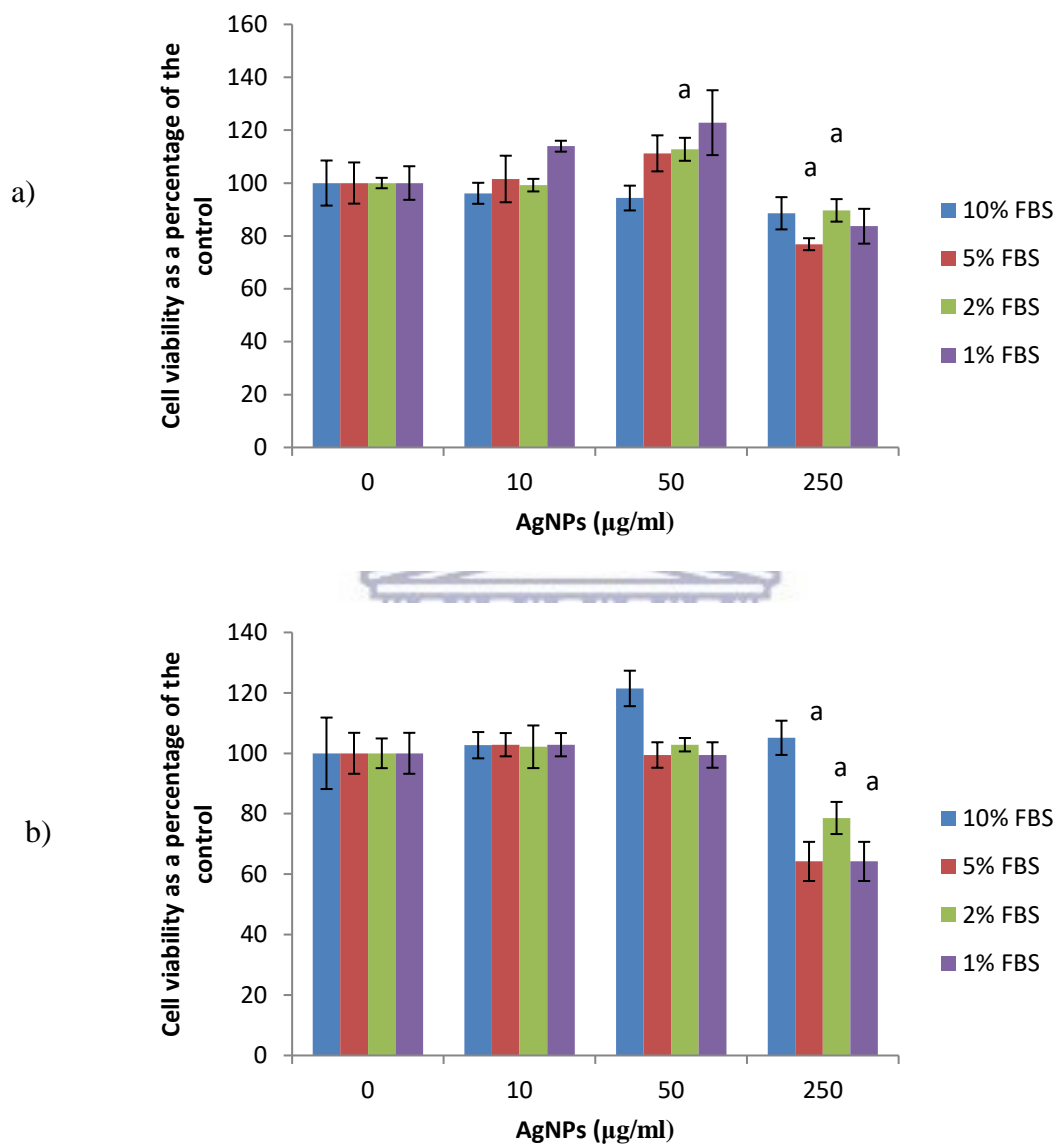
Figure 4.1. Cell viability of RAW 264.7 macrophage cells exposed to AgNPs in the (a) media only or (b) media in the presence of LPS. Data represents mean ± SD with n = 3. Bars marked with the letter a indicate significantly different (P < 0.001) compared to 0 μg/ml AgNPs**.**

112

4.3.1.1.2. The effects of AgNPs on the inflammatory biomarker, NO

Silver nanoparticle exposure at 50 μg/ml in the presence of 2 % FBS significantly upregulated (P < 0.001) NO production by unstimulated RAW cells (Figure 4.2 a). NO production by unstimulated RAW cells was also upregulated by 250 μg/ml AgNP exposures in the presence of 1-10 % FBS.

Silver nanoparticle exposure at 250 μg/ml in medium containing 1 and 5 % FBS significantly reduced (P < 0.001) NO production by LPS stimulated RAW cells (Figure 4.2 b). No effects were seen at other AgNP and FBS concentrations.

113
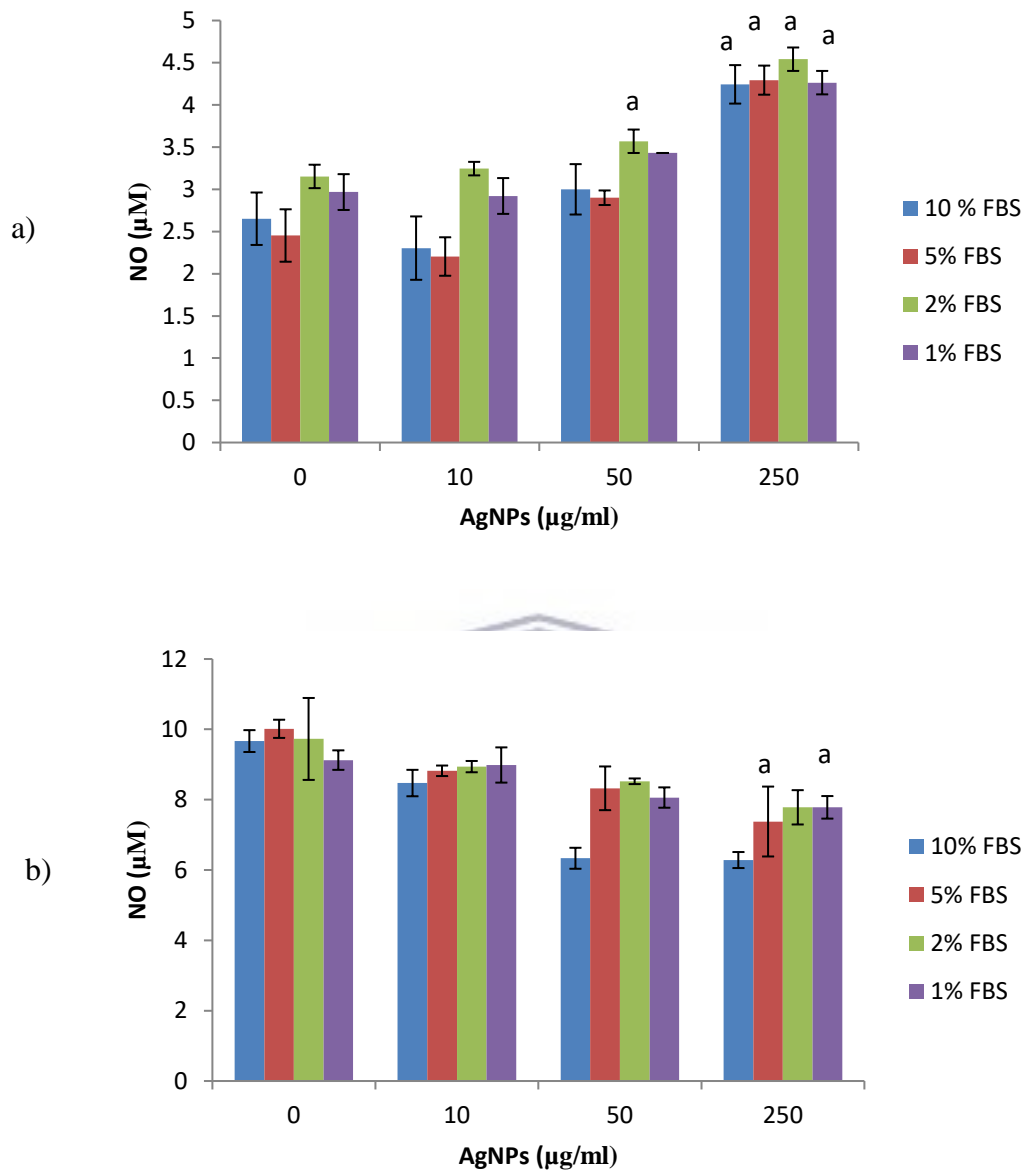
Figure 4.2. Nitric oxide (NO) production by RAW 264.7 macrophage cells exposed to AgNPs in (a) media only or (b) media in the presence of LPS. Data represents mean ± SD with n = 3. Bars marked with the letter a indicate significantly different (P < 0.001) compared to 0 μg/ml AgNPs.

114

4.3.1.1.3. The effects of AgNPs on the inflammatory biomarker IL-6

Silver nanoparticles at 50 and 250 μg/ml in the presence of 10 % FBS significantly reduced ($P < 0.001$) IL-6 production by LPS stimulated RAW cells (Figure 4.3). Silver nanoparticle and FBS concentrations did not affect IL-6 synthesis by unstimulated RAW cells.
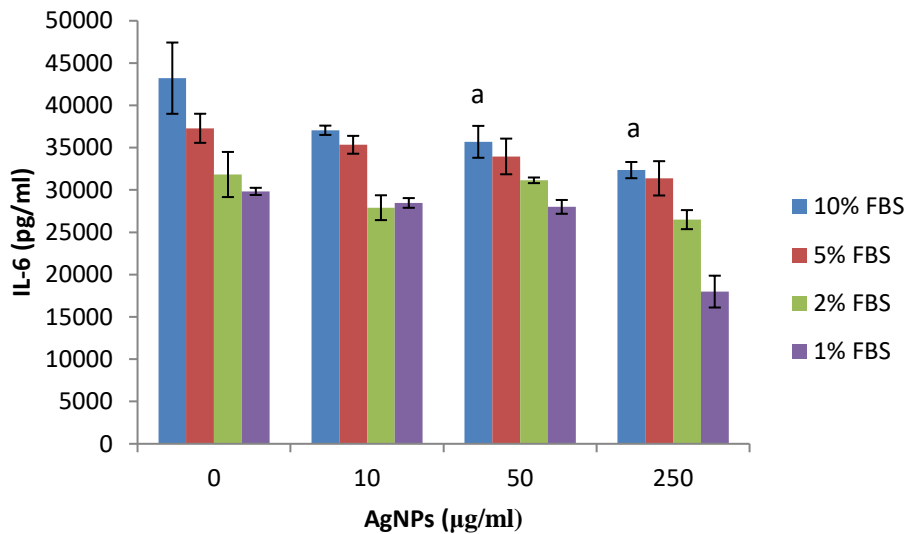
Figure 4.3. Interleukin 6 (IL-6) production by RAW 264.7 macrophage cells exposed to AgNPs in LPS stimulated cell cultures. Data represents mean ± SD with n = 3. Unstimulated cultures did not synthesize IL-6 (data not presented). Bars marked with the letter a indicate significantly different ($P < 0.001$) compared to 0 μg/ml AgNPs.

4.3.1.2. The effects of AgNPs on RAW 264.7 cell viability

AgNP between 0-250 μg/ml had no effect on the viability of cells (Figure 4.4). However, in the absence of LPS, AgNP concentrations ≥ 15.625 μg/ml significantly upregulated ($P < 0.001$) cell metabolic activity compared to the culture control.
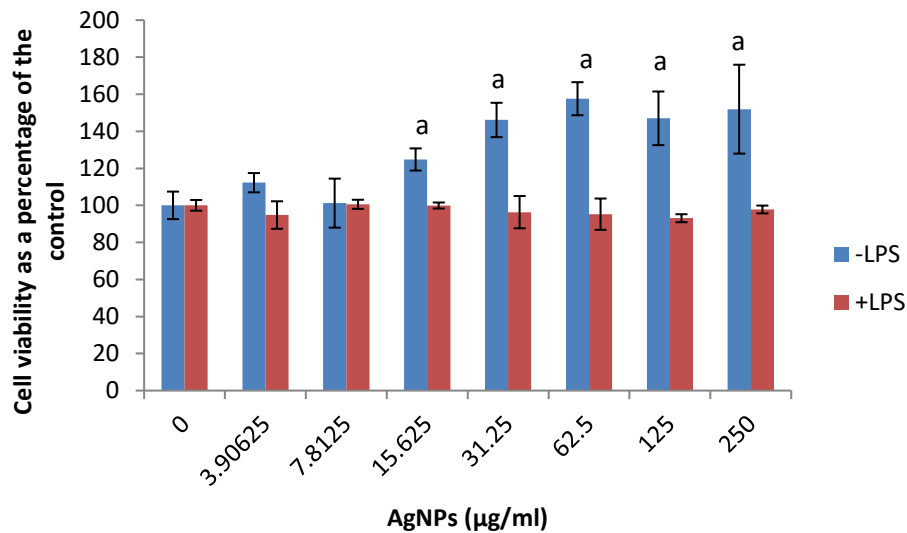
115

Figure 4.4. Cell viability of RAW 264.7 macrophage cells exposed to AgNPs. Data represents mean ± SD with n = 9. Bars marked with the letter a indicate significantly different (P < 0.001) compared to negative control, 0 μg/ml AgNPs.

4.3.1.3. The effects of AgNPs on the inflammatory biomarker, NO

Similar to the viability data (Figure 4.4), AgNP concentrations ≥ 62.5 μg/ml significantly upregulated (P < 0.001) NO production in cultures not stimulated by LPS (Figure 4.5). However, NO was notably inhibited (P < 0.001) by the highest concentration of AgNP (250 μg/ml) in LPS stimulated cultures compared to the culture control.
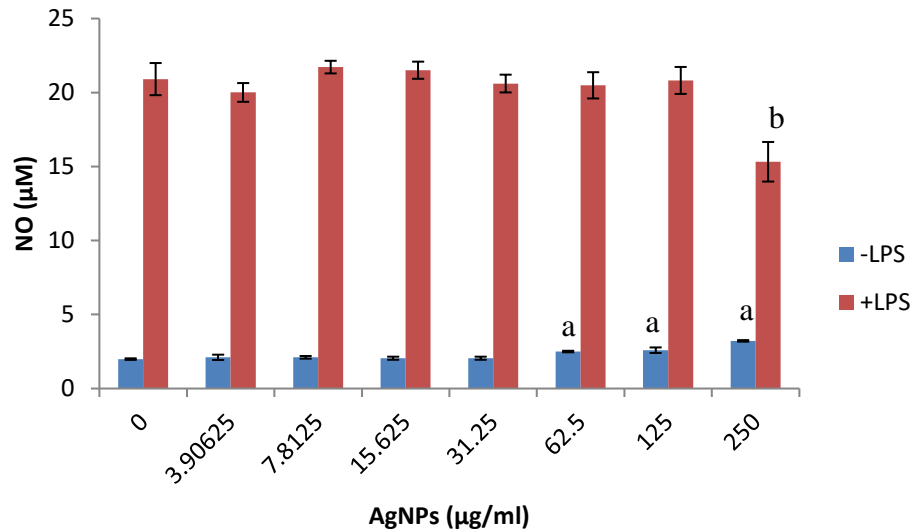
Figure 4.5. Nitric oxide (NO) production by RAW 264.7 macrophage cells exposed to AgNPs. Data represents mean ± SD with n = 9. Bars marked with letters indicate significant difference (P < 0.01) to control. Significance demarcated by: a- significantly different (P < 0.001) compared to 0 μg/ml AgNPs, -LPS; b- significantly different (P < 0.001) compared to 0 μg/ml AgNPs, +LPS.

4.3.1.4. The effects of AgNPs on the inflammatory biomarker IL-6

AgNP between 0-250 μg/ml did not affect IL-6 synthesis in unstimulated cultures (Figure 4.6). The LPS stimulated cultures mirrored the NO data (Figure 4.5), as the highest concentration of AgNP (250 μg/ml) significantly inhibited (P < 0.001) IL-6 synthesis compared to the culture control.
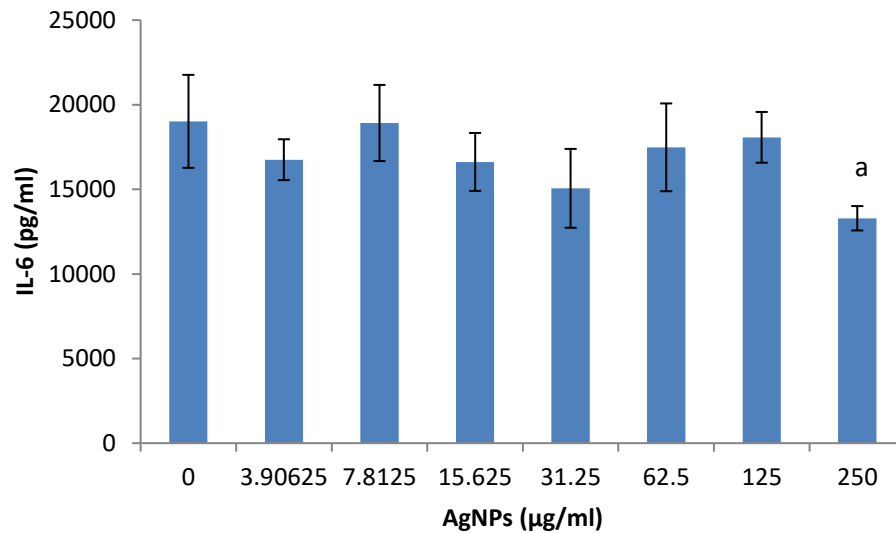
Figure 4.6. Interleukin 6 (IL-6) production by stimulated RAW 264.7 macrophage cells exposed to AgNPs. Data represents mean ± SD with n = 9. Unstimulated cultures did not synthesize IL-6 (data not presented). Bars marked with the letter a indicate significantly different ($P < 0.001$) compared to 0 μg/ml AgNPs.

4.3.1.5. The effects of AgNPs on the secretory cytokine and chemokine profile of RAW 264.7 cells not treated with LPS

Culture supernatants were screened using a cytokine and chemokine array to monitor the effects AgNPs had on their secretion. Screening of the cytokines and chemokines were expected to identify potential biomarkers that can be monitored to assess the effects of AgNPs on the RAW cells.

Culture supernatants from cells not stimulated with LPS and without the presence of AgNPs (negative control) revealed that intracellular adhesion molecule-1 (CD54/sICAM-1) and macrophage inflammatory protein-1 alpha (CCL3/MIP-1α)

118

were present (Figure 4.7 a). Other cytokines and chemokines were present in 250 μg/ml AgNP treated culture supernatants that were not evident in culture supernatants from cells not exposed to AgNPs. These were tumour necrosis factor alpha (TNF-α); monocyte chemoattractant protein-1 (CCL2/MCP-1/JE); macrophage inflammatory protein-1 beta (CCL4/MIP-1β) and macrophage inflammatory protein-2 (CXCL2/MIP-2) (Figure 4.7 c). Therefore, AgNPs stimulated the upregulation of these cytokines and chemokines, along with MIP-1α and CD54. These results were corroborated by the quantification of the membranes. CD54/sICAM-1; TNF-α; CCL2/MCP-1/JE; CCL3/MIP-1α ; CCL4/MIP-1β and CXCL2/MIP-2 were statistically different ($P < 0.001$) and upregulated in 250 μg/ml AgNP exposed culture supernatants when compared to the supernatants of cells not exposed to AgNPs (Table 4.1).
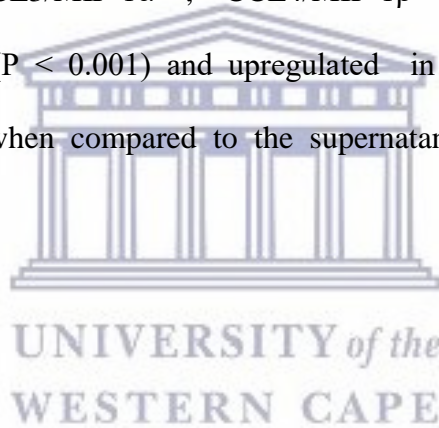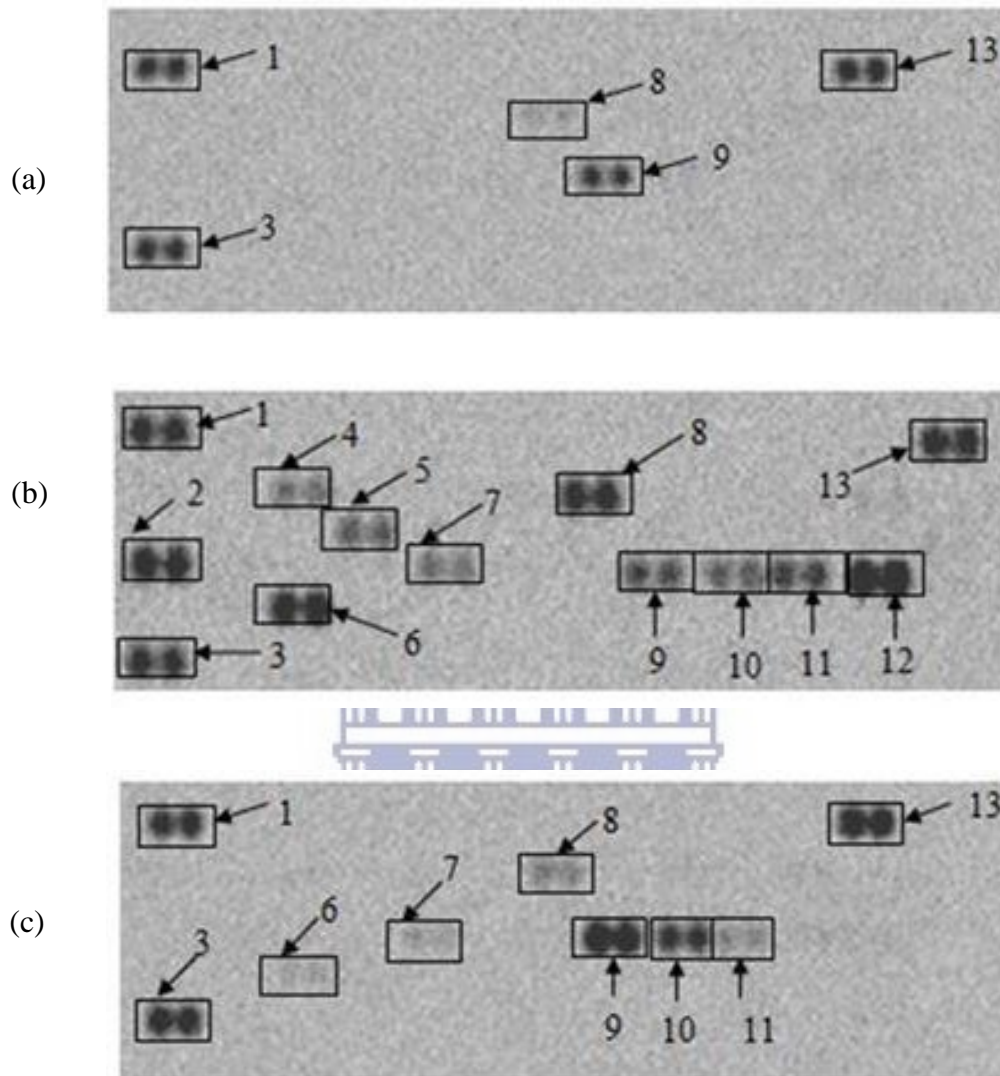
119

Figure 4.7. The effect of AgNPs on RAW 264.7 cells. Cells were incubated with (a) medium only, (b) medium containing LPS or (c) 250 μg/ml AgNPs in the absence of LPS. Supernatants were probed using the proteome profiler array as described in methods. Cytokines/ chemokines that were detected were allocated numbers: 1,3, and 13 are reference spots;   6- TNF-α ;   7- CCL2/MCP-1/JE;   8-CD54/ sICAM-1;   9-CCL3/MIP-1α;   10- CCL4/MIP-1β; and 11- CXCL2/MIP-2.

120

Table 4.1. Quantification of cytokines and chemokines secreted by RAW 264.7 cultures not stimulated with LPS after treatment with medium only (negative control), medium containing LPS (positive control) or medium containing 250 μg/ml AgNPs. Membranes were subjected to 3 min 30 sec chemiluminescence exposure. Data is represented as mean ± SD. Significance indicated by a- AgNP at 250 μg/ml significantly different (P < 0.001) compared to negative control, b- AgNP at 250 μg/ml significantly different (P < 0.001) compared to the positive control.

Cytokines and Chemokines	Positive Control	Negative Control	250 μg/ml AgNPs
Reference Spot	100 ± 11.79	100 ± 6.37	100 ± 14.90
IP-10	106.54 ± 11.68	0 ± 0	0 ± 0[b]
G-CSF	48.37 ± 3.60	0 ± 0	0 ± 0[b]
TNF-α	110.24 ± 1.23	0 ± 0	11.77 ± 4.41[a,b]
IL-6	50.93 ± 2.71	0 ± 0	0 ± 0[b]
MCP-1/JE	45.84 ± 4.66	0 ± 0	11.34 ± 0.87[a,b]
sICAM	113.94 ± 6.41	15.86 ± 6.55	34.09 ± 4.31[a,b]
MIP-1α	69.18 ± 11.03	83.69 ± 9.50	121.33 ± 21.87[a,b]
MIP-1β	59.34 ± 0.18	0 ± 0	95.88 ± 14.94[a,b]
MIP-2	77.57 ± 11.12	0 ± 0	31.53 ± 4.09[a,b]
RANTES	125.14 ± 8.71	0 ± 0	0 ± 0[b]

4.3.1.6. The effects of AgNPs on the secretory cytokine and chemokine profile of LPS treated RAW 264.7 cells

Proteome profile of culture supernatants of LPS treated RAW 264.7 cells cultured in medium only or in medium containing 250 μg/ml AgNPs (Figure 4.8) identified the same cytokines and chemokines. These cytokines and chemokines identified were interferon gamma induced protein 10 (CXCL10/CRG-2/IP-10); granulocyte colony-stimulating factor (G-CSF); IL-6; TNF-α; CCL2/MCP-1/JE; CD54/ sICAM-1; CCL3/MIP-1α; CCL4/MIP-1β; CXCL2/MIP-2 and regulated on activation, normal T

121

cell expressed and secreted (CCL5/RANTES). Quantification of the membranes showed no statistical differences between the various cytokine and chemokine levels (Table 4.2).
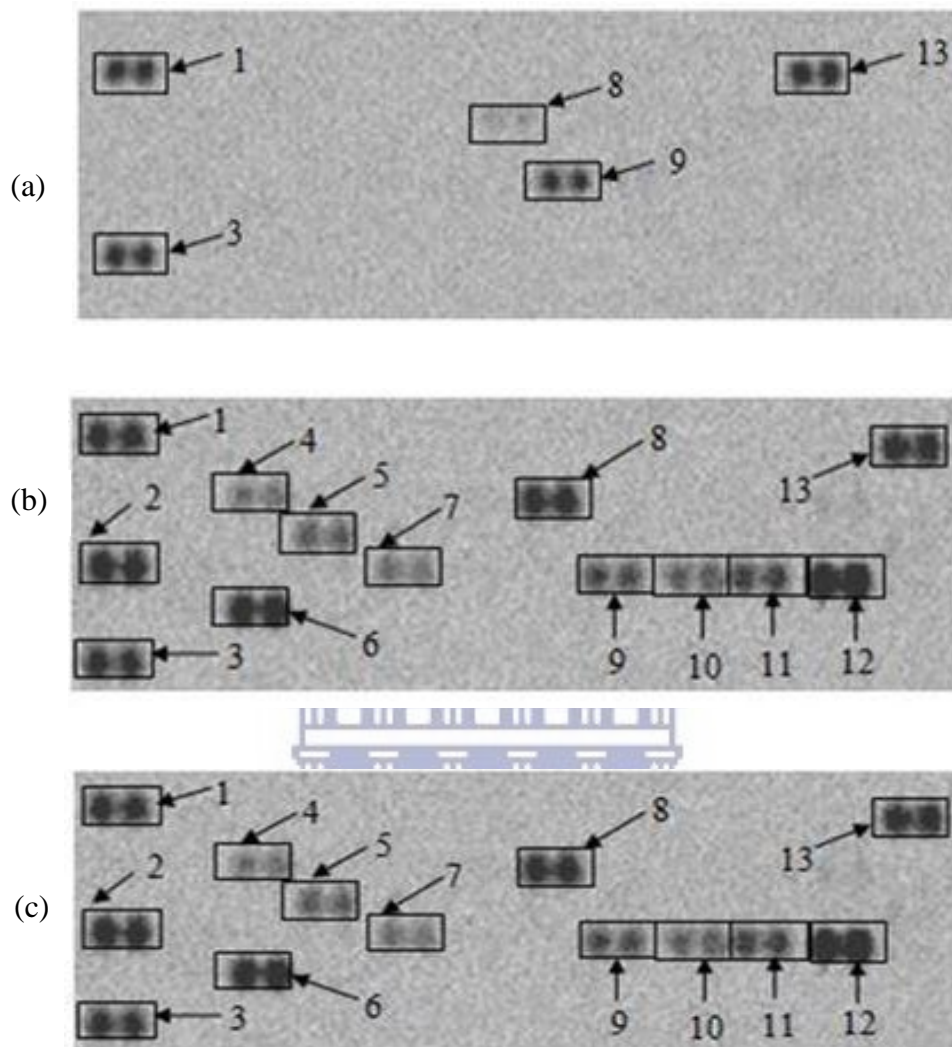
Figure 4.8. The effect of AgNPs on RAW 264.7 cells. Cells were incubated with (a) medium only, (b) medium in the presence of LPS or (c) 250 μg/ml AgNPs in the presence of LPS. Supernatants were probed using the proteome profiler array as described in methods. Cytokines/ chemokines that were detected were allocated numbers: 1,3,and 13 are reference spots; 2-CXCL10/CRG-2/IP-10; 4- G-CSF; 5- IL-6; 6- TNF-α; 7- CCL2/MCP-1/JE; 8- CD54/ sICAM-1; 9- CCL3/MIP-1α; 10-CCL4/MIP-1β; 11- CXCL2/MIP-2; and 12-CCL5/RANTES.

123

Table 4.2. Quantification of cytokines and chemokines secreted by RAW 264.7 cultures stimulated with LPS after treatment with medium only (negative control), medium containing LPS (positive control) or medium containing LPS and 250 μg/ml AgNPs. Membranes were subjected to 3 min 30 sec chemiluminescence exposure. Data is represented as mean ± SD. Significance indicated by a- AgNP at 250 μg/ml significantly different (P < 0.001) compared to negative control.

Cytokines and Chemokines	Positive Control	Negative Control	250 μg/ml AgNPs in the presence of LPS
Reference Spot	100 ± 11.79	100 ± 6.37	100 ± 16.19
IP-10	106.54 ± 11.68	0 ± 0	110.74 ± 0.19[a]
G-CSF	48.37 ± 3.60	0 ± 0	45.20 ± 2.99[a]
TNF-α	110.24 ± 1.23	0 ± 0	108.26 ± 3.40[a]
IL-6	50.93 ± 2.71	0 ± 0	51.35 ± 2.31[a]
MCP-1/JE	45.84 ± 4.66	0 ± 0	44.79 ± 1.01[a]
sICAM	113.94 ± 6.41	15.86 ± 6.55	114.98 ± 0.54[a]
MIP-1α	69.18 ± 11.03	83.69 ± 9.50	73.83 ± 10.58[a]
MIP-1β	59.34 ± 0.18	0 ± 0	66.79 ± 1.64[a]
MIP-2	77.57 ± 11.12	0 ± 0	87.94 ± 7.98[a]
RANTES	125.14 ± 8.71	0 ± 0	127.67 ± 9.44[a]

4.3.1.7. The effects of AgNPs on RAW 264.7 cells not treated with LPS and the effect on the secretion of MIP family chemokines (MIP-1α, MIP-1β and MIP-2)

The proteome profile analysis of the samples not stimulated by a mitogen revealed that members of the MIP family, namely; MIP-1α, MIP-1β and MIP-2 were upregulated by 250 μg/ml AgNPs. The ELISA quantification of these respective chemokines all showed that 250 μg/ml AgNPs significantly upregulated (P < 0.001) their secretion compared to the culture control (Figure 4.9). This trend was also seen

in the NO data, where this biomarker was also upregulated in the unstimulated

samples exposed to the same concentration (Figure 4.5).

125
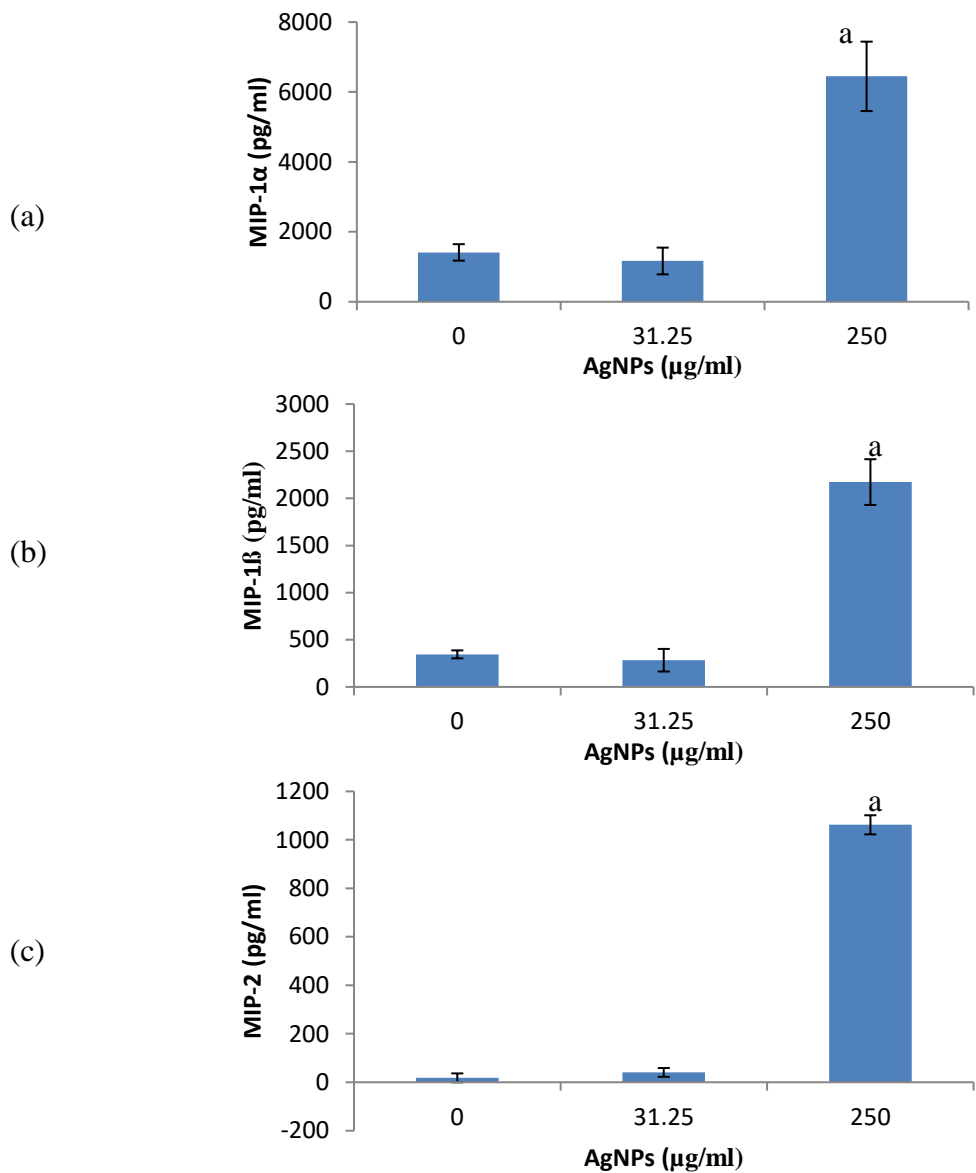
Figure 4.9. The effect of AgNPs exposure on RAW cells not stimulated by LPS. The quantification of the effects of AgNPs on the secretion of the chemokines: a) MIP-1α, b) MIP-1β and c) MIP-2. Data is presented as mean ± SD with n = 9. Bars marked with letters indicate significant difference ($P < 0.01$) to unstimulated control. Significance demarcated by: a- significantly different ($P < 0.001$) compared to the unstimulated control.

4.3.1.8. The effects of AgNPs on RAW 264.7 cells treated with LPS and the resultant effect on the secretion of MIP family chemokines (MIP-1α, MIP-1β and MIP-2)

The ELISA quantification of culture supernatants exposed to AgNPs and in the presence of LPS revealed no significant effects on the secretion for all the MIP family chemokines monitored in this study (Figure 4.12). These results reflected that of the proteome profiling analysis of the culture supernatants (Figure 4.8).

127
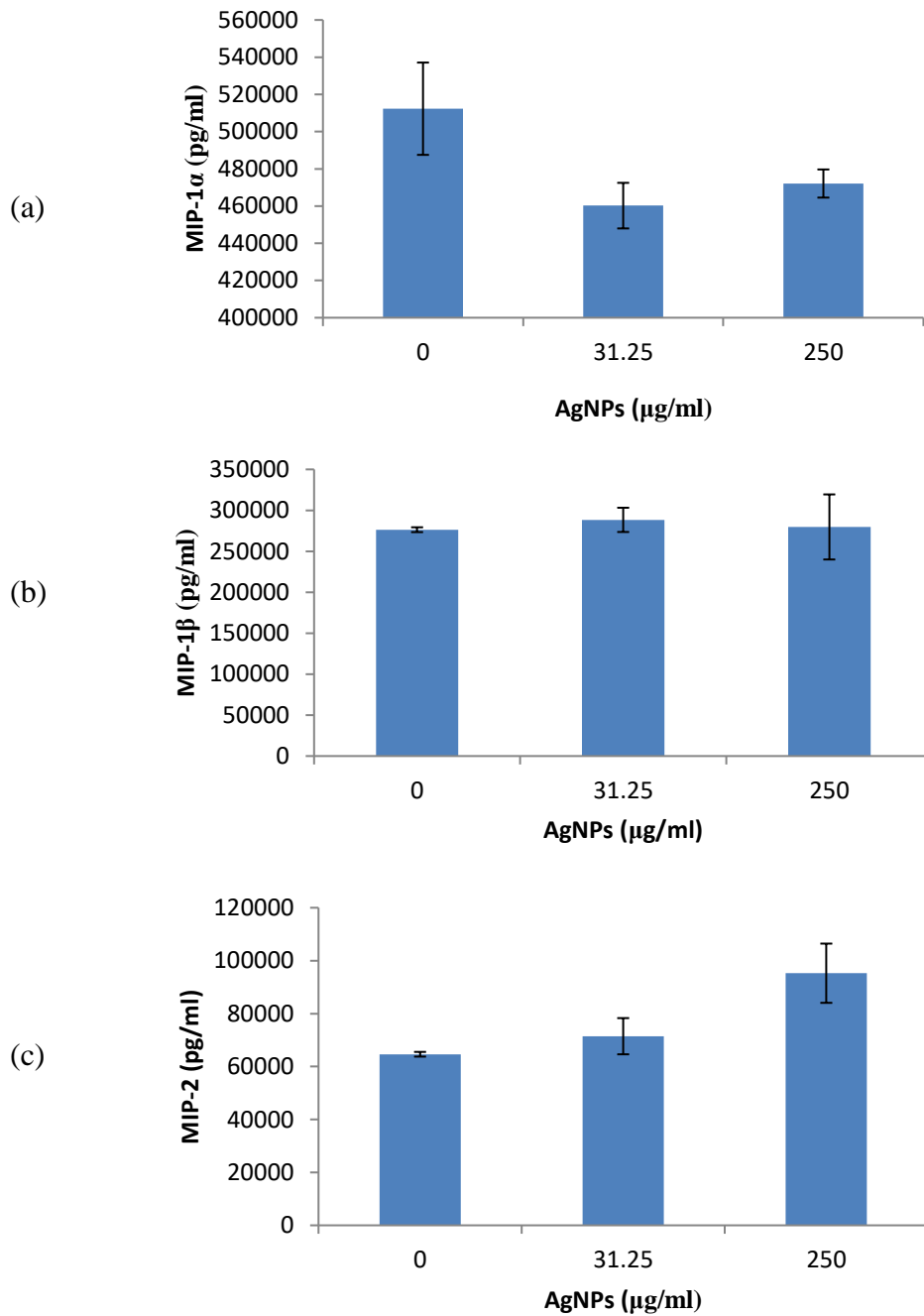
Figure 4.10. The effect of AgNPs exposure on RAW cells stimulated by LPS. The quantification of the effects of AgNPs on the secretion of the chemokines: a) MIP-1α, b) MIP-1β and c) MIP-2. Data is represented as mean ± SD with n = 9.

4.3.2. The effects of AgNPs on WBCs

4.3.2.1. Cytotoxicity

AgNP concentrations ≤ 25 µg/ml did not affect cell viability (Figure 4.11). However, the highest concentration of AgNP (250 µg/ml) significantly reduced (P < 0.001) cell viability compared to the culture control.
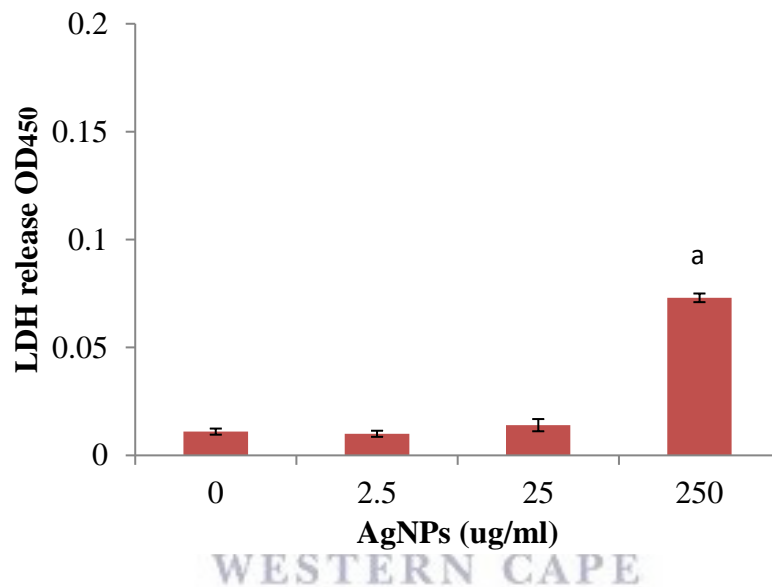
Figure 4.11. Cell viability of WBCs exposed to AgNPs. Data represents mean ± SD with n = 4. Bars marked with letters indicate significant differences (P < 0.01). Significance demarcated by: a- significantly different compared to negative control, 0 µg/ml AgNPs (-LPS) (P < 0.001).

4.3.2.2. The effects of AgNPs on the inflammatory biomarker IL-6 using WBCs

Unstimulated cultures exposed to AgNP concentrations ≤ 25 µg/ml did not affect IL-6 synthesis (Figure 4.12). IL-6 was significantly upregulated (P < 0.001) by 250 µg/ml AgNP in cultures not stimulated by LPS. AgNP concentrations ≤ 25 µg/ml

129

notably upregulated (P < 0.001) IL-6 synthesis in LPS stimulated cultures. However, in the presence of a mitogen, 250 μg/ml AgNP significantly inhibited (P < 0.001) IL-6 synthesis compared to the culture control.
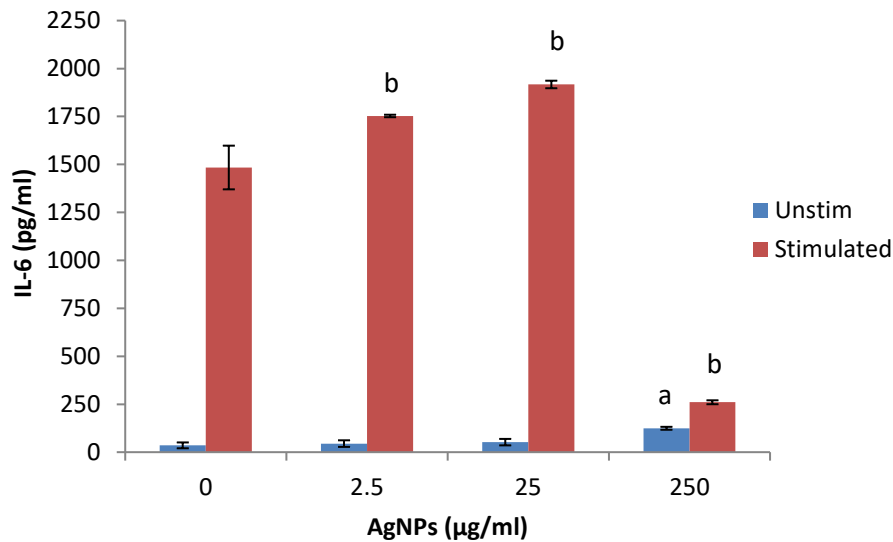
Figure 4.12. IL-6 synthesis by WBCs exposed to AgNPs. Data represents mean ± SD with n = 4. Bars marked with letters indicate significant difference to 0 μg/ml AgNPs (P < 0.01). Significance demarcated by: a- significantly different (P < 0.001) compared to negative control (0 μg/ml AgNPs; -LPS); b- significantly different (P < 0.001) compared to positive control (0 μg/ml AgNPs; +LPS).

4.3.2.3. The effects of AgNPs on the inflammatory chemokine, MIP-1β using WBCs

AgNP concentrations ≥ 25 μg/ml significantly upregulated (P < 0.001) MIP-1β synthesis in cultures not stimulated by LPS (Figure 4.13). However, in LPS

stimulated cultures, the highest concentration of AgNP (250 μg/ml) significantly reduced ($P < 0.001$) MIP-1β synthesis compared to the culture control.
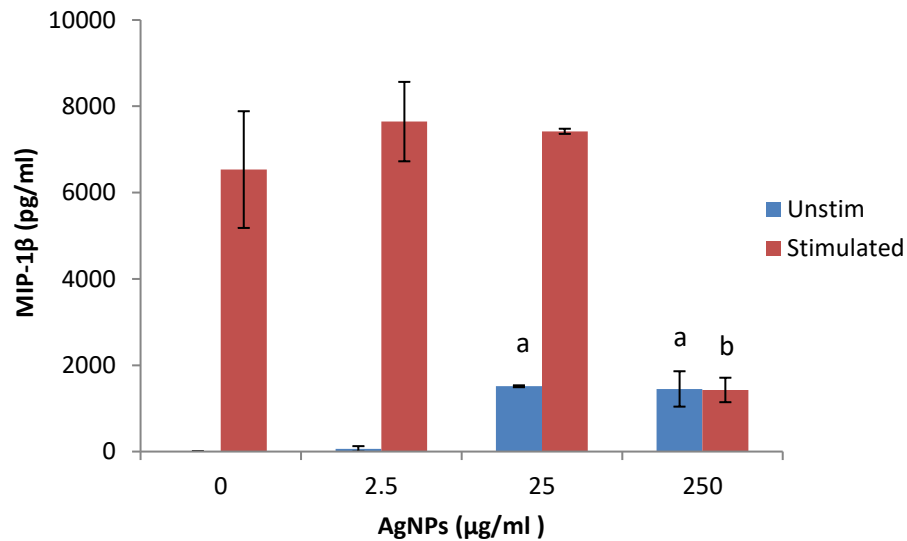
Figure 4.13. MIP-1β synthesis by WBCs exposed to AgNPs. Data represents mean ± SD with n = 4. Bars marked with letters indicate significant difference ($P < 0.01$) to 0 μg/ml AgNPs. Significance demarcated by: a- significantly different ($P < 0.001$) compared to negative control (0 μg/ml AgNPs; -LPS); b- significantly different ($P < 0.001$) compared to positive control (0 μg/ml AgNPs; +LPS).

4.3.2.4. The effects of AgNPs on the humoral immune system biomarker IL-10 using WBCs

AgNP concentrations ≤ 25 μg/ml had no effect on IL-10 production in cultures both in the presence or absence of PHA (Figure 4.14). At the highest AgNP concentration (250 μg/ml), IL-10 was significantly upregulated ($P < 0.001$) in cultures not stimulated by LPS. However, in cultures stimulated by PHA and exposed to 250

131

μg/ml AgNPs, IL-10 was notably inhibited (P < 0.001) compared to the culture control. This inhibition of IL-10 allowed for an IC_{50} of 29.67 μg/ml to be calculated (Figure 4.15).
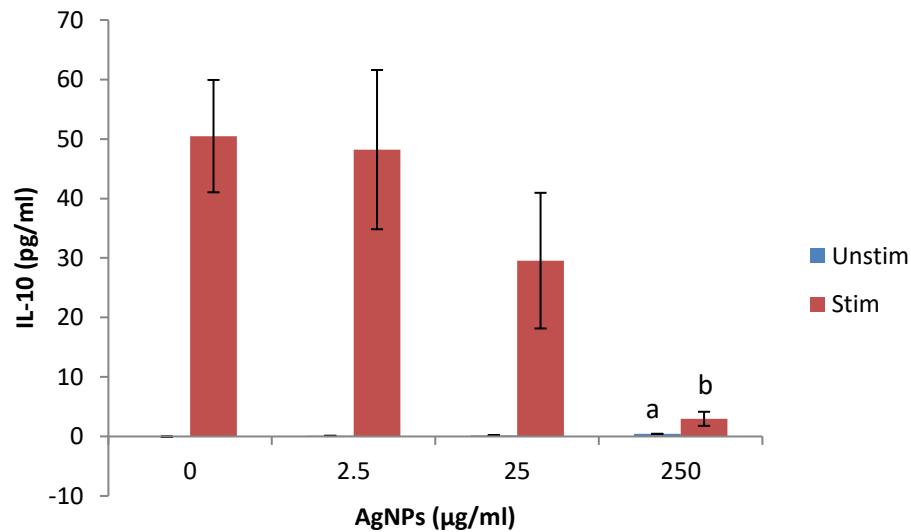
Figure 4.14. IL-10 synthesis by WBCs exposed to AgNPs. Data represents mean ± SD with n = 4. Bars marked with letters indicate significant difference (P < 0.01) to 0 μg/ml AgNPs. Significance demarcated by: significantly different (P < 0.001) compared to negative control (0 μg/ml AgNPs; -PHA); b- significantly different (P < 0.001) compared to positive control (0 μg/ml AgNPs; +PHA).
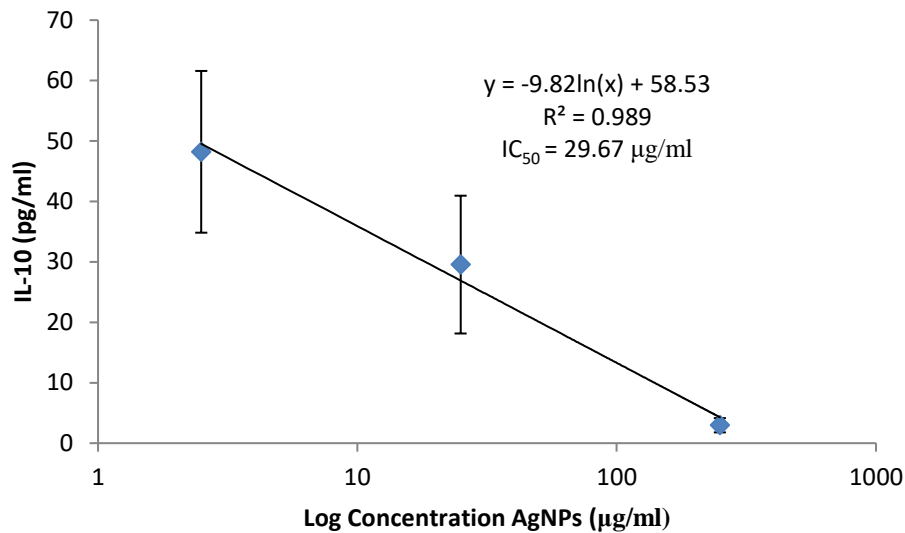
Figure 4.15. IC_{50} determination of AgNPs on IL-10 production by PHA stimulated WBCs.

4.3.2.5. The effects of AgNPs on the cell mediated immune system biomarker, IFNγ using WBCs

AgNP concentrations had no effect on IFNγ production in cultures stimulated by PHA (Figure 4.16). However, at 250 μg/ml AgNP, IFNγ was significantly upregulated (P < 0.001) in cultures not stimulated by PHA compared to the culture control.
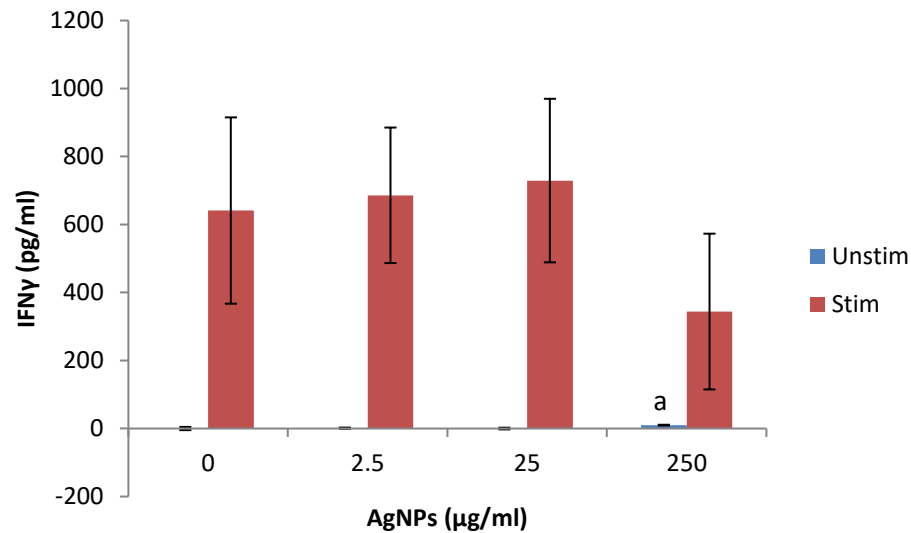
133

Figure 4.16. IFNγ synthesis by WBCs exposed to AgNPs. Data represents mean ± SD with n = 4. Bars marked with letters indicate significant difference (P < 0.01) to 0 μg/ml AgNPs. Significance demarcated by: a- significantly different (P < 0.001) compared to negative control (0 μg/ml AgNPs; -PHA).

4.3.2.6. The effects of AgNPs on the secretory cytokine and chemokine profile of WBCs not treated with LPS

A proteome profile of WBCs exposed to 25 μg/ml AgNPs under unstimulated conditions and media only revealed the respective cytokines and chemokines expressed by WBCs under these conditions (Figure 4.17). Quantification of the membranes revealed that the AgNPs significantly suppressed (P < 0.001) the synthesis of macrophage migration inhibitory factor (MIF) and RANTES (Table 4.3) compared to 0 μg/ml AgNP control. Whereas, the other cytokines and chemokines expressed upon exposure to media only and AgNPs are virtually indistinguishable from each other (Figure 4.17 and Table 4.30).

134
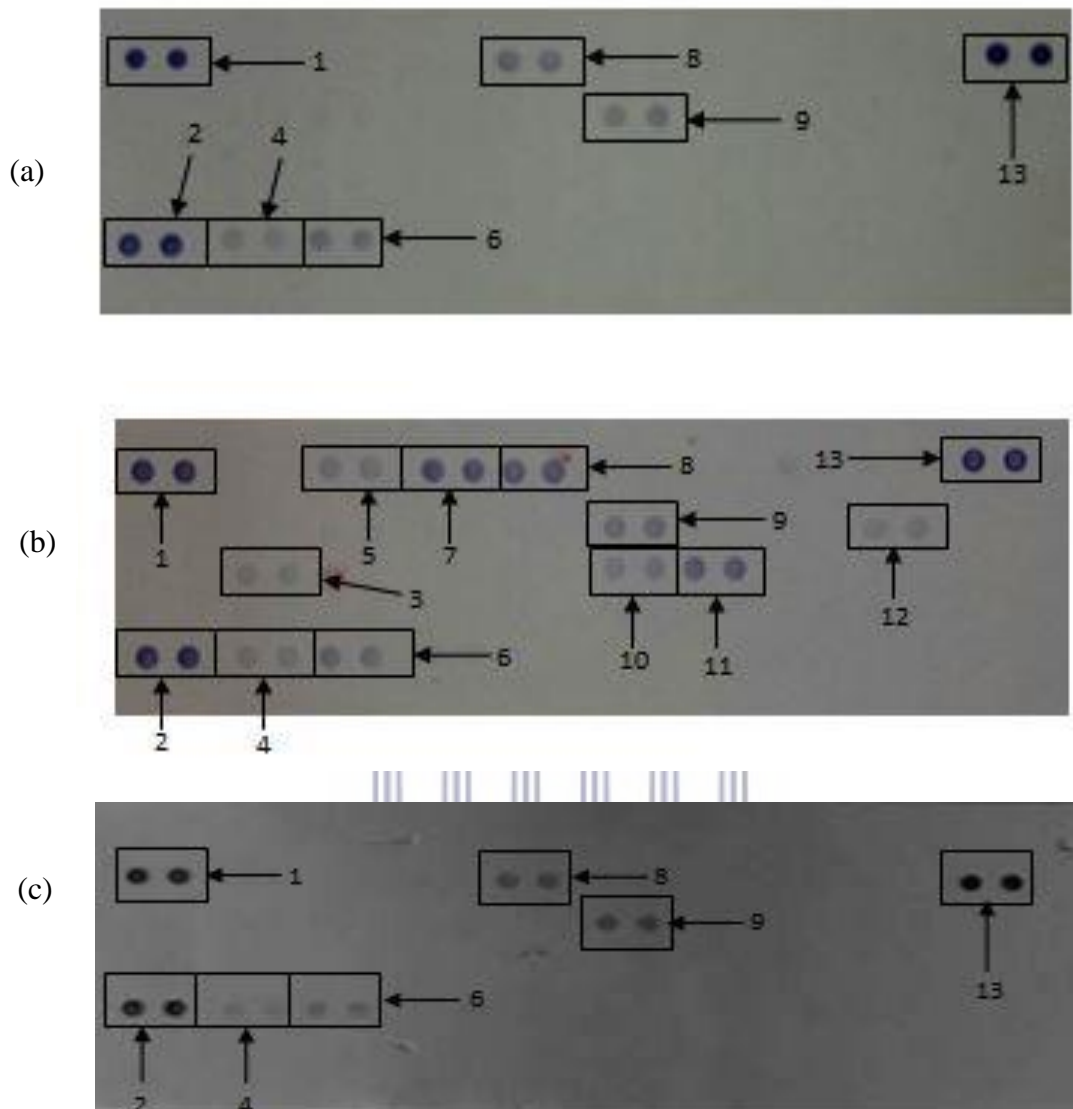
Figure 4.17. The effect of AgNPs on WBCs. Cells were incubated with (a) medium only, (b) medium containing LPS or (c) 25 μg/ml AgNPs in the absence of LPS. Supernatants were probed using the proteome profiler array as described in methods. Cytokines/ chemokines that were detected were allocated numbers: 1,2, and 13 are reference spots; 4- MIF; 6- Serpin E1; 8- RANTES; 9-ICAM-1.

Table 4.3. Quantification of cytokines and chemokines secreted by WBCs not stimulated with LPS after treatment with medium only (negative control), medium containing LPS (positive control) or medium containing 25 μg/ml AgNPs. Membranes were subjected to chromogenic exposure. Data is represented as mean ± SD. Significance indicated by a- AgNP at 25 μg/ml significantly different (P < 0.001) compared to negative control, b- AgNP at 25 μg/ml significantly different (P < 0.001) compared to the positive control.

Cytokines and Chemokines	Positive Control	Negative Control	25 µg/ml AgNPs
Reference Spot	100 ± 7.28	100 ± 14.51	100 ± 5.57
IL-1ra	16.92 ± 1.46	0 ± 0	0 ± 0[b]
MIF	17.56 ± 1.51	19.57 ± 1.65	10.57 ± 1.91[a,b]
MCP-1	26.26 ± 2.54	0 ± 0	0 ± 0[b]
Serpin E1	32.40 ± 2.49	27.39 ± 0.66	24.26 ± 2.26[b]
MIP-1α/β	70.22 ± 4.11	0 ± 0	0 ± 0[b]
RANTES	62.94 ± 2.55	41.71 ± 0.45	34.27 ± 1.37[a,b]
sICAM	37.15 ± 0.59	32.33 ± 1.00	35.98 ± 2.19
IL-6	29.31 ± 4.81	0 ± 0	0 ± 0[b]
IL-8	50.27 ± 8.41	0 ± 0	0 ± 0[b]
IL-1β	20.29 ± 0.99	0 ± 0	0 ± 0[b]

4.3.2.7. The effects of AgNPs on the secretory cytokine and chemokine profile of LPS treated WBCs cells

The proteome profile analysis of WBCs treated with a mitogen or in the presence of 25 μg/ml AgNPs showed that MCP-1 was inhibited by the AgNPs (Figure 4.18). Upon the quantification of the membranes, a significant reduction (P < 0.001) of the following cytokines and chemokines was exhibited due to AgNP exposure. Those cytokines and chemokines are: IL-1ra; MIF; Serpin E1; RANTES; ICAM-1 and IL-1β (Table 4.4).
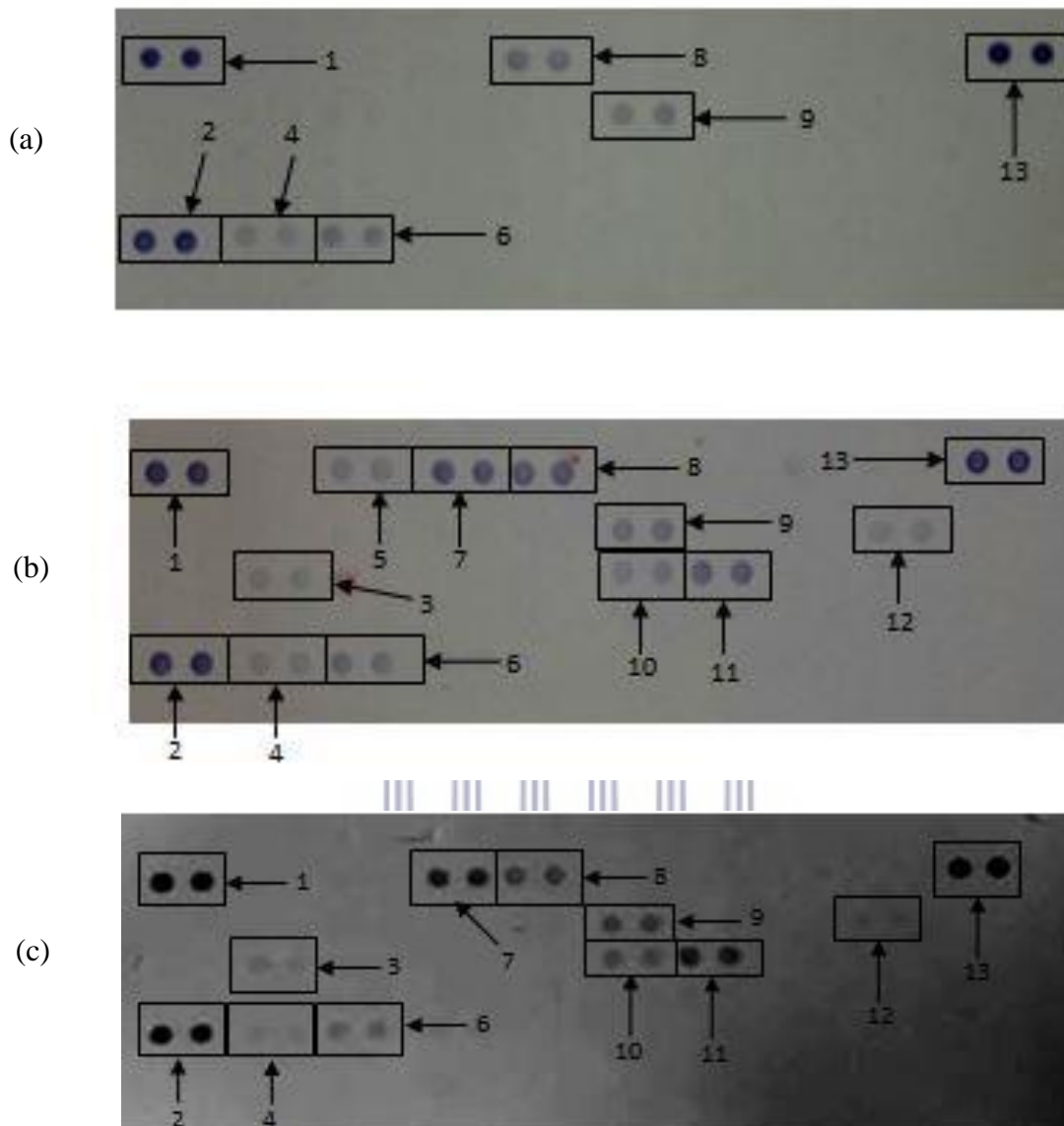
Figure 4.18. The effect of AgNPs on WBCs. Cells were incubated with (a) medium only, (b) medium containing LPS or (c) 25 μg/ml AgNPs in the presence of LPS. Supernatants were probed using the proteome profiler array as described in methods. Cytokines/ chemokines that were detected were allocated numbers: 1,2, and 13 are reference spots; 3- IL-1ra ; 4- MIF; 5-MCP-1; 6- Serpin E1; 7- MIP-1α/β; 8- RANTES; 9-ICAM-1, 10- IL-6, 11- IL-8 and 12- IL-1β.

137

Table 4.4. Quantification of cytokines and chemokines secreted by WBCs stimulated with LPS after treatment with medium only (negative control), medium containing LPS (positive control) or medium containing LPS and 25 μg/ml AgNPs. Membranes were subjected to chromogenic exposure. Data is represented as mean ± SD. Significance indicated by a- AgNP at 25 μg/ml significantly different (P < 0.001) compared to negative control, b- AgNP at 25 μg/ml significantly different (P < 0.001) compared to the positive control.

Cytokines and Chemokines	Positive Control	Negative Control	25 μg/ml AgNPs in the presence of LPS
Reference Spot	100 ± 7.28	100 ± 14.51	100 ± 5.98
IL-1ra	16.92 ± 1.46	0 ± 0	8.36 ± 0.17[a,b]
MIF	17.56 ± 1.51	19.57 ± 1.65	6.99 ± 0.50[a,b]
MCP-1	26.26 ± 2.54	0 ± 0	0 ± 0[b]
Serpin E1	32.40 ± 2.49	27.39 ± 0.66	19.97 ± 1.10[a,b]
MIP-1α/β	70.22 ± 4.11	0 ± 0	62.27 ± 2.16[a,b]
RANTES	62.94 ± 2.55	41.71 ± 0.45	34.99 ± 0.42[a,b]
sICAM	37.15 ± 0.59	32.33 ± 1.00	26.97 ± 0.01[a,b]
IL-6	29.31 ± 4.81	0 ± 0	23.18 ± 0.29[a]
IL-8	50.27 ± 8.41	0 ± 0	49.47 ± 0.26[a]
IL-1β	20.29 ± 0.99	0 ± 0	6.97 ± 0.32[a,b]

4.4. Discussion

Nanoparticles possess unique characteristics due to their higher surface to volume ratio compared to bulk chemicals. This result in superior reactivity compared to their bulk products (Chen and Schluesener, 2008). The unique characteristics of the nanoparticles aid in their translocation into cells where they are speculated to result in cytotoxicity and other cellular responses (Chen and Schluesener, 2008, Fabrega et al., 2011, Liu et al., 2011, Martínez-Gutierrez et al., 2012). Macrophages are believed to

138

be one of the main cell types that encounter and process nanoparticles, resulting in the modulation of biological responses such as immune reactions (Gustafson et al., 2015). Given the extent of AgNP use, it is important to monitor the effects of AgNPs on macrophages and the immune system in its entirety.

Due to the uncertainty of final FBS concentrations of cells exposed to AgNPs (Park et al., 2011, Asharani et al., 2012, Singh and Ramarao, 2012, Kaur and Tikoo, 2013). As a preliminary evaluation in this study, RAW cells were exposed to various AgNP concentrations, 10, 5, 2, and 1 % FBS and either in the absence or presence of LPS. The highest FBS concentration, 10%, aided in protecting the cell from the cytotoxic and anti-inflammatory (NO) effects of the AgNPs.

AgNP concentrations ≥ 15.625 μg/ml stimulated RAW cell growth in unstimulated cultures. Kaur and Tikoo (2013) found that RAW cells exposed to AgNPs synthesized by the reduction with sodium borohydride (BSNPs) had no effect on viability across a 0 – 100 μg/ml concentration range. However, Park et al. (2010) found that RAW cells exposed to AgNPs resulted in a 20 % reduction in cell viability when exposed to 1.6 μg/ml for 24 hrs. In another study, 10 μg/ml of AgNPs caused a 30 % reduction in cell viability of RAW cells after a 24 hr exposure period (Giovanni et al., 2015). These results further add to conflicting reports on how AgNPs affect macrophages. Both Park et al. (2010) and Giovanni et al. (2015) reported a particle size > 100 nm and this could account for the reduction in cell viability. The > 100 nm size of the nanoparticles would impact on other factors such as the zeta potential and agglomerative effect of the AgNPs, thus altering the properties of nanoparticles.

139

Change in particle size would impact on how the nanoparticles are translocated into the cell.

Conversely, WBC viability was reduced by 250 μg/ml AgNPs. Greulich et al. (2011) found that no cytotoxicity was evident when PMBCs were exposed to a concentration range of 5-30 μg/ml for 24 hrs. The nanoparticles, however, had a notable stimulatory effect on unstimulated monocytes at 25 and 30 μg/ml respectively; and had no effect on T-cells. The results of this study, reflect the findings of Greulich et al. (2011) as AgNP concentrations ≤ 25 μg/ml had no cytotoxic effects. However, a larger concentration range was investigated in this study, which revealed AgNPs to be cytotoxic at 250 μg/ml.

This study shows that AgNPs inhibits NO and IL-6 at 250 μg/ml in stimulated RAW cell cultures. NO was stimulated at AgNP concentrations ≥ 62.5 μg/ml in unstimulated RAW cultures. Park et al. (2010) noted that NO increased by two fold in unstimulated RAW cell cultures at 1.6 μg/ml AgNPs compared to the control. Current results are similar to what was seen in this study, however, the effects were at higher concentrations. Martínez-Gutierrez et al. (2012) reported that AgNPs stimulated IL-6 secretion in human THP-1 monocytes at 5 and 10 μg/ml. In another study, where alveolar macrophages were exposed to AgNPs, no detectable levels of IL-6 were found in culture supernatants after a 24 hr exposure (Carlson et al., 2008). This data corroborates conflicting reports of the effects AgNPs has on inflammation, as unstimulated cultures did not synthesize IL-6 in this study.

140

AgNP concentrations > 25 μg/ml stimulated IL-6 and MIP-1β synthesis in unstimulated WBC cultures. These inflammatory biomarkers were inhibited by 250 μg/ml AgNPs in LPS stimulated cultures. The only other study conducted on PBMCs found that AgNPs had an immunostimulatory effect. Greulich et al. (2011) found that inflammatory biomarkers were upregulated by the AgNP concentration range 5 – 20 μg/ml, which is similar to what was found here.

The acquired immune cytokines, IL-10 and IFNγ was upregulated in unstimulated WBC cultures by 250 μg/ml AgNP. IL-10 was inhibited in PHA stimulated cultures at the same AgNP concentration. Martinez-Gutierrez et al. (2012) found that a AgNP concentration range of 5 – 10 μg/ml induced IL-10 production in phorbol 12-myristate 13-acetate (PMA) stimulated THP-1 cells. On the contrary, no effects were seen on IL-10 production at the above mentioned concentration range in this study. Conversely, Shin et al. (2007) found that PBMCs inhibited IFNγ production in PHA stimulated cultures at AgNP concentrations ≥ 3 μg/ml, compared to no effect in this study.

The stimulation of IL-6, MIP-1β, IL-10 and IFNγ under basal conditions and the suppression of these cytokines under a simulated immune response could potentially be detrimental to the immune system, as it could result in immunostimulation or immunosuppression respectively.

The proteome profile of RAW 264.7 cells without and after AgNP treatment gives indications of cytokines and chemokines modulated by the particles. Culture

141

supernatants in the presence of the mitogen, LPS, with and without AgNP exposure revealed no differences in the levels of cytokines and chemokines monitored. Clear differences were seen in the culture supernatants of cells not stimulated with LPS, for unexposed and exposed 250 μg/ml AgNPs supernatants. The 250 μg/ml AgNPs supernatants of cells not treated with LPS showed that the following cytokines and chemokines were upregulated by AgNPs compared to the 0 μg/ml AgNP control: TNF-α; CCL2/MCP-1/JE; CCL4/MIP-1β and CXCL2/MIP-2. The above mentioned cytokines and chemokines have various, different but interconnective functions (Table 4.5). TNF-α, plays a vital role in controlling the production of other cytokines which are mainly produced by macrophages (Wajant et al., 2003). Whereas, the MIPs (CCL4/MIP-1β and CXCL2/MIP-2) have chemotactic properties which are specific to neutrophils and aids in their recruitment in response to infection, injury and cancer (Zlotnik et al., 2006). Similar results were seen using a Multiplex system, where TNF-α; CCL4/MIP-1β and CXCL2/MIP-2 were upregulated regardless of the size of the AgNPs as this trend was seen at 20, 80 and 113 nm. However, only nine cytokines and chemokines were monitored at one time (Park et al., 2010). The current proteome profiler system allows 40 cytokines and chemokines to be monitored at the same time compared to only nine using Multiplex assays. CCL2/MCP-1/JE is one of the major chemokines known for tissue healing and regulates the migration and infiltration of monocytes/macrophages to the site of infection. This involves the migration of monocytes from the blood stream across the vascular endothelium. (Deshmane et al., 2009). MCP-1 exhibits all four elements of inflammatory mediated wound healing by activating macrophage migration and infiltration, fibroblast

142

proliferation, connective tissue proliferation and capillary arteriogenesis (Hoh et al., 2011). Therefore, TNF-α, MIP-1β, MIP-2 and MCP-1 all assist in the defense of the immune system and macrophages when it encounters AgNPs. Hoh et al. (2011) proposed a pathway whereby the above mentioned cytokines work together to promote wound healing when analyzing the repair of murine carotid aneurysms under both *in vivo* and *in vitro* conditions (Figure 4.19). This proposed pathway could apply to the exposure of the murine cell line RAW 264.7 to AgNPs and indicates the way the immune system would react in order to promote cell and tissue healing as the cell would sense damaging effects upon AgNP exposure and during an aneurysm. These specific cytokines and chemokines will be released in order to combat cellular damage and promote cellular healing.

143
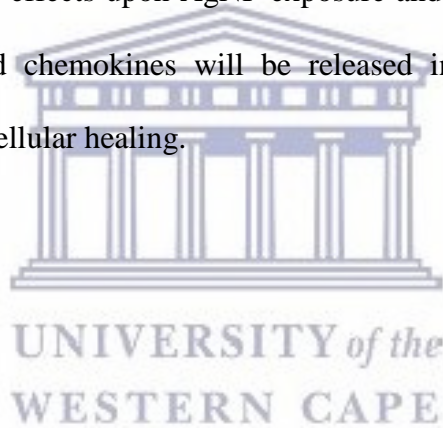
Table 4.5. Mediators and their effects on target cells of innate and adaptive immunity

(Cardamone et al., 2016, Lin and Du, 2017)

Mediators	Target Cell	Cellular Effect
CXCL10/IP-10; TNF-α	Neutrophils	Proliferation
CCL3/MIP-1α; CCL4/MIP-1β; CXCL10/IP-10	Th1 CD4$^+$ cells	Migration, proliferation, activation, differentiation
CCL2/MCP-1	Th17 CD4$^+$ cells	Proliferation, migration
CCL4/MIP-1β; CXCL10/IP-10	CD8$^+$ cells	Migration, proliferation, activation, differentiation
CCL2/MCP-1; G-CSF	B cells	Maturation, proliferation, IgG and IgM production
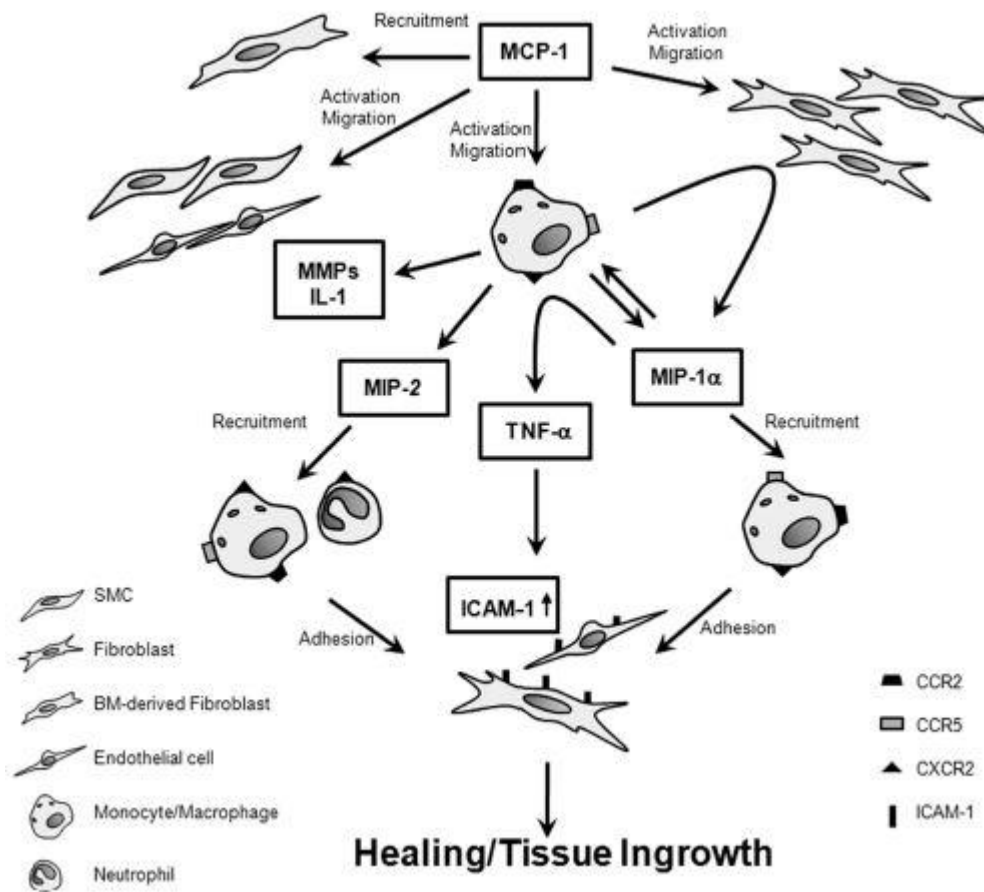
Figure 4.19. Hoh et al. (2011) proposed pathway whereby various cytokines play different but interconnective roles in order to promote wound healing in murine carotid aneurysms under both *in vivo* and *in vitro* conditions.

The proteome profile of WBCs exposed to media only and 25 μg/ml AgNP under basal conditions indicated no major differences between cytokines and chemokines synthesized. However, 25 μg/ml AgNP exposure of LPS treated cell inhibited MCP-1, IL-1ra and IL-1β under a simulated inflammatory response compared LPS treated cells in the absence of AgNP. This indicates that inflammation and the recruitment of cells to promote tissue healing would be inhibited if an individual already

145

experiencing an inflammatory response would be exposed to a AgNP concentration of 25 μg/ml. This is conflicting, as IL-6 was significantly upregulated under stimulated conditions. These results are also contradictory to the RAW cell data although it could be attributed to the higher concentration investigated.

To date only a few studies have looked at the proteome profile of RAW cells, but none on WBCs when exposed to certain 'substances'. These include the Chinese herbal formula, "Zuojin Pill" extract, Bi-Qi capsule, resveratrol, polished and sandblasted (surface roughness) of titanium disks to name a few (Wang et al., 2011a, Capiralla et al., 2012, Wang et al., 2012, Barth et al., 2013). No investigative work has looked at the effects silver or any other nanoparticle on the proteome profile of RAW macrophages and WBCs. Therefore, this assay allows investigators to focus on potential targets of the nanoparticles using a quick method that can monitor multiple end-points.
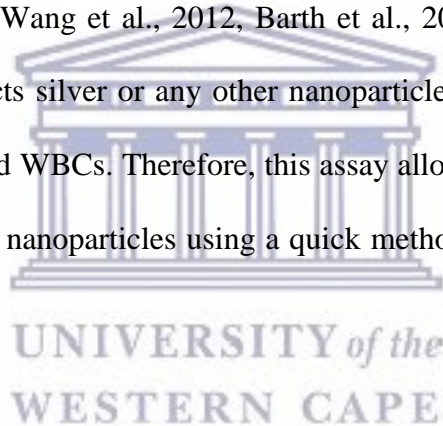
4.5. Conclusion

Silver nanoparticles upregulated RAW cell metabolism and NO production under basal conditions. However, RAW cell NO and IL-6 responses were inhibited by 250 μg/ml. Notable changes in RAW cytokines and chemokines were seen upon proteome profiling analysis. The cytokines and chemokines upregulated by AgNPs in unstimulated cultures could potentially be used to assess the effects of AgNPs on macrophages. These cytokines and chemokines identified are: TNF-α; CCL2/MCP-1/JE; CCL4/MIP-1β; CXCL2/MIP-2; CD54/sICAM-1 and CCL3/MIP-1α. Thus, in

146

depth studies on AgNP toxicity should be conducted using these potential biomarkers.

The highest AgNP concentration (250 μg/ml) exhibited cytotoxic effects on WBCs. Inflammation was upregulated by AgNPs under basal conditions but inhibited in a simulated inflammatory response. A similar trend was seen with adaptive immune responses, humoral and cell mediated immunity. A proteome profile revealed that AgNPs would inhibit inflammation in an individual already experiencing an inflammatory response.

**Effects of graphene oxide nanoparticles on the immune system biomarkers
produced by RAW 264.7and human whole blood cell cultures**

Abstract

Graphene oxide nanoparticles (GONPs) have attracted a lot of attention due to their
many applications. These applications include batteries, super capacitors, drug
delivery and biosensing. However, few studies have investigated the effects of these
nanoparticles on the immune system. In this study the *in vitro* effects of GONPs on
the immune system was evaluated by exposing murine macrophages, RAW 264.7
cells and human whole blood cell cultures (WBCs) to GONPs. The effects of GONPs
on RAW cells were monitored under basal conditions. The WBCs were exposed to
GONPs in the presence or absence of the mitogens lipopolysaccaharide (LPS) and
phytohaemmagglutinin (PHA). A number of parameters were monitored for both
RAW and WBCs, these included cytotoxicity, inflammatory biomarkers, cytokines of
the acquired immune system and a proteome profile analysis. The GONPs were
cytotoxic to both RAW and WBCs at 500 μg/ml. In the absence of mitogens, GONPs
elicited an inflammatory response from RAW and WBCs at 15.6 and 5 μg/ml
respectively. This activation was further corroborated by proteome profile analysis of
both experimental cultures. GONPs inhibited LPS induced IL-6 synthesis and PHA
induced IFNγ synthesis by WBCs in a dose dependent manner. In the absence of
mitogens, GONPs stimulated IL-10 synthesis by WBCs. The current study shows

148

that GONPs modulate immune system biomarkers and that these may pose a health risk to individuals exposed to this type of nanoparticle.

Keywords: graphene oxide nanoparticles, cytotoxicity, macrophage activation, humoral immune response

5.1. Introduction

Graphene (G) is a two-dimensional (2-D) carbon material, with a hexagonal structure (honeycomb lattice) consisting of sp^2 hybridized atoms, which has been isolated from its three dimensional parent material, graphite (Chen et al., 2016a, Chen et al., 2016b, Liu et al., 2016). Graphene oxide (GO) is a single carbon layer graphene derivative, containing oxygen-bearing functional groups such as carboxyl and hydroxyl groups (Chen et al., 2016b, Lu et al., 2017, Sotirelis and Chrysikopoulos, 2017). These groups are acquired when graphene undergoes oxidization (Chen et al., 2016b). These oxidized graphene nanoparticles possess unique characteristics such as electronic and thermal conductivity, superior mechanical strength and optical properties (Cherian et al., 2014). Due to these exceptional physiochemical properties of graphene oxide nanoparticles (GONPs), it has a broad range of applications in a number of fields. These fields include electrochemistry, biomedicine, biosensing, drug delivery, high energy capacity batteries and super capacitors to name a few (Chen et al., 2016b, Sotirelis and Chrysikopoulos, 2017).

Due to the applications of GONPs it is inevitable that these nanoparticles will be released into the environment and may directly or indirectly affect human health.

149

Therefore it is imperative that the effects of GO be investigated. GO was only discovered in 2004, and since its discovery, few studies have reported on its effects on the immune system (Chen et al., 2016b). Graphene oxide induced oxidative stress and immunotoxicity *in vivo* in zebrafish (Chen et al., 2016a). Upon *in vitro* exposure to GONPs, decrease in cell viability, deoxyribonucleic acid (DNA) damage, increased reactive oxygen species (ROS) production and induction of inflammatory factors were recorded (Lu et al., 2017, Peruzynska et al., 2017, Yan et al., 2017). Studies also showed that GONPs exhibited antibacterial effects against both gram negative and gram positive bacteria (Akhavan and Ghaderi, 2010).

The aim of current study was to investigate the *in vitro* effects of GONPs on the immune system by exposing the murine macrophage cell line, RAW 264.7 and human whole blood cell cultures to GONPs. A number of immune system biomarkers were monitored such as cytotoxicity, inflammatory biomarkers, cytokines of the acquired immune system and a proteome profile analysis of cytokines and chemokines expressed upon GONPs exposure.

5.2. Materials and Methods

5.2.1. Synthesis and characterization of graphene oxide nanoparticles (GONPs)

The graphene oxide nanoparticles were synthesized according to a modified Hummer's method (Hummers and Offeman, 1958), characterized and obtained from the University of Missouri. Graphene sheets were visualized (540 nm) via transmission electron microscopy (TEM). Further characterization revealed the

150

particles had a maximum absorbance at 227 nm with ultraviolet-visible spectrophotometry (UV-vis), a number of hydroxyl and carboxyl groups with Fourier-transform infrared spectroscopy (FTIR), and particles had an average zeta potential, an indicator of surface potential of -49.2 mV at pH 7.

5.2.2. Preparation of GONPs

A 10 mg/ml stock of GONPs in distilled water was prepared. The GONPs were sonicated (QSonica, LLC. Misonix sonicators, XL-200 Series) using a tip sonicator in short busts, one ice for a total of approximately 90 min. Aliquots of the stock solution were frozen at -80 °C until use. Before use in experiments, nanoparticles were thawed and further sonicated in short bursts on ice for 5 min.

5.2.3. RAW 264.7 Cells

5.2.3.1. Cell culture and exposures

The murine macrophage cell line, RAW 264.7, was obtained from American Type Culture Collection (ATCC TIB-71). The RAW 264.7 cells were cultured in Dulbecco's modified Eagle's medium (DMEM) (Lonza) supplemented with 10 % heat inactivated fetal bovine serum (FBS) (Hyclone), glutamax (Sigma-aldrich), antibiotic/antimycotic (Sigma-aldrich) and gentamicin (Sigma-aldrich). The cells were incubated in a humidified atmosphere of 5 % CO_2 at 37 ºC and the cells were sub-cultured every 2-3 days.

The RAW 264.7 cells (1 x 10^5 cells/ml) were cultured in cell culture treated 48 well plates and incubated in a humidified atmosphere of 5 % CO_2 at 37 ºC for

151

approximately 48 hrs until the cells reached 80-90 % confluence. After the incubation period, media was removed and replace with media containing 2.5 % FBS. The subsequent procedures occurred in serum free media. The cells were pre-exposed for 2 hrs to various concentrations of GONPs. Thereafter the cells were left unstimulated and a positive control was also present. The positive control were cells only stimulated by lipopolysaccharide (LPS) (1 µg/ml) without the presence of nanoparticle. The final concentration of FBS/well was 0.5 %. Cultures were incubated overnight (~18 hrs) under standard tissue culture conditions. Culture supernatants were collected for nitric oxide (NO), interleukin 6 (IL-6), macrophage inflammatory protein 1α (MIP-1α), MIP-1β, MIP-2 and proteome profiling analysis.

5.2.3.2. Cytotoxicity Assay

After the removal of the supernatants, cells were washed with Dulbecco's Phosphate Buffered Saline (DPBS) (Lonza), supplemented with glutamax, antibiotic/antimycotic solution. Cytotoxicity was measured by adding 150 µl of a 1/10 dilution of2-(4-Iodophenyl)-3-(4-nitrophenyl)-5-(2,4-disulfophenyl)-2H-tetrazolium (WST-1) (Roche)reagent in serum free medium to each well. Metabolically active cells convert WST-1 reagent to a formazan that can be measured spectrophotometrically. Formazan formation was determined by reading the plate at 450 nm (Multiskan Ex, Thermo Electron Corporation) immediately after WST-1 addition and again after an incubation period of 1 hr at 37 °C. The increase in absorbance at 450 nm is proportional to formazan formation. The level of fomazan formed is directly proportional to cell viability.

5.2.3.3. NO Determination

After the overnight incubation of the RAW 264.7 cells, the amount of nitrite that was produced by the cells was measured in the culture supernatant as an indication of NO production. The NO assay is based on the Griess reaction (Granger et al., 1996). The amount of NO production was measured against a doubling dilution range of an 100 µM nitrite standard (Sigma-Aldrich). Nitrite standards or culture supernatant collected (100 µl) were mixed with 100 µl of Griess reagent (1:1 of 1 % sulfanilamide and 0.1 % naphtylethlemidimine-dihydrochloride in 2.5 % phosphoric acid) (all reagents obtained from Sigma-Aldrich). Thereafter, the plate was incubated at room temperature for 15 min. The absorbance was read at 540 nm by a microplate reader (Multiskan Ex, Thermo Electron Corporation) and the amount of NO produced by the RAW cells quantified.

5.2.3.4. Mouse IL-6 Double Antibody Sandwich (DAS) Enzyme Linked Immunosorbent Assay (ELISA)

The mouse IL-6 ELISA (e-Bioscience, Ready-Set-Go) kits were used to measure IL-6 cytokine levels in the cell culture supernatants. The LPS stimulated control was assayed at (1/40) while the negative control (not treated with LPS) was assayed at (1/5) in assay diluent. Assays were performed in 96 well Nunc maxisorb plates. The kit contained all the reagents for the assay and was performed as per the manufacturer's instructions.

153

5.2.3.5. Mouse MIPs (MIP-1α, MIP-1β and MIP-2) DAS ELISAs

Mouse MIP-1α, MIP-1β and MIP-2 ELISAs (R & D Systems) was performed on the samples and the LPS stimulated culture supernatants. The kits contained all the reagents required for the experiment and experiments were performed as per the manufacturer's instructions. The samples were all diluted in reagent diluent, 1% human serum albumin (HSA) (w/v). The MIP-1α samples were assayed at 1/270 v/v and the LPS stimulated supernatant at 1/10 000 v/v in diluent. For the MIP-1β ELISA, the unstimulated culture supernatants were assayed at 1/20 v/v while the LPS stimulated supernatants were assayed at 1/5 000 v/v in assay diluent. The MIP-2 ELISA unstimulated supernatants were assayed at 1/100 v/v and the mitogen stimulated supernatant was at 1/1 000 v/v in diluent.

5.2.3.6. Mouse Proteome Profiling Assay

A commercially available antibody array kit (Proteome Profiler, Mouse cytokine Array Panel A, R & D Systems) which was coated with 40 capturing antibodies in duplicate on a nitrocellulose membrane (dot blot) was used. The kit contained all the reagents for the assay and was performed as per the manufacturer's instructions. This cytokine and chemokine antibody array was used to determine the effects of GONPs exposure on cytokine and chemokine by RAW 264.7 macrophage cells. The assay required 500 μl of cell culture supernatants (unstimulated 0 μg/ml GONPs, LPS stimulated 0 μg/ml GONPs, and unstimulated 15.6 μg/ml GONPs). Membranes were subjected to a ultra sensitive chromogenic 3,3',5,5'-Tetramethylbenzidine (TMB) membrane substrate (Thermo Scientific) to reveal sample-antibody complexes

154

labeled with streptavidin-HRP. Photographs were taken of the blots after the exposure to the substrate.

5.2.3.7. Quantification of pixel density for cytokine and chemokine membranes

Membrane images were quantified using image processing and analysis Java software, ImageJ. Levels of cytokines and chemokines were expressed as a percentage of the reference spot. Microsoft Excel was used to calculate the percentages which is expressed as mean ± standard deviation (SD).

5.2.4. Whole Blood Cell (WBC) Culture

5.2.4.1. Blood collection

Blood was collected by a doctor/nurse from a healthy male who was not using any medication. The blood was collected using venipuncture directly into 3.2% sodium citrate vacuum tubes (Greiner bio-one). The blood was processed immediately. The whole blood cell cultures were performed under sterile conditions. Ethical clearance was obtained from the University of the Western Cape (Ethics No.10/9/43). Informed consent was also obtained from the participant.

5.2.4.2. Cell Culture

Human whole blood was diluted with Roswell Parks Memorial Institute (RPMI) 1640 media (Sigma-Aldrich) to give rise to a 10% (v/v) mixture. Blood was either left unstimulated or stimulated with LPS (Sigma-Aldrich) (0.1 μg/ml) or phytohaemmagglutinin (PHA) (Sigma-Aldrich) (1.6 μg/ml). Unstimulated or

155

stimulated whole blood cell cultures were incubated overnight at 37°C with high, intermediate and low concentrations of GONPs in a 24 well tissue culture treated plate (Nunc). Along with the nanoparticle exposure, a positive control of 0.01 % Tween20 (Merck) was also present. After the incubation period, culture supernatants were screened for cytotoxicity by a lactate dehydrogenase (LDH) assay, inflammatory markers IL-6 and MIP-1β, interleukin 10 (IL-10) and interferon gamma (IFNγ).

5.2.4.3. LDH Assay

After the overnight incubation, an aliquot of the unstimulated WBC supernatants were screened for cytotoxicity and measured the release of LDH from the cells (LDH-cytotoxicity colourimetric kit II, BioVision). The kit contained all the reagents for the assay and was performed as per the manufacturer's instructions.

5.2.4.4. Cytokine Analysis using DAS ELISAs

Commercially available kits (e-Bioscience, Ready-Set-Go) were used to analyse the level of cytokine secretion from the whole blood cell cultures. The kits were used as per the manufacturer's instructions and contained all the reagents to complete the assay. The unstimulated and LPS stimulated samples were analysed using a 1/10 dilution for the IL-6 assay. While the unstimulated and PHA stimulated samples were assayed neat for IL-10 and IFNγ analysis. The same protocol was used as previously described for the mouse cytokine ELISA.

5.2.4.5. Human MIP-1β DAS ELISAs

A human MIP-1β ELISA (R & D Systems) was performed on the unstimulated and LPS stimulated culture supernatants of the WBCs. The samples were diluted 1/10 in reagent diluent, 0.1 % bovine serum albumin (BSA) (Sigma). The same protocol was followed as the mouse MIPs ELISAs.

5.2.4.6. Human Proteome Profiling

A commercially available antibody array kit (Proteome Profiler, Human Cytokine Array Kit, R & D Systems) which was coated with 36 capturing antibodies in duplicate on a nitrocellulose membrane (dot blot) was used. The kit contained all the reagents for the assay and was performed as per the manufacturer's instructions. This cytokine and chemokine antibody array was used to determine the effects of GONPs on cytokine and chemokine secretion when exposed to WBCs. The assay required 500 µl of cell culture supernatants (unstimulated 0 µg/ml GONPs, LPS stimulated 0 µg/ml GONPs, and unstimulated 5µg/ml GONPs). The subsequent steps were carried out as described for the mouse cytokine and chemokine proteome profiling.

5.2.5. Statistical Analysis

All experiments were performed in triplicate and the data was calculated using Microsoft Excel. Data is presented as mean ± standard deviation (SD). One way analysis of variance (ANOVA) using SigmaPlot 12.0 was used to assess statistical differences with $P < 0.01$ being deemed significant.

157

5.3. Results

5.3.1. The effects of GONPs on RAW 264.7 cells

5.3.1.1. Cytotoxicity

GONPs at concentrations ≤ 31.25 µg/ml did not have an effect on cell viability (Figure 5.1). However, GONPs concentrations ≥ 62.5 µg/ml significantly reduced (P < 0.001) cell viability. At the highest concentration of GONP screened (500 µg/ml), the viability of cells were less than 60 % of the control cell viability (cells that did not receive GONP).
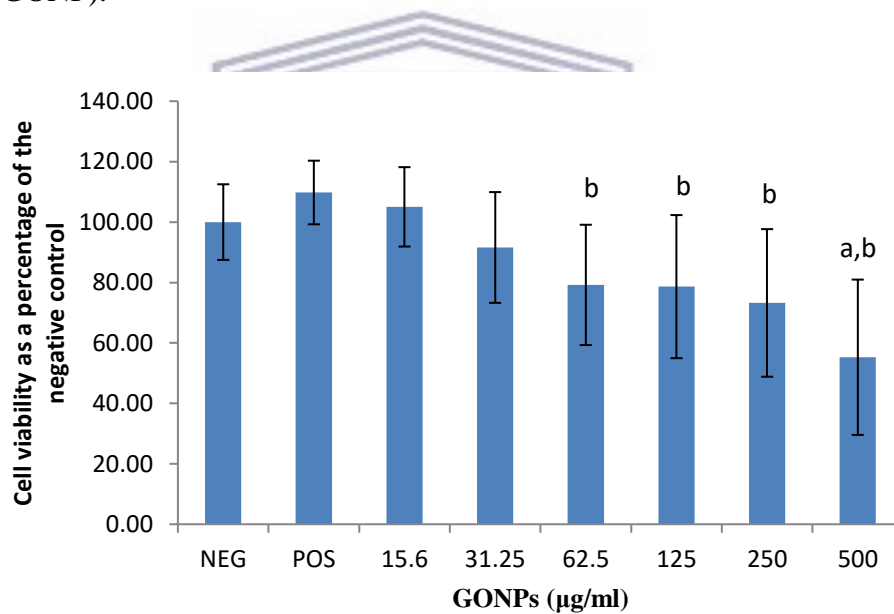
Figure 5.1. Cell viability of RAW 264.7 macrophage cells exposed to GONPs. Data represents mean ± SD with n = 9. Bars marked with letters indicate significant difference (P < 0.01) to control. Significance demarcated by: a- significantly different (P < 0.001) compared to negative control, b- significantly different (P ≤ 0.005) compared to positive control.

5.3.1.2. The effects of GONPs on the inflammatory system biomarker NO using RAW 264.7 cells

GONPs had no effect on the inflammatory response from the cells in an unstimulated environment across all the concentrations monitored in this study (Figure 5.2). A LPS stimulated control without any nanoparticle is included in the results to verify that the data obtained is not due to any artefacts that were generated due to the exposure of GONPs to cells.

Figure 5.2. NO levels of RAW 264.7 cell cultures exposed to GONPs. Data represents mean ± SD with n = 9. Bars marked with letters indicate significant differences (P < 0.01). Significance demarcated by: a- significantly different (P < 0.001) compared to the positive control.

5.3.1.3. The effects of GONPs on the inflammatory system biomarker IL-6 using RAW 264.7 cells

GONPs under unstimulated conditions induced a significant upregulation ($P < 0.001$) of IL-6 at 15.6 and 31.25 μg/ml respectively, when compared to the control culture that was not exposed to GONP (Figure 5.3). Conversely, IL-6 synthesis was not affected when cultures were exposed to GONP concentrations $\geq$ 62.5 μg/ml. The results representing LPS stimulated cultures without any nanoparticle (80862 ± 24175 pg/ml IL-6) is not included on the figure.
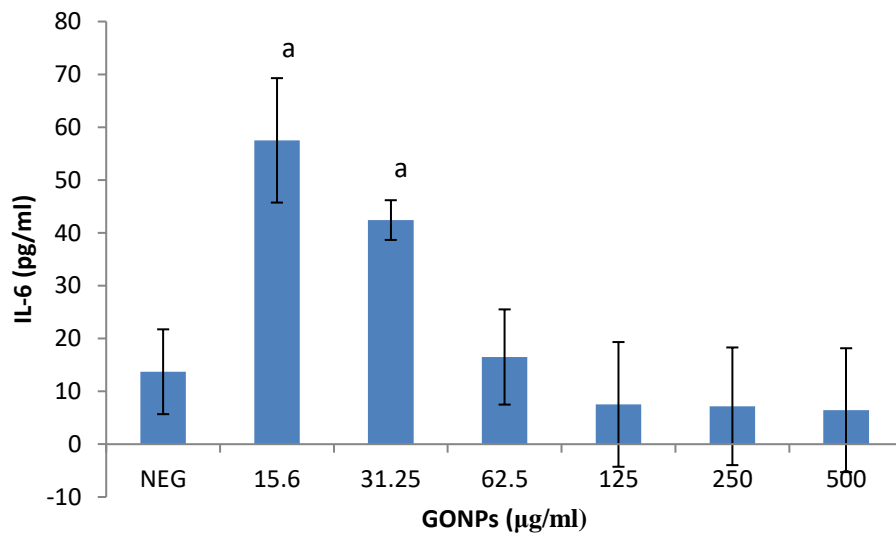
Figure 5.3. IL-6 levels of unstimulated RAW 264.7 cell cultures exposed to GONPs. Data represents mean ± SD with n = 9. Positive control not represented (80862 ± 24175 pg/ml IL-6). Bars marked with letters indicate significant differences ($P < 0.01$). Significance demarcated by: a- significantly different ($P < 0.001$) compared to 0 μg/ml GONP.

5.3.2. The effects of GONPs on the MIPs chemokines using RAW 264.7 cells

5.3.2.1. The effects of GONPs on MIP-1α using RAW 264.7 cells

GONPs in the range of 15.6 – 62.5 μg/ml in media only notably increased ($P < 0.001$) the synthesis of MIP-1α, compared to the culture control not exposed to GONP (Figure 5.4). However, GONPs concentrations ≥ 125 μg/ml significantly decreased the synthesis of MIP-1α compared to the culture control which was not exposed to GONP. The results for control cultures exposed to media in the presence of a mitogen only (803 852 ± 353 697 pg/ml MIP-1α) are not included on the figure.
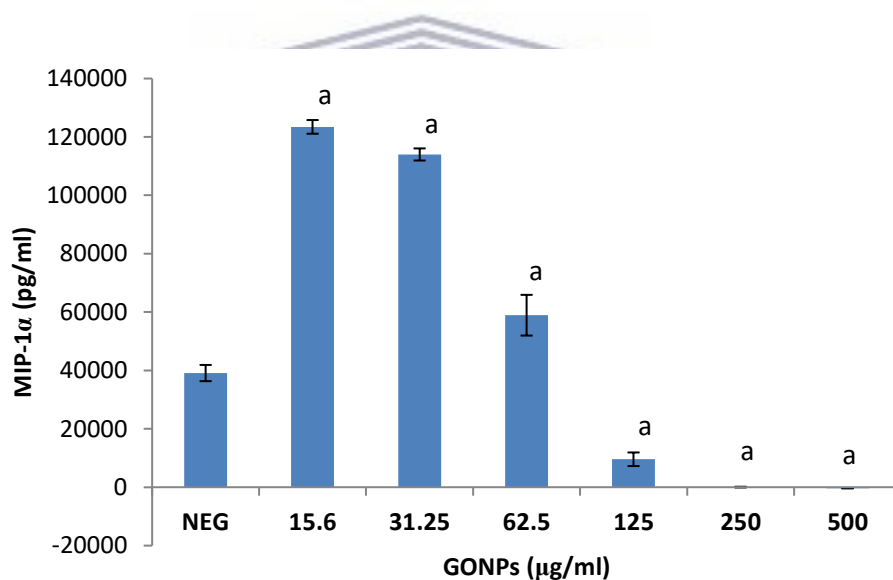
Figure 5.4. MIP-1α levels of unstimulated RAW 264.7 cell cultures exposed to GONPs. Data represents mean ± SD with n = 9. Positive control not represented (803 852 ± 353 697 pg/ml MIP-1α). Bars marked with letters indicate significant differences ($P < 0.01$). Significance demarcated by: a- significantly different ($P < 0.001$) compared to 0 μg/ml GONP.

5.3.2.2. The effects of GONPs on MIP-1β using RAW 264.7 cells

Cultures exposed to GONP concentrations in the range of 15.6 – 31.25 significantly upregulated (P < 0.001) the amount of MIP-1β secreted by the unstimulated RAW cells compared to the culture control not exposed to GONP (Figure 5.5). GONP concentrations ≥ 62.5 μg/ml, on the other hand significantly reduced MIP-1β synthesis compared to the culture control containing no nanoparticle. Results of media only exposed to LPS in the absence of GONP (1 127 185 ± 468 693 pg/ml MIP-1β) are not included in the figure.
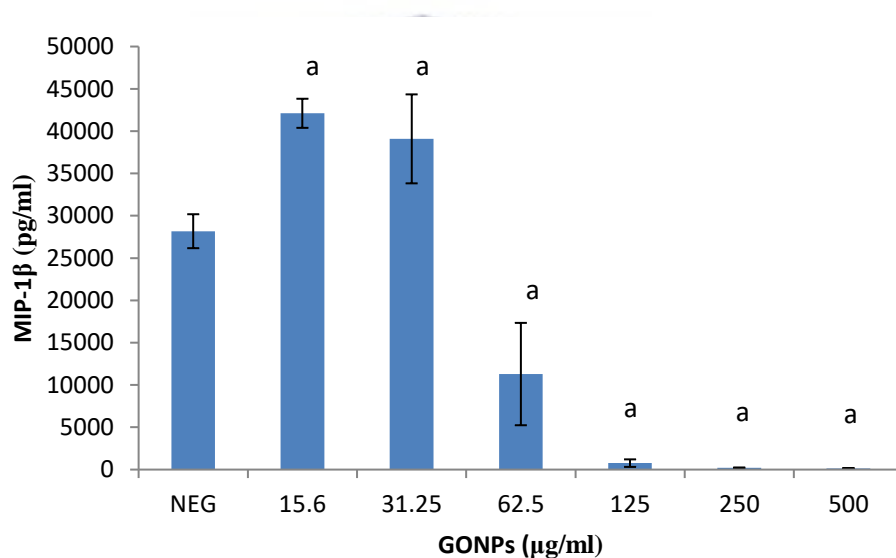
Figure 5.5. MIP-1β levels of unstimulated RAW 264.7 cell cultures exposed to GONPs. Data represents mean ± SD with n = 9. Positive control not represented (1 127 185 ± 468 693 pg/ml MIP-1β). Bars marked with letters indicate significant differences (P < 0.01). Significance demarcated by: a- significantly different (P < 0.001) compared to 0 μg/ml GONP.

5.3.2.3. The effects of GONPs on MIP-2 using RAW 264.7 cells

GONP concentrations $\leq$ 62.5 µg/ml significantly increased (P < 0.001) MIP-2 synthesis compared to the control cultures exposed to media only without any nanoparticle (Figure 5.6). MIP-2 synthesis was not affected by GONP concentrations $\geq$ 125 µg/ml. Media in the presence of LPS without GONP (307 390 ± 171 856 pg/ml MIP-2) is not included on the figure.
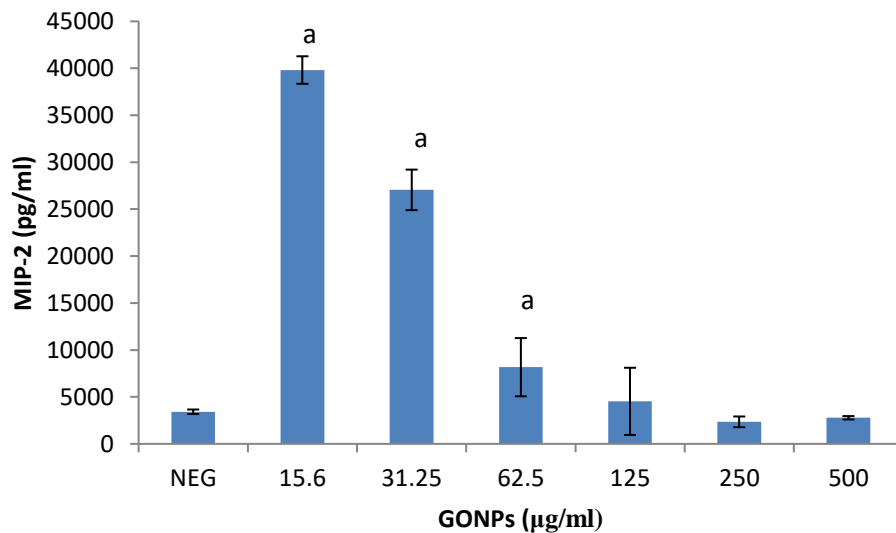
Figure 5.6. MIP-2 levels of unstimulated RAW 264.7 cell cultures exposed to GONPs. Data represents mean ± SD with n = 9. Positive control not represented (307 390 ± 171 856 pg/ml MIP-2). Bars marked with letters indicate significant differences (P < 0.01). Significance demarcated by: a- significantly different (P < 0.001) compared to 0 µg/ml GONP.

163

5.3.3. The effects of GONPs on the secretory cytokine and chemokine profile of RAW 264.7 cells

Membranes exposed to media only, media in the presence of a mitogen, and 15.6 μg/ml GONPs allowed for the analysis of various cytokines and chemokines expressed by the cells upon the relative exposure (Figure 5.7). Quantification of the membranes showed that the simulated inflammatory response (media in the presence of LPS) allowed the cells to secrete certain cytokines and chemokines that were not synthesized by the cells when exposed to media only and 15.6 μg/ml GONPs. These proteins include: IFNγ-inducible protein 10 (IP-10); Granulocyte-macrophage colony-stimulating factor (GM-CSF); IL-6; macrophage colony-stimulating factor (M-CSF); interleukin 27 (IL-27); interleukin 1 receptor antagonist (IL-1ra); and IL-β.

However, the exposure of WBCs to 15.6 μg/ml GONP in the absence of a mitogen affected the synthesis of certain proteins that significantly differed ($P < 0.001$) from both the negative (media only) and positive (media in the presence of LPS) controls. These cytokines and chemokines include: Granulocyte -colony stimulating factor (G-CSF); tumour necrosis factor α (TNF-α); monocyte chemoattractant protein 1 (MCP-1)/JE; intracellular adhesion molecule 1 (ICAM-1); MIP-1α; MIP-1 β; MIP-2; regulated on activation, normal T cell expressed and secreted (RANTES); and stromal cell-derived factor 1 (SDF-1) (Table 5.1).
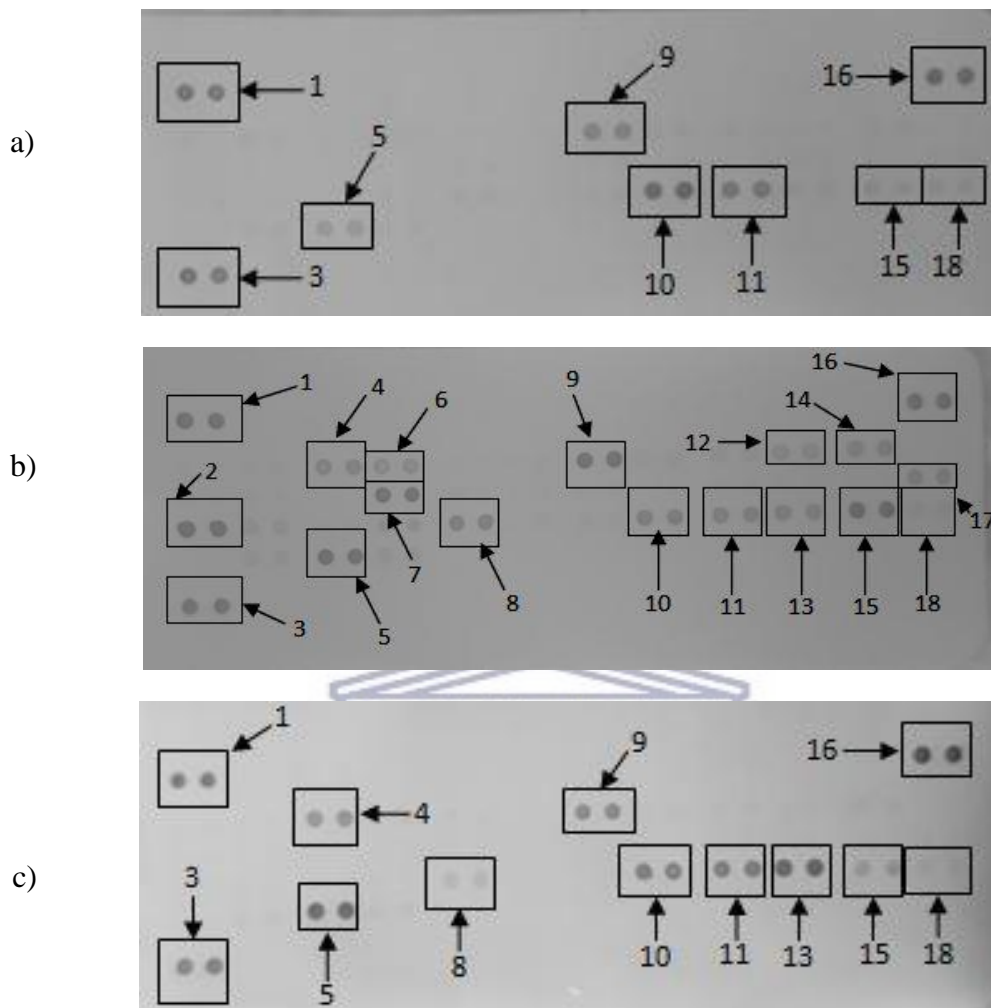
Figure 5.7. The effect of GONPs on RAW 264.7 cells. Cells were incubated with (a) media only (negative control), (b) media in the presence of LPS and (c) 15.6 μg/ml GONPs in the absence of a mitogen. Supernatants were probed using the proteome profiler array as described in methods. Cytokines/ chemokines that were detected were allocated numbers: 1,3, and 16 are reference spots; 2- IP-10; 4- G-CSF; 5- TNF-α; 6- GM-CSF; 7- IL-6; 8- JE; 9-sICAM-1; 10- MIP-1α; 11- MIP-1β; 12- IL-1β; 13-MIP-2; 14- IL-1ra; 15- RANTES; 17- IL-27; 18-SDF-1.

Table 5.1. Quantification of cytokines and chemokines secreted by RAW 264.7 cultures not stimulated with LPS after treatment with medium only (negative control), medium containing LPS (positive control) or medium containing 15.6 μg/ml GONPs. Membranes were subjected to chromogenic exposure. Data is represented as mean ± SD. Significance indicated by a- GONP at 15.6 μg/ml significantly different (P < 0.001) compared to negative control, b- GONP at 15.6 μg/ml significantly different (P < 0.001) compared to the positive control.

Cytokines and Chemokines	Positive Control	Negative Control	15.6 μg/ml GONPs
Reference Spot	100 ± 8.62	100 ± 10.49	100 ± 14.75
IP-10	114.74 ± 5.24	0 ± 0	0 ± 0[b]
G-CSF	58.27 ± 2.55	0 ± 0	70.48 ± 1.93[a,b]
TNF-α	102.01 ± 5.91	17.96 ± 0.13	119.99 ± 3.19[a,b]
GM-CSF	47.32 ± 3.02	0 ± 0	0 ± 0[b]
IL-6	91.94 ± 3.60	0 ± 0	0 ± 0[b]
M-CSF	25.12 ± 3.03	0 ± 0	0 ± 0[b]
MCP-1	78.97 ± 4.48	0 ± 0	23.50 ± 2.27[a,b]
sICAM-1	109.05 ± 6.00	34.76 ± 0.02	68.23 ± 2.39[a,b]
MIP-1α	72.87 ± 4.22	57.00 ± 1.94	93.70 ± 1.69[a,b]
MIP-1β	62.77 ± 3.35	37.68 ± 0.33	82.05 ± 0.74[a,b]
MIP-2	55.51 ± 2.75	14.75 ± 0.69	111.00 ± 3.85[a,b]
RANTES	100.57 ± 4.42	17.93 ± 0.83	37.13 ± 1.12[a,b]
SDF-1	16.41 ± 1.61	21.75 ± 1.01	1.01 ± 0.02[a,b]
IL-27	54.97 ± 4.05	0 ± 0	0 ± 0[b]
IL-1ra	55.84 ± 1.66	0 ± 0	0 ± 0[b]
IL-1β	39.16 ± 3.31	0 ± 0	0 ± 0[b]

5.3.4. The effects of GONPs on WBCs

5.3.4.1. Cytotoxicity

GONP concentrations ≤ 50 μg/ml had no effect on cell viability (Figure 5.8). However the highest concentration of GONP evaluated, 500 μg/ml, significantly

reduced (P < 0.003) viability compared to cultures exposed to media only in the absence of GONP.
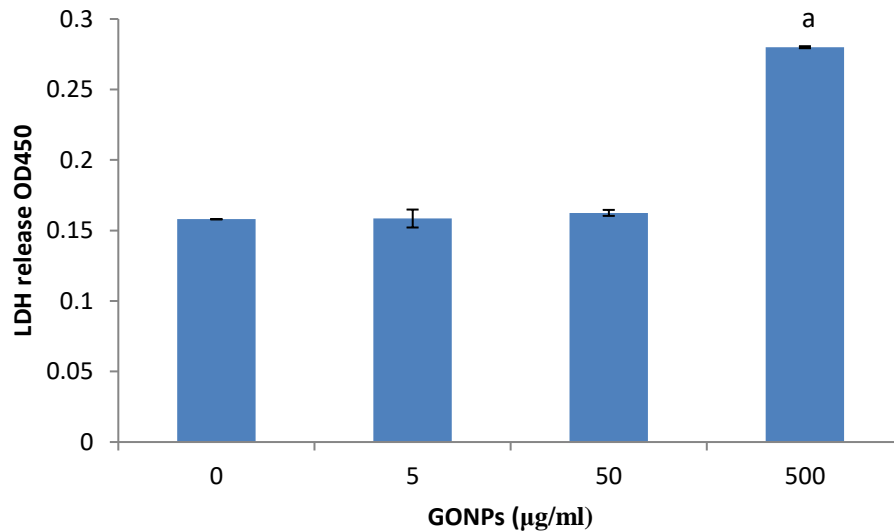
Figure 5.8. Cell viability of WBCs exposed to GONPs. Data represents mean ± SD with n = 4. Bars marked with letters indicate significant difference (P < 0.01) to control. Significance demarcated by: a- significantly different (P < 0.003) compared to 0 µg/ml GONP.

5.3.4.2. The effects of GONPs on the inflammatory system biomarker IL-6 using WBCs

Cultures exposed to GONPs alone significantly increased (P < 0.001) the IL-6 release from the cells at all the concentrations monitored when compared to the culture control exposed to media only (Figure 5.9). Conversely, GONPs concentrations in the presence of LPS significantly reduced (P < 0.002) the secretion of IL-6 from the cells in a dose dependent manner compared to the control, exposed to media only

167

containing the mitogen. Based on the reduction in IL-6, an $IC_{50} = 289.88$ μg/ml was calculated (Figure 5.10).
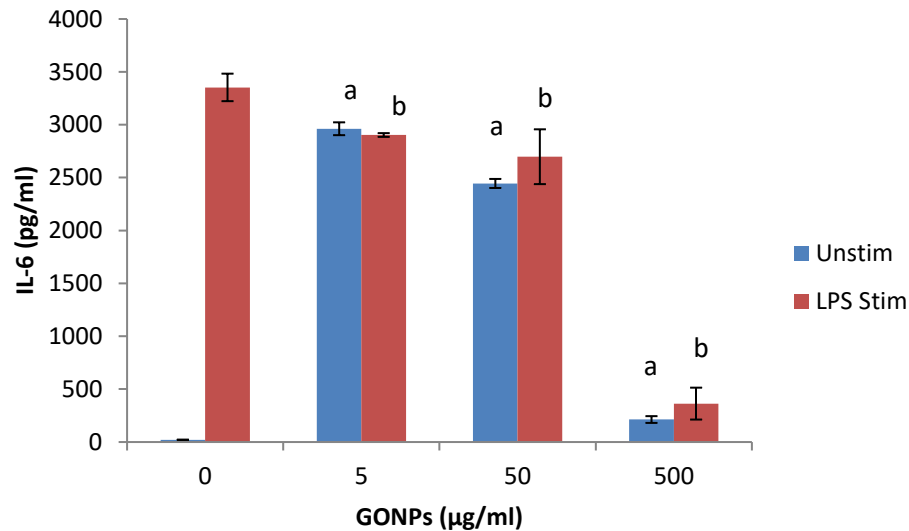
Figure 5.9. IL-6 levels of WBCs exposed to GONPs. Data represents mean ± SD with n = 4. Bars marked with letters indicate significant differences (P < 0.01). Significance demarcated by: a- GONP treated, unstimulated WBCs significantly different (P < 0.001) compared to 0 μg/ml GONP, b- GONP treated, LPS stimulated WBCs significantly different (P < 0.002) compared to 0 μg/ml GONP control.

The plot shows IL-6 (pg/ml) on the y-axis versus Log Concentration GONPs (μg/ml) on the x-axis with the equation:

$$y = -0.001x^2 - 4.494x + 2925.$$
$$R^2 = 1$$
$$IC_{50} = 289.88 \ \mu g/ml$$
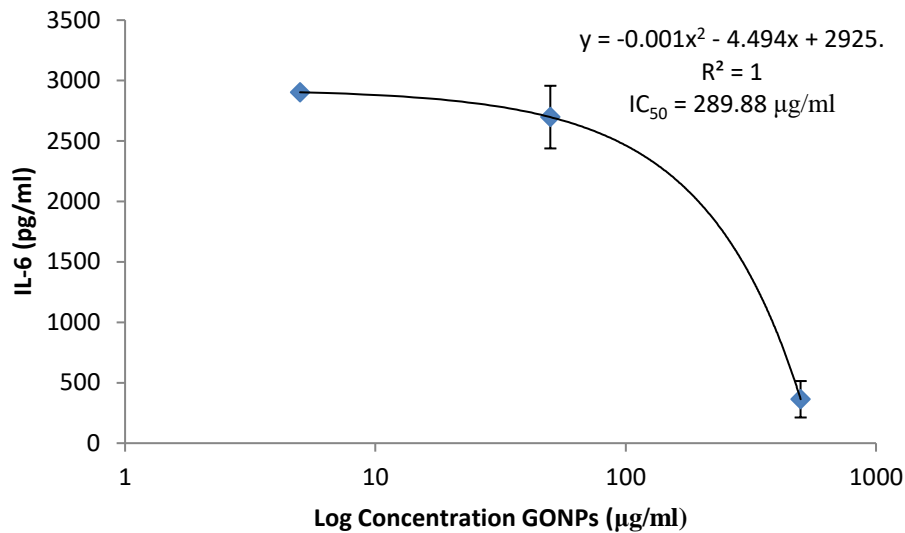
Figure 5.10. IC_{50} determination of GONPs on IL-6 production by LPS stimulated WBCs.

5.3.4.3. The effects of GONPs on the inflammatory chemokine, MIP-1β using WBCs

MIP-1β was significantly upregulated (P < 0.001) by GONPs under unstimulated conditions at 5 and 50 μg/ml respectively, when compared to the culture control, not containing any nanoparticle (Figure 5.11). However, under a simulated inflammatory response, GONPs exhibited a prominent reduction (P < 0.001) in MIP-1β synthesis at concentrations ≥ 50 μg/ml when compared to the culture control, media only containing LPS. Exposure of cells to 37.41 μg/ml GONPs in the presence of a mitogen would reduce MIP-1β synthesis by half (Figure 5.12).
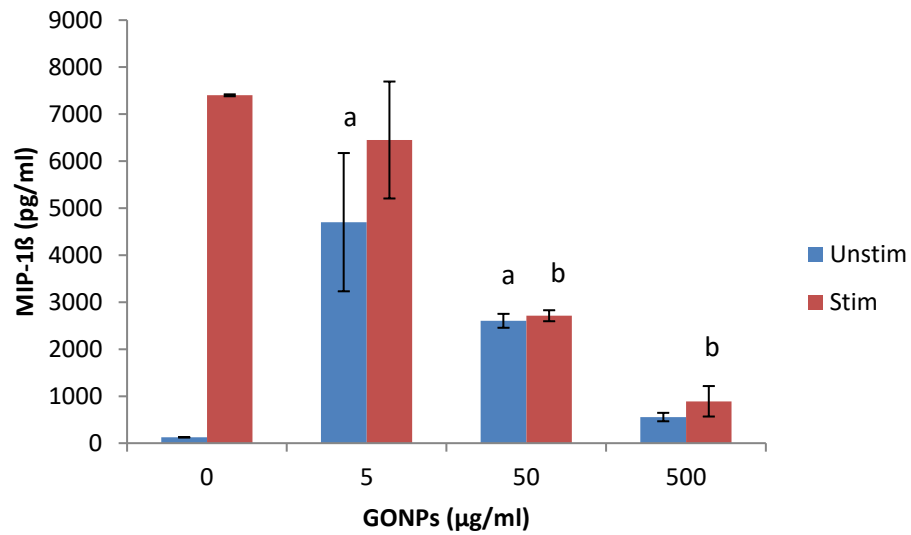
169

Figure 5.11. MIP-1β of WBCs exposed to GONPs. Data represents mean ± SD with n = 4. Bars marked with letters indicate significant differences (P < 0.01). Significance demarcated by: a- significantly different (P < 0.001) compared to 0 µg/ml GONP in unstimulated cultures, b- significantly different (P < 0.001) compared to 0 µg/ml GONP for stimulated cultures.

The graph shows MIP-1β (pg/ml) on the y-axis (ranging from 0 to 9000) versus Log Concentration GONPs (µg/ml) on the x-axis (ranging from 1 to 1000).

$$y = -1207\ln(x) + 8072.$$
$$R^2 = 0.961$$
$$IC_{50} = 37.41 \ \mu g/ml$$
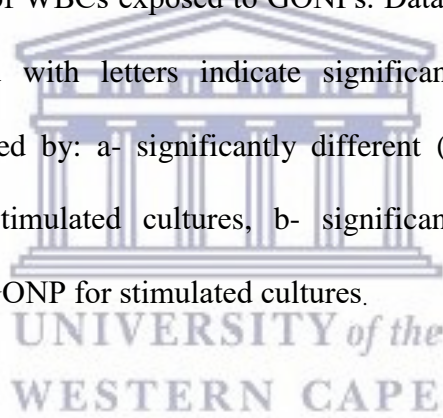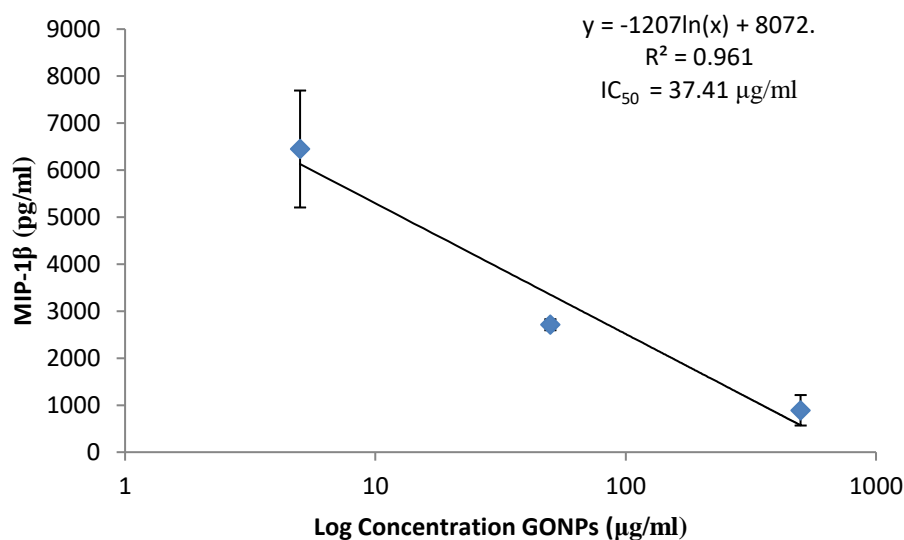
Figure 5.12. IC_{50} determination of GONPs on MIP-1β production by LPS stimulated WBCs.

5.3.4.4. The effects of GONPs on the humoral immune system biomarker IL-10 using WBCs

GONP concentrations ≤ 50 µg/ml in the absence of PHA significantly upregulated ($P < 0.002$) IL-10 production compared to the culture control, not containing nanoparticle (Figure 5.13). However, the highest concentration (500 µg/ml) of the unstimulated cultures had no effect on the adaptive immune response. On the other hand, GONPs concentrations in the presence of PHA significantly inhibited ($P < 0.001$) IL-10 secretion in a dose dependent manner compared to the culture control, which only contained PHA. Therefore, IL-10 secretion would be reduced by 50 % when exposed to 11.7 µg/ml GONPs (Figure 5.14).

171
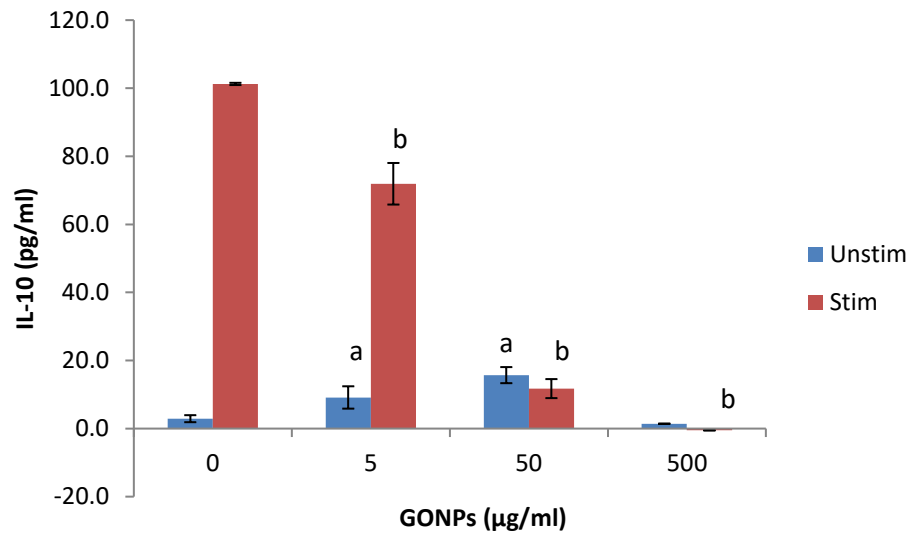
Figure 5.13. IL-10 levels of WBCs exposed to GONPs. Data represents mean ± SD with n = 4. Bars marked with letters indicate significant differences (P < 0.01). Significance demarcated by: a- significantly different (P < 0.002) compared to 0 μg/ml for unstimulated cultures, b- significantly different (P < 0.001) compared to 0 μg/ml for PHA stimulated cultures.
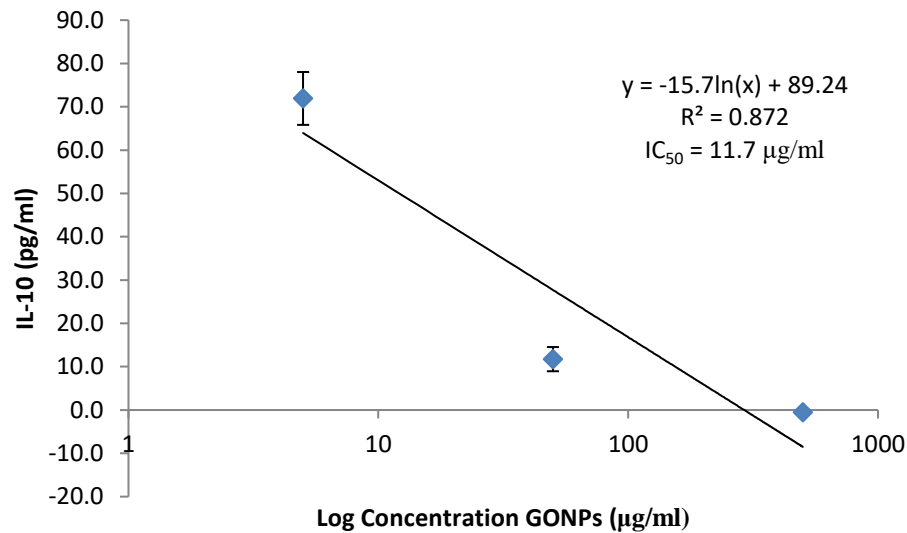
Figure 5.14. IC_{50} determination of GONPs on IL-10 production by PHA stimulated WBCs.

5.3.4.5. The effects of GONPs on the cell mediated immune system biomarker, IFNγ using WBCs

GONP concentrations did not affect the cell mediated cytokine, IFNγ under normal conditions (i.e. in the absence of PHA) (Figure 5.15). However, GONPs notably reduced ($P < 0.001$) the synthesis of IFNγ in a dose dependent manner in PHA stimulated cultures compared to media only containing PHA (culture control). IFNγ secretion would be reduced by half when exposed to 9.95 µg/ml GONPs (Figure 5.16). This dose dependent decrease of IFNγ mimicked the response of the other adaptive immune cytokine, IL-10 (Figure 5.13).
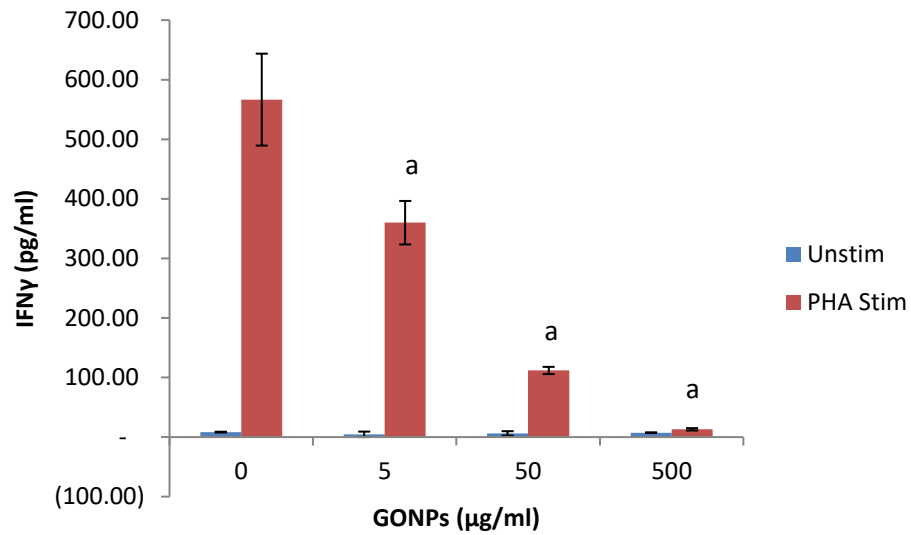
173

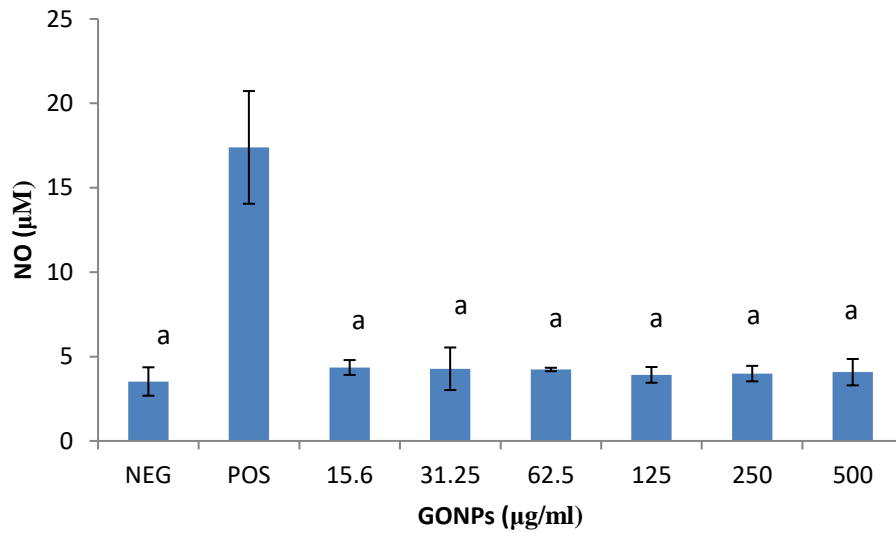**Figure 5.15.** IFNγ levels of WBCs exposed to GONPs. Data represents mean ± SD with n= 4.Bars marked with letters indicate significant differences (P < 0.01). Significance demarcated by: a- significantly different (P< 0.001) compared to 0 μg/ml for PHA stimulated cultures.

The chart shows a plot with the equation and statistics in the upper right:

$$y = -75.3\ln(x) + 456.3$$
$$R^2 = 0.941$$
$$IC_{50} = 9.95 \; \mu g/ml$$
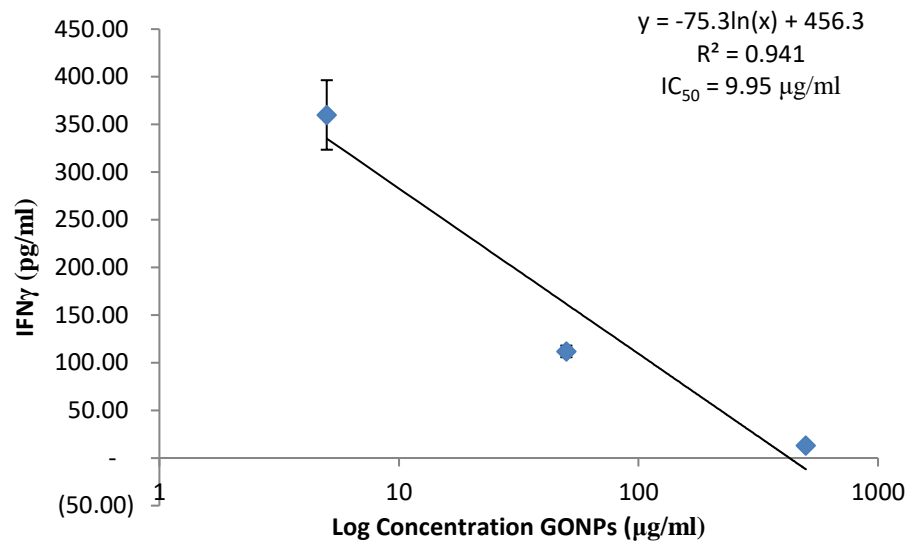
Figure 5.16. IC_{50} determination of GONPs on IFNγ production by PHA stimulated WBCs.

5.3.5. The effects of GONPs on the secretory cytokine and chemokine profile of WBCs

The proteome profile of WBCs exposed to media only (negative control), media containing the mitogen, LPS (positive control) and 5 μg/ml GONPs in the absence of a mitogen revealed notable changes in the synthesis or inhibition of a number of cytokines and chemokines (Figure 5.17).

Table 5.2 represents the quantification of the membranes. The WBCs exposed to GONPs caused the significant upregulation of macrophage migration inhibitory factor (MIF), MCP-1, and interleukin 8 (IL-8) compared to both controls. The GONPs also notably upregulated serpin E1, RANTES, and ICAM-1 compared to the negative control. Cytokines and chemokines that were prominently down regulated compared to the positive control include IL-1ra, MIP-1α/β, IL-6 and IL-1β (Table

175

5.2). Whole blood cells exposed to media only (negative control) did not synthesize the following cytokines: IL-1ra, MCP-1, MIP-1α/β, IL-6, IL-8 and IL-1β.
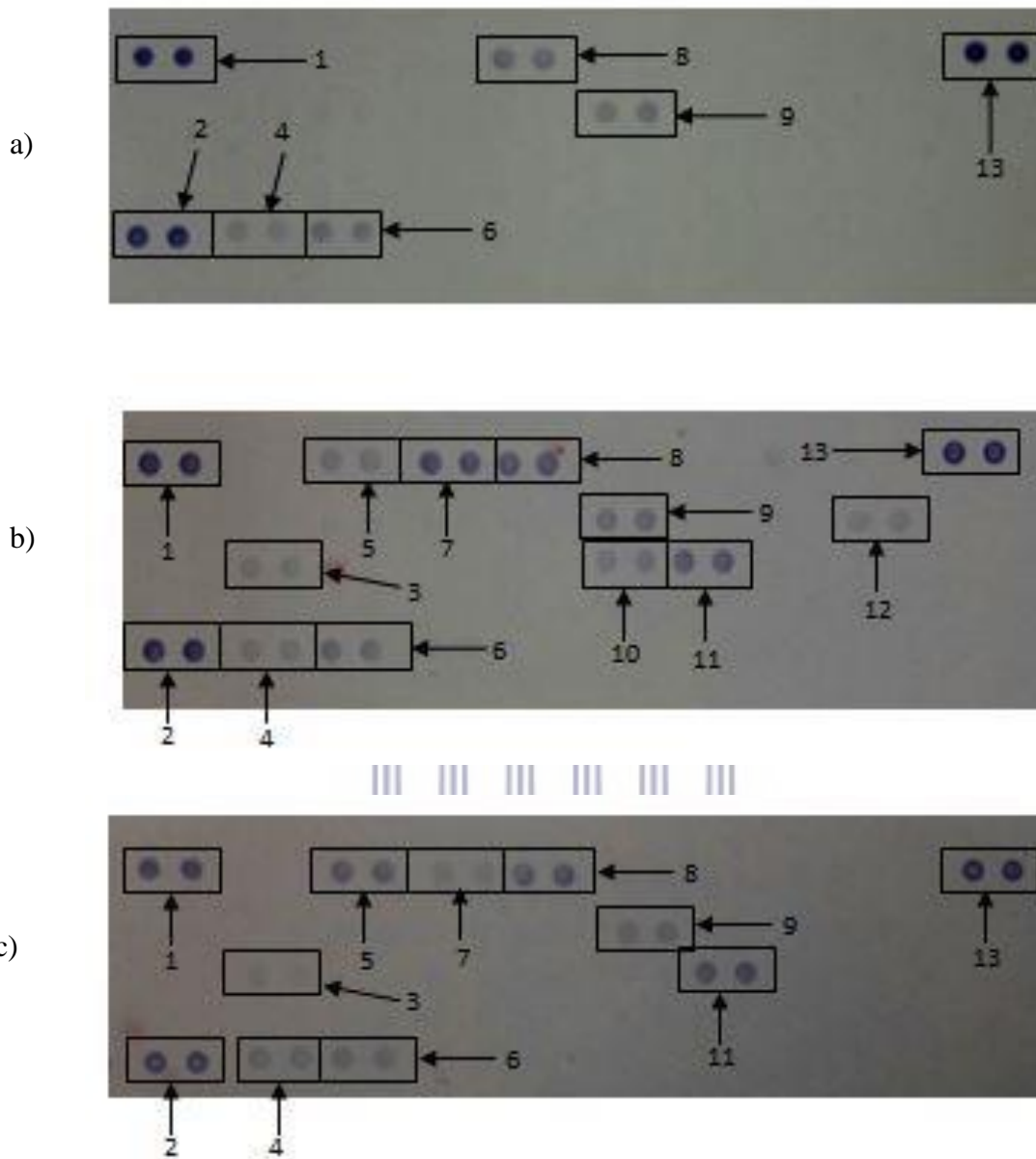
Figure 5.18. The effects of GONPs on whole blood cells. Cells were incubated with (a) media only, (b) media and LPS, (c) 5 µg/ml GONPs in the absence of LPS. Cytokines/ chemokines that were detected were allocated numbers: 1,2, and 13 are reference spots; 3- IL-1ra; 4- MIF; 5-MCP-1; 6- Serpin E1; 7- MIP-1α/β; 8- RANTES; 9-ICAM-1, 10- IL-6, 11- IL-8 and 12- IL-1β.

Table 5.2. Quantification of cytokines and chemokines secreted by WBCs not stimulated with LPS after treatment with medium only (negative control), medium containing LPS (positive control) or medium containing 5 μg/ml GONPs. Membranes were subjected to chromogenic exposure. Data is represented as mean ± SD. Significance indicated by a- GONP at 5 μg/ml significantly different (P < 0.001) compared to negative control, b- GONP at 5 μg/ml significantly different (P < 0.001) compared to the positive control.

Cytokines and Chemokines	Positive Control	Negative Control	5 μg/ml GONPs
Reference Spot	100 ± 7.28	100 ± 14.51	100 ± 8.24
IL-1ra	16.92 ± 1.46	0 ± 0	$10.28 \pm 1.85^{a,b}$
MIF	17.56 ± 1.51	19.57 ± 1.65	$33.27 \pm 2.35^{a,b}$
MCP-1	26.26 ± 2.54	0 ± 0	$73.52 \pm 5.69^{a,b}$
Serpin E1	32.40 ± 2.49	27.39 ± 0.66	37.94 ± 4.04^{a}
MIP-1α/β	70.22 ± 4.11	0 ± 0	$27.70 \pm 2.33^{a,b}$
RANTES	62.94 ± 2.55	41.71 ± 0.45	74.00 ± 8.17^{a}
sICAM	37.15 ± 0.59	32.33 ± 1.00	41.93 ± 4.04^{a}
IL-6	29.31 ± 4.81	0 ± 0	0 ± 0^{b}
IL-8	50.27 ± 8.41	0 ± 0	$73.74 \pm 5.00^{a,b}$
IL-1β	20.29 ± 0.99	0 ± 0	0 ± 0^{b}

5.4. Discussion

Graphene has attracted lots of attention due its numerous potential industrial and medical applications. However, very little is known about the effects of these nanoparticles on the immune system. The exposure of RAW cells to GONPs induced cytotoxicity at the highest concentration (500 μg/ml). Similar data was obtained by Li et al. (2012) who exposed pristine graphene to RAW 264.7 cells. They proposed that GONPs exerted its cytotoxic effects by depleting the mitochondrial membrane potential and increased the production of ROS. The decrease in cell viability could

also be attributed to the higher capacity of macrophages to internalize GO and this could have affected the assembly of actin within the cell (Feito et al., 2014, Zhang et al., 2016). A reduction in cell viability was also reported when exposing human THP-1 cells to GONPs, indicating consistent cytotoxic effects against macrophages and monocytes regardless of species (Lu et al., 2017).

Orecchioni et al. (2016b) reported that in primary and immortalized murine macrophages, GONPs significantly stimulated the secretion of Th_1/Th_2 cytokines, such as IL-1ra, IL-6, IL-10, TNF-α, and GM-CSF, as well as chemokines such as MCP-1, MIP-1α, MIP-1β and RANTES. This indicates activation of the macrophages by GONPs. These findings were corroborated by the inflammatory data and proteome profiling data obtained for the current study. GONPs, at basal conditions, increased the synthesis of inflammatory cytokines and chemokines such as NO, IL-6, TNF-α, MIPs and RANTES. Feito et al. (2014) found that RAW 264.7 cells exposed to poly(ethylene glycol-amine) (PEG) functionalized GO upregulated TNF-α under both basal and LPS stimulated conditions. IL-6 was down regulated at 25 and 100 μg/ml GO in a simulated inflammatory response (+LPS). No differences were seen in IL-6 levels under basal conditions. The TNF-α result obtained by Feito et al. (2014) is consistent with what was found in the current study using proteome profiling. The inflammatory cytokine, IL-6 was significantly upregulated at 15.6 and 31.25 μg/ml in the absence of a mitogen in the current study. This is contradictory to what was found by Feito et al. (2014) but could be attributed to the functionalization of GO. Functionalization, along with size and size distribution of the nanoparticles

179

with biocompatible polymers increases their stability under physiological conditions. It also minimizes their interactions with other biomolecules and reduce immunological responses (Feito et al., 2014, Peruzynska et al., 2017). The effects of GONPs on RAW cells, under LPS stimulated conditions, were not evaluated in the current study.

Similarly to the RAW cells, GONPs also induced cytotoxicity in WBCs at 500 μg/ml. Cherian et al. (2014) and Orecchioni et al. (2016a) exposed GONPs to peripheral blood mononuclear cells (PBMCs) and found that it induced its cytotoxic effects by inducing ROS-mediated apoptosis. Zhi et al. (2013) also found that GO induced apoptosis in T lymphocytes in a dose dependent manner.

Exposing WBCs to GONPs also induced the upregulation of the inflammatory cytokines IL-6 and MIP-1β under unstimulated/basal conditions. This activation of the inflammatory response could be attributed to the activation of the complement system which results in the production of anaphylatoxins (proinflammatory mediators). This may occur as GO may be sensed by components of the complement system as soon as GO is introduced into a biological system (Saleem et al., 2017). The activation of the complement system was studied by Wibroe et al. (2016), who found that there was an increase in C5a, which is a marker of the activation of the complement system when exposing human serum to GO. Wibroe et al. (2016) also found that GO reduced the synthesis of IL-6 when human serum was stimulated by LPS, which is consistent with what was found in this study. Proteome profiling data obtained in the current study confirmed that inflammatory cytokines and chemokines

180

were activated when WBCs were exposed to 5 μg/ml GONPs. Notably, IL-1ra, MCP-1, MIP-1α/β and IL-8 were upregulated by the GONPs.

GONPs not only inhibited an inflammatory response in a dose dependent manner, but also modulated cytokines regulating the adaptive immune responses. The GONPs stimulated the synthesis of the humoral immune regulating cytokine, IL-10, but did not affect the cell mediated response regulating cytokine, IFNγ, from WBCs under unstimulated/basal conditions. This indicates that GONPs would induce the differentiation of Th_0 cell to Th_2 cells. The B-lymphocytes are then stimulated to produce antibodies by interleukin 4 and 10 (IL-4 and IL-10) to combat the exposure to GONPs (Tan and Coussens, 2007). However, both IL-10 and IFNγ responses by WBCs under PHA stimulated conditions were down regulated by GONPs.

This study clearly indicates that GONPs are cytotoxic at high concentrations and stimulates the activation of inflammatory responses under unstimulated/basal conditions. This activation/stimulation of an inflammatory response could cause autoimmunity to individuals exposed to GONPs (De Jong and Van Loveren, 2007). Under unstimulated/basal conditions GONPs would also stimulate a humoral immune response in individuals exposed to them. However, under stimulated conditions mimicking an infection, both humoral and cell mediated responses were down regulated, indicating potential immunosuppression by GONPs exposure to individuals with an infection.

181

The data obtained in the current study is crucial for risk management of people upon GONP exposure, as these nanoparticles could be used *in vivo* as drug delivery systems, among other applications. GONPs may also be released into the environment and can potentially impact on human health.

Chapter 6:

The effects of carbon dots on immune system biomarkers, using the murine macrophage cell line RAW 264.7 and human whole blood cell cultures

Abstract

Carbon dots (CDs) are engineered nanoparticles that are used in a number of bioapplications such as bioimaging, drug delivery and theranostics. The effects of CDs on the immune system have not been evaluated. The effects of CDs on the immune system were assessed by using RAW 264.7 cells and whole blood cell cultures (WBCs). RAW cells were exposed to CD concentrations under basal conditions. WBCs were exposed to CD concentrations under basal conditions or in the presence of the mitogens lipopolysaccharide (LPS) or phytohaemmagglutinin (PHA). After exposure, a number of parameters were assessed, such as cell viability, biomarkers of inflammation, cytokine biomarkers of the acquired immune system and a proteome profile analysis. CDs were cytotoxic to RAW and WBCs at 62.5, 250 and 500 μg/ml respectively. Biomarkers associated with inflammation was induced by CD concentrations $\geq$ 250 and 500 μg/ml under basal conditions for both RAW and WBCs respectively. The humoral immune cytokine IL-10 was increased at 500 μg/ml CD under both basal and PHA activated WBC conditions. Proteome analysis supported the inflammatory data as upregulated proteins identified are associated

183

with inflammation. The upregulated proteins provide potential biomarkers of risk that can be assessed upon CD exposure.

Keywords: carbon dots, cytotoxicity, induced inflammation

6.1. Introduction

In 2004, carbon dots (CDs) were accidentally discovered, when they were isolated from single-walled carbon nanotubes (SWCNTs) via gel electrophoresis (Peng et al., 2017). CDs, also known as carbon quantum dots or carbon nanoparticles are a relatively new fluorescent quasi spherical, zero dimensional nanomaterial with a diameter less than 10 nm (Bayati et al., 2017, Sun and Lei, 2017, Tuerhong et al., 2017). Recently, there has been an increase in CD popularity as they possess unique optical properties, biocompatibility, low toxicity, facile synthesis and aqueous stability (Peng et al., 2017, Sun and Lei, 2017, Tao et al., 2017). These unique properties have allowed CDs to be used in bioapplications, such as bioimaging, drug delivery and theranostic developments (Peng et al., 2017).

Due to these applications, human exposure is unavoidable. However, very few studies have evaluated the potential effects of CDs on cells and the immune system. *In vivo* and *in vitro* studies have mainly focused on sensing and bioimaging of cells via the photoluminescent properties of CDs (Pierrat et al., 2015, Kudr et al., 2017, Pandey et al., 2017, Wang et al., 2017). Only a few studies have reported on the toxicity of CDs, and agree with the reports of their low toxicity. However, the toxicity is dependent on the functionalization of the CDs (Havrdova et al., 2016, Yuan et al.,

184

2017). To our knowledge, no studies have reported on the effects of CDs on the immune system. Reports have been published on the effects of carbon nanotubes (CNTs) on the immune system (Inoue et al., 2009, Kayat et al., 2011, Qu et al., 2012). In these studies, CNTs were reported to induced allergic airway inflammation, pulmonary inflammation, and inflammatory cytokines, interleukin 1β (IL-1β) and interleukin 6 (IL-6) under both *in vivo* and *in vitro* conditions.

This current study aimed to evaluate the effects of CDs on the murine macrophage cell line, RAW 264.7 and human whole blood cell cultures (WBCs). A number of parameters were assessed, which includes cell viability, inflammatory biomarkers, cytokines of the acquired immune system and a proteome profile analysis.

6.2. Materials and Methods

6.2.1. Synthesis and characterization of carbon dots (CDs)

The CDs were obtained from the University of Missouri where they were synthesized and characterized as previously published by Bayati et al. (2017). Briefly, transmission electron microscopy (TEM) revealed an average size range of 1-3 nm and an average zeta potential of -16.83 mV at a neutral pH in 1 mM sodium chloride (NaCl).

6.2.2. Preparation of CD stock solutions

A 10 mg/ml stock solution of CDs in distilled water was prepared. The CDs were sonicated, using a tip sonicator, in short intermittent bursts, on ice for approximately

185

5 min (QSonica, LLC. Misonix sonicators, XL-200 Series). The CDs were sonicated prior to use in cultures.

6.2.3. RAW 264.7 Cells

6.2.3.1. Cell culture and exposures

The murine macrophage cell line, RAW 264.7, was obtained from American Type Culture Collection (ATCC TIB-71). The RAW 264.7 cells were cultured in Dulbecco's modified Eagle's medium (DMEM) (Lonza) supplemented with 10 % heat inactivated fetal bovine serum (FBS) (Hyclone), glutamax (Sigma-aldrich), antibiotic/antimycotic (Sigma-aldrich) and gentamicin (Sigma-aldrich). The cells were incubated in a humidified atmosphere of 5 % CO_2 at 37 ºC and the cells were sub-cultured every 2-3 days.

The RAW 264.7 cells (1×10^5 cells/ml) were cultured in cell culture treated 48 well plates and incubated in a humidified atmosphere of 5 % CO_2 at 37 ºC for approximately 48 hrs until the cells reached 80-90 % confluence. After the incubation period, media was removed and replaced with media containing 2.5 % FBS. The subsequent procedures occurred in serum free media. The cells were pre-exposed for 2 hrs to various concentrations of CDs. Thereafter, the cells were left unstimulated and a positive control was also present. The positive control was cells only stimulated by lipopolysaccharide (LPS) (1 µg/ml) without the presence of nanoparticle. The final concentration of FBS/well was 0.5 %. Cultures were incubated overnight (~18 hrs) under standard tissue culture conditions. Culture supernatants were collected and

used for nitric oxide (NO), interleukin 6 (IL-6), macrophage inflammatory protein 1α (MIP-1α), MIP-1β, MIP-2 and proteome profiling analysis.

6.2.3.2. Cytotoxicity Assay

After the removal of the supernatants, cells were washed with Dulbecco's Phosphate Buffered Saline (DPBS) (Lonza), supplemented with glutamax, antibiotic/antimycotic solution. Cytotoxicity was measured by adding 150 µl of a 1/10 dilution of 2-(4-Iodophenyl)-3-(4-nitrophenyl)-5-(2,4-disulfophenyl)-2H-tetrazolium (WST-1) (Roche) reagent in serum free medium to each well. Metabolically active cells convert WST-1 reagent to a formazan that can be measured spectrophotometrically. Formazan formation was determined by reading the plate at 450 nm (Multiskan Ex, Thermo Electron Corporation) immediately after WST-1 addition and again after an incubation period of 1 hr at 37 °C. The increase in absorbance at 450 nm is proportional to formazan formation. The level of fomazan formed is directly proportional to cell viability.

6.2.3.3. NO Determination

After the overnight incubation of the RAW 264.7 cells, the amount of nitrite that was produced by the cells was measured in the culture supernatant as an indication of NO production. The NO assay is based on the Griess reaction (Granger et al., 1996). The amount of NO production was measured against a doubling dilution range of an 100 µM nitrite standard (Sigma-Aldrich). Nitrite standards or culture supernatant collected (100 µl) were mixed with 100 µl of Griess reagent (1:1 of 1 %

187

sulfanilamide and 0.1 % naphtylethlemidimine-dihydrochloride in 2.5 % phosphoric acid) (all reagents obtained from Sigma-Aldrich). Thereafter, the plate was incubated at room temperature for 15 min. The absorbance was read at 540 nm using a microplate reader (Multiskan Ex, Thermo Electron Corporation) and the amount of NO produced by the RAW cells quantified.

6.2.3.4. Mouse IL-6 Double Antibody Sandwich (DAS) Enzyme Linked Immunosorbent Assay (ELISA)

The mouse IL-6 ELISA (e-Bioscience, Ready-Set-Go) kits were used to measure IL-6 cytokine levels in the cell culture supernatants. The LPS stimulated control was assayed at (1/40 v/v) while the negative control (not treated with LPS) was assayed at (1/5 v/v) in assay diluent. Assays were performed in 96 well Nunc maxisorb plates. The kit contained all the reagents for the assay and was performed as per the manufacturer's instructions.

6.2.3.5. Mouse MIPs (MIP-1α, MIP-1β and MIP-2) DAS ELISAs

Mouse MIP-1α, MIP-1β and MIP-2 ELISAs (R & D Systems) was performed on the samples and the LPS stimulated culture supernatants. The kits contained all the reagents required for the experiment and experiments were performed as per the manufacturer's instructions. The samples were all diluted in reagent diluent, 1% human serum albumin (HSA) (w/v). The MIP-1α in unstimulated samples were assayed at 1/270 v/v and the LPS stimulated supernatant at 1/2 000 v/v in diluent. For the MIP-1β ELISA, the unstimulated culture supernatants were assayed at 1/100 v/v

while the LPS stimulated supernatants were assayed at 1/5 000 v/v in diluent. The MIP-2 ELISA unstimulated supernatants were assayed at 1/20 v/v and the mitogen stimulated supernatant was at 1/500 v/v in assay diluent.

6.2.3.6. Mouse Proteome Profiling Assay

A commercially available antibody array kit (Proteome Profiler, Mouse cytokine Array Panel A, R & D Systems) which was coated with 40 capturing antibodies in duplicate on a nitrocellulose membrane (dot blot) was used. The kit contained all the reagents for the assay and was performed as per the manufacturer's instructions. This cytokine and chemokine antibody array was used to determine the effects of CD exposure on cytokine and chemokine synthesis by RAW 264.7 macrophage cells. The assay required 500 μl of cell culture supernatants (unstimulated containing 0 μg/ml CDs, LPS stimulated containing 0 μg/ml CDs, and unstimulated containing 500 μg/ml CDs). Membranes were subjected to a ultra sensitive chromogenic 3,3',5,5'-Tetramethylbenzidine (TMB) membrane substrate (Thermo Scientific) to reveal sample-antibody complexes labeled with streptavidin-HRP. Photographs were taken of the blots after the exposure to the substrate.

6.2.3.7. Quantification of pixel density for cytokine and chemokine membranes
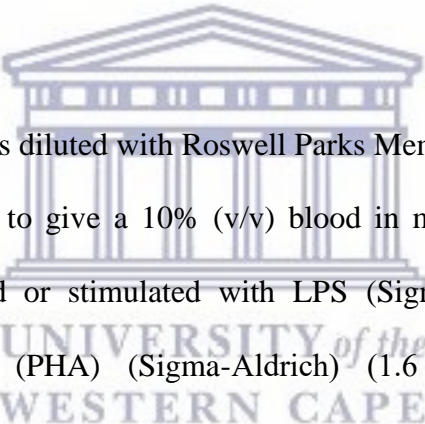
Membrane images were quantified using image processing and analysis Java software, ImageJ. Levels of cytokines and chemokines were expressed as a percentage of the reference spot. Microsoft Excel was used to calculate the percentage which is expressed as mean ± standard deviation (SD).

189

6.2.4. Whole Blood Cell (WBC) Culture

6.2.4.1. Blood collection

Blood was collected by a doctor/nurse from healthy males not using any medication. The blood was collected using venipuncture directly into 3.2% sodium citrate vacuum tubes (Greiner bio-one). The blood was processed immediately. The whole blood cell cultures were performed under sterile conditions. Ethical clearance was obtained from the University of the Western Cape (Ethics No.10/9/43). Informed consent was also obtained from the participant.

6.2.4.2. Cell Culture

Human whole blood was diluted with Roswell Parks Memorial Institute (RPMI) 1640 media (Sigma-Aldrich) to give a 10% (v/v) blood in medium mixture. Blood was either left unstimulated or stimulated with LPS (Sigma-Aldrich) (0.1 μg/ml) or phytohaemmagglutinin (PHA) (Sigma-Aldrich) (1.6 μg/ml). Unstimulated or stimulated whole blood cell cultures were incubated overnight at 37°C with high, intermediate and low concentrations of CDs in 24 well tissue culture treated plates (Nunc). A positive cytotoxicity control (medium containing 0.01 % v/v Tween20 (Merck)) was also present. After the incubation period the culture supernatants were collected and assayed for cytotoxicity, cytokines and chemokines.

6.2.4.3. Cytotoxicity Assay

Cytotoxicity was measured by monitoring lactate dehydrogenase (LDH) release by damaged cells. LDH activity was monitored spectrophotometrically using an LDH kit

(LDH-cytotoxicity colourometric kit II, BioVision). The kit contained all the reagents required for the assay and assays were performed as per the manufacturer's instructions.

6.2.4.4. Cytokine Analysis using DAS ELISAs

Commercially available kits (e-Bioscience, Ready-Set-Go) were used to analyse the level of cytokine secretion from the whole blood cell cultures. The kits were used as per the manufacturer's instructions and contained all the reagents to complete the assay. The unstimulated and LPS stimulated samples were analysed using a 1/10 v/v dilution for the IL-6 assay. While the unstimulated and PHA stimulated samples were assayed neat for IL-10 and IFNγ analysis. The same protocol was used as previously described for the mouse cytokine ELISA.

6.2.4.5. Human MIP-1β DAS ELISA

A human MIP-1β ELISA (R & D Systems) was performed on the unstimulated and LPS stimulated culture supernatants of the WBCs. The samples were diluted 1/10 v/v in reagent diluent, 0.1 % v/v bovine serum albumin (BSA) (Sigma). The same protocol was followed as for the mouse MIPs ELISAs.

6.2.4.6. Human Proteome Profiling

A commercially available antibody array kit (Proteome Profiler, Human Cytokine Array Kit, R & D Systems) which was coated with 36 capturing antibodies in duplicate on a nitrocellulose membrane (dot blot) was used. The kit contained all the reagents for the assay and was performed as per the manufacturer's instructions. This

cytokine and chemokine antibody array was used to determine the effects of CD exposure on cytokine and chemokine secretion by WBCs. The assay required 500 μl of cell culture supernatants (unstimulated containing 0 μg/ml CDs, LPS stimulated containing 0 μg/ml CDs, and unstimulated containing 500 μg/ml CDs). The subsequent steps were carried out as described for the mouse cytokine and chemokine proteome profiling.

6.2.5. Statistical Analysis

All experiments were performed in triplicate and the data was calculated using Microsoft Excel. Data is presented as mean ± standard deviation (SD). One way analysis of variance (ANOVA) using SigmaPlot 12.0 was used to assess statistical differences with P < 0.01 being deemed significant.

6.3. Results

6.3.1. The effects of CDs on RAW 264.7 cells

6.3.1.1. Cytotoxicity

RAW cell viability, under basal conditions was significantly reduced (P < 0.001) by CD concentrations of 62.5 and 250 μg/ml compared to the culture control (Figure 6.1). However, viability was notably upregulated (P < 0.001) at 31.25 μg/ml CD compared to the positive control (LPS only). The other CD concentrations evaluated in this study had no effect on viability.

192
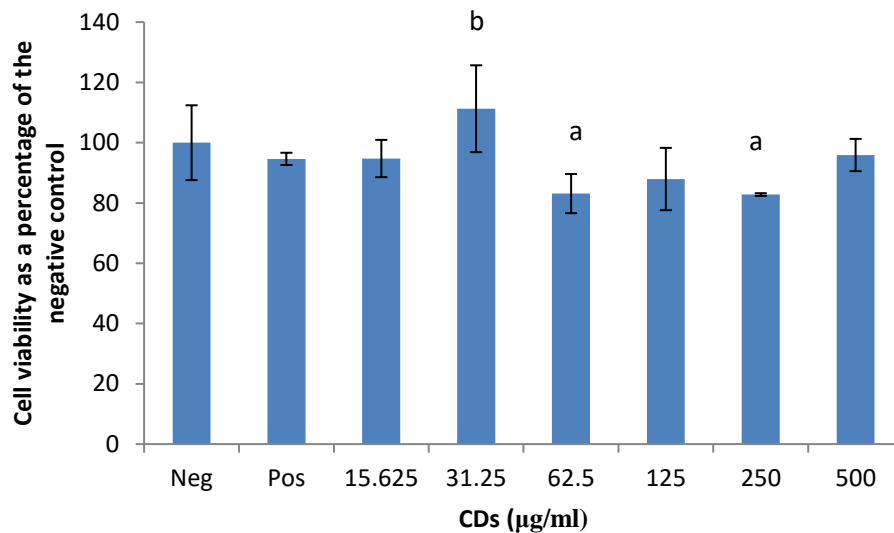
Figure 6.1. Cell viability of RAW 264.7 macrophage cells exposed to CDs. Data represents mean ± SD with n = 9. Bars marked with letters indicate significant differences (P < 0.01). Significance demarcated by: a- significantly different (P < 0.001) compared to 0 μg/ml CD control, b- significantly different (P < 0.001) compared to LPS stimulated 0 μg/ml CD control.

6.3.1.2. The effects of CDs on the inflammatory biomarker NO using RAW 264.7 cells

CDs at the concentrations tested, had no effect on NO production by unstimulated RAW 264.7 cells (Figure 6.2). RAW cells treated with LPS in the absence of CDs was included as a positive control for inflammation.

193
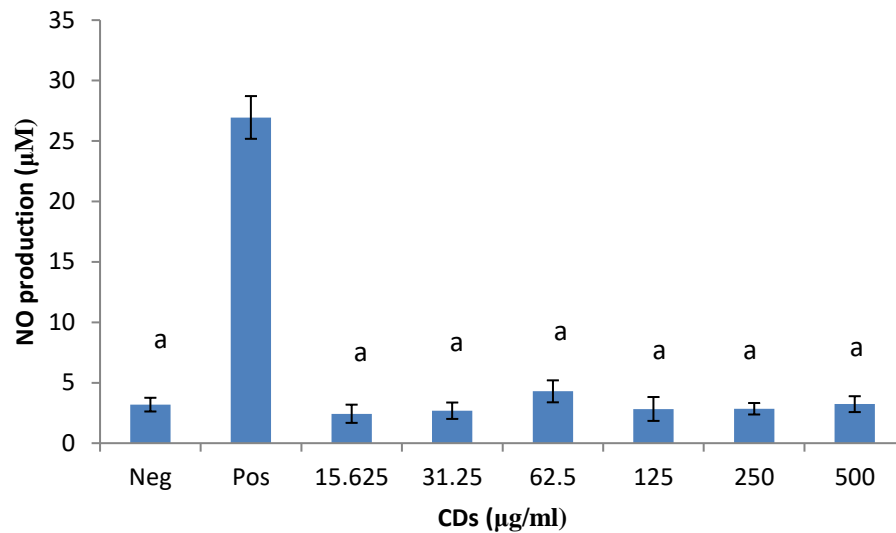
Figure 6.2. NO levels of unstimulated RAW 264.7 cell cultures exposed to CDs. Data represents mean ± SD with n = 9. Bars marked with letters indicate significant differences (P < 0.01). Significance demarcated by: a- significantly different (P < 0.001) compared to the LPS stimulated 0 μg/ml CD control.

6.3.1.3. The effects of CDs on the inflammatory biomarker IL-6 using RAW 264.7 cells

CD concentrations ≤ 31.25 μg/ml had no effect on IL-6 in an unstimulated environment (Figure 6.3). However, CD concentrations ≥ 62.5 μg/ml significantly inhibited (P < 0.001) IL-6 synthesis from cells under basal conditions compared to the culture control. The positive control (56 748 ± 9 591.8 pg/ml IL-6) is not included on the figure.
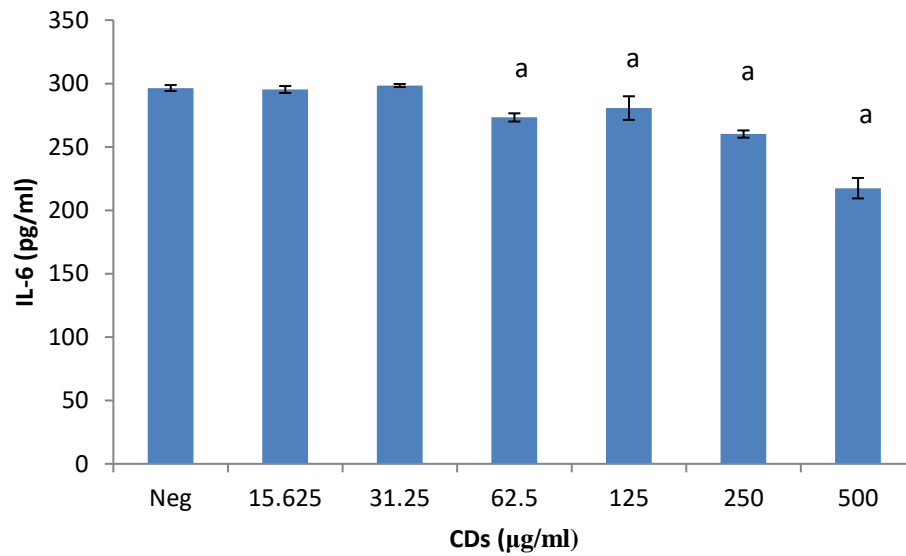
Figure 6.3. IL-6 levels of unstimulated RAW 264.7 cell cultures exposed to CDs. Data represents mean $\pm$ SD with n = 9. Positive control (+ LPS) not presented (56 748 $\pm$ 9 591.8 pg/ml IL-6). Bars marked with letters indicate significant differences (P < 0.01). Significance demarcated by: a- significantly different (P < 0.001) compared to 0 µg/ml CD control.

6.3.2. The effects of CDs on the MIPs chemokines using RAW 264.7 cells

6.3.2.1. The effects of CDs on MIP-1α using RAW 264.7 cells

CD concentrations $\leq$ 31.25 µg/ml did not affect MIP-1α synthesis from RAW cells under unstimulated conditions (Figure 6.4). However, CD concentrations $\geq$ 62.5 µg/ml significantly upregulated (P < 0.002) MIP-1α synthesis under basal conditions compared to the culture control. The positive control (LPS only) is not presented (1 637 093 $\pm$ 199 883.8 pg/ml MIP-1α) on figure 6.4.
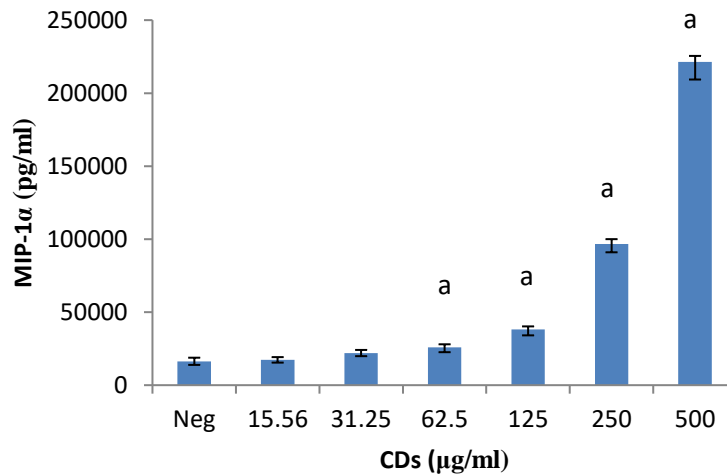
195

Figure 6.4. MIP-1α levels of unstimulated RAW 264.7 cell cultures exposed to CDs. Data represents mean ± SD with n = 9. Positive control (+ LPS) not presented (1 637 093 ± 199 883.8 pg/ml MIP-1α). Bars marked with letters indicate significant differences (P < 0.01). Significance demarcated by: a- significantly different (P < 0.002) compared to 0 μg/ml CD control.

6.3.2.2. The effects of CDs on MIP-1β using RAW 264.7 cells

MIP-1β synthesis was not affected by CD concentrations ≤ 125 μg/ml (Figure 6.5). CD concentrations ≥ 250 μg/ml significantly upregulated (P < 0.001) MIP-1β synthesis from RAW cells under basal conditions compared to the culture control. The positive control, LPS (343 965 ± 52 044 pg/ml MIP-1β) is not presented on figure 6.5.
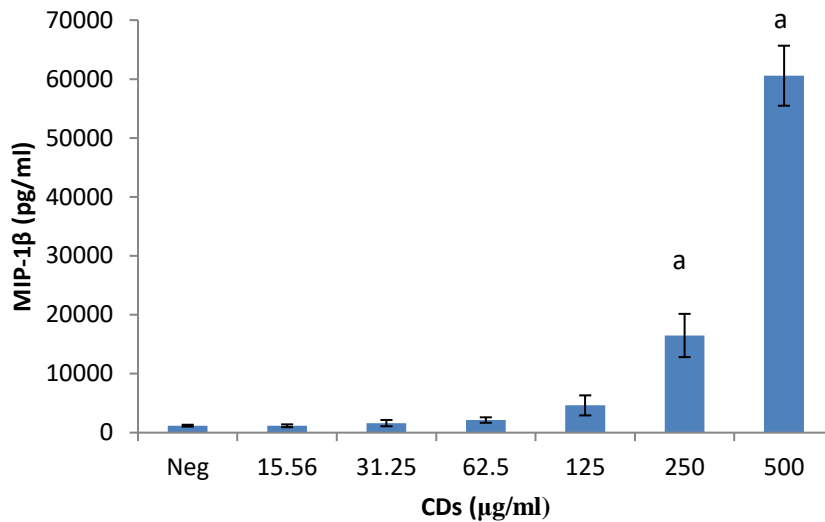
Figure 6.5. MIP-1β levels of unstimulated RAW 264.7 cell cultures exposed to CDs. Data represents mean ± SD with n = 9. Positive control (+ LPS) not presented (343 965 ± 52 044 pg/ml MIP-1β). Bars marked with letters indicate significant differences (P < 0.01). Significance demarcated by: a- significantly different (P < 0.001) compared to 0 μg/ml CD control.

6.3.2.3. The effects of CDs on MIP-2 using RAW 264.7 cells

MIP-2 synthesis from RAW cells exposed to CD concentrations mimicked the MIP-1β data under basal conditions (Figure 6.5). MIP-2 was unaffected by CD concentrations ≤ 125 μg/ml (Figure 6.6). However, CD concentrations ≥ 250 μg/ml significantly upregulated (P < 0.001) MIP-2 synthesis from RAW cells under unstimulated conditions. The LPS stimulated positive control (302 089 ± 68 868 pg/ml MIP-2) is not presented on figure 6.6.

197
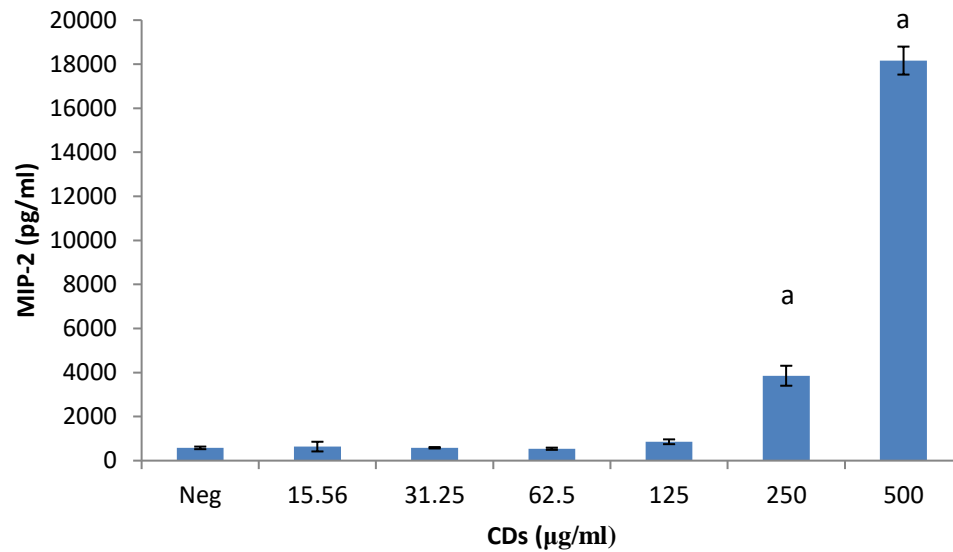
Figure 6.6. MIP-2 levels of unstimulated RAW 264.7 cell cultures exposed to CDs. Data represents mean ± SD with n = 9. Positive control (+ LPS) not presented (302 089 ± 68 868 pg/ml MIP-2). Bars marked with letters indicate significant differences (P < 0.01). Significance demarcated by: a- significantly different (P < 0.001) compared to 0 µg/ml CD control.

6.3.3. The effects of CDs on the secretory cytokine and chemokine profile of RAW 264.7 cells

Membranes exposed to culture supernatants of RAW 264.7 cells exposed to media only, media in the presence of a mitogen, and 500 µg/ml CDs in the absence of a mitogen allowed for the analysis of various cytokines and chemokines expressed by the cells upon the exposure (Figure 6.7). Quantification of the membranes showed that RAW cells exposed to media containing LPS allowed the cells to synthesize certain proteins that were not synthesized by cells exposed to media only and 500

198

μg/ml CDs (Table 6.1). These proteins include macrophage colony-stimulating factor (M-CSF), interleukin 27 (IL-27) and interleukin 1 β (IL-β).

Similarly, certain proteins were significantly upregulated (P < 0.001) by cells exposed to 500 μg/ml CD compared to cells exposed to media only. These proteins include IFNγ-inducible protein 10 (IP-10), granulocyte -colony stimulating factor (G-CSF), tumour necrosis factor α (TNF-α), granulocyte-macrophage colony-stimulating factor (GM-CSF), IL-6, monocyte chemoattractant protein 1 (MCP-1)/JE, MIP-1α, MIP-1β, MIP-2, intracellular adhesion molecule 1 (ICAM-1) and interleukin 1 receptor antagonist (IL-1ra).

199
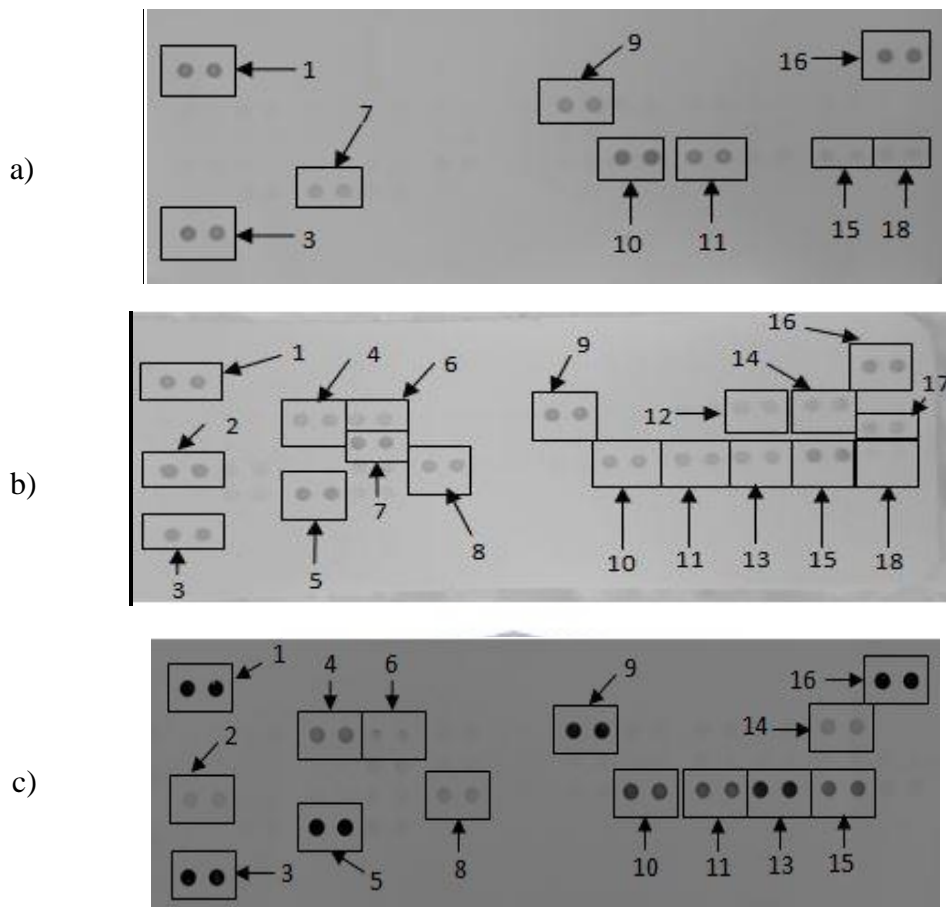
Figure 6.7. The effect of CDs on RAW 264.7 cells. Cells were incubated with (a) media only (negative control), (b) media in the presence of LPS and (c) 500 μg/ml CDs in the absence of a mitogen. Supernatants were probed using the proteome profiler array as described in methods. Cytokines/ chemokines that were detected were allocated numbers: 1,3, and 16 are reference spots; 2- IP-10; 4- G-CSF; 5- TNF-α; 6- GM-CSF; 7- IL-6; 8- JE; 9-sICAM-1; 10- MIP-1α; 11- MIP-1β; 12- IL-1β; 13-MIP-2; 14- IL-1ra; 15- RANTES; 17- IL-27; 18-SDF-1.

Table 6.1. Quantification of cytokines and chemokines secreted by RAW 264.7 cultures not stimulated with LPS after treatment with medium only (negative control), medium containing LPS (positive control) or medium containing 500 µg/ml CDs. Membranes were subjected to chromogenic exposure. Data is represented as mean ± SD. Significance indicated by a- CD at 500 µg/ml significantly different (P < 0.001) compared to negative control, b- CD at 500 µg/ml significantly different (P < 0.001) compared to the positive control.

Cytokines and Chemokines	Positive Control	Negative Control	500 µg/ml CDs
Reference Spot	100 ± 8.62	100 ± 10.49	100 ± 15.19
IP-10	114.74 ± 5.24	0 ± 0	8.20 ± 0.11[a,b]
G-CSF	58.27 ± 2.55	0 ± 0	26.76 ± 0.51[a,b]
TNF-α	102.01 ± 5.91	17.96 ± 0.13	101.00 ± 0.60[a]
GM-CSF	47.32 ± 3.02	0 ± 0	3.72 ± 0.03[a,b]
IL-6	91.94 ± 3.60	0 ± 0	0 ± 0[b]
M-CSF	25.12 ± 3.03	0 ± 0	0 ± 0[b]
JE	78.97 ± 4.48	0 ± 0	10.47 ± 0.01[a,b]
sICAM	109.05 ± 6.00	34.76 ± 0.02	78.65 ± 0.98[a,b]
MIP-1α	72.87 ± 4.22	57.00 ± 1.94	64.87 ± 1.87[a,b]
MIP-1β	62.77 ± 3.35	37.68 ± 0.33	45.40 ± 0.81[a,b]
MIP-2	55.51 ± 2.75	14.75 ± 0.69	76.63 ± 0.06[a,b]
RANTES	100.57 ± 4.42	17.93 ± 0.83	36.09 ± 0.78[a,b]
SDF-1	16.41 ± 1.61	21.75 ± 1.01	0 ± 0[a,b]
IL-27	54.97 ± 4.05	0 ± 0	14.96 ± 0.21[a,b]
IL-1ra	55.84 ± 1.66	0 ± 0	0 ± 0[b]
IL-1β	39.16 ± 3.31	0 ± 0	0 ± 0[b]

6.3.4. The effects of CDs on WBCs

6.3.4.1. Cytotoxicity

CD concentrations ≤ 50 µg/ml did not affect WBC viability (Figure 6.8). However, significant cytotoxicity (P < 0.002) was induced at the highest concentration of CD (500 µg/ml) screened.

WESTERN CAPE
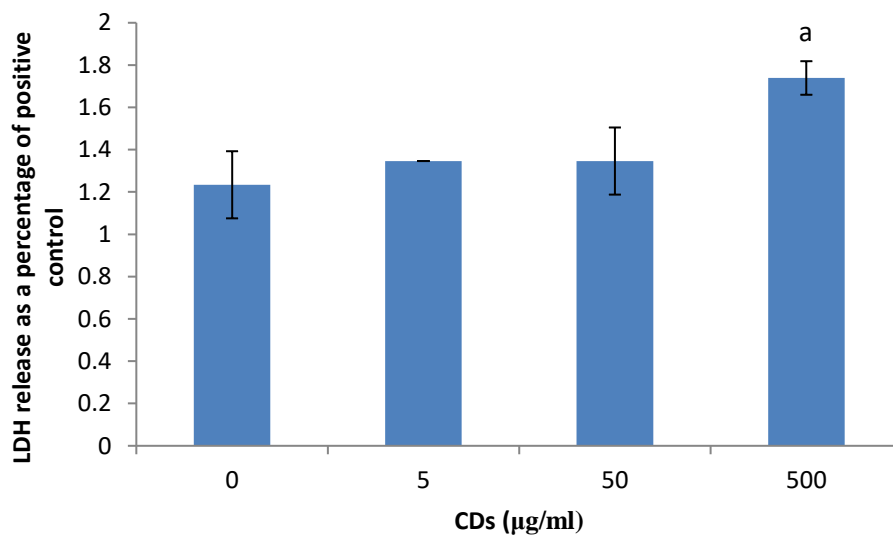
Figure 6.8. Cell viability of WBCs exposed to CDs. Data represents mean ± SD with n = 4. Bars marked with letters indicate significant difference (P < 0.01) to control. Significance demarcated by: a- significantly different (P < 0.002) compared to 0 µg/ml CD control.

6.3.4.2. The effects of CDs on the inflammatory system biomarker IL-6 using WBCs

CD concentrations ≤ 50 µg/ml did not affect IL-6 levels in cultures not stimulated with LPS (Figure 6.9). However, at 500 µg/ml CD significantly induced the

202

upregulation (P < 0.001) of IL-6 compared to 0 μg/ml CD in unstimulated cultures. CD concentrations in the presence of LPS did not affect the synthesis of IL-6 by cultures.
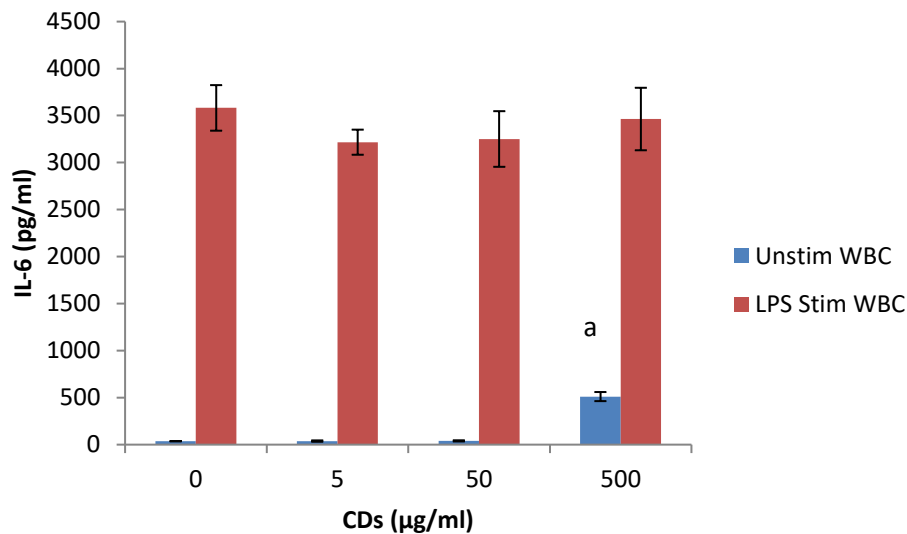
Figure 6.9. IL-6 levels of WBCs exposed to CDs. Data represents mean ± SD with n = 4. Bars marked with letters indicate significant differences (P < 0.01). Significance demarcated by: a- significantly different compared (P < 0.002) to 0 μg/ml CD control.

6.3.4.3. The effects of CDs on the inflammatory chemokine, MIP-1β using WBCs

MIP-1β synthesis followed the same trend as the IL-6 data for both the unstimulated and stimulated cultures exposed to CDs. CD at concentrations tested had no effect on MIP-1β synthesis by LPS stimulated WBCs (Figure 6.10). At concentrations ≤ 50 μg/ml, CD did not affect MIP-1β synthesis by unstimulated cells. However, CD at

500 μg/ml resulted in a significant stimulation (P < 0.001) of MIP-1β synthesis by unstimulated WBCs.
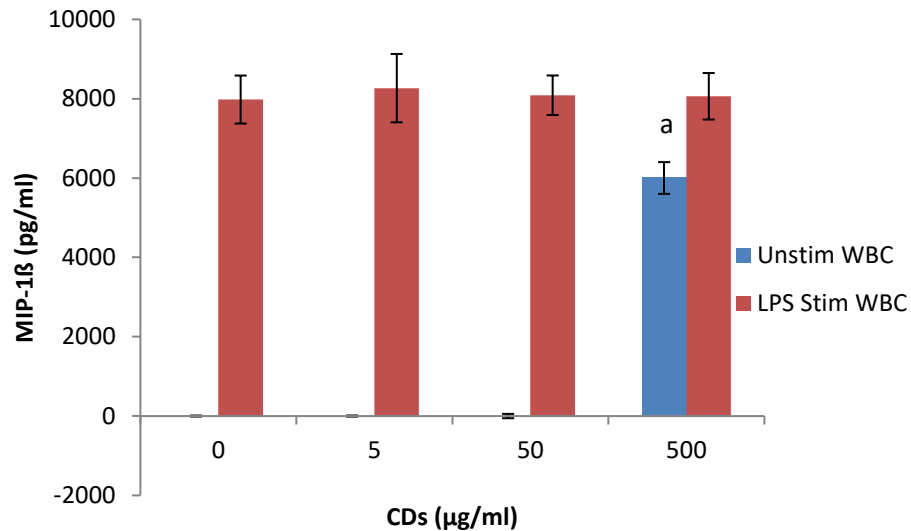
Figure 6.10. MIP-1β of WBCs exposed to CDs. Data represents mean ± SD with n = 4. Bars marked with letters indicate significant differences (P < 0.01). Significance demarcated by: a- significantly different (P < 0.001) compared to 0 μg/ml CD control.

6.3.4.4. The effects of CDs on the humoral immune system biomarker IL-10 using WBCs

CD at 0, 5 and 50 μg/ml did not synthesize IL-10 (Figure 6.11) under unstimulated conditions. However, significant levels (P < 0.001) of IL-10 was detected at 500 μg/ml CD compared to the 0 μg/ml CD control. PHA stimulated WBC at 5 and 50 μg/ml had no effect on IL-10 produced compared to the 0 μg/ml CD control.

However, at 500 μg/ml CD the PHA stimulated WBC produced significantly more IL-10 compared to the 0 μg/ml CD control.
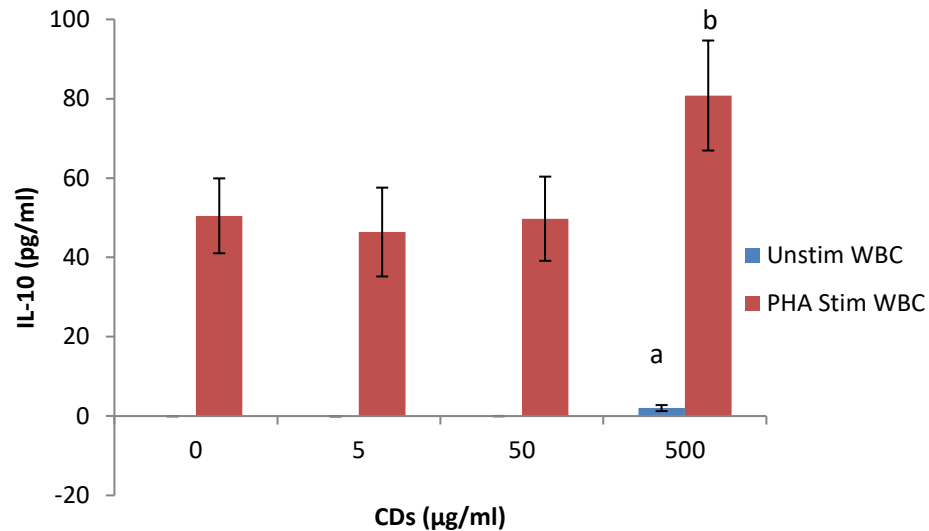
Figure 6.11. IL-10 levels of WBCs exposed to CDs. Data represents mean ± SD with n = 4. Bars marked with letters indicate significant differences (P < 0.01). Significance demarcated by: a- significantly different (P < 0.001) compared to 0 μg/ml CD control, b- significantly different (P < 0.008) compared to PHA stimulated 0 μg/ml CD control.

6.3.4.5. The effects of CDs on the cell mediated immune system biomarker IFNγ using WBCs

None of the CD concentrations tested had an affect IFNγ synthesis by PHA stimulated cultures (Figure 6.12). IFNγ was not detected in unstimulated cultures.
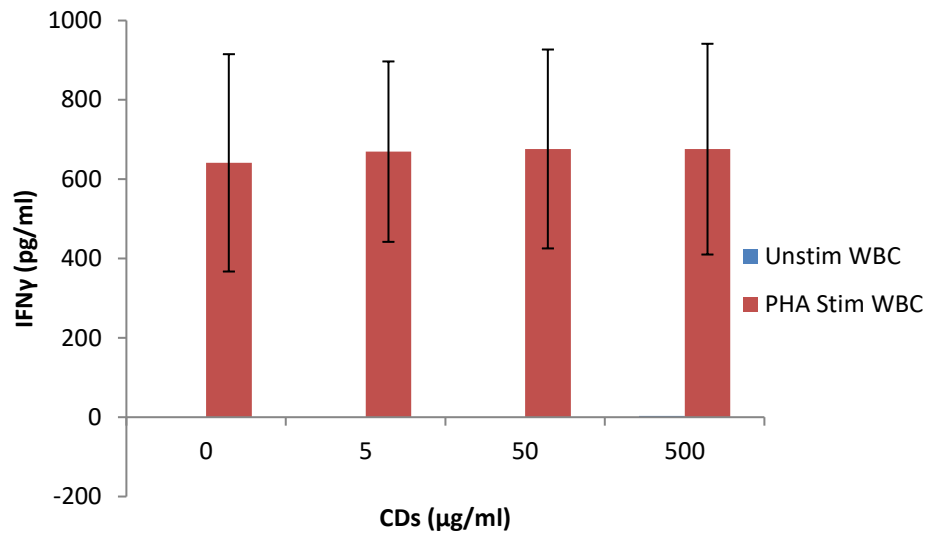
Figure 6.12. IFNγ levels of WBCs exposed to CDs. Data represents mean ± SD with n = 4.

6.3.5. The effects of CDs on the secretory cytokine and chemokine profile of WBCs

The proteome profile of WBCs exposed to media only, media in the presences of LPS and 500 μg/ml CD in media only revealed the synthesis or inhibition of certain proteins (Figure 6.13).

Quantification of the membranes showed that certain proteins were significantly upregulated ($P < 0.001$) in supernatants at WBCs incubated in the presence of 500 μg/ml CD compared to the negative control (media only) (Table 6.2). These proteins include IL-1ra, macrophage migration inhibitory factor (MIF), MIP-1α/β and IL-8. Cytokines and chemokines that were prominently down regulated compared to the LPS positive control include IL-1ra, MCP-1, MIP-1α/β, regulated on activation, normal T cell expressed and secreted (RANTES), IL-6, IL-8 and IL-1β.

206
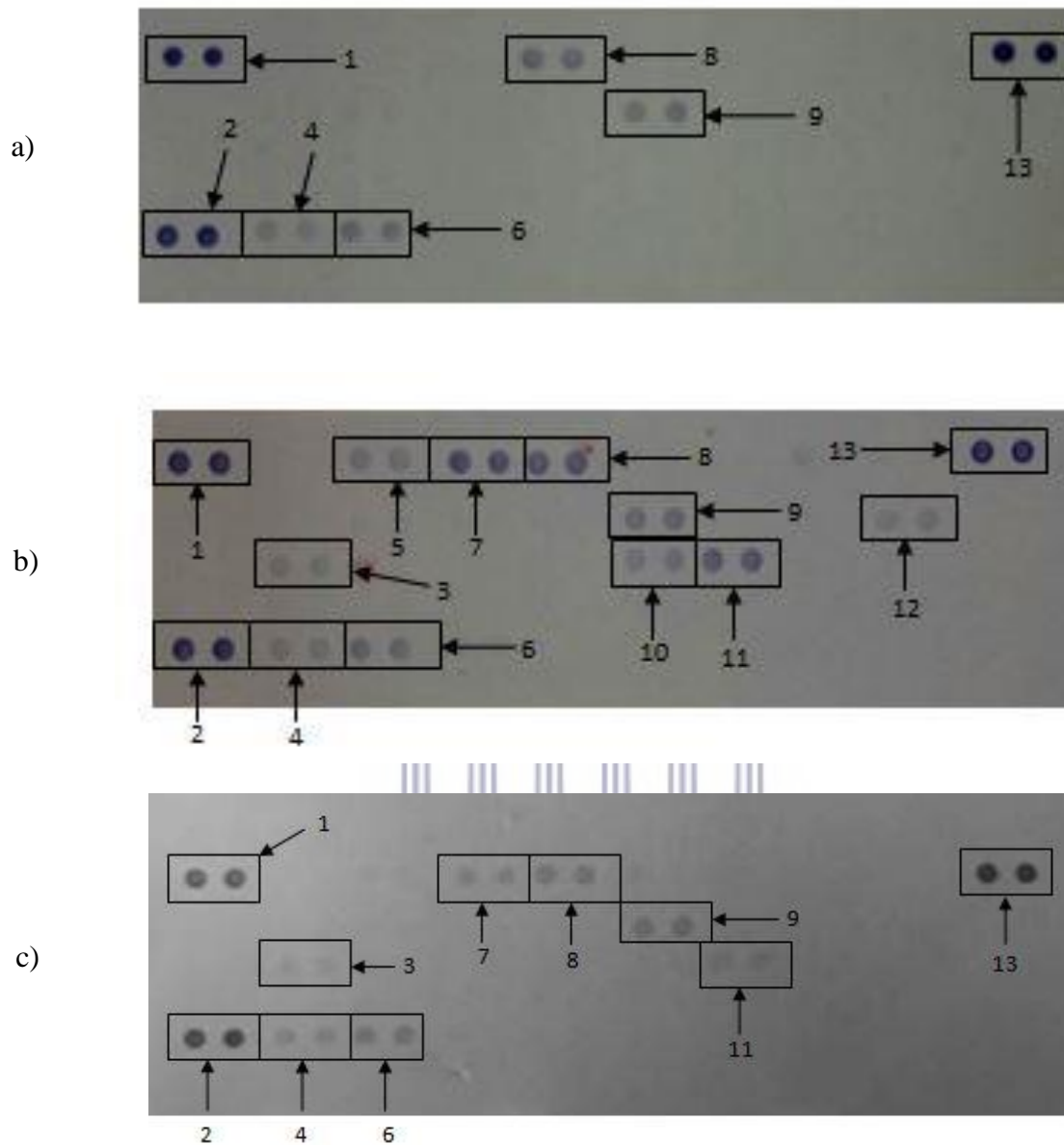
Figure 6.13. The effects of CDs on whole blood cells. Cells were incubated with (a) media only, (b) media and LPS, (c) 500 μg/ml CDs in the absence of LPS. Cytokines/ chemokines that were detected were allocated numbers: 1,2, and 13 are reference spots; 3- IL-1ra; 4- MIF; 5-MCP-1; 6- Serpin E1; 7- MIP-1α/β; 8- RANTES; 9- ICAM-1, 10- IL-6, 11- IL-8 and 12- IL-1β.

207

Table 6.2. Quantification of cytokines and chemokines secreted by WBCs not stimulated with LPS after treatment with medium only (negative control), medium containing LPS (positive control) or medium containing 500 μg/ml CDs. Membranes were subjected to chromogenic exposure. Data is represented as mean ± SD. Significance indicated by a- CDs at 500 μg/ml significantly different (P < 0.001) compared to negative control, b- CDs at 500 μg/ml significantly different (P < 0.001) compared to the positive control.

Cytokines and Chemokines	Positive Control	Negative Control	500 μg/ml CDs
Reference Spot	100 ± 7.28	100 ± 5.57	100 ± 11.35
IL-1ra	16.92 ± 1.46	0 ± 0	12.57 ± 1.27[a,b]
MIF	17.56 ± 1.51	10.57 ± 1.91	20.41 ± 4.00[a]
MCP-1	26.26 ± 2.54	0 ± 0	0 ± 0[b]
Serpin E1	32.40 ± 2.49	24.26 ± 2.26	31.81 ± 4.38
MIP-1α/β	70.22 ± 4.11	0 ± 0	25.84 ± 2.17[a,b]
RANTES	62.94 ± 2.55	34.28 ± 1.37	32.95 ± 2.75[b]
sICAM	37.15 ± 0.59	35.98 ± 2.19	32.38 ± 4.52
IL-6	29.31 ± 4.81	0 ± 0	0 ± 0[b]
IL-8	50.27 ± 8.41	0 ± 0	13.56 ± 2.53[a,b]
IL-1β	20.29 ± 0.99	0 ± 0	0 ± 0[b]

6.4. Discussion

In recent years, CDs have attracted lots of interest due to their many bioapplications, such as bioimaging, drug delivery and theranostics (Peng et al., 2017). However, no studies have evaluated the effects these CDs have on the immune system.

Exposing RAW cells to CD concentrations, (62.5 and 250 μg/ml) reduced cell viability by less than 20 %. Viability was also reduced in WBCs exposed to the highest concentration of CDs (500 μg/ml). The results obtained in this study for both

208

RAW cells and WBCs supports previous reports of CDs having low toxicity levels (Sun and Lei, 2017, Tao et al., 2017). Studies have mainly monitored the bioimaging of cells using CDs (Pierrat et al., 2015, Kudr et al., 2017, Pandey et al., 2017). Although Wang et al. (2011b) evaluated the cytotoxic effects of CDs on two different cell types, HT-29 and MCF-7. Cytotoxicity was induced in both cell lines, although cytotoxicity was also dependent on the functionalization of the CDs. However, Yang et al. (2009) had contradictory results to what was found by Wang et al. (2011b) as they reported no effects on all parameters monitored, using the same cell lines, but only poly(ethylene glycol-amine) (PEG) functionalization of CDs. The effects of SWCNTs on RAW cells was evaluated and it was found that CDs induced oxidative stress (Kagan et al., 2006). However, Crouzier et al. (2010) found that carbon nanotubes reduced oxidative stress in the lungs of mice.

Under basal conditions, the RAW cell inflammatory marker IL-6 was partially inhibited by CD concentrations ≥ 62.5 µg/ml. However, NO remained unaffected by CD exposure. Contradictory to the RAW cell inflammatory markers, the MIP chemokines were significantly upregulated by CD exposure at concentrations ≥ 250 µg/ml. A similar trend was seen with the WBCs, where the highest concentration assessed (500 µg/ml) induced IL-6 and MIP-1β in unstimulated cultures. No studies have been conducted on the effects of CDs on the immune system. *In vitro* monocyte cultures exposed to carbon nanotubes induced the formation of inflammatory genes IL-6 and IL-1β (Qu et al., 2012). Kayat et al. (2011) and Crouzier et al. (2010) also found that carbon nanotubes induced inflammatory markers. Another study

209

conducted by Murray et al. (2009) found that SWCNTs induced pro-inflammatory cytokines such as IL-6, MCP-1 and TNF-α in dermal cells. Zhang et al. (2012) also found that RAW cells exposed to multi-wall carbon nanotubes (MWCNTs) induced inflammatory proteins. The induction of inflammatory markers was supported by the proteome profile analysis of both RAW and WBCs. The inflammatory proteins induced included TNF-α, MIPs, MCP-1, IL-6, IL-8, IL-1ra and IL-1β. However, Liu et al. (2012) found that CDs did not affect inflammatory genes such as IL-6 and TNF-α.

The humoral immune response cytokine, IL-10, was upregulated at 500 μg/ml CD in both unstimulated and PHA stimulated cultures. Whereas, the cell mediated immune response cytokine, IFNγ, remained unaffected under both conditions. The induction of IL-10 in unstimulated conditions would provoke a humoral immune response, when one is not required and upregulated such a response under stimulated conditions. This could lead to hypersensitivity and autoimmunity reactions (De Jong and Van Loveren, 2007).

This study clearly demonstrates that CDs are cytotoxic at high concentrations, although the levels of cytotoxicity are low. CDs also induce inflammation under basal conditions at relatively high concentrations, supported by the proteome analysis. The proteome analysis revealed potential biomarkers to be assessed upon CD exposure. These include MIP-1α, MIP-1β, MIP-2, TNF-α, IL-8 and SDF-1. The humoral immune response is also modulated at high levels of CDs. This stimulation of immune responses could lead to hypersensitivity and autoimmunity (De Jong and

210

Van Loveren, 2007). The current study provides an important insight into the effects of CDs on the immune system as these nanoparticles are geared to be used *in vivo* for a number of bioapplications.

Chapter 7:

Conclusions and recommendations

7.1. General conclusions

This study was designed to investigate how heavy metals, metallic based nanoparticles and carbon based nanoparticles interact with the immune system. This study also intended to identify potential biomarkers that may be monitored upon relative exposure. This was evaluated by exposing the respective compounds to representatives of the immune system under various conditions. These representatives were the murine macrophage RAW 264.7 cell line and human whole blood cell cultures (WBCs). Both cultures were exposed to the heavy metals and nanoparticles under various conditions. These conditions included basal levels and simulated inflammatory and humoral immune responses. The research needed to be undertaken as heavy metals may be released into the environment due to industry. Heavy metals may then run off into receiving waters and impact environmental health and potentially human health as heavy metals are known to bio-accumulate. Similarly, the production of nanoparticles is rapidly increasing and is frequently found in a number of consumer products. This will inevitably result in the release of these nanopaticles into the environment. Yet, very little is known about how these nanoparticles interact with the environment, let alone the impact these nanoparticles have on biological systems.

212

Chapter 3 investigated how the heavy metals cadmium, copper and silver interacted with the immune system. The results show that RAW cells exhibited various sensitivities to the metals. Cadmium was more cytotoxic than silver, with copper not affecting cell viability. The same trend was seen when evaluating the inflammatory biomarkers, nitric oxide (NO) and interleukin 6 (IL-6). Evaluating the effects of the metals on WBCs and the cytokines representing the innate (IL-6), humoral (IL-10) and cell mediated immunity (IFNγ) found that all the cytokines were reduced by the metals. The results show that IL-6 was more sensitive to Cu than Cd, while Ag upregulated its synthesis. IL-10 was most sensitive to Cd, followed by Cu and then Ag. IFNγ was most reduced by Ag, followed by Cu, and then by Cd. Therefore, all the metals monitored would negatively impact the immune system and cause autoimmunity where cytokines are upregulated or immunosuppression where cytokines are inhibited.
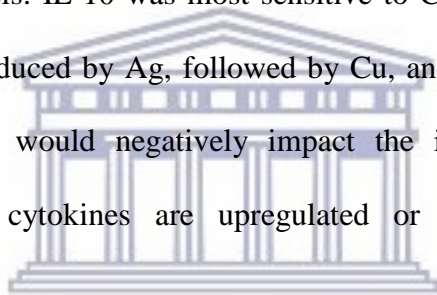
Chapter 4 found that silver nanoparticles (AgNP) caused immunomodulation as it induced an immune response under basal conditions but inhibited an immune response under simulated conditions at high AgNP concentrations (250 μg/ml). However, AgNPs were cytotoxic to WBCs at high concentrations (250 μg/ml). Macrophage inflammatory proteins (MIPs) were identified as potential biomarkers to be monitored due to AgNP exposure.

Chapter 5 established that graphene oxide nanoparticles (GONPs) were cytotoxic to both RAW and WBCs at high concentrations (500 μg/ml). Similar to the AgNPs, exposure to GONPs resulted in immunomodulation. Inflammation was induced at

213

concentrations ≤ 31.25 μg/ml in RAW cells. WBCs showed a dose dependent increase of inflammation and humoral immune response under basal conditions. However, a similar dose dependent decrease of inflammation, humoral and immune response were seen under simulated immune responses. MIPs along with TNF-α were identified as potential biomarkers for GONPs exposure.

Chapter 6 found that carbon dots (CDs) cause low levels of toxicity in WBCs. Similar to AgNPs, inflammation (RAW and WBCs) and humoral immune responses (WBCs) were induced at high concentrations (≥ 250 and 500 μg/ml). Proteome profiling identified inflammatory proteins (MIPs) as potential biomarkers for CD exposure.

All nanoparticles evaluated in this study revealed that they can potentially induce immunomodulatory effects. Inflammatory biomarkers were identified as potential biomarker for nanoparticle exposure via proteome profiling.

7.2. Future perspectives and recommendations

- The nanoparticles were characterized in aqueous solutions and at room temperature. The nanoparticles should in future be characterized in the culture medium and at the incubation temperature that they will be used in.
- Toxicity caused by the AgNPs (Chapter 4) should be monitored to definitively say whether the toxicity was induced by the nanoparticle or due to the leaching of silver ions from the nanoparticle.

214

- Only acute exposures were evaluated in this study. Chronic exposures should be considered for nanoparticle exposure as this may potentially change the extracellular biomarkers that were identified by the proteome profile.

- In this study, only extracellular cytokines and chemokines were monitored. A proteome profile of intracellular proteins, indicative of cell stress, apoptosis, and receptor kinases should be considered for future studies as this would give an overall picture of how the nanoparticles interact with the cells and the potential pathways that they may affect or interfere with.

215

8. References

Aderem, A. (2003). Phagocytosis and the inflammatory response. *The Journal of infectious diseases,* 187**,** S340-5.

Ahamed, M., Alsalhi, M. S. and Siddiqui, M. K. (2010). Silver nanoparticle applications and human health. *Clin Chim Acta,* 411**,** 1841-8.

Ahluwalia, S. S. and Goyal, D. (2007). Microbial and plant derived biomass for removal of heavy metals from wastewater. *Bioresour Technol,* 98**,** 2243-57.

Akhavan, O. and Ghaderi, E. (2010). Toxicity of graphene and graphene oxide nanowalls against bacteria. *ACS nano,* 4**,** 5731-5736.

Arai, Y., Miyayama, T. and Hirano, S. (2015). Difference in the toxicity mechanism between ion and nanoparticle forms of silver in the mouse lung and in macrophages. *Toxicology,* 328**,** 84-92.

Araujo, C. S. T., Carvalho, D. C., Rezende, H. C., Almeida, I. L. S., Coelho, L. M., Coelho, N. M. M., Marques, T. L. and Alves, V. N. (2013). Bioremediation of Waters Contaminated with Heavy Metals Using Moringa oleifera Seeds as Biosorbent.

Asghari, S., Johari, S. A., Lee, J. H., Kim, Y. S., Jeon, Y. B., Choi, H. J., Moon, M. C. and Yu, I. J. (2012). Toxicity of various silver nanoparticles compared to silver ions in Daphnia magna. *J Nanobiotechnol,* 10**,** 1-14.

Asharani, P., Sethu, S., Lim, H. K., Balaji, G., Valiyaveettil, S. and Hande, M. P. (2012). Differential regulation of intracellular factors mediating cell cycle, DNA repair and inflammation following exposure to silver nanoparticles in human cells. *Genome Integr,* 3**,** 2.

216

Ataie-Kachoie, P., Pourgholami, M. H. and Morris, D. L. (2013). Inhibition of the IL-6 signaling pathway: a strategy to combat chronic inflammatory diseases and cancer. *Cytokine Growth Factor Rev,* 24**,** 163-73.

Aziz, R., Rafiq, M., Yang, J., Liu, D., Lu, L., He, Z., Daud, M., Li, T. and Yang, X. (2014). Impact assessment of cadmium toxicity and its bioavailability in human cell lines (Caco-2 and HL-7702). *BioMed research international,* 2014.

Balch, G. C., Evans, R. D., Welbourn, P. and Prairie, R. (2000). Weight loss and net abnormalities of Hydropsyche betteni (caddisfly) larvae exposed to aqueous zinc. *Environmental toxicology and chemistry,* 19**,** 3036-3043.

Baldi, C., Minoia, C., Di Nucci, A., Capodaglio, E. and Manzo, L. (1988). Effects of silver in isolated rat hepatocytes. *Toxicology letters,* 41**,** 261-268.

Baldo, B. A. and Pham, N. H. 2013. Classification and descriptions of allergic reactions to drugs. *Drug Allergy.* Springer.

Banchereau, J. and Steinman, R. M. (1998). Dendritic cells and the control of immunity. *Nature,* 392**,** 245.

Barnhoorn, I. and Van Vuuren, J. (2001). Sublethal effects of manganese on the haematology and osmoregulation of Oreochromis mossambicus after acute exposure. *Southern African Journal of Aquatic Sciences,* 26**,** 1-7.

Barth, K. A., Waterfield, J. D. and Brunette, D. M. (2013). The effect of surface roughness on RAW 264.7 macrophage phenotype. *Journal of Biomedical Materials Research Part A,* 101**,** 2679-2688.

217

Bayati, M., Dai, J., Zambrana, A., Rees, C. and De Cortalezzi, M. F. (2017). Effect of water chemistry on the aggregation and photoluminescence behavior of carbon dots. *Journal of Environmental Sciences*.

Bertin, G. and Averbeck, D. (2006). Cadmium: cellular effects, modifications of biomolecules, modulation of DNA repair and genotoxic consequences (a review). *Biochimie,* 88**,** 1549-59.

Bia, M. J. and Defronzo, R. A. (1981). Extrarenal potassium homeostasis. *American Journal of Physiology-Renal Physiology,* 240**,** F257-F268.

Binning, K. and Baird, D. (2001). Survey of heavy metals in the sediments of the Swartkops River Estuary, Port Elizabeth South Africa. *Water SA,* 27**,** 461-466.

Brewer, J. W. (2013). Phospholipids: "greasing the wheels" of humoral immunity. *Biochim Biophys Acta,* 1831**,** 642-51.

Bystrzejewska-Piotrowska, G., Golimowski, J. and Urban, P. L. (2009). Nanoparticles: their potential toxicity, waste and environmental management. *Waste Manag,* 29**,** 2587-95.

Campanella, L., Cubadda, F., Sammartino, M. and Saoncella, A. (2001). An algal biosensor for the monitoring of water toxicity in estuarine environments. *Water Research,* 35**,** 69-76.

Canesi, L., Ciacci, C., Betti, M., Fabbri, R., Canonico, B., Fantinati, A., Marcomini, A. and Pojana, G. (2008). Immunotoxicity of carbon black nanoparticles to blue mussel hemocytes. *Environment international,* 34**,** 1114-1119.

Capiralla, H., Vingtdeux, V., Zhao, H., Sankowski, R., Al-Abed, Y., Davies, P. and Marambaud, P. (2012). Resveratrol mitigates lipopolysaccharide-and Aβ-mediated microglial inflammation by inhibiting the TLR4/NF-κB/STAT signaling cascade. *Journal of neurochemistry,* 120**,** 461-472.

Cardamone, C., Parente, R., De Feo, G. and Triggiani, M. (2016). Mast cells as effector cells of innate immunity and regulators of adaptive immunity. *Immunology letters,* 178**,** 10-14.

Carlson, C., Hussain, S. M., Schrand, A. M., K. Braydich-Stolle, L., Hess, K. L., Jones, R. L. and Schlager, J. J. (2008). Unique cellular interaction of silver nanoparticles: size-dependent generation of reactive oxygen species. *The journal of physical chemistry B,* 112**,** 13608-13619.

Cavas, T., Garanko, N. N. and Arkhipchuk, V. V. (2005). Induction of micronuclei and binuclei in blood, gill and liver cells of fishes subchronically exposed to cadmium chloride and copper sulphate. *Food Chem Toxicol,* 43**,** 569-74.

Cebo, C., Dambrouck, T., Maes, E., Laden, C., Strecker, G., Michalski, J. C. and Zanetta, J. P. (2001). Recombinant human interleukins IL-1alpha, IL-1beta, IL-4, IL-6, and IL-7 show different and specific calcium-independent carbohydrate-binding properties. *J Biol Chem,* 276**,** 5685-91.

Cesta, M. F. (2006). Normal structure, function, and histology of the spleen. *Toxicol Pathol,* 34**,** 455-65.

Chae, Y. J., Pham, C. H., Lee, J., Bae, E., Yi, J. and Gu, M. B. (2009). Evaluation of the toxic impact of silver nanoparticles on Japanese medaka (Oryzias latipes). *Aquatic Toxicology,* 94**,** 320-327.

Chaplin, D. D. (2006). 1. Overview of the human immune response. *J Allergy Clin Immunol,* 117**,** S430-5.

Chaplin, D. D. (2010). Overview of the immune response. *J Allergy Clin Immunol,* 125**,** S3-23.

Chapman, D., Jackson, J. and Krebs, F. (1996). Water quality monitoring–A practical guide to the design and implementation of Freshwater Quality Studies and Monitoring Programmes, Chapter 11. *Bartram J. and Balance R.(eds.), Biological monitoring, UNEP/WHO***,** 267-305.

Chen, M., Yin, J., Liang, Y., Yuan, S., Wang, F., Song, M. and Wang, H. (2016a). Oxidative stress and immunotoxicity induced by graphene oxide in zebrafish. *Aquatic Toxicology,* 174**,** 54-60.

Chen, W., Yi, P., Zhang, Y., Zhang, L., Deng, Z. and Zhang, Z. (2011). Composites of aminodextran-coated Fe3O4 nanoparticles and graphene oxide for cellular magnetic resonance imaging. *ACS applied materials & interfaces,* 3**,** 4085-4091.

Chen, X., Hai, X. and Wang, J. (2016b). Graphene/graphene oxide and their derivatives in the separation/isolation and preconcentration of protein species: a review. *Analytica chimica acta,* 922**,** 1-10.

Chen, X. and Schluesener, H. (2008). Nanosilver: a nanoproduct in medical application. *Toxicology letters,* 176**,** 1-12.

Cherian, R. S., Sreejith, R., Syama, S., Sruthi, S., Gayathri, V., Maekawa, T., Sakthikumar, D. and Mohanan, P. (2014). Evaluation of toxicity of Maura reduced graphene oxide using in vitro systems.

Chiroma, T., Ebewele, R. and Hymore, F. (2014). Comparative Assessement of Heavy Metal Levels in Soil, Vegetables and Urban Grey Waste Water used for Irrigation in Yola and Kano. *IRJES,* 3**,** 01-09.

Clemens, S. (2006). Toxic metal accumulation, responses to exposure and mechanisms of tolerance in plants. *Biochimie,* 88**,** 1707-1719.

Colombo, M., Hamelin, C., Kouassi, E., Fournier, M. and Bernier, J. (2004). Differential effects of mercury, lead, and cadmium on IL-2 production by Jurkat T cells. *Clin Immunol,* 111**,** 311-22.

Connolly, M., Fernandez-Cruz, M.-L., Quesada-Garcia, A., Alte, L., Segner, H. and Navas, J. M. (2015). Comparative Cytotoxicity Study of Silver Nanoparticles (AgNPs) in a Variety of Rainbow Trout Cell Lines (RTL-W1, RTH-149, RTG-2) and Primary Hepatocytes. *International journal of environmental research and public health,* 12**,** 5386-5405.

Corsini, E., Sokooti, M., Galli, C., Moretto, A. and Colosio, C. (2013). Pesticide induced immunotoxicity in humans: a comprehensive review of the existing evidence. *Toxicology,* 307**,** 123-135.

Cota, A. M. and Midwinter, M. J. (2009). The immune system. *Anaesthesia & intensive care medicine,* 10**,** 215-217.

Couper, K. N., Blount, D. G. and Riley, E. M. (2008). IL-10: the master regulator of immunity to infection. *The Journal of Immunology,* 180**,** 5771-5777.

Crouzier, D., Follot, S., Gentilhomme, E., Flahaut, E., Arnaud, R., Dabouis, V., Castellarin, C. and Debouzy, J.-C. (2010). Carbon nanotubes induce inflammation but decrease the production of reactive oxygen species in lung. *Toxicology,* 272**,** 39-45.

De Jong, W. H. and Van Loveren, H. (2007). Screening of xenobiotics for direct immunotoxicity in an animal study. *Methods,* 41**,** 3-8.

De Lurdes Dinis, M. and Fiúza, A. (2011). Exposure Assessment to Heavy Metals in the Environment: Measures to Eliminate or Reduce the Exposure to Critical Receptors. 1**,** 27-50.

DEA (2012). Government Gazette. 561.

Descotes, J. (2004), Immunotoxicology of Drugs and Chemicals: An Experimental and Clinical Approach, Volume 1: Principles and Methods of Immunotoxieology. Elsevier Science Publishing Company

Deshmane, S. L., Kremlev, S., Amini, S. and Sawaya, B. E. (2009). Monocyte chemoattractant protein-1 (MCP-1): an overview. *Journal of interferon & cytokine research,* 29**,** 313-326.

Dewitt, J. C., Peden-Adams, M. M., Keller, J. M. and Germolec, D. R. (2012). Immunotoxicity of perfluorinated compounds: recent developments. *Toxicologic pathology,* 40**,** 300-311.

Dodds, A. W. and Matsushita, M. (2007). The phylogeny of the complement system and the origins of the classical pathway. *Immunobiology,* 212**,** 233-243.

Domouhtsidou, G. and Dimitriadis, V. (2000). Ultrastructural localization of heavy metals (Hg, Ag, Pb, and Cu) in gills and digestive gland of mussels, Mytilus

222

galloprovincialis (L.). *Archives of Environmental Contamination and Toxicology,* 38**,** 472-478.

Donnelly, R. P., Dickensheets, H. and Finbloom, D. S. (1999). The interleukin-10 signal transduction pathway and regulation of gene expression in mononuclear phagocytes. *Journal of interferon & cytokine research,* 19**,** 563-573.

Dunkelberger, J. R. and Song, W. C. (2010). Complement and its role in innate and adaptive immune responses. *Cell Res,* 20**,** 34-50.

Duruibe, J., Ogwuegbu, M. and Egwurugwu, J. (2007). Heavy metal pollution and human biotoxic effects. *International Journal of Physical Sciences,* 2**,** 112-118.

DWAF (1996), South African Water Quality Guidelines. Volume 7: Aquatic Ecosystems. Department of Water Affairs and Forestry Pretoria

Eisenbrand, G., Pool-Zobel, B., Baker, V., Balls, M., Blaauboer, B., Boobis, A., Carere, A., Kevekordes, S., Lhuguenot, J.-C. and Pieters, R. (2002). Methods of in vitro toxicology. *Food and Chemical Toxicology,* 40**,** 193-236.

Elsabahy, M. and Wooley, K. L. (2013). Cytokines as biomarkers of nanoparticle immunotoxicity. *Chemical Society Reviews,* 42**,** 5552-5576.

Eom, H.-J. and Choi, J. (2010). p38 MAPK activation, DNA damage, cell cycle arrest and apoptosis as mechanisms of toxicity of silver nanoparticles in Jurkat T cells. *Environmental science & technology,* 44**,** 8337-8342.

Fabrega, J., Luoma, S. N., Tyler, C. R., Galloway, T. S. and Lead, J. R. (2011). Silver nanoparticles: behaviour and effects in the aquatic environment. *Environ Int,* 37**,** 517-31.

Feito, M., Vila, M., Matesanz, M., Linares, J., Gonçalves, G., Marques, P., Vallet-Regí, M., Rojo, J. and Portolés, M. (2014). In vitro evaluation of graphene oxide nanosheets on immune function. *Journal of colloid and interface science,* 432**,** 221-228.

Fernández-Luqueño, F., López-Valdez, F., Gamero-Melo, P., Luna-Suárez, S., Aguilera-González, E., Martínez, A., García-Guillermo, M., Hernández-Martínez, G., Herrera-Mendoza, R. and Álvarez-Garza, M. (2013). Heavy metal pollution in drinking water-a global risk for human health: A review. *African Journal of Environmental Science and Technology,* 7**,** 567-584.

Fitzgerald, K. A., Rowe, D. C. and Golenbock, D. T. (2004). Endotoxin recognition and signal transduction by the TLR4/MD2-complex. *Microbes Infect,* 6**,** 1361-7.

Florea, A. M. and Busselberg, D. (2006). Occurrence, use and potential toxic effects of metals and metal compounds. *Biometals,* 19**,** 419-27.

Flores, L. E., Aguilar, E. J., Barbosa, V. C. and De Carvalho, L. A. (2004). A graph model for the evolution of specificity in humoral immunity. *J Theor Biol,* 229**,** 311-25.

Gaetke, L. (2003). Copper toxicity, oxidative stress, and antioxidant nutrients. *Toxicology,* 189**,** 147-163.

Gill, S. K., Islam, N., Shaw, I., Ribeiro, A., Bradley, B., Kilcoyne, M., Ceredig, R. and Joshi, L. (2016). Immunomodulatory effects of natural polysaccharides assessed in human whole blood culture and THP-1 cells show greater sensitivity of whole blood culture. *International immunopharmacology,* 36**,** 315-323.

Giovanni, M., Yue, J., Zhang, L., Xie, J., Ong, C. N. and Leong, D. T. (2015). Pro-inflammatory responses of RAW264. 7 macrophages when treated with ultralow concentrations of silver, titanium dioxide, and zinc oxide nanoparticles. *Journal of hazardous materials,* 297**,** 146-152.

Goswami, M., Yadav, K., Dubey, A., Sharma, B. S., Konwar, R., Kumar, R., Nagpure, N. S. and Lakra, W. S. (2014). In vitro cytotoxicity assessment of two heavy metal salts in a fish cell line (RF). *Drug and chemical toxicology,* 37**,** 48-54.

Granger, D. L., Taintor, R. R., Boockvar, K. S. and Hibbs, J. B. (1996). Measurement of nitrate and nitrite in biological samples using nitrate reductase and Griess reaction. *Methods in enzymology,* 268**,** 142-151.

Greulich, C., Diendorf, J., Gessmann, J., Simon, T., Habijan, T., Eggeler, G., Schildhauer, T., Epple, M. and Köller, M. (2011). Cell type-specific responses of peripheral blood mononuclear cells to silver nanoparticles. *Acta biomaterialia,* 7**,** 3505-3514.

Gubbins, E. J., Batty, L. C. and Lead, J. R. (2011). Phytotoxicity of silver nanoparticles to Lemna minor L. *Environmental Pollution,* 159**,** 1551-1559.

225

Gustafson, H. H., Holt-Casper, D., Grainger, D. W. and Ghandehari, H. (2015). Nanoparticle uptake: The phagocyte problem. *Nano today,* 10**,** 487-510.

Haase, H., Ober-Blöbaum, J. L., Engelhardt, G., Hebel, S. and Rink, L. (2010). Cadmium ions induce monocytic production of tumor necrosis factor-alpha by inhibiting mitogen activated protein kinase dephosphorylation. *Toxicology letters,* 198**,** 152-158.

Hadrup, N. and Lam, H. R. (2014). Oral toxicity of silver ions, silver nanoparticles and colloidal silver–a review. *Regulatory Toxicology and Pharmacology,* 68**,** 1-7.

Handy, R. D. (2003). Chronic effects of copper exposure versus endocrine toxicity: two sides of the same toxicological process? *Comparative Biochemistry and Physiology Part A: Molecular & Integrative Physiology,* 135**,** 25-38.

Hartwig, A. (2001). Role of magnesium in genomic stability. *Mutation Research/Fundamental and Molecular Mechanisms of Mutagenesis,* 475**,** 113-121.

Harvey, R., Mccaughan, C., Wise, L. M., Mercer, A. A. and Fleming, S. B. (2015). Orf virus inhibits interferon stimulated gene expression and modulates the JAK/STAT signalling pathway. *Virus research,* 208**,** 180-188.

Havrdova, M., Hola, K., Skopalik, J., Tomankova, K., Petr, M., Cepe, K., Polakova, K., Tucek, J., Bourlinos, A. B. and Zboril, R. (2016). Toxicity of carbon dots– Effect of surface functionalization on the cell viability, reactive oxygen species generation and cell cycle. *Carbon,* 99**,** 238-248.

226

Hawlisch, H. and Kohl, J. (2006). Complement and Toll-like receptors: key regulators of adaptive immune responses. *Mol Immunol,* 43**,** 13-21.

He, Z., Zhang, H., Yang, C., Zhou, Y., Zhou, Y., Han, G., Xia, L., Ouyang, W., Zhou, F. and Zhou, Y. (2011). The interaction between different types of activated RAW 264.7 cells and macrophage inflammatory protein-1 alpha. *Radiation Oncology,* 6**,** 86.

Heinrich, P. C., Behrmann, I., Serge, H., Hermanns, H. M., Müller-Newen, G. and Schaper, F. (2003). Principles of interleukin (IL)-6-type cytokine signalling and its regulation. *Biochemical journal,* 374**,** 1-20.

Herzog, F., Clift, M. J., Piccapietra, F., Behra, R., Schmid, O., Petri-Fink, A. and Rothen-Rutishauser, B. (2013). Exposure of silver-nanoparticles and silver-ions to lung cells in vitro at the air-liquid interface. *Particle and fibre toxicology,* 10**,** 11.

Hibi, M., Nakajima, K. and Hirano, T. (1996). IL-6 cytokine family and signal transduction: a model of the cytokine system. *Journal of molecular medicine,* 74**,** 1-12.

Hidalgo, E. and Domınguez, C. (1998). Study of cytotoxicity mechanisms of silver nitrate in human dermal fibroblasts. *Toxicology letters,* 98**,** 169-179.

Hoh, B. L., Hosaka, K., Downes, D. P., Nowicki, K. W., Fernandez, C. E., Batich, C. D. and Scott, E. W. (2011). Monocyte chemotactic protein-1 promotes inflammatory vascular repair of murine carotid aneurysms via a macrophage inflammatory protein-1α and macrophage inflammatory protein-2–dependent pathway. *Circulation,* 124**,** 2243-2252.

227

Horvat, T., Vidaković-Cifrek, Ž., Oreščanin, V., Tkalec, M. and Pevalek-Kozlina, B. (2007). Toxicity assessment of heavy metal mixtures by Lemna minor L. *Science of the total environment,* 384**,** 229-238.

House, R. V. (2001). Cytokine measurement techniques for assessing hypersensitivity. *Toxicology,* 158**,** 51-58.

Hummers, W. and Offeman, R. (1958). Preparation of graphitic oxide [J]. *J Am Chem Soc,* 80**,** 1339.

Inoue, K.-I., Koike, E., Yanagisawa, R., Hirano, S., Nishikawa, M. and Takano, H. (2009). Effects of multi-walled carbon nanotubes on a murine allergic airway inflammation model. *Toxicology and applied pharmacology,* 237**,** 306-316.

Ivask, A., Bondarenko, O., Jepihhina, N. and Kahru, A. (2010). Profiling of the reactive oxygen species-related ecotoxicity of CuO, ZnO, TiO2, silver and fullerene nanoparticles using a set of recombinant luminescent Escherichia coli strains: differentiating the impact of particles and solubilised metals. *Analytical and bioanalytical chemistry,* 398**,** 701-716.

Jackson, V. A., Paulse, A. N., Odendaal, J. P. and Khan, W. (2009). Investigation into the metal contamination of the Plankenberg and Diep Rivers, Western Cape, South Africa. *Water SA,* 35**,** 289-299.

Jaishankar, M., Tseten, T., Anbalagan, N., Mathew, B. B. and Beeregowda, K. N. (2014). Toxicity, mechanism and health effects of some heavy metals. *Interdisciplinary toxicology,* 7**,** 60-72.

Jan, A. T., Azam, M., Siddiqui, K., Ali, A., Choi, I. and Haq, Q. M. R. (2015). Heavy metals and human health: Mechanistic insight into toxicity and counter

228

defense system of antioxidants. *International journal of molecular sciences,* 16**,** 29592-29630.

Janeway, C. A., Jr. and Medzhitov, R. (2002). Innate immune recognition. *Annu Rev Immunol,* 20**,** 197-216.

Jansson, G. and Harms-Ringdahl, M. (1993). Stimulating effects of mercuric-and silver ions on the superoxide anion production in human polymorphonuclear leukocytes. *Free radical research communications,* 18**,** 87-98.

Jaworski, S., Sawosz, E., Kutwin, M., Wierzbicki, M., Hinzmann, M., Grodzik, M., Winnicka, A., Lipińska, L., Włodyga, K. and Chwalibog, A. (2015). In vitro and in vivo effects of graphene oxide and reduced graphene oxide on glioblastoma. *International journal of nanomedicine,* 10**,** 1585.

Jezierska, B. and Witeska, M. (2001). Metal toxicity to fish. *Monografie. University of Podlasie (Poland).*

Jin, Y., Liu, L., Zhang, S., He, R., Wu, Y., Chen, G. and Fu, Z. (2016). Cadmium exposure to murine macrophages decreases their inflammatory responses and increases their oxidative stress. *Chemosphere,* 144**,** 168-175.

Jomova, K. and Valko, M. (2011). Advances in metal-induced oxidative stress and human disease. *Toxicology,* 283**,** 65-87.

Kagan, V., Tyurina, Y., Tyurin, V., Konduru, N., Potapovich, A., Osipov, A., Kisin, E., Schwegler-Berry, D., Mercer, R. and Castranova, V. (2006). Direct and indirect effects of single walled carbon nanotubes on RAW 264.7 macrophages: role of iron. *Toxicology letters,* 165**,** 88-100.

Kaufmann, S. H. (1999). Cell-mediated immunity: dealing a direct blow to pathogens. *Current biology,* 9**,** R97-R99.

Kaur, J. and Tikoo, K. (2013). Evaluating cell specific cytotoxicity of differentially charged silver nanoparticles. *Food Chem Toxicol,* 51**,** 1-14.

Kawai, T. and Akira, S. (2007). TLR signaling. *Semin Immunol,* 19**,** 24-32.

Kawata, K., Osawa, M. and Okabe, S. (2009). In vitro toxicity of silver nanoparticles at noncytotoxic doses to HepG2 human hepatoma cells. *Environmental science & technology,* 43**,** 6046-6051.

Kayat, J., Gajbhiye, V., Tekade, R. K. and Jain, N. K. (2011). Pulmonary toxicity of carbon nanotubes: a systematic report. *Nanomedicine: Nanotechnology, Biology and Medicine,* 7**,** 40-49.

Khan, S., Cao, Q., Zheng, Y. M., Huang, Y. Z. and Zhu, Y. G. (2008). Health risks of heavy metals in contaminated soils and food crops irrigated with wastewater in Beijing, China. *Environ Pollut,* 152**,** 686-92.

Kishimoto, T. (2006). Interleukin-6: discovery of a pleiotropic cytokine. *Arthritis Res Ther,* 8 Suppl 2**,** S2.

Kishimoto, T. (2010). IL-6: from its discovery to clinical applications. *Int Immunol,* 22**,** 347-52.

Koukal, B., Gueguen, C., Pardos, M. and Dominik, J. (2003). Influence of humic substances on the toxic effects of cadmium and zinc to the green alga Pseudokirchneriella subcapitata. *Chemosphere,* 53**,** 953-961.

Kudr, J., Richtera, L., Xhaxhiu, K., Hynek, D., Heger, Z., Zitka, O. and Adam, V. (2017). Carbon dots based FRET for the detection of DNA damage. *Biosensors and Bioelectronics,* 92**,** 133-139.

Kumar, H., Kawai, T. and Akira, S. (2009). Toll-like receptors and innate immunity. *Biochem Biophys Res Commun,* 388**,** 621-5.

Lacerda, C. M. and Reardon, K. F. (2009). Environmental proteomics: applications of proteome profiling in environmental microbiology and biotechnology. *Briefings in functional genomics & proteomics,* 8**,** 75-87.

Ladics, G. S. (2007). Use of SRBC antibody responses for immunotoxicity testing. *Methods,* 41**,** 9-19.

Lan, C.-H. and Lin, T.-S. (2005). Acute toxicity of trivalent thallium compounds to Daphnia magna. *Ecotoxicology and environmental safety,* 61**,** 432-435.

Langezaal, I., Hoffmann, S., Hartung, T. and Coecke, S. (2001). Evaluation and prevalidation of an immunotoxicity test based on human whole-blood cytokine release. *Alternatives to laboratory animals: ATLA,* 30**,** 581-595.

Larosa, D. F. and Orange, J. S. (2008). 1. Lymphocytes. *Journal of Allergy and Clinical Immunology,* 121**,** S364-S369.

Lewis, M. A. (1995). Use of freshwater plants for phytotoxicity testing: a review. *Environmental Pollution,* 87**,** 319-336.

Li, Y., Liu, Y., Fu, Y., Wei, T., Le Guyader, L., Gao, G., Liu, R.-S., Chang, Y.-Z. and Chen, C. (2012). The triggering of apoptosis in macrophages by pristine graphene through the MAPK and TGF-beta signaling pathways. *Biomaterials,* 33**,** 402-411.

Liebsch, M. and Spielmann, H. (2002). Currently available in vitro methods used in the regulatory toxicology. *Toxicology letters,* 127**,** 127-134.

Lin, L. and Du, L. (2017). The role of secreted factors in stem cells-mediated immune regulation. *Cellular Immunology*.

Liu, B., Salgado, S., Maheshwari, V. and Liu, J. (2016). DNA adsorbed on graphene and graphene oxide: Fundamental interactions, desorption and applications. *Current Opinion in Colloid & Interface Science,* 26**,** 41-49.

Liu, J.-H., Yang, S.-T., Chen, X.-X. and Wang, H. (2012). Fluorescent carbon dots and nanodiamonds for biological imaging: preparation, application, pharmacokinetics and toxicity. *Current drug metabolism,* 13**,** 1046-1056.

Liu, W., Zhou, Q., Liu, J., Fu, J., Liu, S. and Jiang, G. (2011). Environmental and biological influences on the stability of silver nanoparticles. *Chinese Science Bulletin,* 56**,** 2009-2015.

Liu, X., Vinson, D., Abt, D., Hurt, R. H. and Rand, D. M. (2009). Differential toxicity of carbon nanomaterials in Drosophila: larval dietary uptake is benign, but adult exposure causes locomotor impairment and mortality. *Environmental science & technology,* 43**,** 6357-6363.

Lu, C.-J., Jiang, X.-F., Junaid, M., Ma, Y.-B., Jia, P.-P., Wang, H.-B. and Pei, D.-S. (2017). Graphene oxide nanosheets induce DNA damage and activate the base excision repair (BER) signaling pathway both in vitro and in vivo. *Chemosphere*.

Lu, Y. C., Yeh, W. C. and Ohashi, P. S. (2008). LPS/TLR4 signal transduction pathway. *Cytokine,* 42**,** 145-51.

Maddaly, R., Pai, G., Balaji, S., Sivaramakrishnan, P., Srinivasan, L., Sunder, S. S. and Paul, S. F. (2010). Receptors and signaling mechanisms for B-lymphocyte activation, proliferation and differentiation--insights from both in vivo and in vitro approaches. *FEBS Lett,* 584**,** 4883-94.

Maier, J. A., Malpuech-Brugere, C., Zimowska, W., Rayssiguier, Y. and Mazur, A. (2004). Low magnesium promotes endothelial cell dysfunction: implications for atherosclerosis, inflammation and thrombosis. *Biochim Biophys Acta,* 1689**,** 13-21.

Malan, M., Muller, F., Cyster, L., Raitt, L. and Aalbers, J. (2015). Heavy metals in the irrigation water, soils and vegetables in the Philippi horticultural area in the Western Cape Province of South Africa. *Environ Monit Assess,* 187**,** 4085.

Marc, D. and Olson, K. (2009). Hypersensitivity reactions and methods of detection. *NeuroScience, Inc*.

Marth, E., Jelovcan, S., Kleinhappl, B., Gutschi, A. and Barth, S. (2001). The effect of heavy metals on the immune system at low concentrations. *International journal of occupational medicine and environmental health,* 14**,** 375-386.

Martínez-Gutierrez, F., Thi, E. P., Silverman, J. M., De Oliveira, C. C., Svensson, S. L., Hoek, A. V., Sánchez, E. M., Reiner, N. E., Gaynor, E. C. and Pryzdial, E. L. (2012). Antibacterial activity, inflammatory response, coagulation and cytotoxicity effects of silver nanoparticles. *Nanomedicine: Nanotechnology, Biology and Medicine,* 8**,** 328-336.

Martinez-Gutierrez, F., Thi, E. P., Silverman, J. M., De Oliveira, C. C., Svensson, S. L., Vanden Hoek, A., Sanchez, E. M., Reiner, N. E., Gaynor, E. C., Pryzdial,

E. L., Conway, E. M., Orrantia, E., Ruiz, F., Av-Gay, Y. and Bach, H. (2012). Antibacterial activity, inflammatory response, coagulation and cytotoxicity effects of silver nanoparticles. *Nanomedicine,* 8**,** 328-36.

Mcglauchlen, K. S. and Vogel, L. A. (2003). Ineffective humoral immunity in the elderly. *Microbes and Infection,* 5**,** 1279-1284.

Mebius, R. E. and Kraal, G. (2005). Structure and function of the spleen. *Nat Rev Immunol,* 5**,** 606-16.

Medzhitov, R. (2007). Recognition of microorganisms and activation of the immune response. *Nature,* 449**,** 819-26.

Miretzky, P., Saralegui, A. and Cirelli, A. F. (2004). Aquatic macrophytes potential for the simultaneous removal of heavy metals (Buenos Aires, Argentina). *Chemosphere,* 57**,** 997-1005.

Mishra, K. P. (2009). Lead exposure and its impact on immune system: a review. *Toxicol In Vitro,* 23**,** 969-72.

Mishra, V. K. and Tripathi, B. (2008). Concurrent removal and accumulation of heavy metals by the three aquatic macrophytes. *Bioresource technology,* 99**,** 7091-7097.

Mogensen, T. H. (2009). Pathogen recognition and inflammatory signaling in innate immune defenses. *Clin Microbiol Rev,* 22**,** 240-73, Table of Contents.

Mohr, B. (2013). The current status of laboratory animal ethics in South Africa. *Altern Lab Anim,* 41**,** 48-51.

Moser, M. and Leo, O. (2010). Key concepts in immunology. *Vaccine,* 28 Suppl 3**,** C2-13.

Mouchet, F., Landois, P., Sarremejean, E., Bernard, G., Puech, P., Pinelli, E., Flahaut, E. and Gauthier, L. (2008). Characterisation and in vivo ecotoxicity evaluation of double-wall carbon nanotubes in larvae of the amphibian Xenopus laevis. *Aquatic Toxicology,* 87**,** 127-137.

Mühl, H. and Pfeilschifter, J. (2003). Anti-inflammatory properties of pro-inflammatory interferon-γ. *International immunopharmacology,* 3**,** 1247-1255.

Münzinger, A. (1990). Effects of nickel on Daphnia magna during chronic exposure and alterations in the toxicity to generations pre-exposed to nickel. *Water Research,* 24**,** 845-852.

Murphy, K. and Weaver, C. (2016). *Janeway's immunobiology*, Garland Science.

Murray, A., Kisin, E., Leonard, S., Young, S., Kommineni, C., Kagan, V., Castranova, V. and Shvedova, A. (2009). Oxidative stress and inflammatory response in dermal toxicity of single-walled carbon nanotubes. *Toxicology,* 257**,** 161-171.

Musee, N., Oberholster, P., Sikhwivhilu, L. and Botha, A.-M. (2010). The effects of engineered nanoparticles on survival, reproduction, and behaviour of freshwater snail, Physa acuta (Draparnaud, 1805). *Chemosphere,* 81**,** 1196-1203.

Niemand, C., Nimmesgern, A., Haan, S., Fischer, P., Schaper, F., Rossaint, R., Heinrich, P. C. and Muller-Newen, G. (2003). Activation of STAT3 by IL-6 and IL-10 in Primary Human Macrophages Is Differentially Modulated by

Suppressor of Cytokine Signaling 3. *The Journal of Immunology,* 170**,** 3263-3272.

Nordberg, J. and Arner, E. S. (2001). Reactive oxygen species, antioxidants, and the mammalian thioredoxin system. *Free radical biology and medicine,* 31**,** 1287-1312.

Noris, M. and Remuzzi, G. Overview of complement activation and regulation. Seminars in nephrology, 2013. Elsevier, 479-492.

O'Connor, D. 2004 *OECD Country Economic and Environmental Policies: What Implications for East Asia?* [Online]. Available: http://www.oecd.org/pcd/31970833.pdf.

Okonkwo, J. O. and Mothiba, M. (2005). Physico-chemical characteristics and pollution levels of heavy metals in the rivers in Thohoyandou, South Africa. *Journal of Hydrology,* 308**,** 122-127.

Olabarrieta, I., L'azou, B., Yuric, S., Cambar, J. and Cajaraville, M. (2001). In vitro effects of cadmium on two different animal cell models. *Toxicology in vitro,* 15**,** 511-517.

Oluyemi, E., Feuyit, G., Oyekunle, J. and Ogunfowokan, A. (2008). Seasonal variations in heavy metal concentrations in soil and some selected crops at a landfill in Nigeria. *African Journal of Environmental Science and Technology,* 2**,** 089-096.

Orecchioni, M., Jasim, D. A., Pescatori, M., Manetti, R., Fozza, C., Sgarrella, F., Bedognetti, D., Bianco, A., Kostarelos, K. and Delogu, L. G. (2016a). Molecular and genomic impact of large and small lateral dimension graphene

236

oxide sheets on human immune cells from healthy donors. *Advanced healthcare materials,* 5**,** 276-287.

Orecchioni, M., Ménard-Moyon, C., Delogu, L. G. and Bianco, A. (2016b). Graphene and the immune system: Challenges and potentiality. *Advanced drug delivery reviews,* 105**,** 163-175.

Pandey, S., Gedda, G. R., Thakur, M., Bhaisare, M. L., Talib, A., Khan, M. S., Wu, S.-M. and Wu, H.-F. (2017). Theranostic carbon dots 'clathrate-like'nanostructures for targeted photo-chemotherapy and bioimaging of cancer. *Journal of Industrial and Engineering Chemistry*.

Panyala, N. R., Peña-Méndez, E. M. and Havel, J. (2008). Silver or silver nanoparticles: a hazardous threat to the environment and human health. *J Appl Biomed,* 6**,** 117-129.

Paris-Palacios, S., Biagianti-Risbourg, S. and Vernet, G. (2000). Biochemical and (ultra) structural hepatic perturbations of Brachydanio rerio (Teleostei, Cyprinidae) exposed to two sublethal concentrations of copper sulfate. *Aquatic Toxicology,* 50**,** 109-124.

Park, E. J., Yi, J., Kim, Y., Choi, K. and Park, K. (2010). Silver nanoparticles induce cytotoxicity by a Trojan-horse type mechanism. *Toxicol In Vitro,* 24**,** 872-8.

Park, M. V., Neigh, A. M., Vermeulen, J. P., De La Fonteyne, L. J., Verharen, H. W., Briede, J. J., Van Loveren, H. and De Jong, W. H. (2011). The effect of particle size on the cytotoxicity, inflammation, developmental toxicity and genotoxicity of silver nanoparticles. *Biomaterials,* 32**,** 9810-7.

Parkin, J. and Cohen, B. (2001). An overview of the immune system. *The Lancet,* 357**,** 1777-1789.

Pathak, N. and Khandelwal, S. (2006). Oxidative stress and apoptotic changes in murine splenocytes exposed to cadmium. *Toxicology,* 220**,** 26-36.

Peng, Z., Han, X., Li, S., Al-Youbi, A. O., Bashammakh, A. S., El-Shahawi, M. S. and Leblanc, R. M. (2017). Carbon Dots: Biomacromolecule Interaction, Bioimaging and Nanomedicine. *Coordination Chemistry Reviews*.

Peruzynska, M., Cendrowski, K., Barylak, M., Tkacz, M., Piotrowska, K., Kurzawski, M., Mijowska, E. and Drozdzik, M. (2017). Comparative in vitro study of single and four layer graphene oxide nanoflakes—Cytotoxicity and cellular uptake. *Toxicology in Vitro,* 41**,** 205-213.

Pierrat, P., Wang, R., Kereselidze, D., Lux, M., Didier, P., Kichler, A., Pons, F. and Lebeau, L. (2015). Efficient in vitro and in vivo pulmonary delivery of nucleic acid by carbon dot-based nanocarriers. *Biomaterials,* 51**,** 290-302.

Pinto, E., Sigaud-Kutner, T., Leitao, M. A., Okamoto, O. K., Morse, D. and Colepicolo, P. (2003). Heavy metal–induced oxidative stress in algae1. *Journal of Phycology,* 39**,** 1008-1018.

Piotrowska-Niczyporuk, A., Bajguz, A., Zambrzycka, E. and Godlewska-Żyłkiewicz, B. (2012). Phytohormones as regulators of heavy metal biosorption and toxicity in green alga Chlorella vulgaris (Chlorophyceae). *Plant Physiology and Biochemistry,* 52**,** 52-65.

Ploetz, D., Fitts, B. and Rice, T. (2007). Differential accumulation of heavy metals in muscle and liver of a marine fish,(King Mackerel, Scomberomorus cavalla Cuvier) from the Northern Gulf of Mexico, USA. *Bulletin of Environmental Contamination and Toxicology,* 78**,** 134-137.

Pulit-Prociak, J. and Banach, M. (2016). Silver nanoparticles–a material of the future…? *Open Chemistry,* 14**,** 76-91.

Qu, C., Wang, L., He, J., Tan, J., Liu, W., Zhang, S., Zhang, C., Wang, Z., Jiao, S. and Liu, S. (2012). Carbon nanotubes provoke inflammation by inducing the pro-inflammatory genes IL-1β and IL-6. *Gene,* 493**,** 9-12.

Radwan, M., El-Gendy, K. and Gad, A. (2010). Oxidative stress biomarkers in the digestive gland of Theba pisana exposed to heavy metals. *Archives of environmental contamination and toxicology,* 58**,** 828-835.

Rahman, I. and Macnee, W. (2000). Oxidative stress and regulation of glutathione in lung inflammation. *European Respiratory Journal,* 16**,** 534-554.

Rainbow, P. S. (2002). Trace metal concentrations in aquatic invertebrates: why and so what? *Environmental Pollution,* 120**,** 497-507.

Ravera, O. (2001). Monitoring of the aquatic environment by species accumulator of pollutants: a review. *Journal of Limnology,* 60**,** 63-78.

Reardon, C. L. and Lucas, D. O. (1987). Heavy-metal mitogenesis: Zn++ and Hg++ induce cellular cytotoxicity and interferon production in murine T lymphocytes. *Immunobiology,* 175**,** 455-469.

Reinecke, A., Reinecke, S. and Lambrechts, H. (1997). Uptake and toxicity of copper and zinc for the African earthworm, Eudrilus eugeniae (Oligochaeta). *Biology and fertility of soils,* 24**,** 27-31.

Reinecke, A., Snyman, R. and Nel, J. (2003). Uptake and distribution of lead (Pb) and cadmium (Cd) in the freshwater crab, Potamonautes perlatus (Crustacea) in the Eerste River, South Africa. *Water, Air, and Soil Pollution,* 145**,** 395-408.

Reinecke, S., Prinsloo, M. and Reinecke, A. (1999). Resistance ofEisenia fetida (Oligochaeta) to cadmium after long-term exposure. *Ecotoxicology and Environmental Safety,* 42**,** 75-80.

Ribatti, D., Crivellato, E. and Vacca, A. (2006). Miller's seminal studies on the role of thymus in immunity. *Clinical & Experimental Immunology,* 144**,** 371-375.

Richards, D. M. and Endres, R. G. (2014). The mechanism of phagocytosis: two stages of engulfment. *Biophysical journal,* 107**,** 1542-1553.

Riemschneider, S., Herzberg, M. and Lehmann, J. (2015). Subtoxic doses of cadmium modulate inflammatory properties of murine RAW 264.7 macrophages. *BioMed research international,* 2015.

Riley, J. K., Takeda, K., Akira, S. and Schreiber, R. D. (1999). Interleukin-10 Receptor Signaling through the JAK-STAT Pathway requirement for two distinct receptor-derived signals for anti-inflammatory action. *Journal of Biological Chemistry,* 274**,** 16513-16521.

Rodda, N., Carden, K., Armitage, N. and Du Plessis, H. (2011). Development of guidance for sustainable irrigation use of greywater in gardens and small-scale agriculture in South Africa. *Water SA,* 37**,** 727-737.

Roozendaal, R., Mebius, R. E. and Kraal, G. (2008). The conduit system of the lymph node. *Int Immunol,* 20**,** 1483-7.

Rosales, C. and Uribe-Querol, E. (2017). Phagocytosis: A Fundamental Process in Immunity. *BioMed Research International,* 2017.

Rossi, A., Poverini, R., Di Lullo, G., Modesti, A., Modica, A. and Scarino, M. (1996). Heavy metal toxicity following apical and basolateral exposure in the human intestinal cell line Caco-2. *Toxicology in vitro,* 10**,** 27-36.

Ruparelia, J. P., Chatterjee, A. K., Duttagupta, S. P. and Mukherji, S. (2008). Strain specificity in antimicrobial activity of silver and copper nanoparticles. *Acta biomaterialia,* 4**,** 707-716.

Ryu, J. C., Park, S. M., Hwangbo, M., Byun, S. H., Ku, S. K., Kim, Y. W., Kim, S. C., Jee, S. Y. and Cho, I. J. (2013). Methanol Extract of Artemisia apiacea Hance Attenuates the Expression of Inflammatory Mediators via NF- kappa B Inactivation. *Evid Based Complement Alternat Med,* 2013**,** 494681.

Said, W. and Lewis, D. (1991). Quantitative assessment of the effects of metals on microbial degradation of organic chemicals. *Applied and Environmental Microbiology,* 57**,** 1498-1503.

Saleem, J., Wang, L. and Chen, C. (2017). Immunological effects of graphene family nanomaterials. *NanoImpact*.

Sauvé, S., Brousseau, P., Pellerin, J., Morin, Y., Senécal, L., Goudreau, P. and Fournier, M. (2002). Phagocytic activity of marine and freshwater bivalves: in vitro exposure of hemocytes to metals (Ag, Cd, Hg and Zn). *Aquatic toxicology,* 58**,** 189-200.

Schroder, K., Hertzog, P. J., Ravasi, T. and Hume, D. A. (2004). Interferon-γ: an overview of signals, mechanisms and functions. *Journal of leukocyte biology,* 75**,** 163-189.

Shin, S. H., Ye, M. K., Kim, H. S. and Kang, H. S. (2007). The effects of nano-silver on the proliferation and cytokine expression by peripheral blood mononuclear cells. *Int Immunopharmacol,* 7**,** 1813-8.

Singh, R. P. and Ramarao, P. (2012). Cellular uptake, intracellular trafficking and cytotoxicity of silver nanoparticles. *Toxicol Lett,* 213**,** 249-59.

Sotirelis, N. P. and Chrysikopoulos, C. V. (2017). Heteroaggregation of graphene oxide nanoparticles and kaolinite colloids. *Science of the Total Environment,* 579**,** 736-744.

Stavnezer, J., Guikema, J. E. and Schrader, C. E. (2008). Mechanism and regulation of class switch recombination. *Annual review of immunology,* 26.

Stavnezer, J. and Schrader, C. E. (2014). IgH chain class switch recombination: mechanism and regulation. *The Journal of Immunology,* 193**,** 5370-5378.

Steiner, E., Kleinhappl, B., Gutschi, A. and Marth, E. (1998). Analysis of hsp70 mRNA levels in HepG2 cells exposed to various metals differing in toxicity. *Toxicology letters,* 96**,** 169-176.

Stone, V., Nowack, B., Baun, A., Van Den Brink, N., Kammer, F., Dusinska, M., Handy, R., Hankin, S., Hassellov, M., Joner, E. and Fernandes, T. F. (2010). Nanomaterials for environmental studies: classification, reference material issues, and strategies for physico-chemical characterisation. *Sci Total Environ,* 408**,** 1745-54.

Storni, T., Kündig, T. M., Senti, G. and Johansen, P. (2005). Immunity in response to particulate antigen-delivery systems. *Advanced drug delivery reviews,* 57**,** 333-355.

Sun, X. and Lei, Y. (2017). Fluorescent carbon dots and their sensing applications. *TrAC Trends in Analytical Chemistry*.

Sun, X., Liu, Z., Welsher, K., Robinson, J. T., Goodwin, A., Zaric, S. and Dai, H. (2008). Nano-graphene oxide for cellular imaging and drug delivery. *Nano research,* 1**,** 203-212.

Takeda, K. and Akira, S. (2004). TLR signaling pathways. *Seminars in Immunology,* 16**,** 3-9.

Takeda, K. and Akira, S. (2005). Toll-like receptors in innate immunity. *Int Immunol,* 17**,** 1-14.

Talas, Z. S., Orun, I., Ozdemir, I., Erdogan, K., Alkan, A. and Yılmaz, I. (2008). Antioxidative role of selenium against the toxic effect of heavy metals (Cd+ 2, Cr+ 3) on liver of rainbow trout (Oncorhynchus mykiss Walbaum 1792). *Fish physiology and biochemistry,* 34**,** 217-222.

Tan, F., Wang, M., Wang, W. and Lu, Y. (2008). Comparative evaluation of the cytotoxicity sensitivity of six fish cell lines to four heavy metals in vitro. *Toxicology in vitro,* 22**,** 164-170.

Tan, T. T. and Coussens, L. M. (2007). Humoral immunity, inflammation and cancer. *Curr Opin Immunol,* 19**,** 209-16.

Tao, S., Zhu, S., Feng, T., Xia, C., Song, Y. and Yang, B. (2017). The polymeric characteristics and photoluminescence mechanism in polymer carbon dots: A review. *Materials Today Chemistry,* 6**,** 13-25.

Trouw, L. A. and Daha, M. R. (2011). Role of complement in innate immunity and host defense. *Immunology letters,* 138**,** 35-37.

Tsangaris, G. T. and Tzortzatou-Stathopoulou, F. (1998). Cadmium induces apoptosis differentially on immune system cell lines. *Toxicology,* 128**,** 143-150.

Tuerhong, M., Yang, X. and Xue-Bo, Y. (2017). Review on Carbon Dots and Their Applications. *Chinese Journal of Analytical Chemistry,* 45**,** 139-150.

Turrens, J. F. (2003). Mitochondrial formation of reactive oxygen species. *The Journal of physiology,* 552**,** 335-344.

US EPA (2000). Heavy Metal Soil Contamination. *Soil Quality-Urban Technical Note,* 3.

Van Lynden, G., Mantel, S. and Oostrum, A. V. (2004). Guiding principles for the quantitative assessment of soil degradation: with a focus on salinization, nutrient decline and soil pollution. *Guiding principles for the quantitative assessment of soil degradation: with a focus on salinization, nutrient decline and soil pollution*.

Vinodhini, R. and Narayanan, M. (2008). Bioaccumulation of heavy metals in organs of fresh water fish Cyprinus carpio (Common carp). *International Journal of Environmental Science & Technology,* 5**,** 179-182.

Vosloo, A., Van Aardt, W. and Mienie, L. (2002). Sublethal effects of copper on the freshwater crab Potamonautes warreni. *Comparative Biochemistry and Physiology Part A: Molecular & Integrative Physiology,* 133**,** 695-702.

Wajant, H., Pfizenmaier, K. and Scheurich, P. (2003). Tumor necrosis factor signaling. *Cell Death & Differentiation,* 10**,** 45-65.

Walters, C., Pool, E. and Somerset, V. (2013). Aggregation and dissolution of silver nanoparticles in a laboratory-based freshwater microcosm under simulated environmental conditions. *Toxicological & Environmental Chemistry,* 95**,** 1690-1701.

Wang, J., Li, Q., Zhou, J., Wang, Y., Yu, L., Peng, H. and Zhu, J. (2017). Synthesis, characterization and cells and tissues imaging of carbon quantum dots. *Optical Materials,* 72**,** 15-19.

Wang, Q.-S., Cui, Y.-L., Wang, Y.-F. and Chi, W. (2011a). Effects of compounds from Bi-Qi Capsule on the expression of inflammatory mediators in lipopolysaccharide-stimulated RAW 264.7 macrophages. *Journal of ethnopharmacology,* 136**,** 480-487.

Wang, Q. S., Cui, Y. L., Dong, T. J., Zhang, X. F. and Lin, K. M. (2012). Ethanol extract from a Chinese herbal formula, "Zuojin Pill", inhibit the expression of inflammatory mediators in lipopolysaccharide-stimulated RAW 264.7 mouse macrophages. *J Ethnopharmacol,* 141**,** 377-85.

Wang, Y., Anilkumar, P., Cao, L., Liu, J.-H., Luo, P. G., Tackett, K. N., Sahu, S., Wang, P., Wang, X. and Sun, Y.-P. (2011b). Carbon dots of different composition and surface functionalization: cytotoxicity issues relevant to

245

fluorescence cell imaging. *Experimental Biology and Medicine,* 236**,** 1231-1238.

Wang, Y., Li, Z., Hu, D., Lin, C.-T., Li, J. and Lin, Y. (2010). Aptamer/graphene oxide nanocomplex for in situ molecular probing in living cells. *Journal of the American Chemical Society,* 132**,** 9274-9276.

WHO (2006). Guidelines for Drinking-water Quality.

Wibroe, P. P., Petersen, S. V., Bovet, N., Laursen, B. W. and Moghimi, S. M. (2016). Soluble and immobilized graphene oxide activates complement system differently dependent on surface oxidation state. *Biomaterials,* 78**,** 20-26.

Willard-Mack, C. L. (2006). Normal structure, function, and histology of lymph nodes. *Toxicol Pathol,* 34**,** 409-24.

Yan, J., Chen, L., Huang, C.-C., Lung, S.-C. C., Yang, L., Wang, W.-C., Lin, P.-H., Suo, G. and Lin, C.-H. (2017). Consecutive evaluation of graphene oxide and reduced graphene oxide nanoplatelets immunotoxicity on monocytes. *Colloids and Surfaces B: Biointerfaces,* 153**,** 300-309.

Yang, E. J., Kim, S., Kim, J. S. and Choi, I. H. (2012). Inflammasome formation and IL-1beta release by human blood monocytes in response to silver nanoparticles. *Biomaterials,* 33**,** 6858-67.

Yang, S.-T., Wang, X., Wang, H., Lu, F., Luo, P. G., Cao, L., Meziani, M. J., Liu, J.-H., Liu, Y. and Chen, M. (2009). Carbon dots as nontoxic and high-performance fluorescence imaging agents. *The Journal of Physical Chemistry C,* 113**,** 18110-18114.

Ye, J. L., Mao, W. P., Wu, A. L., Zhang, N. N., Zhang, C., Yu, Y. J., Zhou, L. and Wei, C. J. (2007). Cadmium-induced apoptosis in human normal liver L-02 cells by acting on mitochondria and regulating Ca(2+) signals. *Environ Toxicol Pharmacol,* 24**,** 45-54.

Yuan, Y., Guo, B., Hao, L., Liu, N., Lin, Y., Guo, W., Li, X. and Gu, B. (2017). Doxorubicin-loaded environmentally friendly carbon dots as a novel drug delivery system for nucleus targeted cancer therapy. *Colloids and Surfaces B: Biointerfaces,* 159**,** 349-359.

Zhang, B., Wei, P., Zhou, Z. and Wei, T. (2016). Interactions of graphene with mammalian cells: Molecular mechanisms and biomedical insights. *Advanced drug delivery reviews,* 105**,** 145-162.

Zhang, T., Tang, M., Kong, L., Li, H., Zhang, T., Zhang, S., Xue, Y. and Pu, Y. (2012). Comparison of cytotoxic and inflammatory responses of pristine and functionalized multi-walled carbon nanotubes in RAW 264.7 mouse macrophages. *Journal of hazardous materials,* 219**,** 203-212.

Zhang, W., Yao, Y., Li, K., Huang, Y. and Chen, Y. (2011). Influence of dissolved oxygen on aggregation kinetics of citrate-coated silver nanoparticles. *Environ Pollut,* 159**,** 3757-62.

Zhao, E., Xu, H., Wang, L., Kryczek, I., Wu, K., Hu, Y., Wang, G. and Zou, W. (2012). Bone marrow and the control of immunity. *Cell Mol Immunol,* 9**,** 11-9.

247

Zhi, X., Fang, H., Bao, C., Shen, G., Zhang, J., Wang, K., Guo, S., Wan, T. and Cui, D. (2013). The immunotoxicity of graphene oxides and the effect of PVP-coating. *Biomaterials,* 34**,** 5254-5261.

Zhou, Q., Zhang, J., Fu, J., Shi, J. and Jiang, G. (2008). Biomonitoring: an appealing tool for assessment of metal pollution in the aquatic ecosystem. *Analytica chimica acta,* 606**,** 135-150.

Zhu, X., Chang, Y. and Chen, Y. (2010). Toxicity and bioaccumulation of TiO 2 nanoparticle aggregates in Daphnia magna. *Chemosphere,* 78**,** 209-215.

Zipfel, P. F. (2009). Complement and immune defense: from innate immunity to human diseases. *Immunology letters,* 126**,** 1-7.

Zlotnik, A., Yoshie, O. and Nomiyama, H. (2006). The chemokine and chemokine receptor superfamilies and their molecular evolution. *Genome biology,* 7**,** 1.

Zufferey, A., Speck, E. R., Machlus, K. R., Aslam, R., Guo, L., Mcvey, M. J., Kim, M., Kapur, R., Boilard, E. and Italiano, J. E. (2017). Mature murine megakaryocytes present antigen-MHC class I molecules to T cells and transfer them to platelets. *Blood Advances,* 1**,** 1773-1785.